Downloaded from UvA-DARE, the Institutional Repository of the University of Amsterdam (UvA)
http://dare.uva.nl/document/49088

File ID	49088
Filename	pyrc.pdf

SOURCE, OR PART OF THE FOLLOWING SOURCE:

Type	Dissertation
Title	Virus discovery and human coronavirus NL63
Author	K.A. Pyrc
Faculty	Faculty of Medicine
Year	2007
Pages	278

FULL BIBLIOGRAPHIC DETAILS:
http://dare.uva.nl/record/224746

Copyrights

It is not permitted to download or to forward/distribute the text or part of it without the consent of the copyright holder (usually the author), other then for strictly personal, individual use.

UvA-DARE is a service provided by the Library of the University of Amsterdam (http://dare.uva.nl)

Virus Discovery and Human Coronavirus NL63



Krzysztof Pyrc

Virus Discovery and Human Coronavirus NL63

The research described in this thesis was conducted in the Laboratory of Experimental Virology, Department of Medical Microbiology, Center for Infection and Immunity Amsterdam (CINIMA), Academic Medical Center, University of Amsterdam, The Netherlands

© Krzysztof Pyrc, 2007. No part of this publication may be reproduced, stored in a retrieval system, or transmitted, in any form or by any means, electronic, mechanical, photocopying, recording, or otherwise, without prior permission of the author.

Cover: The corona of the sun during eclipse, by Robert J. Peters

Virus Discovery and Human Coronavirus NL63

ACADEMISCH PROEFSCHRIFT

ter verkrijging van de graad van doctor

aan de Universiteit van Amsterdam

op gezag van de Rector Magnificus

prof.dr. J.W. Zwemmer

ten overstaan van een door het college voor promoties ingestelde

commissie, in het openbaar te verdedigen in de Aula der Universiteit

op vrijdag 29 juni 2007, te 10:00 uur

door

Krzysztof Antoni Pyrc

geboren te Krakow, Poland

Promotiecommissie:

Promotor: Prof.dr. B. Berkhout

Co-promotor: Dr. C.M. van der Hoek

Overige leden: Prof.dr. T. van der Poll

Prof.dr. J. Goudsmit

Dr. R. Lutter

Dr. H.L. Zaaijer

Prof.dr. R.S. Baric

Prof.dr. M. Van Ranst

Prof.dr. W.J.M Spaan

Faculteit der Geneeskunde

Contents

Chapter I	General introduction	5
Chapter II	Identification of a new human coronavirus	13
Chapter III	Genome structure and transcriptional regulation of human coronavirus NL63	35
Chapter IV	Molecular characterization of human coronavirus NL63	53
Chapter V	Mosaic structure of human coronavirus NL63, one thousand years of evolution	79
Chapter VI	Human coronavirus NL63 employs the SARS-CoV receptor for cellular entry	97
Chapter VII	Downregulation of angiotensin converting enzyme 2 protein during HCoV-NL63 infection	113
Chapter VIII	HCoV-NL63 induces interleukin-6 and interleukin-8 expression	121
Chapter IX	Inhibition of human coronavirus NL63 infection at early stages of the replication cycle	133
Chapter X	Antiviral strategies against human coronaviruses	153
Chapter XI	Identification of new human coronaviruses	179
Chapter XII	VIDISCA analyses of untypable picornaviruses reveals two novel human type B enteroviruses and one novel rhinovirus	195
Chapter XIII	Epilogue	211
Appendix A	VIDISCA: Unraveling the unknown	233
	Summary	253
	Samenvatting	257
	Podsumowanie	263
	Acknowledgments	269
	Curriculum Vitae	273

Chapter I

General Introduction

Viral infections impose an enormous disease burden on humanity, but our knowledge about pathogenic viruses is rather incomplete. The impression that we know almost everything about viral diseases and that medicine can cope with every possible infection was crushed by the appearance of several lethal viruses that are still out of our control, including HIV, Ebola, avian influenza and many others[4,7,9,18,20,23-25]. Fast evolution of these viruses and the presence of an enormous reservoir of unknown viruses in the animal world made us realize that the path to reach the point where no viral infection will be a threat for us, is just an illusion and the only thing we can do is to be prepared and race with mother nature.

Currently, several research centers are continuously analyzing material derived from patients suffering from atypical illnesses to search for new human pathogens[1,12,22,30,32-34]. These investigations are limited by several factors, including an incomplete map of the existing virus families, low virus titers, or the lack of proper virus detection techniques. There is not one commonly accepted method for identification of novel viruses. The use of random amplification methods, differential display primers or DNA chip screening all have their limitations and most of the novel viruses will be detected only if they can replicate *in vitro* and produce relatively pure material for subsequent analysis.

To overcome at least some of these problems, we developed a novel virus discovery method based on the common presence of restriction enzyme recognition sites in virtually every genome. The method is based on a previously known technique used for determination of gene expression levels called cDNA amplification fragment length polymorphism (cDNA-AFLP)[3] and we therefore named the new method VIDISCA (Virus discovery based on cDNA-AFLP)[26,30].

Respiratory tract infections are the leading cause for hospitalization of infants and young children[27]. The most important viral agents in this patient group are respiratory syncytial virus (RSV) and the picornaviruses[13]. Other agents that cause various respiratory diseases are the influenza and parainfluenza viruses, adenoviruses, coronaviruses, and human metapneumovirus [2,11,14,16,17].

Identification of a novel pathogen is just the beginning of a new story with many unknowns. How does the virus replicate? How does it interact with the host? Where does it come from? How is it related to known viruses? What is the causative role in disease? And ultimately: How can we stop it. The answer to all these questions implies years of careful studies.

Using VIDISCA we discovered a human pathogen – human coronavirus NL63 - that has been circulating in the human population for centuries[30]. We also identified three novel human picornaviruses, illustrating the broad applicability and power of VIDISCA.

Thesis outline

The 30% gap in the diagnostics of human respiratory illnesses needs to be closed. This thesis describes an effort to identify novel respiratory viral pathogens. The novel VIDISCA method was developed to achieve this goal (Chapter II). HCoV-NL63 was identified in 2004 in a cell culture amplified sample derived from a 7-month old child suffering from respiratory illness. Chapter III describes the HCoV-NL63 genome characteristics, e.g. the transcription products generated during virus replication. Chapter IV describes an *in silico* analysis of the HCoV-NL63 genome and encoded proteins using bioinformatics tools, pinpointing several unique features of this pathogen.

Two genetically distinct HCoV-NL63 clusters seem to co-exist. Chapter V analyzes this phenomenon in more detail. It was recognized that these two lineages have recombined. We also analyzed the divergence between HCoV-NL63 and its closest relative HCoV-229E. A molecular clock algorithm revealed that these two viruses may have diverged about 1000 years ago.

Chapter VI describes the identification of angiotensin converting enzyme 2 (ACE2) as receptor for HCoV-NL63 entry into the cell. HCoV-NL63 therefore shares the receptor with SARS-CoV and can possibly be used as a model system to study SARS-CoV pathogenicity. It has been suggested that the development of acute respiratory distress syndrome and severe lung damage in SARS-CoV infected patients is related to downregulation of the ACE2 protein on epithelial cells[15,21]. The influence of HCoV-NL63 infection on ACE2 expression levels was evaluated in chapter VII, indicating a very similar effect. In search for other factors that may explain the difference in pathogenicity between SARS-CoV and HCoV-NL63, we investigated the innate immune response during HCoV-NL63 infection in chapter VIII. HCoV-NL63 infection elevates the level of interleukin 6 and interleukin 8, similar to what has been described for SARS-CoV.

In chapter X, the current status of anti-coronaviral agents is reviewed, and chapter IX describes a detailed study of candidate inhibitors that target different stages of HCoV-NL63 infection. This study led to the identification of six reasonably potent inhibitors, some of which are already approved drugs that - with low risk - can be tested in clinical trials.

As the main subject of my PhD study was the development of the VIDISCA method and the identification of new human pathogens, the existing methods for virus discovery are summarized in chapter XI. In chapter XII, the discovery of three novel viruses that belong to the *Picornaviridae* family is described, confirming the potency of the VIDISCA method.

The main achievements and discoveries of my PhD research project, future directions, and a detailed study of the literature on human coronaviruses are presented in the epilogue chapter XIII.
Appendix A contains the complete and detailed protocol for the VIDISCA method.

References

1. Allander, T., S. U. Emerson, R. E. Engle, R. H. Purcell, and J. Bukh. 2001. A virus discovery method incorporating DNase treatment and its application to the identification of two bovine parvovirus species. Proc Natl Acad Sci U S A 98:11609-11614.
2. Arden, K. E., P. McErlean, M. D. Nissen, T. P. Sloots, and I. M. Mackay. 2006. Frequent detection of human rhinoviruses, paramyxoviruses, coronaviruses, and bocavirus during acute respiratory tract infections. J. Med. Virol. 78:1232-1240.
3. Bachem, C. W., R. S. van der Hoeven, S. M. de Bruijn, D. Vreugdenhil, M. Zabeau, and R. G. Visser. 1996. Visualization of differential gene expression using a novel method of RNA fingerprinting based on AFLP: analysis of gene expression during potato tuber development. Plant J 9:745-753.
4. Barre-Sinoussi, F., J. C. Chermann, F. Rey, M. T. Nugeyre, S. Chamaret, J. Gruest, C. Dauguet, C. Axler-Blin, F. Vezinet-Brun, C. Rouzioux, W. Rozenbaum, and L. Montagnier. 1983. Isolation of a T-lymphotropic retrovirus from a patient at risk for acquired immune deficiency syndrome (AIDS). Science 220:868-871.
5. Bastien, N., K. Anderson, L. Hart, P. Van Caeseele, K. Brandt, D. Milley, T. Hatchette, E. C. Weiss, and Y. Li. 2005. Human coronavirus NL63 infection in Canada. J. Infect. Dis. 191:503-506.
6. Bastien, N., J. L. Robinson, A. Tse, B. E. Lee, L. Hart, and Y. Li. 2005. Human coronavirus NL-63 infections in children: a 1-year study. J. Clin. Microbiol. 43:4567-4573.
7. Bowen, E. T., G. Lloyd, W. J. Harris, G. S. Platt, A. Baskerville, and E. E. Vella. 1977. Viral haemorrhagic fever in southern Sudan and northern Zaire. Preliminary studies on the aetiological agent. Lancet 1:571-573.
8. Choi, E. H., H. J. Lee, S. J. Kim, B. W. Eun, N. H. Kim, J. A. Lee, J. H. Lee, E. K. Song, S. H. Kim, J. Y. Park, and J. Y. Sung. 2006. The association of newly identified respiratory viruses with lower respiratory tract infections in Korean children, 2000-2005. Clin. Infect. Dis. 43:585-592.
9. Drosten, C., S. Gunther, W. Preiser, S. van der Werf, H. R. Brodt, S. Becker, H. Rabenau, M. Panning, L. Kolesnikova, R. A. Fouchier, A. Berger, A. M. Burguiere, J. Cinatl, M. Eickmann, N. Escriou, K. Grywna, S. Kramme, J. C. Manuguerra, S. Muller, V. Rickerts, M. Sturmer, S. Vieth, H. D. Klenk, A. D. Osterhaus, H. Schmitz, and H. W. Doerr. 2003. Identification of a novel coronavirus in patients with severe acute respiratory syndrome. N. Engl. J. Med. 348:1967-1976.
10. Ebihara, T., R. Endo, X. Ma, N. Ishiguro, and H. Kikuta. 2005. Detection of human coronavirus NL63 in young children with bronchiolitis. J. Med. Virol. 75:463-465.
11. Forster, J., G. Ihorst, C. H. Rieger, V. Stephan, H. D. Frank, H. Gurth, R. Berner, A. Rohwedder, H. Werchau, M. Schumacher, T. Tsai, and G. Petersen. 2004. Prospective population-based study of viral lower respiratory tract infections in children under 3 years of age (the PRI.DE study). Eur. J. Pediatr. 163:709-716.
12. Fouchier, R. A., N. G. Hartwig, T. M. Bestebroer, B. Niemeyer, J. C. de Jong, J. H. Simon, and A. D. Osterhaus. 2004. A previously undescribed coronavirus associated with respiratory disease in humans. Proc. Natl. Acad. Sci. U. S. A 101:6212-6216.
13. Freymuth, F., A. Vabret, D. Cuvillon-Nimal, S. Simon, J. Dina, L. Legrand, S. Gouarin, J. Petitjean, P. Eckart, and J. Brouard. 2006. Comparison of multiplex PCR assays and conventional techniques for the diagnostic of respiratory virus infections in children admitted to hospital with an acute respiratory illness. J. Med. Virol. 78:1498-1504.
14. Garbino, J., S. Crespo, J. D. Aubert, T. Rochat, B. Ninet, C. Deffernez, W. Wunderli, J. C. Pache, P. M. Soccal, and L. Kaiser. 2006. A prospective hospital-based study of the clinical impact of non-severe acute respiratory syndrome (Non-SARS)-related human coronavirus infection. Clin. Infect. Dis. 43:1009-1015.

15. Imai, Y., K. Kuba, S. Rao, Y. Huan, F. Guo, B. Guan, P. Yang, R. Sarao, T. Wada, H. Leong-Poi, M. A. Crackower, A. Fukamizu, C. C. Hui, L. Hein, S. Uhlig, A. S. Slutsky, C. Jiang, and J. M. Penninger. 2005. Angiotensin-converting enzyme 2 protects from severe acute lung failure. Nature 436:112-116.
16. Iwane, M. K., K. M. Edwards, P. G. Szilagyi, F. J. Walker, M. R. Griffin, G. A. Weinberg, C. Coulen, K. A. Poehling, L. P. Shone, S. Balter, C. B. Hall, D. D. Erdman, K. Wooten, and B. Schwartz. 2004. Population-based surveillance for hospitalizations associated with respiratory syncytial virus, influenza virus, and parainfluenza viruses among young children. Pediatrics 113:1758-1764.
17. Jartti, T., P. Lehtinen, T. Vuorinen, R. Osterback, H. B. van den, A. D. Osterhaus, and O. Ruuskanen. 2004. Respiratory picornaviruses and respiratory syncytial virus as causative agents of acute expiratory wheezing in children. Emerg. Infect. Dis. 10:1095-1101.
18. Johnson, K. M., J. V. Lange, P. A. Webb, and F. A. Murphy. 1977. Isolation and partial characterisation of a new virus causing acute haemorrhagic fever in Zaire. Lancet 1:569-571.
19. Kaiser, L., N. Regamey, H. Roiha, C. Deffernez, and U. Frey. 2005. Human coronavirus NL63 associated with lower respiratory tract symptoms in early life. Pediatr. Infect. Dis. J. 24:1015-1017.
20. Ksiazek, T. G., D. Erdman, C. S. Goldsmith, S. R. Zaki, T. Peret, S. Emery, S. Tong, C. Urbani, J. A. Comer, W. Lim, P. E. Rollin, S. F. Dowell, A. E. Ling, C. D. Humphrey, W. J. Shieh, J. Guarner, C. D. Paddock, P. Rota, B. Fields, J. DeRisi, J. Y. Yang, N. Cox, J. M. Hughes, J. W. LeDuc, W. J. Bellini, and L. J. Anderson. 2003. A novel coronavirus associated with severe acute respiratory syndrome. N. Engl. J. Med. 348:1953-1966.
21. Kuba, K., Y. Imai, S. Rao, H. Gao, F. Guo, B. Guan, Y. Huan, P. Yang, Y. Zhang, W. Deng, L. Bao, B. Zhang, G. Liu, Z. Wang, M. Chappell, Y. Liu, D. Zheng, A. Leibbrandt, T. Wada, A. S. Slutsky, D. Liu, C. Qin, C. Jiang, and J. M. Penninger. 2005. A crucial role of angiotensin converting enzyme 2 (ACE2) in SARS coronavirus-induced lung injury. Nat. Med. 11:875-879.
22. Lu, Y., S. Y. Wang, and J. M. Lotz. 2004. The use of differential display to isolate viral genomic sequence for rapid development of PCR-based detection methods. A test case using Taura syndrome virus. J Virol Methods 121:107-114.
23. Martini, G. A. 1973. Marburg virus disease. Postgrad. Med. J. 49:542-546.
24. Pattyn, S., G. G. van der, G. Courteille, W. Jacob, and P. Piot. 1977. Isolation of Marburg-like virus from a case of haemorrhagic fever in Zaire. Lancet 1:573-574.
25. Peiris, J. S., S. T. Lai, L. L. Poon, Y. Guan, L. Y. Yam, W. Lim, J. Nicholls, W. K. Yee, W. W. Yan, M. T. Cheung, V. C. Cheng, K. H. Chan, D. N. Tsang, R. W. Yung, T. K. Ng, and K. Y. Yuen. 2003. Coronavirus as a possible cause of severe acute respiratory syndrome. Lancet 361:1319-1325.
26. Pyrc, K., MF. Jebbink, B. Berkhout, and L. van der Hoek. 2006. VIDISCA: unraveling the unknown In D. Cavanagh (ed.), SARS and other coronaviruses: strategies and protocols. Humana Press.
27. Shay, D. K., R. C. Holman, R. D. Newman, L. L. Liu, J. W. Stout, and L. J. Anderson. 1999. Bronchiolitis-associated hospitalizations among US children, 1980-1996. JAMA 282:1440-1446.
28. Suzuki, A., M. Okamoto, A. Ohmi, O. Watanabe, S. Miyabayashi, and H. Nishimura. 2005. Detection of human coronavirus-NL63 in children in Japan. Pediatr. Infect. Dis. J. 24:645-646.
29. Vabret, A., T. Mourez, J. Dina, L. van der Hoek, S. Gouarin, J. Petitjean, J. Brouard, and F. Freymuth. 2005. Human coronavirus NL63, France. Emerg. Infect. Dis. 11:1225-1229.
30. van der Hoek, L., K. Pyrc, M. F. Jebbink, W. Vermeulen-Oost, R. J. Berkhout, K. C. Wolthers, P. M. Wertheim-van Dillen, J. Kaandorp, J. Spaargaren, and B. Berkhout. 2004. Identification of a new human coronavirus. Nat. Med. 10:368-373.
31. van der Hoek, L., K. Sure, G. Ihorst, A. Stang, K. Pyrc, M. F. Jebbink, G. Petersen, J. Forster, B. Berkhout, and K. Uberla. 2005. Croup is associated with the novel coronavirus NL63. PLoS. Med. 2:e240.
32. Wang, D., L. Coscoy, M. Zylberberg, P. C. Avila, H. A. Boushey, D. Ganem, and J. L. DeRisi. 2002. Microarray-based detection and genotyping of viral pathogens. Proc Natl Acad Sci U S A 99:15687-15692.
33. Wang, D., A. Urisman, Y. T. Liu, M. Springer, T. G. Ksiazek, D. D. Erdman, E. R. Mardis, M. Hickenbotham, V. Magrini, J. Eldred, J. P. Latreille, R. K. Wilson, D. Ganem, and J. L. DeRisi. 2003. Viral discovery and sequence recovery using DNA microarrays. PLoS. Biol. 1:E2.

34. Woo, P. C., S. K. Lau, C. M. Chu, K. H. Chan, H. W. Tsoi, Y. Huang, B. H. Wong, R. W. Poon, J. J. Cai, W. K. Luk, L. L. Poon, S. S. Wong, Y. Guan, J. S. Peiris, and K. Y. Yuen. 2005. Characterization and complete genome sequence of a novel coronavirus, coronavirus HKU1, from patients with pneumonia. J. Virol. 79:884-895.

Chapter II

Identification of a new human coronavirus

Adapted from: Nature Medicine, April 2004, vol. 10, p. 368 - 373.

Lia van der Hoek[1], Krzysztof Pyrc[1], Maarten F. Jebbink[1], Wilma Vermeulen-Oost[2], Ron J.M. Berkhout[2], Katja C. Wolthers[1], Pauline M.E. Wertheim-van Dillen[3], Jos Kaandorp[4], Joke Spaargaren[2] and Ben Berkhout[1]

[1]Laboratory of Experimental Virology, Department of Medical Microbiology, Center for Infection and Immunity Amsterdam (CINIMA), Academic Medical Center, University of Amsterdam, Meibergdreef 15, 1105 AZ, Amsterdam, The Netherlands. [2] Public Health Laboratory, Municipal Health Service, Nieuwe Achtergracht 100, 1018 WT, Amsterdam, The Netherlands. [3] Department of Medical Microbiology/Clinical Virology, Academic Medical Center, University of Amsterdam, Meibergdreef 15, 1105 AZ, Amsterdam, The Netherlands. [4] Pediatric Department, Slotervaart Hospital, Louwesweg 6, 1066 EC Amsterdam, The Netherlands.

Three human coronaviruses are known to exist: human coronavirus 229E (HCoV-229E), HCoV-OC43 and severe acute respiratory syndrome (SARS)-associated coronavirus (SARS-CoV). Here we report the identification of a fourth human coronavirus, HCoV-NL63, using a new method of virus discovery. The virus was isolated from a 7-month-old child suffering from bronchiolitis and conjunctivitis. The complete genome sequence indicates that this virus is not a recombinant, but rather a new group 1 coronavirus. The *in vitro* host cell range of HCoV-NL63 is notable because it replicates on tertiary monkey kidney cells and the monkey kidney LLC-MK2 cell line. The viral genome contains distinctive features, including a unique N-terminal fragment within the spike protein. Screening of clinical specimens from individuals suffering from respiratory illness identified seven additional HCoV-NL63-infected individuals, indicating that the virus was widely spread within the human population.

Introduction

To date, there is still a variety of human diseases with unknown etiology. A viral origin has been suggested for many of these diseases, emphasizing the importance of a continuous search for new viruses[18,36,39]. Major difficulties are encountered, however, when searching for new viruses. First, some viruses do not replicate *in vitro*, at least not in the cells that are commonly used in viral diagnostics. Second, for those viruses that do replicate *in vitro* and cause a cytopathic effect (CPE), the subsequent virus identification methods may fail. Antibodies raised against known viruses may not recognize the cultured virus, and virus-specific PCR methods may not amplify the new viral genome. To solve both problems, we developed a new method for virus discovery based on the cDNA-amplified restriction fragment−length polymorphism technique (cDNA-AFLP)[2]. Here we report the identification of a new coronavirus using this method of Virus-Discovery-cDNA-AFLP (VIDISCA).

Coronaviruses, a genus of the *Coronaviridae* family, are enveloped viruses with a large plus-strand RNA genome. The genomic RNA is 27−32 kb in size, capped and polyadenylated. Three serologically distinct groups of coronaviruses have been described. Within each group, viruses are characterized by their host range and genome sequence. Coronaviruses have been identified in mice, rats, chickens, turkeys, swine, dogs, cats, rabbits, horses, cattle and humans, and can cause a variety of severe diseases including gastroenteritis and respiratory tract diseases[13,17]. Three human coronaviruses have been studied in detail. HCoV-229E and HCoV-OC43 were identified in the mid-1960s, and are known to cause the common cold[1,6,15,16,22,28,29,40,42]. The recently identified SARS-CoV causes a life-threatening pneumonia, and is the most pathogenic human coronavirus identified thus far[8,23,32]. SARS-CoV is likely to reside in an animal reservoir, and has recently initiated the epidemic in humans through zoonotic transmission[12,26]. It has been suggested that SARS-CoV is the first member of a fourth group of coronaviruses, or that it is an outlier of group 2[25,37].

The new coronavirus that we present here was isolated from a child suffering from bronchiolitis and conjunctivitis. This was not an isolated case, as we identified the virus in clinical specimens from seven additional individuals, both infants and adults, during the last winter season. We also resolved the complete sequence of the viral genome, which revealed several unique features.

Methods

Virus isolation

The child, who was living in Amsterdam, was admitted to the hospital (Slotervaart Hospital, Amsterdam) with complaints of coryza and conjunctivitis since 3 days. At admission she had shortness of breath and refused to drink. The patient's temperature was 39°C, the respiratory rate was 50 breaths/min with oxygen saturation of 96% and her pulse was 177 beats/min. Upon auscultation bilateral prolonged expirium and end-expiratory wheezing was found. A chest radiograph showed the typical features of bronchiolitis. The child was treated with salbutamol and ipratropium at the first day, followed by the use of salbutamol only for 5 days. The child was seen daily at the out patient clinic and the symptoms gradually decreased. A nasopharyngeal aspirate was collected 5 days after the onset of symptoms. The specimen was tested for the presence of RSV, adenovirus, influenza A and B virus, and parainfluenza virus type 1, 2 and 3 using the Virus Respiratory Kit (Bartels: Trinity Biotech plc, Wicklow Ireland). In addition, PCR tests for rhinoviruses, enterovirus, meta-pneumovirus and HCoV-OC43 and HCoV-229E were performed[10,43]. The original nasopharyngeal aspirate was inoculated onto a variety of cells. The cultures were kept in a rollerdrum at 34°C and inspected by eye every 3 to 4 days. Maintenance medium was replenished every 3 to 4 days. Two different types of medium were used: Optimem 1 (Invitrogen, Breda, The Netherlands) without bovine fetal serum was used for the tMK cells, and MEM Hanks' /Earle's medium (Invitrogen, Breda, The Netherlands) with 3% bovine fetal serum for the remaining cell types. Cell cultures that were infected with the aspirate specimen were stained for the presence of respiratory viruses after one week of incubation. Direct staining was performed with pools of fluorescent-labeled mouse antibodies against RSV and influenza A and B virus (Imagen, DakoCytomation Ltd, Cambridge, UK). Indirect staining was performed for adenoviruses and parainfluenza virus type 1, 2 or 3 with mouse antibodies (Chemicon International, Temecula, California) and subsequent staining with FITC-labeled rabbit anti-mouse antibodies (Imagen, DakoCytomation Ltd, Cambridge, UK). A sixth passage of the virus was used for VIDISCA and full genome sequencing.

VIDISCA method

The virus was cultured on LLC-MK2 cells. To remove residual cells and mitochondria, 110µl of virus culture supernatant was spun for 10min at maximum speed (13,500r.p.m.) in an Eppendorf microcentrifuge. To remove chromosomal

DNA and mitochondrial DNA from the lysed cells, 100µl of supernatant was transferred to a fresh tube and treated with DNase I for 45min at 37°C (Ambion). Nucleic acids were extracted as described[5]. A reverse transcription reaction was performed with random hexamer primers (Amersham Bioscience) and Moloney murine leukemia virus reverse transcriptase (MMLV-RT; Invitrogen). Second-strand DNA synthesis was carried out with Sequenase II (Amersham Bioscience), without further addition of a primer. A phenol-chloroform extraction was followed by ethanol precipitation.

cDNA-AFLP was performed essentially as described[2], with some modifications. The double-stranded DNA was digested with the HinP1I and MseI restriction enzymes (New England Biolabs). MseI and HinP1I anchors (see below) were subsequently added, along with 5U ligase enzyme (Invitrogen) in the supplied ligase buffer, for 2h at 37°C. The MseI and HinP1I anchors were prepared by mixing a top-strand oligonucleotide (5'-CTCGTAGACTGCGTACC-3' for the MseI anchor and 5'-GACGATGAGTCCTGAC-3' for the HinP1I anchor) with a bottom-strand oligonucleotide (5'-TAGGTACGCAGTC-3' for the MseI anchor and 5'-CGGTCAGGACTCAT-3' for the HinP1I anchor) in a 1:40 dilution of ligase buffer. Twenty cycles of PCR were carried out with 10µl of the ligation mixture, 100ng of HinP1I standard primer (5'-GACGATGAGTCCTGACCGC-3') and 100ng of MseI standard primer (5'-CTCGTAGACTGCGTACCTAA-3'). Five microliters of this PCR product was used as input in the second 'selective' amplification step, along with 100ng HinP1I N-primer and 100ng MseI N-primer (the 'N' indicates that the standard primers were extended with one nucleotide; G, A, T or C). The selective rounds of amplification were done using 'touchdown PCR': 10 cycles of 94°C for 60s, 65°C for 30s, and 72°C for 1min (annealing temperature reduced by 1°C per cycle); 23 cycles of 94°C for 30s, 56°C for 30s, and 72°C for 1min; and finally 1 cycle of 72°C for 10min. Sixteen PCR reactions, each with 1 of the 16 primer combinations, were conducted for each sample in this selective PCR. The PCR products were analyzed on 4% Metaphor agarose gels (Cambrex), and the fragments of interest were cloned and sequenced using BigDye terminator reagents. Electrophoresis and data collection were performed using an ABI 377 instrument. DNA molecular weight markers were from Invitrogen and Eurogentec.

To detect HIV-1, we used VIDISCA with EcoRI digestion instead of HinP1I digestion. VIDISCA was modified for parvovirus B19 detection as follows: the reverse transcription step was excluded; only HinP1I digestion and adaptor ligation were performed; the first PCR reaction was performed with 35 cycles instead of 20; and the first PCR fragments were visualized by agarose gel electrophoresis.

cDNA library construction and full genome sequencing

The cDNA library was generated as described by Marra *et al*[25] with minor modifications. Random hexamer primers instead of the oligo-dT primer were used for reverse transcription, and the amplified cDNA was cloned into the PCR2.1-TOPO TA cloning vector. Colonies were picked and suspended in Brain Heart Infusion medium. The E. coli suspension was used as input in PCR amplification with T7 and M13 RP primers. The PCR products were subsequently sequenced with the same primers and the BigDye terminator reagent. Electrophoresis and data collection was performed on an ABI 377 instrument. Sequences were assembled using the AutoAssembler DNA sequence Assembly software version 2.0 (Applied Biosystems, Nieuwerkerk aan de IJssel, The Netherlands).

Diagnostic RT-PCR

A total of 614 respiratory samples were collected from 493 individuals between December 2002 and August 2003 at the Academic Medical Center in Amsterdam. The specimens included oral and nasopharyngeal aspirates, throat swabs, bronchoalveolar lavage and sputum. The samples had been collected for routine viral diagnostic screening of people suffering from upper and/or lower respiratory tract diseases, and the patients consented that their samples be used for testing of respiratory viruses that included coronaviruses. We used 100µl of each sample in a Boom extraction[5]. The diagnostic assay was designed based on the sequence of the 1b gene. The reverse transcription was performed with MMLV-RT (Invitrogen), using 10ng of reverse transcription primer (repSZ-RT, 5′-CCACTATAAC-3′; coordinate 16232 in HCoV-NL63). The entire reverse transcription mixture was added to the first PCR mixture containing 100ng of primer repSZ-1 (5′-GTGATGCATATGCTAATTTG-3′; coordinate 15973) and 100ng of primer repSZ-3 (5′-CTCTTGCAGGTATAATCCTA-3′; coordinate 16210). The PCR reaction consisted of the following steps: 95°C for 5min; then 35 cycles of 95°C for 1min, 55°C for 1min, and 72°C for 2min; then 72°C for 10min.

A nested PCR was started using 5µl of the first PCR product with 100ng of primer repSZ-2 (5′-TTGGTAAACAAAAGATAACT-3′; coordinate 16012) and 100ng of primer repSZ-4 (5′-TCAATGCTATAAACAGTCAT-3′; coordinate 16181). Twenty-five PCR cycles were performed using the same profile as the first PCR. Ten microliters of each PCR product was analyzed by agarose gel electrophoresis. All positive samples were repeated and sequenced to confirm the presence of HCoV-NL63. To verify negative and positive PCR results, an additional diagnostic RT-PCR assay was conducted using the 1a gene primers 5′-AATATGTCTAACAAATAAAACGATT-3′ (reverse transcriptase primer P4H10-3; coordinate 6667), 5′-CTTTTGATAACGGTCACTATG-3′ (SS 5852-5P; coordinate 5777) and 5′-CTCATTACATAAAACATCAAACGG-3′ (P4G1M-5-3P; coordinate 6616) in the first PCR; and 5′-GGTCACTATGTAGTTTATGATG-3′ (P3E2-5P; coordinate 5788) and 5′-GGATTTTTCATAACCACTTAC-3′ (SS 6375-3P; coordinate 6313) in the nested PCR.

Sequence analysis

Sequences were compared to all sequences in the GenBank database using the BLAST tool of the NCBI webpage: http://www.ncbi.nlm.nih.gov/blast. For phylogenetic analysis the sequences were aligned using the ClustalX software package with the following settings: Gap opening penalties:10.00; Gap extension penalty 0.20; Delay divergent sequences switch at 30% and transition weight 0.5[41]. Phylogenetic analysis was carried out using the neighbourjoining method of the MEGA program. The nucleotide distance matrix was generated either by Kimura's 2 parameter estimation or by the *p*-distance estimation[19]. Bootstrap resampling (500 replicates) was employed to place approximate confidence limits on individual branches.

The Genbank accession number of the sequences used in this phylogenetic analysis are: MHV (mouse hepatitis virus, strain MHV-A59): NC_001846; HCoV-229E: NC_002645; HCoV-OC43 strain ATCC VR-759: NC_005147; PEDV (porcine epidemic diarrhea virus, strain CV777): AF353511; TGEV (transmissible gastroenteritis virus, strain Purdue): NC_002306; SARS-CoV isolate Tor2: NC_004718; IBV (avian infectious bronchitis virus, strain Beaudette): NC_001451; BCoV (bovine coronavirus, isolate BCoV-ENT): NC_003045; FCoV (feline enteric coronavirus, strain 79-1683): X80799; CCoV (canine coronavirus strain BGF10 and v2): AY342160 and AY390344; PRCoV (porcine respiratory coronavirus, strain HOL87, IA1894 and 86/137004): M94097, U26212 and X60056; FIPV (feline infectious peritonitis virus, strain KU-2, 79-1146 and Black): D32044, AF033000 and AB086903; EqCoV (equine coronavirus): AY316300; TCoV (turkey coronavirus strain NC99): AY342357.

GenBank accession numbers

The HCoV-NL63 sequences were deposited in GenBank under accession numbers AY567487−AY567494.

Results

Virus isolation from a child with acute respiratory disease

In January 2003, a 7-month-old child was admitted to the hospital with coryza, conjunctivitis and fever. Chest radiography revealed typical features of bronchiolitis. A nasopharyngeal aspirate specimen was collected 5d after the onset of disease (sample NL63). Diagnostic tests for respiratory syncytial virus, adenovirus, influenza viruses A and B, parainfluenza virus types 1, 2 and 3, rhinovirus, enterovirus, HCoV-229E and HCoV-OC43 yielded negative results. The clinical sample was subsequently inoculated onto human fetal lung fibroblasts, tertiary monkey kidney cells (Cynomolgus monkey) and HeLa cells. CPE was detected exclusively on tertiary monkey kidney cells, and was first noted 8 d after inoculation. The CPE was diffuse, with a refractive appearance in the affected cells followed by cell detachment. More pronounced CPE was

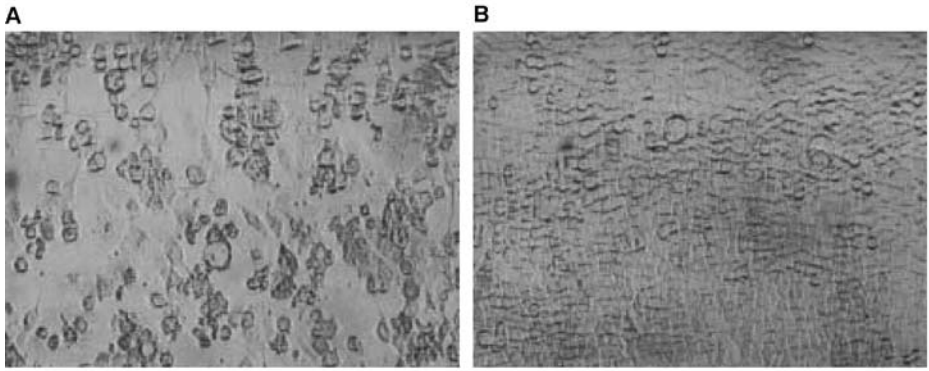


Figure 1. LLC-MK2 cells infected with HCoV-NL63. (a) The CPE of HCoVNL63 in LLC-MK2 cells. (b) Non-infected LLC-MK2 cells.

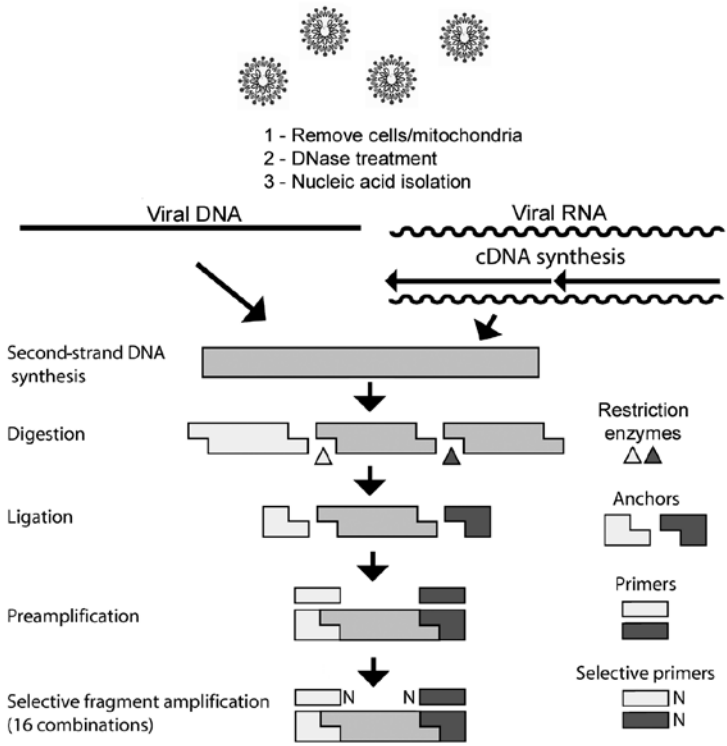


Figure 2. The VIDISCA method. Schematic overview of steps in VIDISCA method.

observed upon passage onto the monkey kidney cell line LLC-MK2, with overall cell rounding and moderate cell enlargement (Fig. 1). Additional subcultures on human fetal lung fibroblasts, rhabdomyosarcoma cells and Vero cells remained negative for CPE. Immunofluorescence assays to detect respiratory syncytial virus, adenovirus, influenza viruses A and B, and parainfluenza virus types 1, 2 and 3 remained negative. Acid lability and chloroform sensitivity tests indicated that the virus was most likely enveloped, and did not belong to the picornavirus group[14].

Virus discovery by the VIDISCA method

Identification of unknown pathogens using molecular biology tools is difficult because the target sequence is not known, so genome-specific PCR primers cannot be designed. To overcome this problem, we developed the VIDISCA method based on the cDNA-AFLP technique[2]. The advantage of VIDISCA is that prior knowledge of the sequence is not required, as the presence of restriction enzyme sites is sufficient to guarantee PCR amplification. The input sample can be either blood plasma or serum, or culture supernatant. Whereas cDNA-AFLP starts with isolated mRNA, VIDISCA begins with a treatment to selectively enrich for viral nucleic acid, including a centrifugation step to remove residual cells and mitochondria (Fig. 2). A DNase treatment is also used to remove interfering chromosomal and mitochondrial DNA from degraded cells (viral nucleic acid is protected within the viral particle). Finally, by choosing frequently cutting restriction enzymes, the method can be fine-tuned such that most viruses will be amplified. We were able to amplify viral nucleic acids in EDTA-treated plasma from a person with hepatitis B viral infection, and from a person with an acute parvovirus B19 infection (Fig. 3). The technique can also detect HIV-1 in cell culture, demonstrating its capacity to identify both RNA and DNA viruses (Fig. 3).

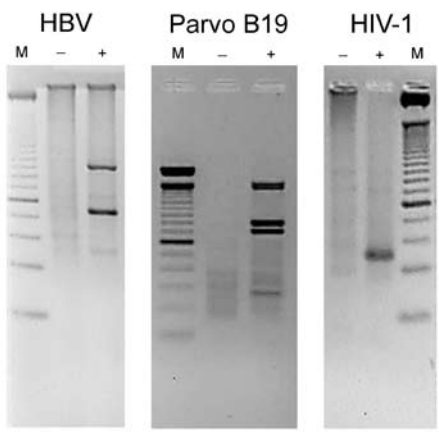


Figure 3. Examples of VIDISCA-mediated virus identification. Specimens were analyzed using ethidium bromide–stained agarose (parvovirus B19) or Metaphor agarose (HBV and HIV-1) gel electrophoresis. Lane M, DNA molecular weight markers; -, negative controls; +, VIDISCA PCR products for HBV (amplified with primers HinP1I-T/MseI-T), parvovirus B19 (HinP1I standard primer only) or HIV-1 (EcoRI-A/MseI-C primers).

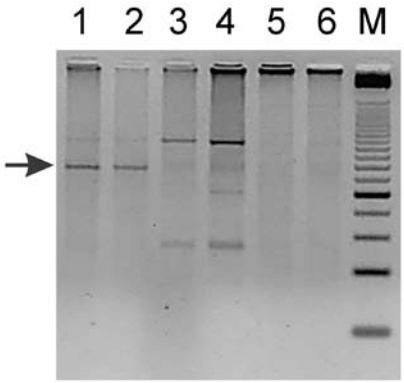


Figure 4. VIDISCA PCR products for HCoV-NL63. HinP1I-G and MseI-A primers were used for selective amplification; products were visualized by Metaphor agarose gel electrophoresis. Lanes 1 and 2, duplicate PCR product of cultured HCoV-NL63 harvested from LLC-MK2 cells; 3 and 4, duplicate control supernatant from uninfected LLC-MK2 cells; 5 and 6, duplicate negative controls containing water; M, 25-bp molecular weight marker. Arrow indicates HCoV-NL63 fragment that was excised from gel and sequenced.

14-6 15073-15279
AACAAAAATTTGAATGAGGGTGTTCTTGAATCTTTTTCTGTTACACTTCTTGATAATCAAGAAGATAAGTTTTGGTGTGAAGAT
TTTTATGCTAGTATGTATGAAAATTCTACAATATTGCAAGCTGCTGGTTTATGTGTTGTTTGTGGTTCACAAACTGTACTTCGT
TGTGGTGATTGTCTGCGTAAGCCTATGTTGTGCACTAAA

10-1 15966-16085
TAATGTCAGTGATGCATATGCTAATTTGGTTCCATATTACCAACTTATTGGTAAACAAAAGATAACTACAATACAGGGTCCTCC
TGGTAGTGGTAAGTCACATTGTTCCATTGGACTTGG

1-2 16110-16237
TGTTTTTGTTGCTTGTGCCCATGCTGCTGTTGATTCCTTATGTGCAAAAGCTATGACTGTTTATAGCATTGATAAGTGTACTAG
GATTATACCTGCAAGAGCTCGGGTTGAGTGTTATAGTGGCTTTA

18-4 18363-18472
TAGTAGTTGTGTTACTCGTTGTAATATAGGTGGTGCTGTTTGTTCAAAACATGCAAATTTGTATCAAAAATATGTTGAGGCATA
TAATACATTTACACAGGCAGGTTTTA

16-6 20403-20685
GAGTGGTAGGTTGTTGTTACGCAATAATGGTCGTTTTGGTGGTTTTAGTAATCATTTAGTCTCAACTAAATGAAACTTTTCTTG
ATTTTGCTTGTTTTGCCCCTGGCCTCTTGCTTTTTCACATGTAATAGTAATGCTAATCTCTCTATGTTACAATTAGGTGTTCCT
GACAATTCTTCAACTATTGTTACGGGTTTATTGCCAACTCATTGGTTTTGTGCTAATCAGAGTACATCTGTTTACTCAGCCAAT
GGTTTCTTTTATATTGATGTTGGTAATCACC

20-1 20699-20762
GCTCCATACTGGTTATTATGATGCTAATCAGTATTATATTTATGTTACTAATGAAATAGGCTTA

23-5 20885-20991
GCCTTTGGGCATAACTATATCTGGTGAAACTGTGCGTCTGCATTTATATAATGTAACTCGTACTTTTTATGTGCCAGCAGCTTA
TAAACTTACTAAACTTAGTGTTA

22-2 21696-21747
GCCACAGATTTTTGGACGGTTGCATTTGCTACTTTTGTTGATGTTTTGGTTA

4-6 22565-22712
TAATGAGTCTAGATATGGCTTGCAAAACTTACTACAGTTACCTAACTTTTATTATGTTAGTAATGGTGGTAACAATTGCACTAC
GGCCGTTATGACTTATTCTAATTTTGGTATTTGTGCTGATGGTTCTTTGATTCCTGTTCGTCCG

11-6 26115-26320
TAATCTAAACTAAACAAAATGGCTAGTGTAAATTGGGCCGATGACAGAGCTGCTAGGAAGAAATTTCCTCCTCCTTCATTTTAC
ATGCCTCTTTTGGTTAGTTCTGATAAGGCACCATATAGGGTCATTCCCAGGAATCTTGTCCCTATTGGTAAGGGTAATAAAGAT
GAGCAGATTGGTTATTGGAATGTTCAAGAGCGTTGGCG

15-1 26327-26400
CAGGGGGCAACGTGTTGATTTGCCTCCTAAAGTTCATTTTTATTACCTAGGTACTGGACCTCATAAGGACCTTA

9-2 27329-27401
ATGATAAGGGTTTAGTCTTACACACAATGGTAGGCCAGTGATAGTAAAGTGTAAGTAATTTGCTATCATATTA

22-3 27471-27526
GCCAACAATGGAAGAGCCAACAACATATCTAAAAATGTTTTGTCTGGTACTTGTTA

Figure 5: VIDISCA fragments of HCoV-NL63. Sequence and coordinates of the 13 VIDISCA fragments of HCoV-NL63

The supernatant of the CPE-positive LLC-MK2 culture NL63 was analyzed by VIDISCA. The supernatant of uninfected cells was used as a negative control. After the second PCR amplification step, unique and prominent DNA fragments were present in the test sample but not in the control (1 of 16 selective PCR reactions is shown in Fig. 4). These fragments were cloned and sequenced. Thirteen of 16 fragments showed sequence similarity to members of the coronavirus family, but significant sequence divergence with known coronaviruses was apparent in all fragments, indicating that we had identified a new coronavirus. The sequences of the 13 VIDISCA fragments are provided in Figure 5.

Detection of HCoV-NL63 in patient specimens

To show that HCoV-NL63 originated from the nasopharyngeal aspirate of the child, we designed a diagnostic RT-PCR that specifically detects HCoV-NL63. This test confirmed the presence of HCoV-NL63 in the clinical sample. The sequence of the RT-PCR product of the 1b gene was identical to that of the virus identified upon *in vitro* passage in LLC-MK2 cells (data not shown).

Having confirmed that the cultured coronavirus originated from the child, the question remained as to whether this was an isolated clinical case, or whether HCoV-NL63 is circulating in humans. To address this question, we used two diagnostic RT-PCR assays to examine respiratory specimens of hospitalized individuals and those visiting the outpatient clinic between December 2002 and August 2003 (Fig. 6). We identified seven additional individuals carrying HCoV-NL63 (Table 1). Sequence analysis of the PCR products indicated the presence of a few characteristic point mutations in several samples, suggesting that several viruses with different molecular markers may be cocirculating (Fig. 7 and Fig. 8).

Table 1. Patients positive for HCoV-NL63.

Patient no.	Age	Symptoms	Specimen	Sample date
72	4 months	URTI	NPA	Dec. 31 2002
251	67 years	Unknown	OPA	Jan. 7 2003
223	52 years	Unknown[b]	OPA	Jan. 8 2003
NL63[a]	7 months	LRTI	NPA	Jan. 10 2003
246	9 months	LRTI	OPA	Jan. 13 2003
248	11 months	URTI	OPA	Jan. 16 2003
466	40 years	LRTI[c]	BAL	Feb. 4 2003
496	7 months	URTI	OPA	Feb. 25 2003

[a] Seven-monyh-old patient from whom HCoV-NL63 was cultured.
[b] Patient received bone marrow transplant.
[c] Patient infected with HIV-1; 20 $CD4^+$ cells per mm^3.
URTI, upper respiratory tract illness; LRTI, lower respiratory tract illness; NPA, nasopharyngeal aspirate; OPA, oropharyngeal aspirate; BAL, bronchoalveolar lavage.

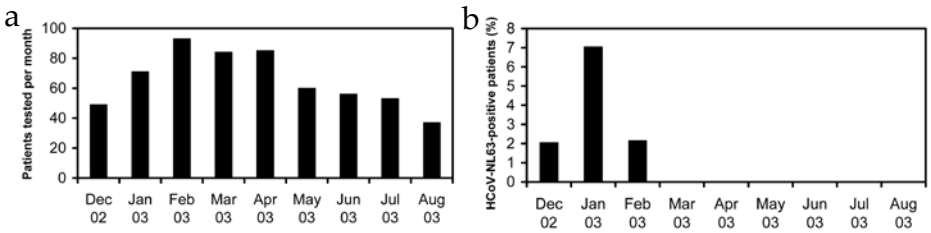


Figure 6. Detection of HCoV-NL63 in winter months of 2002 and 2003. (a) Number of patients tested per month. (b) Percentage of patients positive for HCoV-NL63.

At least five of the HCoV-NL63-positive individuals suffered from respiratory tract illness; the clinical data of two individuals was not available. Including the index case, five of the patients were children less than 1 year old, and three patients were adults. Two adults were likely to be immunosuppressed, as one of them was a bone marrow transplant recipient and the other an HIV-positive patient suffering from AIDS, with very low $CD4^+$ cell counts (Table 1). No clinical data was available for the third adult. One patient was coinfected with respiratory syncytial virus (no. 72), and the HIV-infected patient (no. 466) carried *Pneumocystis carinii*. No other respiratory agent was found in the other patients, suggesting that the respiratory symptoms were caused by HCoV-NL63. All positive samples were collected during the last winter season, with a detection frequency of 7% in January 2003. None of the 306 samples collected in the spring and summer of 2003 contained HCoV-NL63 ($P < 0.01$ by two-tailed t test).

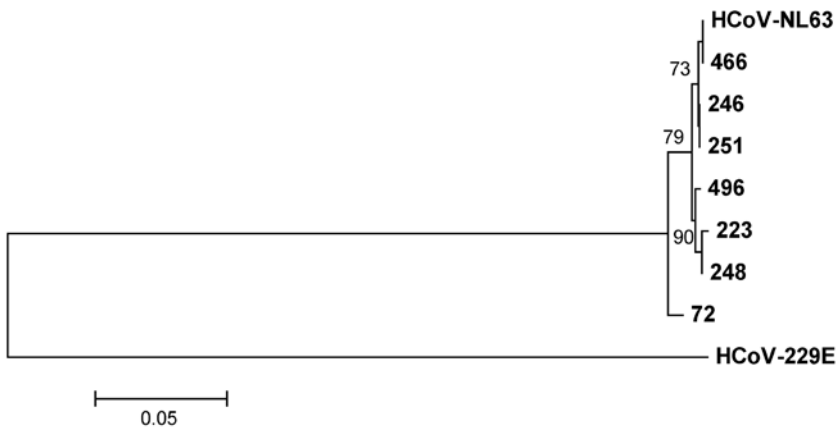


Figure 7. Phylogenetic analysis of RT-PCR sequences of the 1a gene from HCoV-NL63-positive patients. HCoV-229E was used to root the tree.

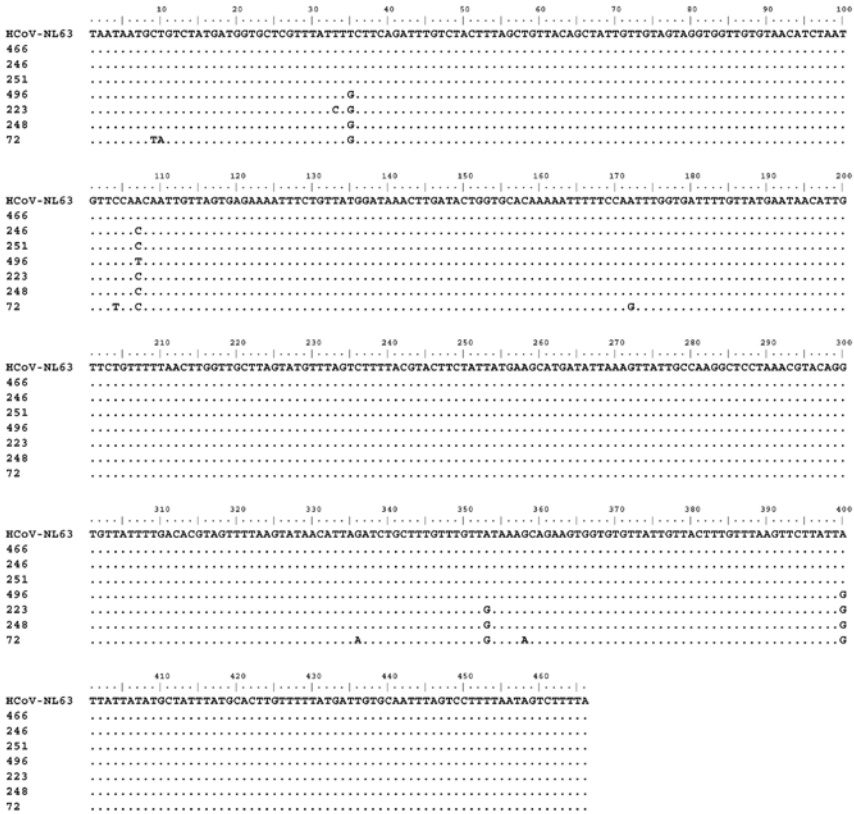


Figure 8. Analysis of the 1a RT-PCR sequences of the HCoV-NL63 positive patients.

Complete genome analysis of HCoV-NL63

The genomes of coronaviruses have a characteristic organization. The 5′ two-thirds contain the 1a and 1b genes that encode the nonstructural polyproteins, followed by the genes encoding four structural proteins: spike (S), envelope (E), membrane (M) and nucleocapsid (N). The genomes of known coronaviruses contain a variable number of unique characteristic open reading frames (ORFs) encoding nonstructural proteins either between the 1b and S genes, between the S and E genes, between the M and N genes, or downstream of the N gene.

To determine whether the HCoV-NL63 genome organization shares these characteristics, we constructed a cDNA library with purified virus stock as input material. A total of 475 genome fragments were analyzed, with an average coverage of seven sequences per nucleotide. Specific PCR reactions were designed to fill in gaps and to sequence regions with low-quality sequence data. We combined this with 5′ and 3′ rapid amplification of cDNA ends to resolve the complete HCoV-NL63 genome sequence.

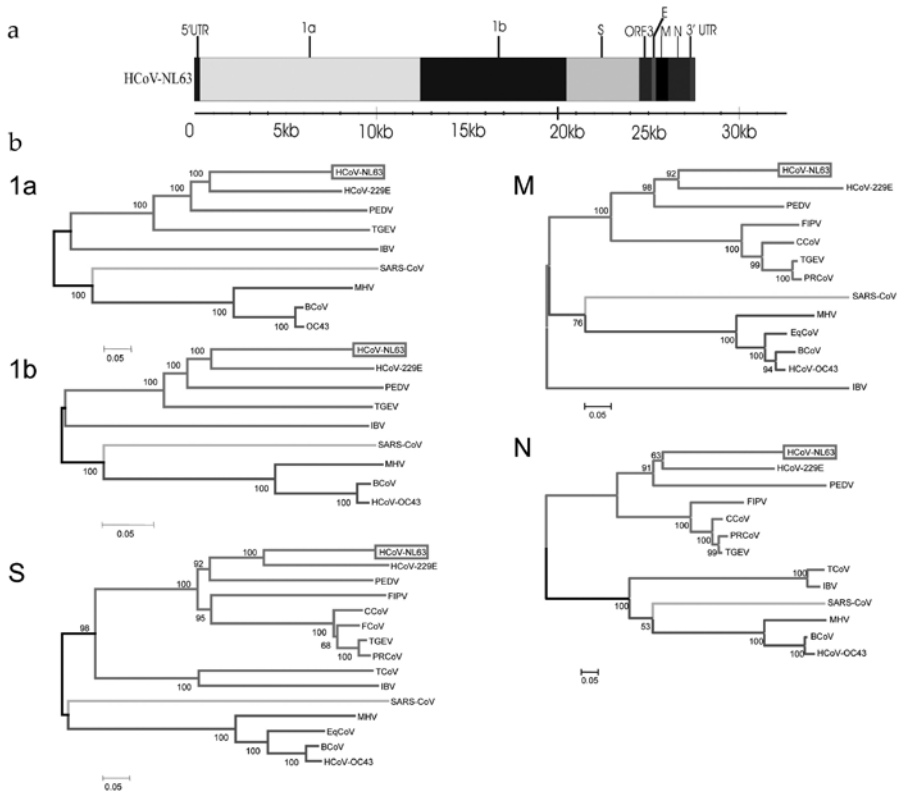


Figure 9. HCoV-NL63 genome organization and phylogenetic analysis. (a) ORFs encoding 1a, 1b, S, ORF3, E, M and N proteins are flanked by 286-nucleotide 5′ UTR and 287-nucleotide 3′ UTR. Coordinates of each ORF are provided in Table 2. (b) Phylogenetic analysis of HCoV-NL63, using nucleotide sequences predicted to encode 1a, 1b, S, M and N proteins. MHV, mouse hepatitis virus; IBV, avian infectious bronchitis virus; BCoV, bovine coronavirus; FCoV, feline enteric coronavirus; CCoV, canine coronavirus; FIPV, feline infectious peritonitis virus; EqCoV, equine coronavirus; TCoV, turkey coronavirus.

The RNA genome of HCoV-NL63 consists of 27,553 nucleotides and a poly-A tail. With a GC content of 34%, HCoV-NL63 has the lowest GC content among the *Coronaviridae*, which range from 37–42%[34]. ZCurve software was used to identify the ORFs[7], and the genome configuration was portrayed using the similarity with known coronaviruses as a guide (Fig. 9a and Table 2). Short untranslated regions (UTRs) of 286 and 287 nucleotides are present at the 5′ and 3′ termini, respectively. The 1a and 1b genes encode the RNA polymerase and proteases that are essential for virus replication. A potential pseudoknot structure is present at position 12,439 (data not shown), which may provide the -1 frameshift signal to translate the 1b polyprotein. Genes predicted to encode the S, E, M and N proteins are found in the 3′ part of the genome. The hemagglutinin-esterase gene, which is present in some group 2 coronaviruses, is not present in HCoV-NL63. ORF3, located between the S and E genes, probably encodes a single accessory

Table 2. Coordinates and sizes of the ORFs of HCoV-NL63

Gene	Start	Stop	Length (bp)	Length (a.a.)	Frame
1a	287	12439	12153	4050	+2
1b	12439	20475	8037	2678	+1
S	20472	24542	4071	1356	+3
ORF 3	24542	25219	678	225	+2
E	25200	25433	234	77	+3
M	25442	26122	681	226	+2
N	26133	27266	1134	377	+3

nonstructural protein; this gene showed only limited similarity to ORF4a and ORF4b of HCoV-229E and ORF3 of porcine epidemic diarrhea virus (PEDV).

The 1a and 1ab polyproteins are translated from the genomic RNA, but the remaining viral proteins are translated from subgenomic mRNAs made by discontinuous transcription during negative strand synthesis[35]. Each subgenomic mRNA has a common 5′ end, derived from the 5′ portion of the genome (the 5′ leader sequence), and common 3′ coterminal parts. Discontinuous transcription requires base-pairing between cis-acting transcription regulatory sequences (TRSs), one located near the 5′ part of the viral genome (the leader TRS) and others located upstream of each of the respective ORFs (the body TRSs)[44]. The cDNA bank that we sequenced contained copies of the subgenomic mRNA for the N protein, thus providing the opportunity to exactly map the leader sequence that is fused to all subgenomic mRNAs. A leader of 72 nucleotides was identified at the 5′ UTR. Eleven of twelve nucleotides of the leader TRS (5′-UCUCAACUAAAC-3′) showed similarity with the body TRS upstream of the N gene. Putative TRSs were also identified upstream of the S, ORF3, E and M genes (Table 3).

We next aligned the sequence of HCoV-NL63 with the complete genomes of other coronaviruses. The percentage nucleotide identity was determined for each gene and is listed in Table 4. All genes except the M gene shared the highest identity with HCoV-229E. To confirm that HCoV-NL63 is a new member of the group 1 coronaviruses, we conducted phylogenetic analysis using the nucleotide sequence of the 1a, 1b, S, M and N genes (Fig. 9b). For each gene analyzed, HCoV-NL63 clustered with the group 1 coronaviruses. The 1a, 1b and S genes of HCoV-NL63 are most closely related to those of HCoV-229E. However, further inspection revealed a subcluster of HCoV-NL63, HCoV-229E and PEDV. Phylogenetic analysis could not be performed for the

Table 3: The leader TRS and putative body TRS of the associated ORF.

	TRS sequence[a]	Position
Leader	CUUCUCAACUAAACGA	60-75
S	AGUCUCAACUAA**AUG**	20460-20474
ORF 3	UGGUUCAACUAAACN$_{37}$**AUG**	24491-24544
E	CUUCUCAACUAUACGAAG**AUG**	25182-25202
M	UGUCUAAACUAAACG**AUG**	25427-25444
N	AAUCUAAACUAAACAAA**AUG**	26116-26135

[a] TRS elements are underlined, startcodons are in bold.

Table 4. Percent nucleotide sequence identity between HCoV-NL63 and other coronaviruses.

	Group 1			Group 2		Group 3	Group 2/4
Gene	HCoV 229E[a]	PEDV	TGEV	BCoV	MHV	IBV	SARS-CoV
1a	63	57	50	40	38	37	38
1b	75	72	69	58	57	59	58
S	56	53	48	35	34	32	32
ORF3	53	49	29	29	25	19	23
E	59	54	49	37	39	25	40
M	64	65	46	47	43	43	42
N	52	38	45	30	29	31	30

[a] GenBank accession numbers for viruses are provided in the Methods section.

ORF3 and E genes because the regions were too variable or too small for analysis, respectively. Bootscan analysis by the Simplot software version 2.5[24] found no signs of recombination (data not shown).

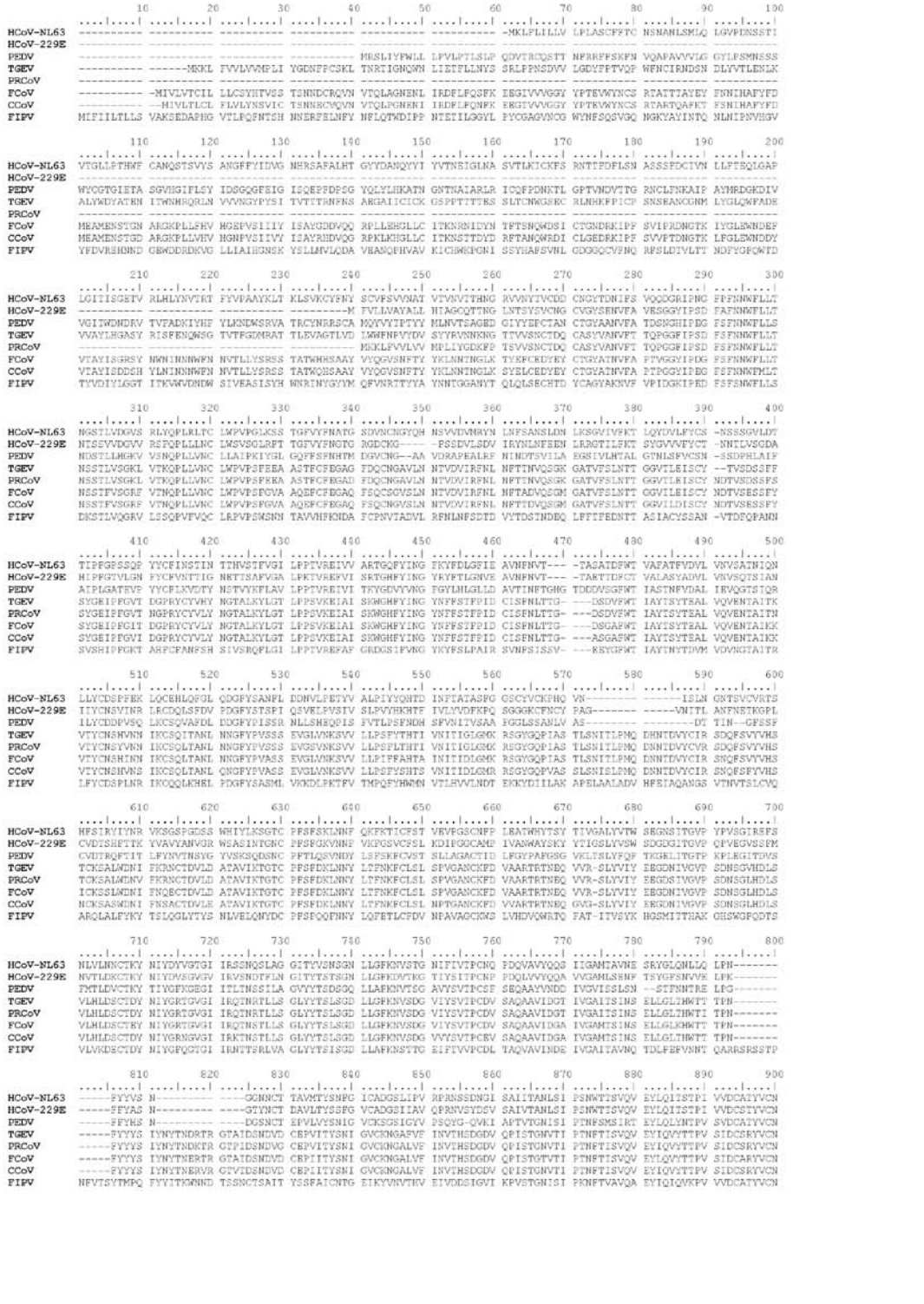
The presence of a single nonstructural gene between the S and E genes is noteworthy because almost all coronaviruses have two or more ORFs in this region, with the exception of PEDV and HCoV-OC43[9,30]. Perhaps most notable is a large insert of 537 nucleotides in the 5′ portion of the S gene of HcoV-NL63, as compared with that of HCoV-229E. A BLAST search found no similarity between this additional 179–amino acid domain of the S protein and any coronavirus or other sequence deposited in GenBank. An alignment of the HCoV-NL63 S protein sequence with those of other group 1 coronaviruses is shown in Figure 10.

Discussion

In this study we present a detailed description of a new human coronavirus. Thus far, only three human coronaviruses have been characterized if we include SARS-CoV; further characterization of HCoV-NL63 as the fourth member will provide important insight into the variation among human coronaviruses. HCoV-NL63 is a member of the group 1 coronaviruses and is most closely related to HCoV-229E, but the differences between them are prominent. First, they share on average only 65% sequence identity. Second, a single gene, ORF3, in HCoV-NL63 takes the place of the 4a and 4b genes of HCoV-229E. Third, the 5′ region of the S gene of HCoV-NL63 contains a large in-frame insertion of 537 nucleotides. The N-terminal region of the S protein has been implicated in binding to aminopeptidase N (group I coronaviruses) and sialic acid[4,11,20], so the 179–amino acid insert in HCoV-NL63 might be involved in receptor binding and may explain the tropism of this virus in cell culture. However, the aminopeptidase N receptor-binding domain of the HCoV-229E S protein has been mapped to amino acids (407–547[4]), so it seems unlikely that the insertion will be directly involved in binding to aminopeptidase N. Fourth, whereas HCoV-229E is fastidious in cell culture with a narrow host range, HCoV-NL63 replicates efficiently in monkey kidney cells. SARS-CoV is also able to replicate in monkey kidney cells (Vero-E6 cells[21]), yet the predicted S proteins of SARS-CoV and HCoV-NL63 do not share a domain that could explain the *in vitro* host cell range of these viruses. Other viral proteins may influence the cell tropism of a virus, but none of the HCoV-NL63 proteins were more closely related to SARS-CoV than to HCoV-229E.

Variability at the 5′ end of the S gene, correlating with alterations in tropism, has also been described for the group 1 coronaviruses porcine respiratory coronavirus (PRCoV) and transmissible gastroenteritis virus (TGEV). These porcine viruses are antigenically and genetically related, but their pathogenicity is markedly different. TGEV replicates in and destroys the enterocytes of the small intestine, causing severe diarrhea with high mortality in neonatal swine. In contrast, PRCoV (which emerged more recently than TGEV) has a selective tropism for respiratory tissue, and very little capacity to replicate in intestinal tissue. The difference between the TGEV and PRCoV S gene sequences is comparable to the difference between those of HCoV-NL63 and HCoV-229E[45]. Compared with TGEV, PRCoV contains a deletion in the 5′ hypervariable region of the S gene. The extra region that is present at the 5′ end of the TGEV S gene is responsible for the hemagglutination activity of TGEV, and its capacity to bind to sialic acid[20]. However, this region shows no similarity to the HCoV-NL63 insert.

The common cold–causing virus HCoV-229E can cause more serious respiratory disease in infants and immunocompromised patients[27,33]. Our data indicate that HCoV-NL63 causes acute respiratory disease in children below the age of 1 year, and in immunocompromised adults. To date, no known viral pathogen can be


HCoV-NL63
HCoV-229E
PEDV
TGEV
PRCoV
FCoV
CCoV
FIPV

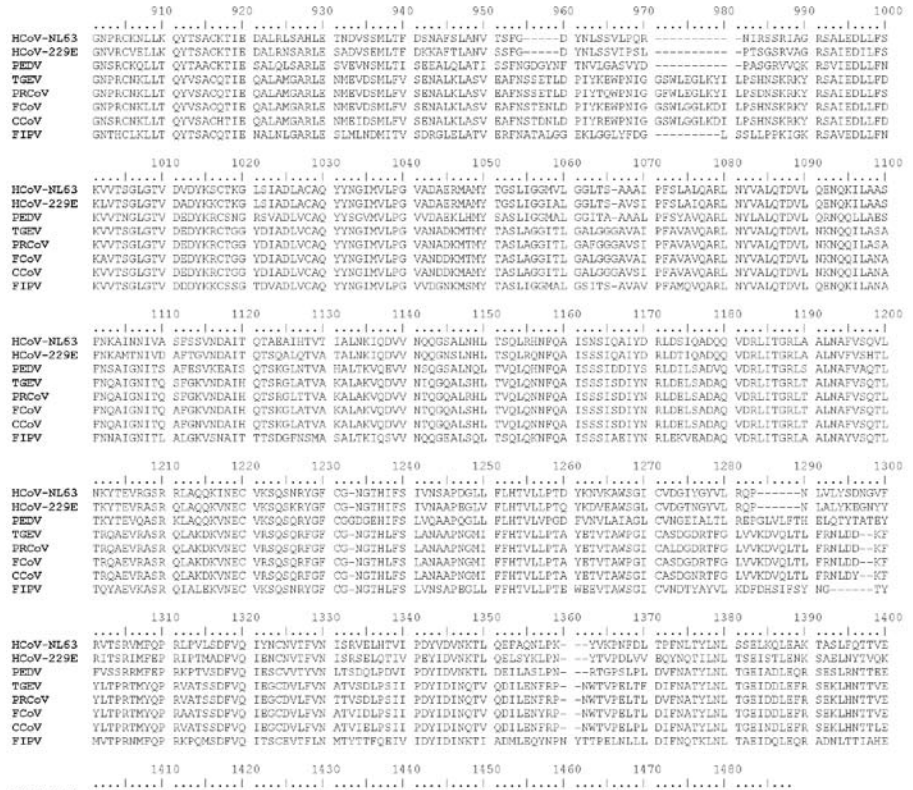


Figure 10: Alignment of the sequence of the deduced Spike protein of the group 1 coronaviruses. The GenBank accession numbers of the sequences are provided in the Methods section.

identified in a substantial portion of respiratory disease cases in humans (20–30%[3]). Several assays have been used to diagnose coronavirus infections. Traditionally, an antibody test is implemented to measure a rise in titers of antibodies to the human coronaviruses HCoV-229E or HCoV-OC43[16]. Antibodies to HCoV-NL63 might cross-react with HCoV-229E, given that these viruses are members of the same serotype. If this were the case, HCoV-NL63 infections might have been misdiagnosed as HCoV-229E. Molecular biology tools such as RT-PCR assays[31,38] were designed to selectively detect the human coronaviruses HCoV-229E and HCoV-OC43, but these assays will not detect HCoV-NL63. Even the RT-PCR assay that was designed to amplify all known coronaviruses[38] is not able to amplify HCoV-NL63 because of several mismatches with the primer sequences. The availability of the complete HCoV-NL63 genome sequence means that these diagnostic assays can be substantially improved.

Our results indicate that HCoV-NL63 is present in a significant number of respiratory tract illnesses of unknown etiology. HCoV-NL63 was detected in patients suffering from respiratory disease, with a frequency of up to 7% in January 2003. The virus was not detected in more recent samples collected in the spring and summer of 2003, which correlates with the fact that human coronaviruses tend to be transmitted predominantly in the winter season[16]. Future experiments with more sensitive diagnostic tools should yield a more accurate picture of the prevalence of this virus and its association with respiratory disease.

References

1. Almeida, J. D. and D. A. Tyrrell. 1967. The morphology of three previously uncharacterized human respiratory viruses that grow in organ culture. J Gen Virol 1:175-178.
2. Bachem, C. W., R. S. van der Hoeven, S. M. de Bruijn, D. Vreugdenhil, M. Zabeau, and R. G. Visser. 1996. Visualization of differential gene expression using a novel method of RNA fingerprinting based on AFLP: analysis of gene expression during potato tuber development. Plant J 9:745-753.
3. Boivin, G., G. De Serres, S. Cote, R. Gilca, Y. Abed, L. Rochette, M. G. Bergeron, and P. Dery. 2003. Human metapneumovirus infections in hospitalized children. Emerg. Infect. Dis. 9:634-640.
4. Bonavia, A., B. D. Zelus, D. E. Wentworth, P. J. Talbot, and K. V. Holmes. 2003. Identification of a receptor-binding domain of the spike glycoprotein of human coronavirus HCoV-229E. J. Virol. 77:2530-2538.
5. Boom, R., C. J. Sol, M. M. Salimans, C. L. Jansen, P. M. Wertheim-van Dillen, and J. van der Noordaa. 1990. Rapid and simple method for purification of nucleic acids. J. Clin. Microbiol. 28:495-503.
6. Bradburne, A. F., M. L. Bynoe, and D. A. Tyrrell. 1967. Effects of a "new" human respiratory virus in volunteers. Br. Med J 3:767-769.
7. Chen, L. L., H. Y. Ou, R. Zhang, and C. T. Zhang. 2003. ZCURVE_CoV: a new system to recognize protein coding genes in coronavirus genomes, and its applications in analyzing SARS-CoV genomes. Biochem. Biophys. Res. Commun. 307:382-388.
8. Drosten, C., S. Gunther, W. Preiser, S. van der Werf, H. R. Brodt, S. Becker, H. Rabenau, M. Panning, L. Kolesnikova, R. A. Fouchier, A. Berger, A. M. Burguiere, J. Cinatl, M. Eickmann, N. Escriou, K. Grywna, S. Kramme, J. C. Manuguerra, S. Muller, V. Rickerts, M. Sturmer, S. Vieth, H. D. Klenk, A. D. Osterhaus, H. Schmitz, and H. W. Doerr. 2003. Identification of a novel coronavirus in patients with severe acute respiratory syndrome. N. Engl. J. Med. 348:1967-1976.
9. Duarte, M., K. Tobler, A. Bridgen, D. Rasschaert, M. Ackermann, and H. Laude. 1994. Sequence analysis of the porcine epidemic diarrhea virus genome between the nucleocapsid and spike protein genes reveals a polymorphic ORF. Virology 198:466-476.
10. Falsey, A. R., E. E. Walsh, and F. G. Hayden. 2002. Rhinovirus and coronavirus infection-associated hospitalizations among older adults. J. Infect. Dis. 185:1338-1341.
11. Godet, M., J. Grosclaude, B. Delmas, and H. Laude. 1994. Major receptor-binding and neutralization determinants are located within the same domain of the transmissible gastroenteritis virus (coronavirus) spike protein. J. Virol. 68:8008-8016.
12. Guan, Y., B. J. Zheng, Y. Q. He, X. L. Liu, Z. X. Zhuang, C. L. Cheung, S. W. Luo, P. H. Li, L. J. Zhang, Y. J. Guan, K. M. Butt, K. L. Wong, K. W. Chan, W. Lim, K. F. Shortridge, K. Y. Yuen, J. S. Peiris, and L. L. Poon. 2003. Isolation and characterization of viruses related to the SARS coronavirus from animals in southern China. Science 302:276-278.
13. Guy, J. S., J. J. Breslin, B. Breuhaus, S. Vivrette, and L. G. Smith. 2000. Characterization of a coronavirus isolated from a diarrheic foal. J. Clin. Microbiol. 38:4523-4526.
14. Hamparian, V. V. 1979. Rhinoviruses., p. 562. In E. H. Lennette and N. J. Schmidt (eds.), Diagnostic procedures for viral, rickettsial, and chlamydial infection. American Public Health Association, Washington, D.C.

15. Hamre, D. and J. J. Procknow. 1966. A new virus isolated from the human respiratory tract. Proc. Soc. Exp. Biol. Med. 121:190-193.
16. Hendley, J. O., H. B. Fishburne, and J. M. Gwaltney, Jr. 1972. Coronavirus infections in working adults. Eight-year study with 229 E and OC 43. Am. Rev. Respir. Dis. 105:805-811.
17. Holmes, K. V. and M. M. C. Lai. 1996. Coronaviridae: The viruses and their replication, p. 1075-1093. In B. N. Fields, D. M. Knipe, P. M. Howley, and et al (eds.), Fields Virology. Lippincott-Raven Publishers, Philadelphia.
18. Jubelt, B. and J. R. Berger. 2001. Does viral disease underlie ALS? Lessons from the AIDS pandemic. Neurology 57:945-946.
19. Kimura, M. 1980. A simple method for estimating evolutionary rates of base substitutions through comparative studies of nucleotide sequences. J. Mol. Evol. 16:111-120.
20. Krempl, C., M. L. Ballesteros, G. Zimmer, L. Enjuanes, H. D. Klenk, and G. Herrler. 2000. Characterization of the sialic acid binding activity of transmissible gastroenteritis coronavirus by analysis of haemagglutination-deficient mutants. J. Gen. Virol. 81:489-496.
21. Ksiazek, T. G., D. Erdman, C. S. Goldsmith, S. R. Zaki, T. Peret, S. Emery, S. Tong, C. Urbani, J. A. Comer, W. Lim, P. E. Rollin, S. F. Dowell, A. E. Ling, C. D. Humphrey, W. J. Shieh, J. Guarner, C. D. Paddock, P. Rota, B. Fields, J. DeRisi, J. Y. Yang, N. Cox, J. M. Hughes, J. W. LeDuc, W. J. Bellini, and L. J. Anderson. 2003. A novel coronavirus associated with severe acute respiratory syndrome. N. Engl. J. Med. 348:1953-1966.
22. Kunkel, F. and G. Herrler. 1993. Structural and functional analysis of the surface protein of human coronavirus OC43. Virology 195:195-202.
23. Lai, M. M. 2003. SARS virus: the beginning of the unraveling of a new coronavirus. J. Biomed. Sci. 10:664-675.
24. Lole, K. S., R. C. Bollinger, R. S. Paranjape, D. Gadkari, S. S. Kulkarni, N. G. Novak, R. Ingersoll, H. W. Sheppard, and S. C. Ray. 1999. Full-length human immunodeficiency virus type 1 genomes from subtype C-infected seroconverters in India, with evidence of intersubtype recombination. J. Virol. 73:152-160.
25. Marra, M. A., S. J. Jones, C. R. Astell, R. A. Holt, A. Brooks-Wilson, Y. S. Butterfield, J. Khattra, J. K. Asano, S. A. Barber, S. Y. Chan, A. Cloutier, S. M. Coughlin, D. Freeman, N. Girn, O. L. Griffith, S. R. Leach, M. Mayo, H. McDonald, S. B. Montgomery, P. K. Pandoh, A. S. Petrescu, A. G. Robertson, J. E. Schein, A. Siddiqui, D. E. Smailus, J. M. Stott, G. S. Yang, F. Plummer, A. Andonov, H. Artsob, N. Bastien, K. Bernard, T. F. Booth, D. Bowness, M. Czub, M. Drebot, L. Fernando, R. Flick, M. Garbutt, M. Gray, A. Grolla, S. Jones, H. Feldmann, A. Meyers, A. Kabani, Y. Li, S. Normand, U. Stroher, G. A. Tipples, S. Tyler, R. Vogrig, D. Ward, B. Watson, R. C. Brunham, M. Krajden, M. Petric, D. M. Skowronski, C. Upton, and R. L. Roper. 2003. The Genome sequence of the SARS-associated coronavirus. Science 300:1399-1404.
26. Martina, B. E., B. L. Haagmans, T. Kuiken, R. A. Fouchier, G. F. Rimmelzwaan, G. van Amerongen, J. S. Peiris, W. Lim, and A. D. Osterhaus. 2003. Virology: SARS virus infection of cats and ferrets. Nature 425:915.
27. McIntosh, K., R. K. Chao, H. E. Krause, R. Wasil, H. E. Mocega, and M. A. Mufson. 1974. Coronavirus infection in acute lower respiratory tract disease of infants. J. Infect. Dis. 130:502-507.
28. McIntosh, K., J. H. Dees, W. B. Becker, A. Z. Kapikian, and R. M. Chanock. 1967. Recovery in tracheal organ cultures of novel viruses from patients with respiratory disease. Proc Natl Acad Sci U S A 57:933-940.
29. Mounir, S., P. Labonte, and P. J. Talbot. 1993. Characterization of the nonstructural and spike proteins of the human respiratory coronavirus OC43: comparison with bovine enteric coronavirus. Adv. Exp. Med. Biol. 342:61-67.
30. Mounir, S. and P. J. Talbot. 1993. Human coronavirus OC43 RNA 4 lacks two open reading frames located downstream of the S gene of bovine coronavirus. Virology 192:355-360.
31. Myint, S., S. Johnston, G. Sanderson, and H. Simpson. 1994. Evaluation of nested polymerase chain methods for the detection of human coronaviruses 229E and OC43. Mol. Cell Probes 8:357-364.
32. Peiris, J. S., C. M. Chu, V. C. Cheng, K. S. Chan, I. F. Hung, L. L. Poon, K. I. Law, B. S. Tang, T. Y. Hon, C. S. Chan, K. H. Chan, J. S. Ng, B. J. Zheng, W. L. Ng, R. W. Lai, Y. Guan, and K. Y. Yuen. 2003. Clinical progression and viral load in a community outbreak of coronavirus-associated SARS pneumonia: a prospective study. Lancet 361:1767-1772.

33. Pene, F., A. Merlat, A. Vabret, F. Rozenberg, A. Buzyn, F. Dreyfus, A. Cariou, F. Freymuth, and P. Lebon. 2003. Coronavirus 229E-related pneumonia in immunocompromised patients. Clin. Infect. Dis. 37:929-932.
34. Rota, P. A., M. S. Oberste, S. S. Monroe, W. A. Nix, R. Campagnoli, J. P. Icenogle, S. Penaranda, B. Bankamp, K. Maher, M. H. Chen, S. Tong, A. Tamin, L. Lowe, M. Frace, J. L. DeRisi, Q. Chen, D. Wang, D. D. Erdman, T. C. Peret, C. Burns, T. G. Ksiazek, P. E. Rollin, A. Sanchez, S. Liffick, B. Holloway, J. Limor, K. McCaustland, M. Olsen-Rasmussen, R. Fouchier, S. Gunther, A. D. Osterhaus, C. Drosten, M. A. Pallansch, L. J. Anderson, and W. J. Bellini. 2003. Characterization of a novel coronavirus associated with severe acute respiratory syndrome. Science 300:1394-1399.
35. Sawicki, S. G. and D. L. Sawicki. 1995. Coronaviruses use discontinuous extension for synthesis of subgenome-length negative strands. Adv. Exp. Med. Biol. 380:499-506.
36. Shingadia, D., A. Bose, and R. Booy. 2002. Could a herpesvirus be the cause of Kawasaki disease? Lancet Infect. Dis. 2:310-313.
37. Snijder, E. J., P. J. Bredenbeek, J. C. Dobbe, V. Thiel, J. Ziebuhr, L. L. Poon, Y. Guan, M. Rozanov, W. J. Spaan, and A. E. Gorbalenya. 2003. Unique and conserved features of genome and proteome of SARS-coronavirus, an early split-off from the coronavirus group 2 lineage. J. Mol. Biol. 331:991-1004.
38. Stephensen, C. B., D. B. Casebolt, and N. N. Gangopadhyay. 1999. Phylogenetic analysis of a highly conserved region of the polymerase gene from 11 coronaviruses and development of a consensus polymerase chain reaction assay. Virus Res. 60:181-189.
39. Stohlman, S. A. and D. R. Hinton. 2001. Viral induced demyelination. Brain Pathol. 11:92-106.
40. Thiel, V., J. Herold, B. Schelle, and S. G. Siddell. 2001. Infectious RNA transcribed in vitro from a cDNA copy of the human coronavirus genome cloned in vaccinia virus. J. Gen. Virol. 82:1273-1281.
41. Thompson, J. D., T. J. Gibson, F. Plewniak, F. Jeanmougin, and D. G. Higgins. 1997. The CLUSTAL_X windows interface: flexible strategies for multiple sequence alignment aided by quality analysis tools. Nucleic Acids Res 25:4876-4882.
42. Tyrrell, D. A. and M. L. Bynoe. 1965. Cultivation of a novel type of common-cold virus in organ cultures. Br. Med. J. 5448:1467-1470.
43. van den Hoogen, B. G., J. C. de Jong, J. Groen, T. Kuiken, R. De Groot, R. A. Fouchier, and A. D. Osterhaus. 2001. A newly discovered human pneumovirus isolated from young children with respiratory tract disease. Nat. Med. 7:719-724.
44. van Marle, G., J. C. Dobbe, A. P. Gultyaev, W. Luytjes, W. J. Spaan, and E. J. Snijder. 1999. Arterivirus discontinuous mRNA transcription is guided by base pairing between sense and antisense transcription-regulating sequences. Proc. Natl. Acad. Sci. U. S. A 96:12056-12061.
45. Vaughn, E. M., P. G. Halbur, and P. S. Paul. 1995. Sequence comparison of porcine respiratory coronavirus isolates reveals heterogeneity in the S, 3, and 3-1 genes. J. Virol. 69:3176-3184.

Chapter III

Genome structure and transcriptional regulation of human coronavirus NL63

Virology Journal, Nobember 2004, vol. 1, nr 7

Krzysztof Pyrc, Maarten F. Jebbink, Ben Berkhout and Lia van der Hoek

Laboratory of Experimental Virology, Department of Medical Microbiology, Center for Infection and Immunity Amsterdam (CINIMA), Academic Medical Center, University of Amsterdam, Meibergdreef 15, 1105 AZ, Amsterdam, The Netherlands.

Two human coronaviruses are known since the 1960s: HCoV-229E and HCoV-OC43. SARS-CoV was discovered in the early spring of 2003, followed by the identification of HCoV-NL63, the fourth member of the *Coronaviridae* family that infects humans. In this study, we describe the genome structure and the transcription strategy of HCoV-NL63 by experimental analysis of the viral subgenomic mRNAs.

The genome of HCoV-NL63 has the following gene order: 1a-1b-S-ORF3-E-M-N. The GC content of the HCoV-NL63 genome is extremely low (34%) compared to other coronaviruses, and we therefore performed additional analysis of the nucleotide composition. Overall, the RNA genome is very low in C and high in U, and this is also reflected in the codon usage. Inspection of the nucleotide composition along the genome indicates that the C-count increases significantly in the last one-third of the genome at the expense of U and G. We document the production of subgenomic (sg) mRNAs coding for the S, ORF3, E, M and N proteins. We did not detect any additional sg mRNA. Furthermore, we sequenced the 5′ end of all sg mRNAs, confirming the presence of an identical leader sequence in each sg mRNA. Northern blot analysis indicated that the expression level among the sg mRNAs differs significantly, with the sg mRNA encoding nucleocapsid (N) being the most abundant.

The presented data give insight into the viral evolution and mutational patterns in coronaviral genome. Furthermore our data show that HCoV-NL63 employs the discontinuous replication strategy with generation of subgenomic mRNAs during the (-) strand synthesis. Because HCoV-NL63 has a low pathogenicity and is able to replicate easily in cell culture, this virus can be a powerful tool to study SARS coronavirus pathogenesis.

Introduction

Until recently only two human coronaviruses were known – human coronavirus (HCoV) 229E and HCoV-OC43, representatives of the group 1 and 2 coronaviruses, respectively. Both were identified in 1960s and are generally considered as common cold viruses. An outbreak of severe acute respiratory syndrome (SARS) in the spring of 2003 led to the rapid identification of SARS-CoV[4,16], which is considered to be a distinct member of the group 2 coronaviruses[6] or the first member of group 4 coronaviruses[18,22]. We identified earlier this year another human pathogen from this family: HCoV-NL63[26], a variant that belongs to group 1 together with HCoV-229E and PEDV. These recent findings may be striking, as since the 1960's not a single new HCoV had been described. The genome features of SARS-CoV and its transcription strategy have been described in detail[4,15,18]. Here, we present such an analysis for HCoV-NL63.

HCoV-NL63 is a member of the *Coronaviridae* family that clusters together with arteri-, toro- and roniviruses in the order of the nidovirales. Coronaviruses are enveloped viruses with a positive, single stranded RNA genome of approximately 27 to 32kb. The 5′ two-third of a coronavirus genome encodes a polyprotein that contains all enzymes necessary for RNA replication. The expression of the complete polyprotein requires a –1 ribosomal frameshift during translation that is triggered by a pseudoknot RNA structure[7,11]. The polyprotein undergoes autocatalytic cleavage by the viral papain-like proteinase and a chymotrypsin-like proteinase. The 3′ one-third of a coronavirus genome encodes several structural proteins such as spike (S), envelope (E), membrane (M) and nucleocapsid (N) that, among other functions, participate in the budding process and are incorporated into the virus particle. Some of the group 2 viruses encode a hemagglutinin esterase (HE)[5,28]. Non-structural protein genes are located between the structural genes. These accessory genes vary significantly in number and sequence among coronavirus species. Their precise function is unknown, but several reports indicate that they can modulate viral pathogenicity[2].

Coronavirus replication is a complex, not yet fully understood mechanism[19,20]. The 5′ end of the genomic RNA contains the untranslated leader (L) sequence with the Transcription Regulation Sequence (TRS) in the downstream part. The L TRS is very similar to sequences that can be found in front of each open reading frame (body TRSs). The RNA-dependent RNA-polymerase has been proposed to pause after a body TRS of a particular gene is copied during (-) strand synthesis, subsequently switching to the L TRS and thus adding a common L sequence to each sg mRNA[23]. This discontinuous transcription mechanism is based on base-pairing of the nascent (-) strand copy RNA with the (+) strand L TRS. The nested set of (-) strand sg mRNAs are subsequently copied into a set of (+) strand sg mRNA. Other factors besides the sequence similarity between body and L TRS influence the efficiency of transcription. The level of transcription of a particular gene has been reported to be inversely related to the distance of a particular TRS to the 3′ end of the genome[3,13,14,21].

In this study, we analyzed the genome structure of HCoV-NL63. First, we focus on the unusual nucleotide composition of the RNA genome. We describe in detail the bias in the nucleotide composition and its influence on the codon usage of this virus. We provide a possible mechanistic explanation for a shift in nucleotide bias at two-third of the HCoV-NL63 genome that is based on the RNA replication mechanism. Second, we describe in detail the different sg mRNAs generated during HCoV-NL63 replication and their relative abundance.

Methods

Genome Analysis

The nucleotide content of different *Coronaviridae* family members was assessed using BioEdit software (http://www.mbio.ncsu.edu/BioEdit/bioedit.html). The nucleotide distribution was determined using a Microsoft Excel datasheet (300 nucleotide (nt) window and 10-nt step). Codon usage was assessed using DNA 2.0 software. Data was processed in Microsoft Excel datasheet and all statistical analysis was performed with SPSS 11.5.0 software. The level of significance of the nucleotide bias was established for 300-nt non-overlapping windows with the non-parametric Mann-Whitney U test for two independent samples. Cumulative GC-skew graphs were generated as described previously[9] with the value in step n defined as the sum of (G-C)/(G+C) from step 0 to n (200-nt sliding window, 10-nt step).

Viral RNA isolation

HCoV-NL63 RNA was obtained from virus-infected LLC-MK2 cells (2×10^7) after 6 days of culture (virus passage 7). Mouse Hepatitis Virus (MHV) RNA was obtained by infecting $2x10^7$ LR7 cells with MHV strain A59. The medium was removed and the cells were dissolved in 15ml TRIzol® and RNA was isolated according to the standard TRIzol® procedure. RNA was subsequently precipitated with 0.5 volume of isopropanol, dried and dissolved in 50µl H_2O. Integrity of the RNA was analyzed by electrophoresis on a non-denaturating 0.8% agarose gel. RNA was stored at -150°C.

RT-PCR

The cDNA used for sequencing and probe construction was made by MMLV-RT on viral RNA with 1µg of random hexamer DNA primers in 10mM Tris pH 8.3, 50mM KCl, 0.1% Triton-X100, 6mM of $MgCl_2$ and 50µM of each dNTPs at 37°C for 1 hour. The single stranded cDNA product was made into double-stranded DNA in a standard PCR reaction with 1.25 U of Taq polymerase (Perkin-Elmer) per reaction with appropriate primers (see below).

Northern Blot

Gel electrophoresis of viral RNA was performed on a 1% agarose gel with 7% of formaldehyde at 100 Volt in 1×MOPS buffer (40mM MOPS, 10mM sodium acetate, pH 7.0). Transfer onto a positively charged nylon membrane (Boehringer Mannheim) was done overnight by means of capillary force. RNA was linked to the membrane in a UV crosslinker (Stratagene). For generation of the HCoV-NL63 probe, the RT-PCR product was further amplified with 5′ primer N5PCR1 (CTGTTACTTTGGCTTTAAAGAACTTAGG) and 3′ primer N3PCR1 (CTCACTATCAAAGAATAACGCAGCCTG). Similarly, the MHV probe was amplified with 5′ primer MHV_UTR-B5′ (GATGAAGTAGATAATGTAAGCGT) and 3′ primer MHV_UTR-B3′ (TGCCACAACCTTCTCTATCTGTTAT). Labeling of the probes was done in a standard PCR reaction with specific 3′ primers (N3PCR1 and MHV_UTR-B3′) in presence of [α-^{32}P]dCTP. Prehybridization and hybridization

was done in ULTRAhyb buffer (Ambion) at 50°C for 1 and 12 hours, respectively. The membrane was then washed at room temperature with low-stringency buffer (2×SSC, 0.2% SDS) and at 50°C in high stringency buffer (0.1×SSC, 0.2% SDS). Images were obtained using the STORM 860 phosphorimager (Amersham Biosciences) and data analysis was performed with the ImageQuant software package. The size of sg mRNA fragments of HCoV-NL63 were estimated from their migration on the Northern blot using the sg mRNA of MHV as size marker.

Sequence analysis of TRS motifs

The L/body TRS junctions were PCR-amplified from an HCoV-NL63 cDNA bank. We performed 35 cycle PCR with the 5′ L primer (L5 – TAAAGAATTTTTCTATC-TATAGATAG) and gene specific 3′ primers (S gene – SL3′ – ACTACGGTGATTAC-CAACATCAATATA; ORF3 – 4L3′ – CAAGCAACACGACCTCTAGCAGTAAG; E gene – EL3′ – TATTTGCATATAATCTTGGTAAGC; M gene – ML3′ – GAC-CCAGTCCACATT AAAATTGACA; N gene – 3-163-F15 – ATTACCTAGGTACT-GGACCT). The PCR products were analyzed by electrophoresis on a 0.8% agarose gel and products of discrete size were used for sequencing using the BigDye termi-nator kit (ABI) and ABI Prism 377 sequencer (Perkin Elmer). Sequence analysis was performed by Sequence Navigator and AutoAssembler 2.1 software.

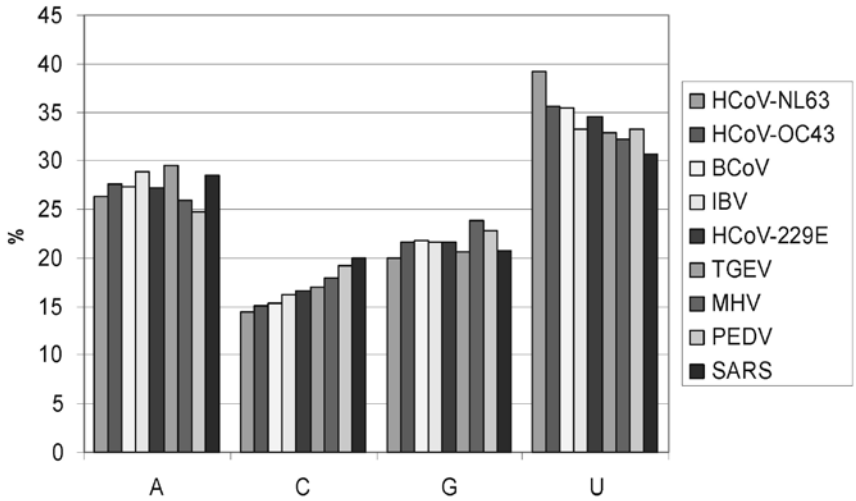


Figure 1. Nucleotide content of Coronaviridae RNA genomes. We arranged the viruses based on their C-count, which ranges from 14% (HCoV-NL63) to 20% (SARS-CoV).

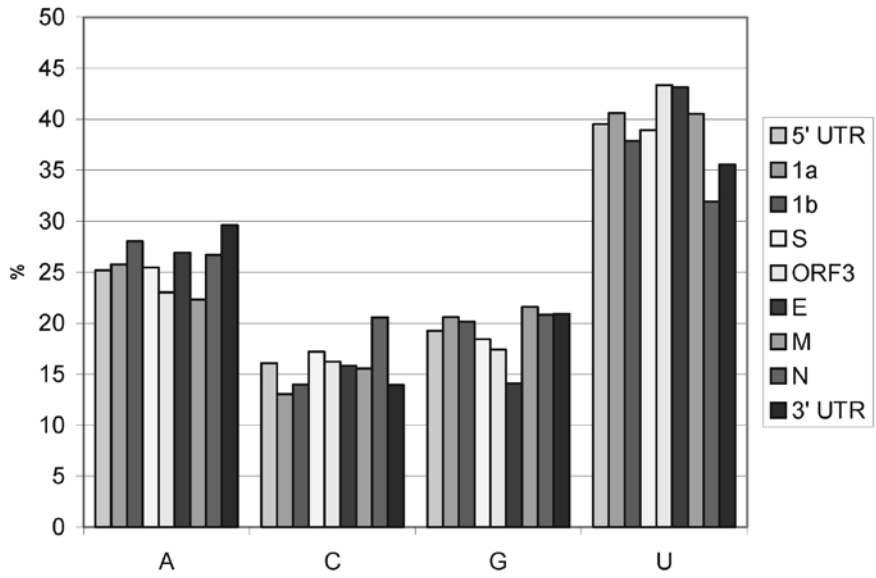


Figure 2. Nucleotide content of individual HCoV-NL63 genes and the 5′/3′ untranslated regions (UTR).

Sequences

The complete genome sequence of HCoV-NL63[26] is deposited in GenBank (accession number: NC_005831). sg mRNA sequences are deposited in GenBank under the accession numbers: AY697419-AY697423. The GenBank accession number of the sequences used in this genome analysis are: MHV (mouse hepatitis virus, strain MHV-A59): NC_001846; HCoV-229E: NC_002645; HCoV-OC43 strain ATCC VR-759: NC_005147; PEDV (porcine epidemic diarrhea virus, strain CV777): AF353511; TGEV (transmissible gastroenteritis virus, strain Purdue): NC_002306; SARS-CoV isolate Tor2: NC_004718; IBV (avian infectious bronchitis virus, strain Beaudette): NC_001451; BCoV (bovine coronavirus, isolate BCoV-ENT): NC_003045.

Results

Nucleotide content of the HCoV-NL63 genome

We described previously that the newly identified HCoV-NL63 virus has a typical coronavirus genome structure and gene order[26]. The nucleotide composition of the genomic (+) strand RNA of several *Coronaviridae* members is presented in Figure 1, demonstrating a common pattern with U as the most abundant nucleotide and G and in particular C as underrepresented nucleotides. HCoV-NL63 has the most extreme nucleotide bias among the *Coronaviridae*, with 39% U and only 14% C. As a general trend, U and C seem to compete directly, because the genomes with the lowest C-count (HCoV-NL63, HCoV-OC43 and BCoV) have the highest U-count and vice versa (Figure 1).

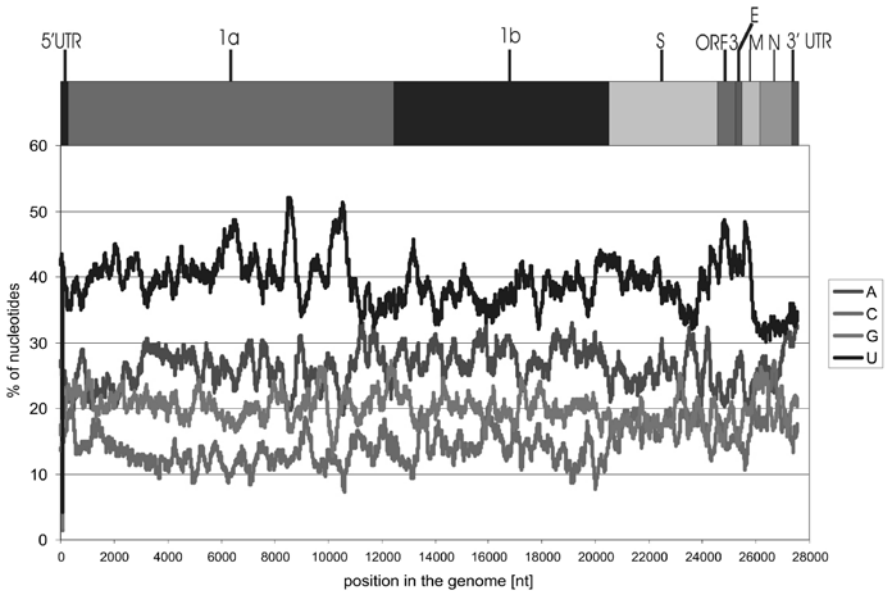


Figure 3. Nucleotide distribution along the HCoV-NL63 genome. The change in the C- and G-count at two-third of the genome is statistically significant for all tested coronaviruses (HCoV-NL63, HCoV-229E, SARS-CoV, HCoV-OC43) with $p<0.01$ for C-count and $p<0.05$ for G-count in Mann-Whitney U test for two independent samples.

To investigate if all coding regions of HCoV-NL63 display a similarly strong preference for U and against C, we also plotted the nucleotide count for the individual genes and 5′ and 3′ non-coding regions (Figure 2). The typical nucleotide bias is observed in all genome segments. The highest U-count is found in the ORF3 and E genes (43%) and the lowest C-count in the 1a/1b genes and the 3′ UTR (13%, 14% and 14%, respectively). The N gene is most moderate in its nucleotide bias, with 21% C and 32% U, confirming the "competition" idea that was already suggested by inspection of Figure 1.

We plotted the nucleotide distribution along the genome (Figure 3) to determine whether there is any significant variation. We observed that local changes in A-count are inversely linked to changes in G-count. This is most striking in the 20400-26000 nt region, where three A peaks are mirrored by three G anti-peaks. Although the typical bias is maintained along the genome, the most notable variation occurs in the last one-third of the genome, where an increase in C and a decrease in G content is apparent. This region encodes the structural proteins.

Recently, Grigoriev reported an interesting feature within coronaviral genomes that is visible when the cumulative GC-skew is plotted[8,9]. Cumulative GC skew graph is a way to visualize the local G:C ratio along the genome, discarding

Table 1. Codon usage of HCoV-NL63 compared with that of human genes

Amino acid	Codon	Human[a]	HCoV-NL63	1ab (20190)	S (4071nt)	ORF3 (678nt)	E (234nt)	M (681nt)	N (1134nt)
Arg	CGA	0.62[b]	0.16	0.12	0.22	0.44	***1.28***	0.00	0.26
	CGC	1.07	0.28	0.21	0.37	0.00	0.00	0.88	1.06
	CGG	***1.16***[c]	0.06	0.04	0.15	0.00	0.00	0.00	0.00
	CGU	0.46	***1.57***	***1.49***	***1.40***	***1.77***	0.00	***2.20***	***3.44***
	AGA	***1.17***	0.78	0.76	0.74	0.88	0.00	1.32	1.06
	AGG	***1.17***	0.47	0.49	0.22	0.00	***1.28***	0.00	1.32
Leu	CUA	0.70	0.39	0.31	0.29	2.65	1.28	0.88	0.26
	CUC	1.97	0.36	0.24	0.74	0.88	2.56	0.44	0.26
	CUG	***4.01***	0.21	0.18	0.37	0.44	1.28	0.00	0.00
	CUU	1.30	***2.97***	2.84	2.87	***4.42***	***3.85***	***5.73***	***2.91***
	UUA	0.74	2.68	2.75	2.51	2.65	***3.85***	4.41	0.79
	UUG	1.28	***2.95***	***2.97***	***3.02***	3.54	2.56	2.20	2.38
Ser	UCA	1.20	1.49	1.38	1.92	1.33	0.00	0.44	2.91
	UCC	1.76	0.33	0.30	0.59	0.00	***1.28***	0.00	0.26
	UCG	0.45	0.08	0.07	0.00	0.44	0.00	0.00	0.26
	UCU	1.49	***3.06***	***2.76***	***3.98***	***2.21***	0.00	***3.52***	***5.82***
	AGC	***1.94***	0.34	0.27	0.59	0.00	0.00	0.88	0.79
	AGU	1.21	2.47	2.51	2.36	***2.21***	***1.28***	3.08	2.12
Thr	ACA	1.49	1.72	1.89	1.33	0.88	***1.28***	***2.64***	0.26
	ACC	***1.91***	0.44	0.40	0.52	0.00	***1.28***	0.44	1.06
	ACG	0.62	0.19	0.13	0.37	0.44	0.00	0.88	0.00
	ACU	1.30	***3.58***	***3.28***	***5.53***	***4.87***	***1.28***	1.76	***2.65***
Pro	CCA	1.68	1.03	1.01	1.11	0.44	***2.56***	0.44	1.59
	CCC	**2.00**	0.18	0.15	0.22	0.00	0.00	0.00	0.79
	CCG	0.70	0.10	0.07	0.22	0.00	0.00	0.44	0.00
	CCU	1.74	***2.10***	***1.93***	***1.92***	***3.10***	1.28	***2.20***	***5.29***
Ala	GCA	1.60	1.51	1.66	1.33	0.00	***2.56***	1.32	0.26
	GCC	***2.83***	0.64	0.55	1.11	0.88	0.00	0.44	0.79
	GCG	0.75	0.14	0.13	0.22	0.00	0.00	0.00	0.26
	GCU	1.86	***3.38***	***3.39***	***3.02***	***3.98***	***2.56***	***2.64***	***4.76***
Gly	GGA	1.64	0.46	0.49	0.44	0.00	0.00	0.44	0.26
	GGC	***2.26***	0.48	0.34	1.18	1.33	0.00	0.44	0.00
	GGG	1.65	0.14	0.13	0.07	0.00	0.00	0.44	0.53
	GGU	1.08	***5.19***	***5.56***	***4.35***	***4.42***	***1.28***	***4.41***	***3.44***
Val	GUA	0.71	1.04	1.19	0.59	0.00	1.28	0.88	0.79
	GUC	1.46	0.89	0.77	0.96	2.65	2.56	1.76	0.79
	GUG	***2.86***	0.77	0.68	1.03	0.88	1.28	2.20	0.26
	GUU	1.10	***7.18***	***7.41***	***6.63***	***7.52***	***3.85***	***7.49***	***5.29***
Lys	AAA	2.40	***3.25***	***3.70***	1.33	***2.65***	***2.56***	1.32	3.70
	AAG	***3.22***	2.25	2.29	***1.77***	1.77	0.00	***1.76***	***4.23***
Asn	AAC	***1.92***	1.27	1.05	2.28	0.44	0.00	0.88	2.38
	AAU	1.67	***4.88***	***4.73***	***6.19***	***3.54***	***3.85***	***3.96***	***4.50***
Gln	CAA	1.2	***1.97***	***1.89***	***2.58***	***1.77***	***5.13***	0.44	1.59
	CAG	***3.44***	1.03	0.76	1.69	0.00	0.00	***2.20***	***3.70***
His	CAC	***1.50***	0.39	0.39	0.52	0.44	0.00	0.00	0.27
	CAU	1.07	***1.50***	***1.6***	***1.03***	***0.88***	***1.28***	***2.64***	***1.06***
Glu	GAA	2.89	***2.20***	***2.35***	***1.55***	***3.10***	***1.28***	***1.32***	2.12
	GAG	***4.00***	1.12	1.17	0.66	0.44	0.00	***1.32***	***2.38***
Asp	GAC	***2.55***	1.19	1.2	1.03	***2.21***	1.28	***1.32***	0.79
	GAU	2.2	***4.27***	***4.67***	***3.10***	1.33	***2.56***	0.88	***5.56***
Tyr	UAC	***1.54***	0.89	0.82	1.03	1.77	1.28	1.32	***1.06***
	UAU	1.21	***3.8***	***3.83***	***4.13***	***5.75***	***5.13***	***3.52***	0.79
Cys	UGC	***1.26***	0.30	0.31	0.29	0.44	0.00	0.00	***0.26***
	UGU	1.03	***3.01***	***3.28***	***3.02***	***1.33***	***2.56***	***1.76***	0.00
Phe	UUC	***2.04***	0.68	0.58	0.74	1.77	2.56	0.88	1.06
	UUU	1.72	***5.76***	***6.02***	***4.94***	***7.52***	***8.97***	***5.29***	***2.65***
Ile	AUA	0.73	1.30	1.29	1.62	1.33	2.56	0.88	0.26
	AUC	***2.11***	0.33	0.30	0.44	0.00	0.00	1.32	0.26
	AUU	1.58	***3.76***	***3.77***	***3.68***	***3.98***	***7.69***	***3.08***	***3.17***

[a] data obtained from GenBank Release 142.0 17.
[b] all values represent the percentage of a specified codon.
[c] the highest value for each codon group is typed bold italics.

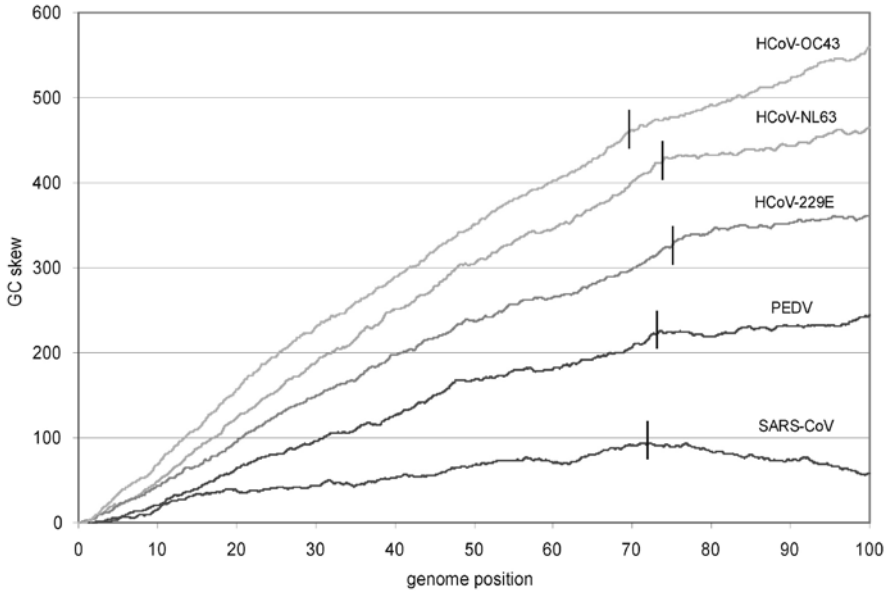


Figure 4. Cumulative GC-skew diagrams for several coronaviral RNA genomes. The vertical bar indicates the border between the 1a/1b and the structural genes.

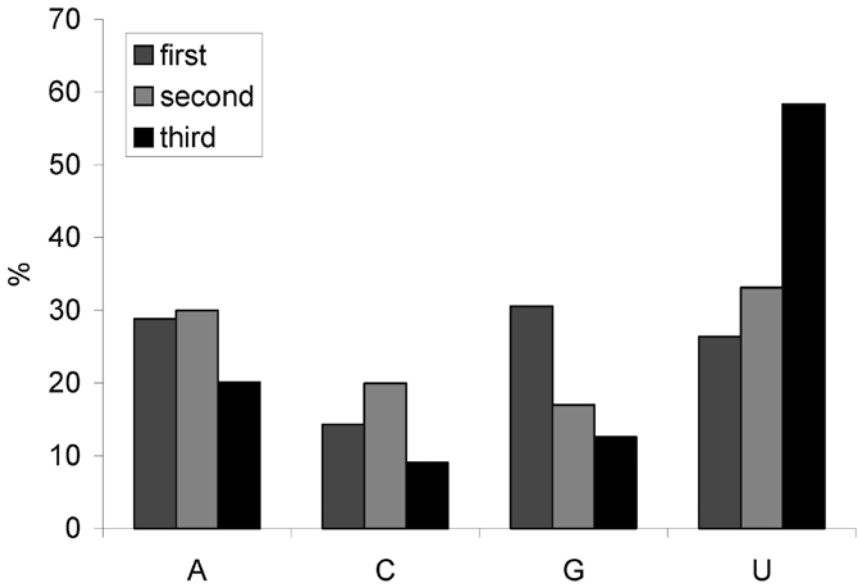


Figure 5. Nucleotide composition of the first, second and third codon positions in the HCoV-NL63 genome.

the local fluctuations. A biphasic pattern was described that separates the 1a/1b polyprotein genes and the structural genes. The cumulative GC-skews for HCoV-NL63 and four other coronaviruses: HCoV-OC43, HCoV-229E, PEDV and SARS-CoV are presented in Figure 4. In the 1a/1b genes, the G:C ratio reaches high levels, whereas for all coronaviruses, including HCoV-NL63, the 3′ end of the genome displays a flattening of the curve, as the G:C ratio reaches value ~1 or less. Grigoriev proposed that this biphasic pattern is due to the discontinuous transcription process[9]. He suggested that the frequent deamination of cytosine on the (-) strand RNA results in a decrease of G on the (+) strand in the region encoding the structural genes. In the discussion section we will present an alternative mechanistic explanation.

HCoV-NL63 codon usage

The bias in the nucleotide count led us to compare the codon usage of HCoV-NL63 with that of human mRNA (Table 1). The codon usage of HCoV-NL63 differs markedly from that of human mRNAs. Third-base choices in the four-codon families (Thr, Pro, Ala, Gly, Val) provide a convenient example of this contrasting codon usage. For instance, the Gly codons in human mRNAs prefer C (34%) over G (25%), A (25%) and U (16%). In contrast, HCoV-NL63 prefers U (83%) over A (7%), C (8%) and G (2%). This result strongly suggests that the codon usage is shaped directly by the unusual nucleotide composition of the viral genome, that is a high U-count and a low G/C-count. All HCoV-NL63 genes, except for the E gene, follow this trend (Table 1). The coronaviral addiction to



Figure 6. Body-leader junctions of all HCoV-NL63 sg mRNAs. Shown on top is the leader (L) sequence and below the specific sequences upstream of the structural genes. The fusion of 5′ L sequences to 3′ sg RNA is indicated by the boxes. Sequence homology between the strands near the junction is marked by asterisks, the conserved AACUAAA TRS core is highlighted in gray.

the U nucleotide is most prominent in the "free" third position of degenerate codons. For the complete genome, the U-count at the third position is up to 58% whereas the A-count is 20%, G-count is 13% and C-count is only 9% (Figure 5). This illustrates that the U-pressure mainly affects the %C and %G.

Identification of the HCoV-NL63 TRS elements

The 5′ end of HCoV-NL63 genome RNA contains the L sequence of 72 nucleotides that ends with the L TRS element. This TRS has a high similarity to short sequences that are located in front of each open reading frame (S-ORF3-E-M-N)[12]. We previously identified the L TRS and body TRS of the N gene using a cDNA bank[26], which allowed us to predict the body TRS of the other genes. To confirm these predictions, we amplified and sequenced all sg mRNA fragments with a general L primer and gene-specific 3′ primers in an RT-PCR protocol. Inspection of sg mRNA junctions indicated that they are indeed composed of the part of the HCoV-NL63 genome that is directly downstream of a particular body TRS, with its 5′ end derived from the leader sequence. Apparently, strand

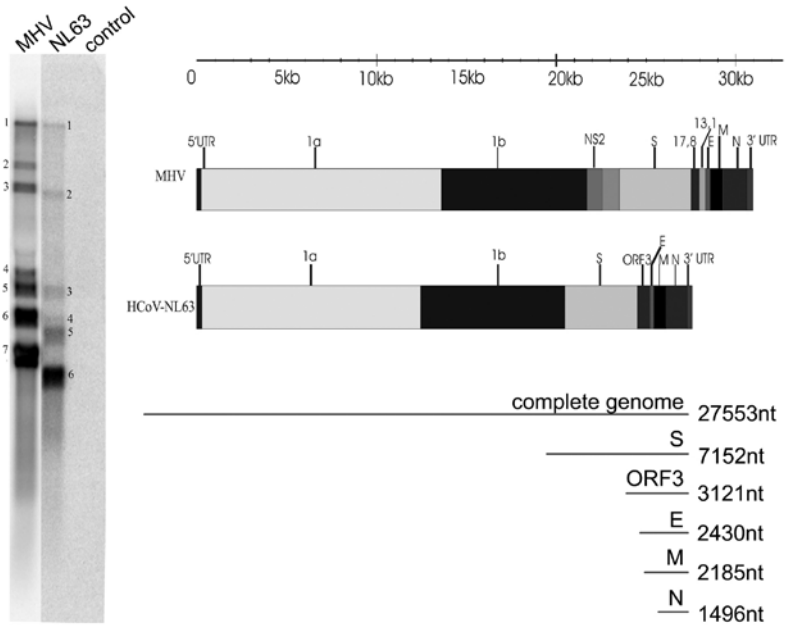


Figure 7. HCoV-NL63 transcription products. The left panel shows the Northern blot analysis of HCoV-NL63 RNA in infected LLC-MK2 cells. RNA of HCoV-NL63 (NL63 lane) was compared with RNA of MHV strain A59 (MHV lane). Non-infected LLC-MK2 cells are included as a negative control (control lane). MHV RNA bands represent the complete genome (1) and sg mRNAs 2a (2), S (3), 17.8 (4), 13.1 and E (5), M (6), N (7). HCoV-NL63 RNA includes the complete genome (1) and sg mRNAs for S (2), ORF3 (3), E (4), M (5) and N (6). The right panel shows the MHV and HCoV-NL63 genome organization and the HCoV-NL63 sg-mRNAs.

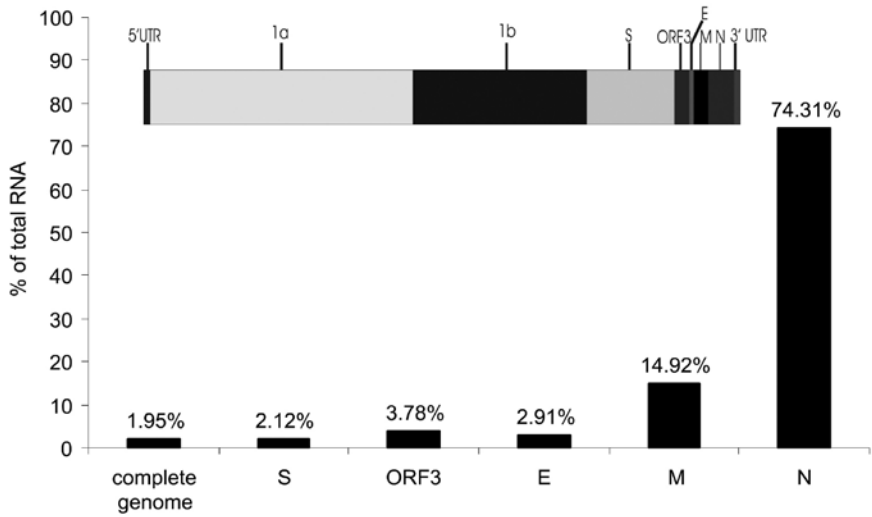


Figure 8: Expression levels of the HCoV-NL63 genomic and sg mRNAs.

transfer occurred on the 5′ end of the body TRS, as indicated in Figure 6.
The most conserved TRS region was defined by multiple sequence alignment as AACUAAA (gray box). This core sequence is conserved in all sg mRNA, except for the E gene that contains the sub-optimal TRS core AACUAUA (Figure 6). Interestingly, the E gene contains a 13-nucleotide sequence upstream of the core sequence with perfect homology to the L sequence. Perhaps the upstream sequence compensates for the absence of an optimal TRS core during discontinuous (-) strand synthesis. This would suggest that these sequences are copied during (-) strand synthesis, and that the actual strand transfer within the E sequences occurred after copying of the core TRS and the next 13 nucleotides. Evidence for such a "delayed" strand transfer is provided by the junction analysis of the M and N sg mRNAs, which clearly demonstrates that the nucleotides directly upstream of the core TRS are derived from the body TRS element and not from the leader (Figure 6).

Analysis of the subgenomic mRNAs of HCoV-NL63

To determine whether the predicted sg mRNAs encoding the S-ORF3-E-M-N proteins are produced in virus-infected cells, we performed Northern blot analysis on total cellular RNA (Figure 7). We used a (-) strand N gene probe that anneals to both genomic RNA and all sg (+) strand mRNAs. We included RNA from MHV-infected cells to obtain discrete size markers. Six distinct mRNAs are produced in HCoV-NL63 infected cells. The sizes of the RNA fragments were estimated and these values nicely fit the size of the genomic RNA and the five predicted sg mRNAs. All HCoV-NL63 ORFs that have the potential to encode viral proteins are indeed transcribed into sg mRNAs (Figure 7).

To determine the expression level of each subgenomic RNA, we measured the intensity of the signals. When plotted as a function of the genome position (Figure 8), there appears a correlation between the relative distance of a gene to the 3′ terminus and its RNA expression level, with the exception of the E gene.

Discussion

We analyzed the nucleotide composition of the HCoV-NL63 genomic (+) RNA, which was found to exhibit a typical coronavirus pattern with an abundance of U (39%) and shortage of G (20%) and C (14%). In fact, HCoV-NL63 has the most pronounced nucleotide bias among the *Coronaviridae*.

There is a significant fluctuation in the nucleotide count among the HCoV-NL63 genes. For instance, ORF3 and M appear as extreme U-rich and A-poor islands. It is possible that the unique nucleotide composition of some structural genes reflects their evolutionary origin, perhaps suggesting that some of these functions were acquired recently from another viral or cellular origin by gene transfer. These properties mimic the pathogenicity islands of prokaryotic genomes[10]. Consistent with this gene transfer hypothesis is the observation that there is a lot of variation in the number and identity of the 3′ genes among *Coronaviridae*.

Inspection of the nucleotide composition along the genome indicates a bi-phasic pattern. The 5′ two-third of the genome encoding the 1ab polyprotein has a stable nucleotide count with the typical U>A>G>C order, but rather striking differences are observed in the 3′ one-third of the genome that encodes the structural proteins (Figure 2). Most notably, the C-count increases significantly at the expense of G and U. Grigoriev recently reported the typical nucleotide bias of coronaviral genomes and the switch in nucleotide count at two-thirds of the genome[9]. He performed an analysis based on cumulative GC-skew, and suggested that the drop in GC-ratio is in fact due to a decrease in G-count. However, inspection of the HCoV-NL63 nucleotide composition indicates that the switch is due to a sudden increase in C-count, with a slight drop in G-count. Inspection of other coronaviral genomes confirms that C goes up (with highest significance in group 1 coronaviruses) and G goes down (with highest significance in group 2 coronaviruses) at two-third of the viral genome (results not shown). Grigoriev presented a possible mechanistic explanation. He suggested that the 3′-terminal one-third of the viral genomic (-) strand is more likely to be single stranded because (-) sg mRNA synthesis on the (+) strand template frequently disrupts the protective duplex in that region. This would make this part of the (-) strand genome more vulnerable to C to U transitions, which would eventually lead to a decrease of the G-count on the (+) strand. This scenario explains the G decrease, but obviously is not consistent with the local increase in C-count. We therefore propose an alternative mechanism that is also dictated by the viral transcription

strategy. The central 1a/1b portion of the viral (+) strand genome is less likely to be annealed to complementary (-) strand during viral replication because most (-) strand RNAs are sub-genomic, which lack this 1a/1b domain. The 1a/1b portion of the genome thus becomes more vulnerable to C to U deamination, which correlates with the high U-count and the low C-count. Obviously, there may be many other cellular conditions and viral properties like higher amount of secondary structures on the 3' part of the genome that could have shaped the coronavirus genome over an evolutionary timescale, but this scenario explains the switch in nucleotide count at two-thirds of the viral genome.

We show that U-counts reach the highest values and C-counts the lowest values at the third position of the HCoV-NL63 codons (Figure 5). Analysis of the synonymous codon usage indicates that codons with a high U and A content are preferred over C and G rich codons (Table 1). Thus, the peculiar genome composition has a direct effect on the codon usage of HCoV-NL63, and possibly even an indirect effect on the amino acid composition of coronaviral proteins by affecting the non-synonymous codon usage[1,24,27]. The synonymous codon usage of HCoV-NL63 clearly differs from that in human cells. Thus, the genome may have been shaped by cytosine deamination over an evolutionary timescale, but it is possible that the translational machinery has restricted this genome drift because of the availability of tRNA molecules.

Inspection of the viral genome sequence led us to predict that the 1ab polyprotein is expressed from the genomic RNA and the 3' structural proteins and ORF3 from 5 distinct sg mRNAs. This was confirmed experimentally. We observed that sg mRNAs are more abundant when the corresponding TRS is located closer to the 3' end of the genome. The exception is formed by the E sg mRNA, which is relatively underexpressed. This may correlate with the low expression level of this protein. The general trend of increased gene expression along the genome has been reported previously for other coronaviruses[3]. A possible mechanistic explanation is that the viral polymerase density is reduced along the genome or that the polymerase becomes less susceptible to execute a transfer from body TRS to L TRS during extended (-) strand synthesis. Fine-tuning of the efficiency of the strand-transfer processes may be modulated by many other features, including the local sequence and structure of the core body TRS and its flanking regions. It was reported previously[25] that the core of the L TRS of group 1 coronaviruses is presented in the single stranded loop of a mini-hairpin. We found similar motif in HCoV-NL63 (results not shown). Although not excessively stable, this structural motif is predicted to fold as part of the complete leader sequence, and it may participate in the strand transfer process.

The core sequence AACUAAA is conserved in the L TRS and all body TRSs, except for the E gene that has a single mismatch AACUAUA. The presence of a

sub-optimal core sequence may in fact explain the lower than expected expression level of this sg mRNA (Figure 8). But there is another striking feature of the E body TRS: it has 13 additional upstream nucleotides in common with the leader TRS. If one assumes that strand transfer does not occur at the core sequence but up to 13 nucleotides further upstream, this sequence homology will result in additional base pairing interactions that may stimulate the strand transfer process. Thus, the extended TRS homology may compensate for the sub-optimal core element. A remarkably similar scenario of sub-optimal core and extended TRS is apparent in the E gene sequence of PEDV (results not shown). A further indication that the viral polymerase frequently copies beyond the core sequence is provided by the actual sequence of the M and N sg mRNAs, which apparently have copied the TRS nucleotide that flanks the core element of body TRS.

Acknowledgements
We thank Berend Jan Bosch and Peter Rottier for providing MHV infected cells and Alexander Nabatov and Barbara van Schaik for technical support.

References

1. Berkhout, B. and F. J. van Hemert. 1994. The unusual nucleotide content of the HIV RNA genome results in a biased amino acid composition of HIV proteins. Nucleic Acids Res. 22:1705-1711.
2. de Haan, C. A., P. S. Masters, X. Shen, S. Weiss, and P. J. Rottier. 2002. The group-specific murine coronavirus genes are not essential, but their deletion, by reverse genetics, is attenuating in the natural host. Virology 296:177-189.
3. de Haan, C. A., L. van Genne, J. N. Stoop, H. Volders, and P. J. Rottier. 2003. Coronaviruses as vectors: position dependence of foreign gene expression. J. Virol. 77:11312-11323.
4. Drosten, C., S. Gunther, W. Preiser, S. van der Werf, H. R. Brodt, S. Becker, H. Rabenau, M. Panning, L. Kolesnikova, R. A. Fouchier, A. Berger, A. M. Burguiere, J. Cinatl, M. Eickmann, N. Escriou, K. Grywna, S. Kramme, J. C. Manuguerra, S. Muller, V. Rickerts, M. Sturmer, S. Vieth, H. D. Klenk, A. D. Osterhaus, H. Schmitz, and H. W. Doerr. 2003. Identification of a novel coronavirus in patients with severe acute respiratory syndrome. N. Engl. J. Med. 348:1967-1976.
5. Gagneten, S., O. Gout, M. Dubois-Dalcq, P. Rottier, J. Rossen, and K. V. Holmes. 1995. Interaction of mouse hepatitis virus (MHV) spike glycoprotein with receptor glycoprotein MHVR is required for infection with an MHV strain that expresses the hemagglutinin-esterase glycoprotein. J. Virol. 69:889-895.
6. Gibbs, A. J., M. J. Gibbs, and J. S. Armstrong. 2004. The phylogeny of SARS coronavirus. Arch. Virol. 149:621-624.
7. Giedroc, D. P., C. A. Theimer, and P. L. Nixon. 2000. Structure, stability and function of RNA pseudoknots involved in stimulating ribosomal frameshifting. J. Mol. Biol. 298:167-185.
8. Grigoriev, A. 1999. Strand-specific compositional asymmetries in double-stranded DNA viruses. Virus Res. 60:1-19.
9. Grigoriev, A. 2004. Mutational patterns correlate with genome organization in SARS and other coronaviruses. Trends Genet. 20:131-135.
10. Hacker, J. and J. B. Kaper. 2000. Pathogenicity islands and the evolution of microbes. Annu. Rev. Microbiol. 54:641-679.
11. Herold, J. and S. G. Siddell. 1993. An 'elaborated' pseudoknot is required for high frequency frameshifting during translation of HCV 229E polymerase mRNA. Nucleic Acids Res. 21:5838-5842.
12. Hiscox, J. A., K. L. Mawditt, D. Cavanagh, and P. Britton. 1995. Investigation of the control of coronavirus subgenomic mRNA transcription by using T7-generated negative-sense RNA transcripts. J. Virol. 69:6219-6227.

13. Hofmann, M. A., R. Y. Chang, S. Ku, and D. A. Brian. 1993. Leader-mRNA junction sequences are unique for each subgenomic mRNA species in the bovine coronavirus and remain so throughout persistent infection. Virology 196:163-171.
14. Konings, D. A., P. J. Bredenbeek, J. F. Noten, P. Hogeweg, and W. J. Spaan. 1988. Differential premature termination of transcription as a proposed mechanism for the regulation of coronavirus gene expression. Nucleic Acids Res. 16:10849-10860.
15. Ksiazek, T. G., D. Erdman, C. S. Goldsmith, S. R. Zaki, T. Peret, S. Emery, S. Tong, C. Urbani, J. A. Comer, W. Lim, P. E. Rollin, S. F. Dowell, A. E. Ling, C. D. Humphrey, W. J. Shieh, J. Guarner, C. D. Paddock, P. Rota, B. Fields, J. DeRisi, J. Y. Yang, N. Cox, J. M. Hughes, J. W. LeDuc, W. J. Bellini, and L. J. Anderson. 2003. A novel coronavirus associated with severe acute respiratory syndrome. N. Engl. J. Med. 348:1953-1966.
16. Kuiken, T., R. A. Fouchier, M. Schutten, G. F. Rimmelzwaan, G. van Amerongen, D. van Riel, J. D. Laman, T. de Jong, G. van Doornum, W. Lim, A. E. Ling, P. K. Chan, J. S. Tam, M. C. Zambon, R. Gopal, C. Drosten, S. van der Werf, N. Escriou, J. C. Manuguerra, K. Stohr, J. S. Peiris, and A. D. Osterhaus. 2003. Newly discovered coronavirus as the primary cause of severe acute respiratory syndrome. Lancet 362:263-270.
17. Nakane, S., S. Shirabe, R. Moriuchi, A. Mizokami, T. Furuya, Y. Nishiura, S. Okazaki, N. Yoshizuka, Y. Suzuki, T. Nakamura, S. Katamine, T. Gojobori, and K. Eguchi. 2000. Comparative molecular analysis of HTLV-I proviral DNA in HTLV-I infected members of a family with a discordant HTLV-I-associated myelopathy in monozygotic twins. J. Neurovirol. 6:275-283.
18. Rota, P. A., M. S. Oberste, S. S. Monroe, W. A. Nix, R. Campagnoli, J. P. Icenogle, S. Penaranda, B. Bankamp, K. Maher, M. H. Chen, S. Tong, A. Tamin, L. Lowe, M. Frace, J. L. DeRisi, Q. Chen, D. Wang, D. D. Erdman, T. C. Peret, C. Burns, T. G. Ksiazek, P. E. Rollin, A. Sanchez, S. Liffick, B. Holloway, J. Limor, K. McCaustland, M. Olsen-Rasmussen, R. Fouchier, S. Gunther, A. D. Osterhaus, C. Drosten, M. A. Pallansch, L. J. Anderson, and W. J. Bellini. 2003. Characterization of a novel coronavirus associated with severe acute respiratory syndrome. Science 300:1394-1399.
19. Sawicki, S. G. and D. L. Sawicki. 1990. Coronavirus transcription: subgenomic mouse hepatitis virus replicative intermediates function in RNA synthesis. J. Virol. 64:1050-1056.
20. Sawicki, S. G. and D. L. Sawicki. 1998. A new model for coronavirus transcription. Adv. Exp. Med. Biol. 440:215-219.
21. Sethna, P. B., S. L. Hung, and D. A. Brian. 1989. Coronavirus subgenomic minus-strand RNAs and the potential for mRNA replicons. Proc. Natl. Acad. Sci. U. S. A 86:5626-5630.
22. Snijder, E. J., P. J. Bredenbeek, J. C. Dobbe, V. Thiel, J. Ziebuhr, L. L. Poon, Y. Guan, M. Rozanov, W. J. Spaan, and A. E. Gorbalenya. 2003. Unique and conserved features of genome and proteome of SARS-coronavirus, an early split-off from the coronavirus group 2 lineage. J. Mol. Biol. 331:991-1004.
23. Spaan, W., H. Delius, M. Skinner, J. Armstrong, P. Rottier, S. Smeekens, B. A. van der Zeijst, and S. G. Siddell. 1983. Coronavirus mRNA synthesis involves fusion of non-contiguous sequences. EMBO J. 2:1839-1844.
24. Sueoka, N. 1961. Correlation between base composition of deoxyribonucleic acid and amino acid composition of protein. Proc. Natl. Acad. Sci. U. S. A 47:1141-1149.
25. Van Den Born, E., A. P. Gultyaev, and E. J. Snijder. 2004. Secondary structure and function of the 5′-proximal region of the equine arteritis virus RNA genome. RNA. 10:424-437.
26. van der Hoek, L., K. Pyrc, M. F. Jebbink, W. Vermeulen-Oost, R. J. Berkhout, K. C. Wolthers, P. M. Wertheim-van Dillen, J. Kaandorp, J. Spaargaren, and B. Berkhout. 2004. Identification of a new human coronavirus. Nat. Med. 10:368-373.
27. van Hemert, F. J. and B. Berkhout. 1995. The tendency of lentiviral open reading frames to become A-rich: constraints imposed by viral genome organization and cellular tRNA availability. J. Mol. Evol. 41:132-140.
28. Zhang, X., D. R. Hinton, S. Park, B. Parra, C. L. Liao, M. M. Lai, and S. A. Stohlman. 1998. Expression of hemagglutinin/esterase by a mouse hepatitis virus coronavirus defective-interfering RNA alters viral pathogenesis. Virology 242:170-183.

Chapter IV

Molecular characterization of human coronavirus NL63

Recent Research in Development of Infection & Immunity, 2005, vol. 3 p. 25-48

Krzysztof Pyrc, Ben Berkhout and Lia van der Hoek

Laboratory of Experimental Virology, Department of Medical Microbiology, Center for Infection and Immunity Amsterdam (CINIMA), Academic Medical Center, University of Amsterdam, Meibergdreef 15, 1105 AZ, Amsterdam, The Netherlands.

Before the SARS outbreak only 2 human coronaviruses (HCoV) were known: HCoV-OC43 and HCoV-229E. With the discovery of SARS-CoV, the third family member was identified. Soon thereafter the fourth human coronavirus (HCoV-NL63) was discovered in the Netherlands and in 2005 a team from the University of Hong Kong reported the finding of the fifth coronavirus, CoV-HKU1. It is now known that, among all human coronaviruses, infection with HCoV-NL63 occurs most frequently. HCoV-NL63 has spread worldwide and infection is associated with acute respiratory tract disease and intriguingly, might also be associated with Kawasaki disease. Coronaviruses possess extremely large plus-strand RNA genomes and employ unique mechanisms for replication, which separate them from all other RNA viruses. In this report we review the molecular characteristics of HCoV-NL63 in comparison to the other coronaviruses, in particular the closest relatives HCoV-229E and porcine epidemic diarrhea virus (PEDV).

Introduction

Coronaviruses, a genus of the *Coronaviridae* family, are enveloped viruses with a large plus-strand RNA genome. The genomic RNA is 27-32 kb in size, capped and polyadenylated. Coronaviruses have been identified in bats, mice, rats, chickens, turkeys, swine, dogs, cats, rabbits, horses, cattle and humans and cause highly prevalent diseases such as respiratory, enteric, cardiovascular and neurological disorders[31,50,59]. Originally, coronaviruses were classified on the basis of antigenic cross-reactivity, and in this manner three antigenic groups were recognized[43,59]. When coronavirus genome sequences began to accumulate, the original antigenic groups were converted into genetic groups based on similarity of the nucleotide sequences (Figure 1).

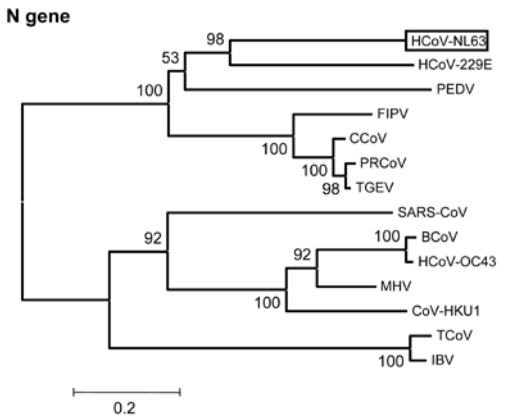


Figure 1. Phylogenetic analysis of the N gene of HCoV-NL63. Numbers on the root of each branch represent the bootstrap value. HCoV-229E: human coronavirus 229E; PEDV: porcine epidemic diarrhea virus; FIPV: feline infectious peritonitis virus; CCoV: canine coronavirus; PRCoV: porcine respiratory coronavirus; TGEV: transmissible gastroenteritis virus; SARS-CoV: severe acute respiratory syndrome coronavirus; BCoV: bovine coronavirus; HCoV-OC43: human coronavirus OC43; MHV: murine hepatitis virus; CoV-HKU1: human coronavirus HKU1; TCoV: turkey coronavirus; IBV: avian infectious bronchitis virus.

Table 1. Open reading frames present in the HCoV-NL63 genome.

ORF	protein name	position in genome (nt)	length (nt)	length (aa)	frame
1	1a	287-12439	12153	4050	+2
1,2	1a/1b	287-20475	20190	6729	+2/+1
3	Spike (S)	20472-24542	4071	1356	+3
4	ORF3	24542-25219	678	225	+2
5	Envelope (E)	25200-25433	234	77	+3
6	Membrane (M)	25442-26122	681	226	+2
7	Nucleocapsid (N)	26133-27266	1134	377	+3

Until recently only two human coronaviruses (HCoV) were known, HCoV-229E and HCoV-OC43, representatives of the group 1 and 2 coronaviruses, respectively. Both were identified in the 1960s and are generally considered to be common cold viruses[1,12,51,54,71,90,125,128]. An outbreak of severe acute respiratory syndrome (SARS) in the spring of 2003 (the outbreak started on November 2002 and had a peak in March 2003) led to the rapid identification of SARS-CoV[28,47,69], which is considered to be a distinct member of the group 2 coronaviruses[41] or the first member of a new group 4[111,121]. SARS-CoV is the most pathogenic human coronavirus identified thus far[73,103]. SARS-CoV is likely to reside in an animal reservoir, and has recently initiated the outbreak in humans through zoonotic transmission[49,85].

HCoV-NL63 was identified in 2003 in a child with bronchiolitis in the Netherlands[129]. Recent reports from several countries (Australia, Japan, Canada, Belgium) indicate that the virus has spread worldwide. The virus is found mainly in young children, elderly and immunocompromised patients with acute respiratory illness during the winter season[5,10,29,37,89,129]. Recent data suggest an association of HCoV-NL63 infection with Kawasaki disease[33], a systemic vasculitis in childhood that may result in aneurysms of the coronary arteries. In the developed world, Kawasaki disease is the most common cause of acquired heart disease in children[65,113]. Further analysis of HCoV-NL63 pathogenicity seems warranted, in particular because of recent evidence that this virus uses the same cellular receptor as SARS-CoV[58].

Genome organization and transcription

Gene order in the HCoV-NL63 genome

The HCoV-NL63 genome encompasses 27553 nucleotides. The RNA genome is predicted to contain seven functional open reading frames flanked by untranslated regions at the 5′ and 3′ ends (Table 1)[107,129]. The two large 5′ terminal ORF's 1a and 1b encode non-structural proteins that are required for viral replication (Table 2)[40]. Remaining ORF's in the 3′ part of the genome encode the four structural proteins S, E, M and N and an accessory ORF3 protein (Figure 2)[107,129].

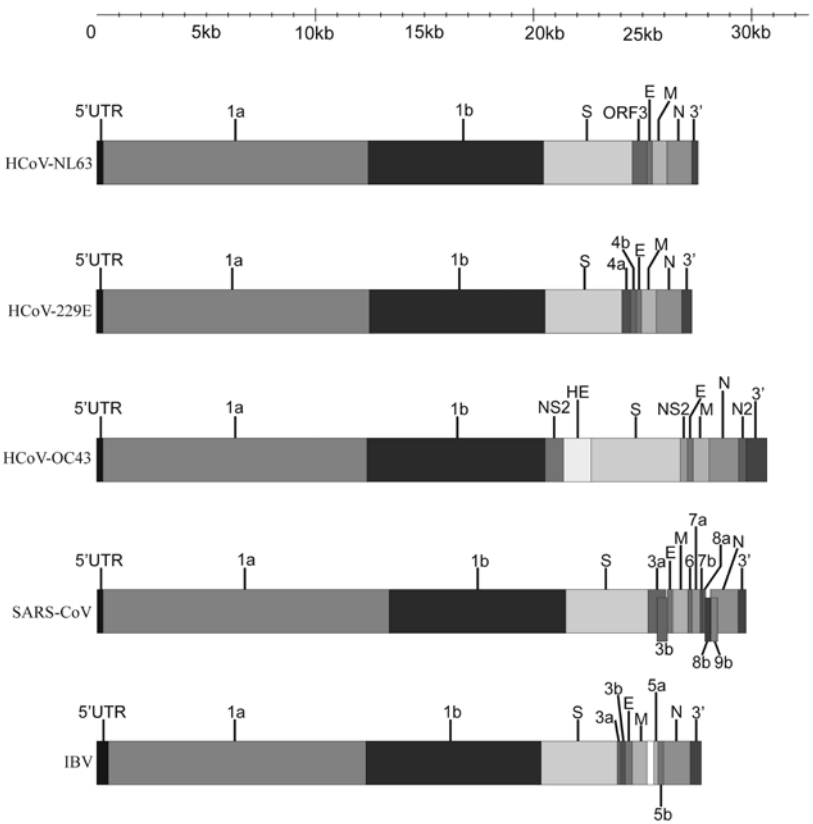


Figure 2. Genome organization of *Coronaviridae* **family members.**

Generation of subgenomic mRNAs employing the discontinuous transcription mechanism

Coronavirus replication is a complex, not yet fully understood mechanism. The 5′ end of the HCoV-NL63 genomic RNA contains the untranslated leader (L) sequence of 72 nucleotides that ends with the L TRS element. The L TRS is very similar to sequences that can be found in front of each open reading frame (body TRSs). The RNA-dependent RNA-polymerase (RdRp) has been proposed to pause after a body TRS of a particular gene is copied during (-) strand synthesis, subsequently switching to the L TRS and thus adding a common L sequence to each (-) strand subgenomic (sg) mRNA. This discontinuous transcription mechanism is based on base-pairing of the nascent (-) strand copy RNA with the (+) strand L TRS. The nested set of (-) strand sg mRNAs is subsequently copied into a set of (+) strand sg mRNA by the RdRp.

Functional sg mRNAs contain at the 5′ terminus the common L sequence followed by the gene of interest with a TRS sequence derived from that particular gene[107,117,140]. HCoV-NL63 generates five distinct sg mRNAs during HCoV-NL63



Figure 3. Full length and sg mRNAs generated in HCoV-NL63 infected cells. The transcript length is indicated in nucleotides.

replication: S, ORF3, E, M and N, from which the corresponding proteins are expressed. The 1a/ab polyprotein is supposed to be translated from the genomic RNA (Figure 3)[107].

The efficiency of discontinuous transcription has been proposed to depend on the efficiency of base pairing of sense body and antisense leader TRS core sequences as well as on the sequences flanking the TRS[2,122,140]. Additionally, the transcription levels of a particular sg mRNA have been reported to be inversely related to the distance between the body TRS and the 3' end of the genome[107].

Translation and post-translational modification of HCoV-NL63 proteins

The frameshift signal

Ribosomal frameshifting in coronaviruses was the first described non-retroviral example of translational frameshifting in higher eukaryotes[14]. It is a mechanism of translational regulation in which a directed change of translational reading frame allows the synthesis of a single protein from two overlapping genes. In coronaviruses, frameshifting appears to be the mechanism for translation of the 1a/1b fusion polyprotein and is used to regulate the level of those replicative proteins[13,14]. Coronaviral ribosomal frameshifting is induced by a complex RNA structure called a pseudoknot, consisting of a hairpin of which the loop interacts with a sequence further downstream, and a slippery site upstream of the hairpin[14]. The pseudoknot structure in HCoV-229E was found to possess an extended loop 2 and stem 3 and was therefore called an "elaborated" pseudoknot and was shown to function as such in *in vitro* experiments[56]. Porcine epidemic diarrhea virus (PEDV) and transmissible gastroenteritis virus (TGEV), taxonomically clustering together with HCoV-NL63 in group 1, also possess a stem 2 region presented in a stable hairpin, although its function was not tested experimentally (Figure 4)[8,88,139]. In the HCoV-NL63 genome, the ribosomal frameshift site is located inside the RNA-dependent RNA-polymerase gene (Figure 5A). The predicted "elaborated" pseudoknot consists of a hairpin with a highly conserved 11 basepair stem, and a loop of 8 nucleotides that interacts with a sequence 167 nucleotides downstream (with 5 nucleotides basepairing) that is presented on a loop of the stem 3 hairpin. The heptanucleotide slippery UUUAAAC sequence is present just upstream of stem 1 at position nt 12433 (Figure 4).

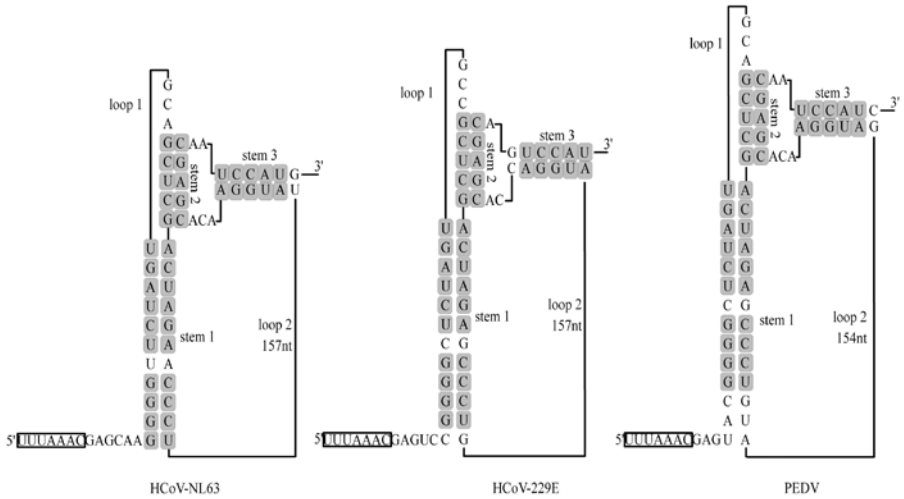


Figure 4. Predicted "elaborated" pseudoknot structures for the translational frameshift signal of HCoV-NL63 and its closest relatives HCoV-229E and PEDV. The slippery sequence UUUAAAC is marked with a box. The shading represents the interacting sites conserved among presented species.

Proteolytic processing of 1a/1b polyprotein

Similar to all other coronaviruses, HCoV-NL63 is supposed to employ post-translational proteolytic processing as a key regulatory mechanism in the expression of its replicative proteins[135-138]. In the genome of HCoV-NL63 two proteinases can be predicted in the 5′ region of the 1a/1b polyprotein. First, papain-like proteinase (PL^{pro}) is encoded in the non-structural protein (nsp) 3 gene situated near the 5′ terminus of the genome (Figure 5A; Table 2,3). The papain-like proteinase of HCoV-NL63 consists of two domains: $PL1^{pro}$ and $PL2^{pro}$, and both are expected to have catalytic activity[7,55,138]. The enzyme is predicted to cleave the 1a/1b protein at three sites between nsp1|nsp2; nsp2|nsp3; nsp3|nsp4, releasing the functional papain-like proteinase protein (nsp3) molecule by auto-cleavage[40]. Analysis of cleavage sites recognized by PL^{pro} of HCoV-NL63 indicates that this enzyme has the specificity to cut between two small amino acids with short uncharged side chains, similar to homologous enzymes in other species from the *Coronaviridae* family[80,135-137] (Figure 6A).

Coronaviral PL^{pro} is expected to be a multi-functional protein with several catalytic domains that mediate different enzymatic activities. The conserved catalytic Cys-His dyad that mediates the proteolysis is present at positions Cys_{164} - His_{314} for $PL1^{pro}$ and Cys_{780} - His_{938} for $PL2^{pro}$ (numbers represent the position in the PL^{pro} protein). Sequence similarity between coronaviral PL^{pro} and other proteinases like the leader proteinase of the picornavirus foot-and-mouth-disease virus can be found at these active sites[46]. The second catalytic domain predicted to be present in HCoV-NL63 PL^{pro} is an ADRP (aa 367-493) domain, a distant homologue of the cellular adenosine diphosphate-ribose 1′′-phosphatase

Table 2. Predicted proteins generated during proteolytical processing of the HCoV-NL63 1a/1b polyprotein.

protein	position in the genome (nt)	position in 1a/1b polyprotein (aa)	length(aa)	cleavage site	processing enzyme
nsp1	287-616	1-110	110	FGHGAG|SVVFVD	PL^{pro}
nsp2	617-2980	111-898	788	FTKLAG|GKISFS	PL^{pro}
nsp3; PL^{pro}	2981-7672	899-2462	1564	VAKQGA|GFKRTY	PL^{pro}
nsp4	7673-9103	2463-2939	477	YNSTLQ|SGLKKM	M^{pro}
nsp5; M^{pro}	9104-10012	2940-3242	303	YGVNLQ|SGKVIF	M^{pro}
nsp6	10013-10849	3243-3521	279	KISTVQ|SKLTDL	M^{pro}
nsp7	10850-11098	3522-3604	83	NSSTLQ|SVASSF	M^{pro}
nsp8	11099-11683	3605-3799	195	RVVKLQ|NNEIMP	M^{pro}
nsp9	11684-12010	3800-3908	109	ATIRLQ|AGKQTE	M^{pro}
nsp10	12011-12415	3909-4043	135	DRTTIQ|SVDISY	M^{pro}
nsp12; RdRp	12416-15195	4044-4970	927	NSTILQ|AAGLCV	M^{pro}
nsp13; MBD, NTPase, Helicase	15196-16986	4971-5567	597	KHADLH|SSQVCG	M^{pro}
nsp14; ExoN	16987-18540	5568-6085	518	IETNLQ|SLENIA	M^{pro}
nsp15; NendoU	18541-19572	6086-6429	344	FYPQLQ|SAEWKC	M^{pro}
nsp16; 2'-O-MT	19573-20472	6430-6729	300	-	-

protein[86]. Additionally, several features suggest that the NL63-PL^{pro} protein might participate in processing of viral RNA e.g. presence of the zinc-finger-like structures (aa 236-278 for $PL1^{pro}$ and aa 859-901 for $PL2^{pro}$) with a conserved $CX_{1-2}CX_{22-31}CX_{1-2}$-[CH] pattern, where X can be any amino acid (Figure 5B, 5C). Several reports show the involvement of PL^{pro} in RNA processing and as an indispensable factor for mRNA synthesis[120,127].

The second proteinase of HCoV-NL63 is encoded by the nsp5 gene. It has a predicted serine-like proteinase activity and is designated "the main proteinase" (M^{pro}) to stress its dominant function (Figure 5A, Table 2). On the level of primary and secondary structure, NL63-M^{pro} is closely related to M^{pro} of HCoV-229E (Table 3). M^{pro} processes the majority of cleavage sites between non-structural proteins in the 1a/1b polyprotein (Figure 5A). The order of cleavage sites was found to be conserved among coronaviruses and appears to depend on the accessibility of specific sites in the context of the polyprotein[105]. Analysis of the cleavage sites of M^{pro} suggests altered substrate specificity of NL63-M^{pro} comparing to homologous enzymes from other *Coronaviridae* species (Figure 6B). Different from any other coronavirus, the cleavage site between nsp13 and nsp14 contains a histidine residue at position P1 instead of glutamine, which is conserved among all other species[35,53,136]. This observation was confirmed for three different HCoV-NL63 isolates (Amsterdam 1, Amsterdam 57 (unpublished results) and NL)[37,129].

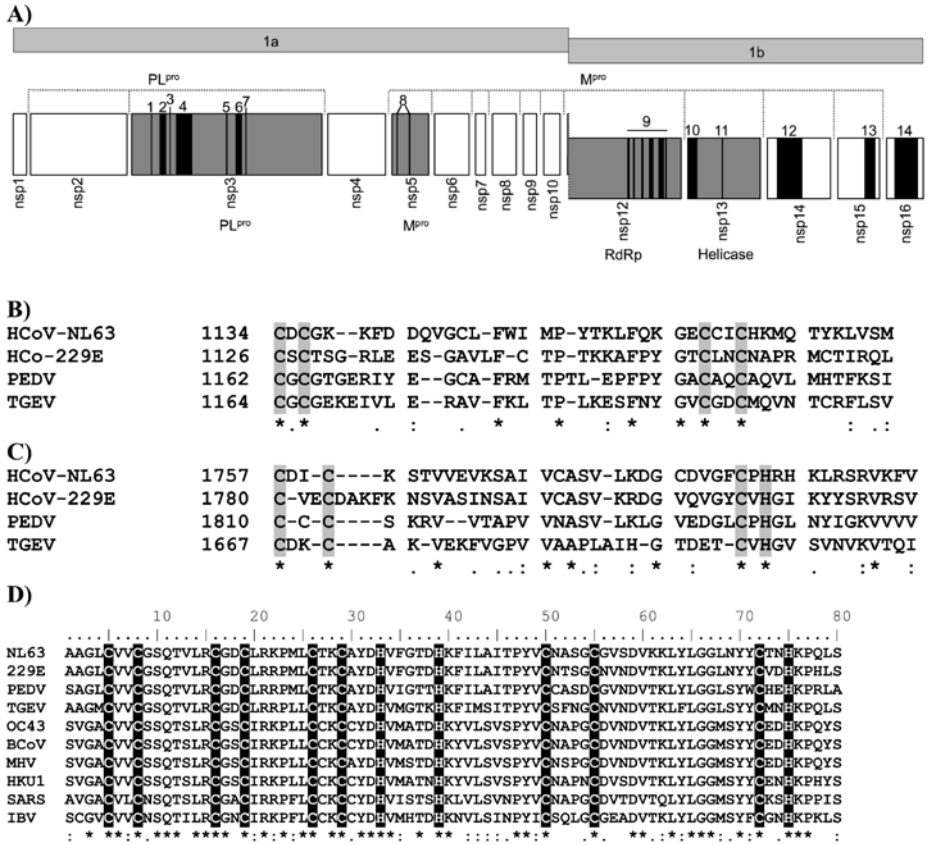


Figure 5. HCoV-NL63 1ab polyprotein A) Organization of the 1a/1b polyprotein of HCoV-NL63. Numbers above the graph represents the domains identified in the genome of HCoV-NL63; 1,3: Cys/His catalytic dyad in PL1^{pro} domain; 2: Zinc finger structure in PL1^{pro} domain; 4: ADRP domain; 5,7 : Cys/His catalytic dyad in PL2^{pro} domain; 6: Zinc finger structure in PL2^{pro} domain; 8: His/ Cys catalytic dyad in Mpro domain; 9:RdRp domains: thumb, fingers, A, B, C, D, E; 10: binuclear zinc-binding cluster in helicase gene; 11: ATP/GTP binding site in helicase gene; 12: Exon domain; 13: NendoU domain; 14: 2′-O-MT domain. The gray regions represent the proteins described in detail in the text. B) Alignment of the zinc finger motif region in the PL1^{pro} domain. C) Alignment of the zinc finger motif region in the PL2^{pro} domain. D) Alignment of the metal binding domain region in the helicase protein. Black shading represents residues participating in catalytic activity of the motif; "*" represents amino acids conserved among all group 1 species; ":" and "." represents partially conserved sites.

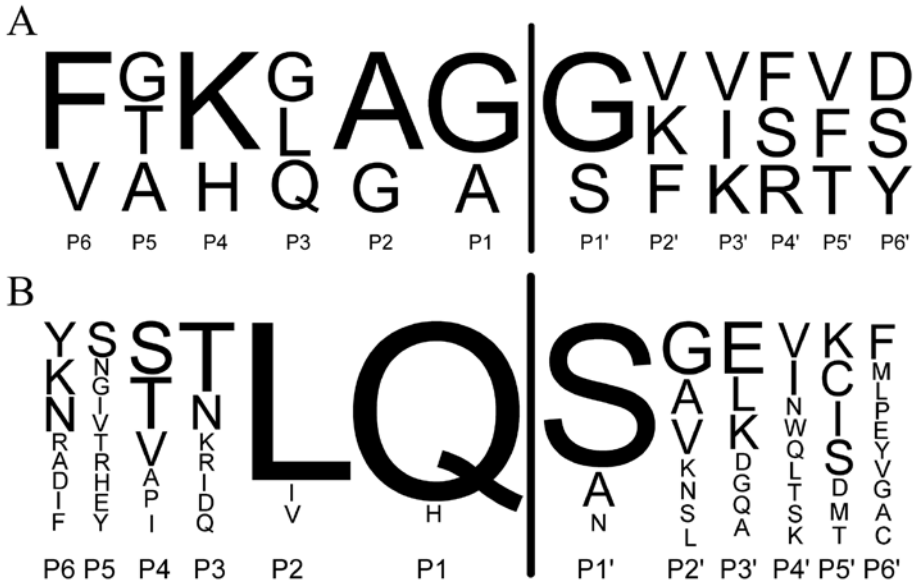


Figure 6. Substrate specificity of HCoV-NL63 PL^{pro} (A) and M^{pro} (B). The vertical line indicates the predicted cleavage site. Letter size corresponds to the frequency of a particular amino acid at the given position.

Table 3. Characteristics of HCoV-NL63 proteins

protein	size [kDa]	theoretical pI	total charge	similarity to HCoV-229E	
				nucleotide level	protein level (identities /similarities)
PL^{pro}	173.97	5.70	-24	60%	51% / 69%
M^{pro}	32.73	6.39	-3	70%	71% / 85%
RdRp	105.50	6.02	-11	76%	81% / 91%
Hel	66.30	8.83	+16	78%	87% / 95%
ORF3	25.66	7.62	-1	44%	43% / 67%
S	149.85	6.83	-2	56%	55% / 71%
E	9.18	6.50	0	59%	47% / 79%
M	25.93	9.21	+6	64%	62% / 78%
N	42.25	9.78	+16	53%	43% / 67%

This unique feature might suggest altered substrate specificity or the absence of a cleavage site. For instance, alteration of the consensus M^{pro} cleavage sequence LQ|(A,S,G) for M^{pro} derived from other coronaviruses resulted in significantly reduced cleavage efficiencies in most cases[35,52,136].

Viral proteins involved in transcription of HCoV-NL63

RNA-dependent-RNA polymerase

Similar to all coronaviruses, HCoV-NL63 encodes an RNA-dependent RNA polymerase (RdRp) (Table 2,3). The RdRp gene (nsp12) is located partially in the 1a protein and mostly in the 1b protein[40,78,119,121]. It is expressed as one protein through the ribosomal frameshift described above (Figure 5A).

For all known positive-strand RNA viruses, RNA polymerase activity is mediated by viral RdRp in replication complexes that are associated with cellular membranes in the host cell cytoplasm[78,131]. The function of RdRp protein has been predicted and membrane-associated RdRp activity has been detected in coronavirus-infected cells, but the enzymatic activity of this putative enzyme has not yet been confirmed experimentally[4,13,48,69,119].

The overall structure of coronaviral RdRp polymerase resembles a right hand structure[133]. The palm domain is remarkably similar to the palm domain of other polymerases (reverse transcriptase, DNA dependent DNA polymerase, DNA dependent RNA polymerase) and contains the four amino acid sequence motifs named A, B, C, D and an additional E motif that is unique for RdRp (Figure 5A). The region located in the 1b protein contains motifs that are conserved for all RdRps, including an RNA-binding motif and a catalytic Ser-Asp-Asp (SDD) core motif (aa 754-756) typical for members of the *Coronaviridae* family[69,118,129].

Helicase

The coronaviral helicase domain was previously identified and shown to be enzymatically active and to efficiently unwind double stranded DNA and RNA[63,126]. The helicase domain of HCoV-NL63 is encoded in ORF1b by the nsp13 gene, which is located downstream of the RdRp gene (nsp12) (Figure 5A, Table 2,3). This arrangement is unique for coronaviruses, as the helicase domain generally precedes RdRp in the replicase polyprotein[67].

Coronaviral helicase was previously reported to share sequences with the superfamily 1 helicases[119]. This enzyme family is common among viruses, being encoded by e.g. alphaviruses, rubiviruses, hepatitis E viruses and arteriviruses[44,45]. Biochemical and genetic data suggest a role of these proteins in diverse aspects of viral replication: transcription, RNA stability, cell-to-cell movement and virus biogenesis[27,64,97,98,101,104,112]. Nidoviral helicase proteins are unique among the positive-stranded RNA viruses because of the presence of an N-terminal

binuclear zinc-binding cluster. This cluster consists of 12 conserved Cys/His residues, arranged in the HCoV-NL63 helicase protein at aa position 5-75[45,57] (Figure 5D). The zinc-binding domain of the arterivirus helicase was previously shown to be involved in diverse processes of the viral life cycle[130].

Another domain linked to the helicase function is an ATP/GTP binding domain motif A (P-loop) at position aa 283-290 of nsp13 (GPPGSGKS). It is a glycine-rich region, which typically forms a flexible loop that interacts with one of the phosphate groups of the nucleotide. Additionally, several motifs similar to structures known to be involved in nucleic acid interaction are present in the HCoV-NL63 helicase protein: a fork head domain (aa 76-89; 80% similarity), a ribosome-binding factor A signature (aa 187 - 208; 70% similarity), and a ribosomal protein S4 motif (aa 488 to 512; 67% similarity)[20].

Other proteins involved in virus replication

The list of putative enzymes involved in coronavirus RNA processing was recently extended by identification of new conserved coronaviral RNA processing domains[121]. A similar analysis for HCoV-NL63 suggests that those domains also exist in the 1a/1b polyprotein of HCoV-NL63. This includes a 3′ to 5′ exonuclease (ExoN) of the DEDD superfamily[141] that is predicted in nsp14 of HCoV-NL63[34]. A poly(U)-specific endoribonuclease NendoU (homologue of XendoU of Xenopus laevis) is predicted in the C-terminal part of nsp15[75], sharing sequences with HCoV-229E NendoU[62]. An S-adenosylmethionine-dependent ribose 2′-O-methylotransferase (2′-O-MT) of the Rrmj family is present in nsp16[16,34], and ADRP domain described above is encoded in PL^{pro} (nsp5)[34,86]. ExoN, XendoU and 2′-O-MT coding regions are arranged in 1a/1b polyprotein gene as a single block downstream of the ribosomal frameshift site and RdRp and helicase domains. The activities of these enzymes resemble the cellular RNA processing pathway leading to the generation of small nucleolar RNAs that guide specific 2′-O-ribose methylation of rRNA (Figure 5A, Table 2)[36,66,121].

Structural proteins of HCoV-NL63

The spike protein

Spike protein (S) of HCoV-NL63 is a large, probably highly glycosylated (Table 4) structural protein that is responsible for the receptor recognition and host cell entry. During incorporation into the viral envelope and budding, the S protein probably interacts with the M protein by its transmembrane and C-terminal region[26,42,99,100]. NL63-S is most similar to 229E-S (Table 3). HCoV-229E uses human aminopeptidase N (APN) as the receptor for viral entry. Other group 1 viruses like TGEV and FIPV also use porcine APN and feline APN, respectively. Surprisingly, NL63-S does not use hAPN. Instead NL63-S interacts with angiotensin converting enzyme 2 (ACE2) and this surface molecule serves as a receptor for HCoV-NL63[58]. The only other coronavirus that employs this receptor is SARS-CoV[79].

Table 4. Predicted N-glycosylation sites in the HCoV-NL63 S protein. Method for analysis will be published by Gupta et al., manuscript in preparation.

position in S protein (aa)	probability of N-glycosylation	
24	+	
35	+	
52	+	
98	+	
111	+	
119	+	
155	+++	Unique spike insert of HCoV-NL63
178	+	
187	+	
193	+	
203	++	
240	+	
276	+	
301	++	
330	+	
354	+	
358	+	
403	+	
426	++	S1 domain
486	+	
506	++	
512	+	
629	+	
645	-	
666	-	
699	+	
723	+	
749	-	
762	+	
768	-	
844	++	
852	++	
1111	+	
1196	+	
1201	-	
1218	++	S2 domain
1242	-	
1247	++	
1277	-	

The spike protein of HCoV-NL63 is organized as follows: an N-terminal S1 domain that has been reported to contain the receptor-recognition site for other coronaviruses[17,39,74]. The S2 domain contains two heptad repeat regions (HR1 and HR2), probably mediating virus-cell membrane fusion[30]. Towards the C-terminus of the S protein, a single transmembrane domain and a short cytoplasmic tail with a C-terminal cysteine cluster are located. The S1 domain of coronaviruses form the globular head of the spike, whereas the S2 subunit constitutes the stalk-like region[24].

The S1 domain

The S1 domain of HCoV-NL63 contains an N-terminal signal peptide[11,96], similar to other coronaviruses[70,84,111], with the cleavage site between amino acid 15 and 16. A unique feature of HCoV-NL63 spike protein is an 179 amino acid "insert" that has no significant similarity to any known sequence[129]. TGEV-S protein also contains an N-terminal insert that is involved in sialic acid binding and that is not present in the S protein of porcine respiratory coronavirus (PRCoV). This results in altered PRCoV pathogenicity and tissue tropism[77,114-116]. The insert in NL63-S might also be involved in receptor or co-receptor recognition.

The S2 domain

The S2 domain of coronaviral spike proteins is thought to contain a fusion peptide[18,82] and two 4,3 hydrophobic heptad repeat (HR) regions designated HR1 and HR2[24]. HR regions are found in fusion proteins of many different viruses and form an important characteristic of class I viral fusion proteins. The NL63-HR structures are located in the spike protein between aa 949-1064 (HR1) and 1234-1293 (HR2). These two HR regions are relatively conserved in position and sequence among the members of the three coronavirus antigenic clusters. They are thought to undergo a conformational switch during virus entry, forming a stable rod-like structure. The fusion peptide inserts into the cell membrane during the fusion event, and the conformational switch results in juxtapositioning of the cellular and viral membrane to facilitate virion-cell fusion[30].

Transmembrane domain and C-terminal domain

the S protein of HCoV-NL63 is predicted to span the viral membrane once, with a highly hydrophobic, α-helical transmembrane domain (aa 1297-1319) dipped in the membrane and the cysteine-rich C-terminal domain located inside the virion (37 C-terminal amino acids).

The ORF3 protein

All coronaviral genomes encode a variable number of accessory genes between the structural genes in the 3' one-third part of the genome. These genes show the highest variation among coronaviral genes. HCoV-NL63 contains one accessory protein of 225 aa that is encoded by the ORF3 gene (Table 1). The ORF3 protein

```
                          10        20        30        40        50        60
                    ....|....|....|....|....|....|....|....|....|....|....|....|
HCoV-229E 4a        1   MALG-LFTLQLVSAVNQSLSNAKVSAEVSRQVIQDVKDGTVTFNLLAYTLMSLFVVYFAL 59
HCoV-NL63 ORF3      1   MPFGGLFQLTLESTINKSVANLKLPPHDVTVLRDNLKPVTTLSTITAYLLVSLFVTYFAL 60
HCoV-229E 4b        1   ------------------------------------------------------------ 1

                          70        80        90       100       110       120
                    ....|....|....|....|....|....|....|....|....|....|....|....|
HCoV-229E 4a        60  FKARSHRGRAALIVFKILILFVYVPLLYWSQAYIYATLIAVILLGRFFHTAWHCWLYKTW 119
HCoV-NL63 ORF3      61  FKPLTARGRVACFVLKLLTLFVYVPLLVLFGMYLDSFIIFSTLLFRFIHVGYYAYLYKNF 120
HCoV-229E 4b        1   ------------------------------------------------------------ 1

                         130       140       150       160       170       180
                    ....|....|....|....|....|....|....|....|....|....|....|....|
HCoV-229E 4a        120 DFIVFNVTTLCYAR--------------------------------------------133
HCoV-NL63 ORF3      121 SFVLFNVTKLCFVSGKCWYLEQSFYENRFAAIYGGDHYVVLGGETITFVSFDDLYVAIRG 80
HCoV-229E 4b        1   ------------MQGKCWFLENKALKP-FVCFYGGDQFLYIGDRIVSYFSTNDLYVALRG 47

                         190       200       210       220
                    ....|....|....|....|....|....|....|....|
HCoV-229E 4a        ----------------------------------------
HCoV-NL63 ORF3      181 SCEKNLQLMRKVDLYNGAVIYIFAEEPVVGIVYSSQLYEDVPSIN 225
HCoV-229E 4b        48  RIDKDLSLSRKVELYNGECVYLFCEHPAVGIVN-TDFKLEIH--- 88
```

Figure 7. Sequence alignment of the ORF3 protein of HCoV-NL63 and the 4a and 4b proteins of HCoV-229E.

is significantly hydrophobic (leucine: 14.7%, valine: 11.1%) with a moderate negative charge that may suggest the presence of transmembrane domains (Table 3). ORF3 protein is expected to span the membrane three times, with predicted transmembrane regions at aa positions 39-61, 70-92, 97-116 with the C terminus on the cytosolic side[68,123]. It is not known whether ORF3 protein of HCoV-NL63 is a structural protein that is incorporated into the virion similar to the 3a protein of SARS-CoV[61]. ORF3 protein has the highest homology to ORF4a and ORF4b of HCoV-229E and the protein alignment shows that although conservation is poor, NL63-ORF3 looks like a fusion protein of ORF4a and ORF4b (Figure 7). The similarity of NL63-ORF3 to the 229E-4a and 229E-4b genes of HCoV-229E is low at the nucleotide level, with some regions of unknown origin. The function of the ORF3 protein is not known, but accessory murine hepatitis virus (MHV) proteins were previously shown to modulate viral pathogenicity[25].

The envelope protein E

The coronaviral E protein, also called small membrane protein, was previously reported to be a trans-membrane protein that is involved in the formation of the viral envelope, encapsidation and virus budding[81]. The E protein of HCoV-NL63 consists of 77 amino acids and is most similar to the E protein of HCoV-229E (Table 1,3). NL63-E protein is expected to span the virion membrane once, with the transmembrane region localized between amino acids 16 and 32 and a short N-terminal tail outside the virion[83]. The hydrophobic α-helical transmembrane region of 17 amino acids occupies 30% of the total size of E protein. Coronaviral E proteins interact with M protein by the transmembrane and the endo domains and are proposed to act as a temporary anchor to relocate M protein into the pre-Golgi compartments to prepare membranes for viral budding[22]. The avian infectious bronchitis virus (IBV) and SARS-CoV E protein is localized mainly in

the pre-Golgi compartments, participates actively in virus budding and is the major factor during generation of virus-like particles[21,22,91].

The endoplasmic reticulum (ER) membrane retention signal XXRR-like (FLRL) is present on the N-terminus of the E protein of HCoV-NL63, which differs from the IBV C-terminal ER retention signal, the KKXX-like motif (RDKLYS)[81].
The body TRS of the NL63-E protein shows a hampered TRS sequence, which may explain the low level of E sg mRNA during virus replication[107]. The E protein concentration may be tightly regulated as it has been reported to localize on the outer membrane of infected cells and to trigger apoptosis[3]. However, it is currently not known whether the low sg mRNA level corresponds with a low E protein level.

The membrane protein M
The M protein is a key player in virus assembly and budding, thereby interacting with other structural viral proteins. The M protein of HCoV-NL63 is predicted to span the virion membrane 3 or 4 times. The N_{exo}-C_{endo} topology is adopted by the M protein of other coronaviruses[6,108], but it has been proposed that the M protein of TGEV is present in the viral envelope in two topological states, N_{exo}-C_{endo} and N_{exo}-C_{exo}[110]. The sequence analysis suggests a similar scenario for HCoV-NL63.

The protein-protein interaction between coronavirus N and M proteins has been reported for MHV and TGEV *in vitro*[32,72,93], and this interaction is essential for coronaviral assembly. Coronaviruses differ from other enveloped viruses such as paramyxoviruses and rhabdoviruses by the absence of a structural matrix protein that links the E and the N protein. Thus replacing the matrix protein in the role of core stabilization appears to be one of the functions of the coronavirus M protein. M protein has also been found to contain an RNA binding domain that interacts with the RNA packaging signal[92], but it is not known if such interaction occurs for HCoV-NL63.

The nucleocapsid protein N
The 1134-nucleotide N gene of HCoV-NL63 resides near the 3′ end of the genome. N protein is expressed from the most abundant sg mRNA species in HCoV-NL63 infected cells[107]. This 42kDa basic phophoprotein has been reported for other coronaviruses to interact with the viral RNA and is a component of the viral core (Table 3)[32,109].

Conservation of the N proteins is relatively poor among coronaviral species[76]. Based on sequence comparison, three domains have been identified in coronaviral N proteins[102]. The middle domain was identified as a potential RNA binding domain[87,94], capable of binding both coronavirus derived and other RNA molecules *in vitro*[87,124]. No functions have been described yet for the other two domains.

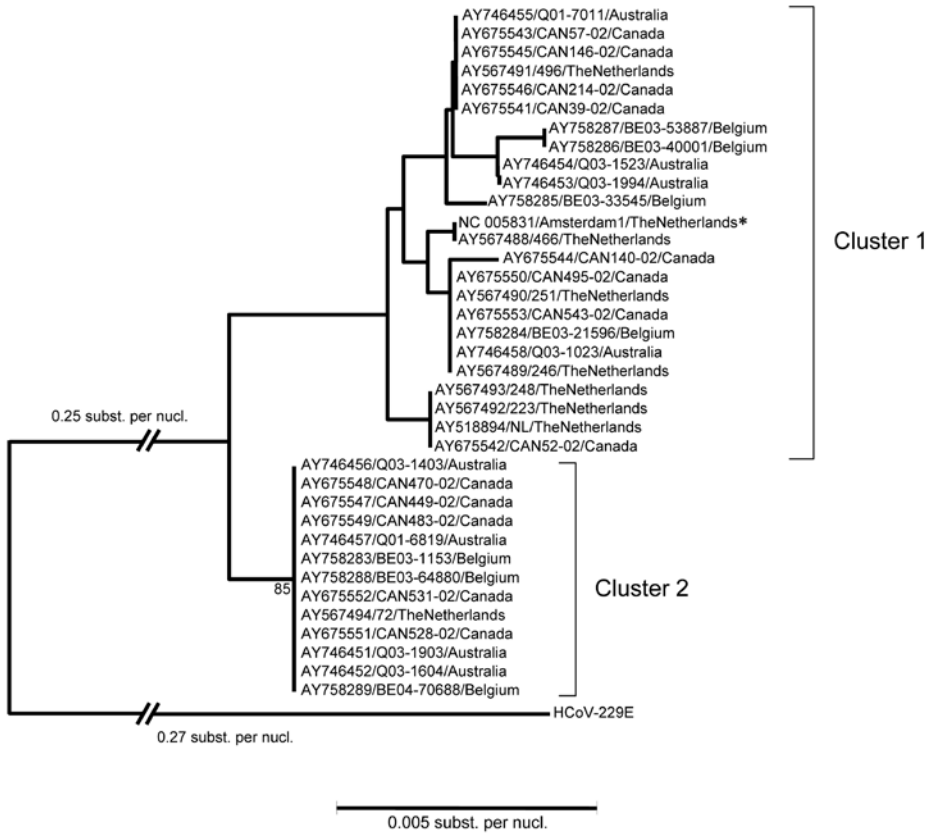


Figure 8. Phylogenetic analysis of different isolates of HCoV-NL63. Analysis includes the partial sequence of the PLpro gene (1a). Name of each taxon consists of its GenBank accession number, isolate name and country of origin. The index strain that was discovered first[129] is marked with an asterix.

It has been postulated that the coronavirus N protein is involved in transcription, translation and virus assembly. N protein complexes with the genomic RNA to form a ribonucleocapsid[23]. The N protein interacts with the L region[9,95] and a sequence at the 3′ end of the genomic RNA[134]. Coronaviral N protein shares homology with the SR superfamily of RNA-binding proteins[102], which contains many splicing regulatory factors[38]. A distinguishing feature of this RNA-binding domain is a tandem repeat of the sequence SRXX present at NL63-N position aa 148-173: (**SR**AS**SR**SS**TR**NN**SR**DS**SR**ST**SR**QQ**SR**). This motif is present in all coronaviral N proteins[15,60,102], supporting the notion that it is important for virus replication[95]. RNA interaction of the NL63-N protein is further supported by its high positive charge.

Previous reports show that N protein might influence the host-cell cycle, triggering inhibition of cell proliferation with a concomitant polyploidy in some cells. This feature of the N protein may be linked to its presence in the cell nucleus[132]. NL63-N protein contains a nuclear localization signal: pat4 (KKPR, aa position 232) or pat7 (PRWKRVP, aa position 234). Viral interference with the cell cycle may improve virus replication, for example by promoting viral RNA transcription or by delaying the cell cycle to allow sufficient time for virion assembly. Alternatively, a delay of the cell cycle in interphase would allow maximal translation of viral mRNAs[19].

Origin and evolution of HCoV-NL63

HCoV-NL63 is closely related to group 1 coronaviruses according to phylogenetic analyses (Figure 1)[129]. Similarity is the highest with HCoV-229E and PEDV, 65% and 61%, respectively. These three viruses cluster with a recently described bat coronavirus[106] in a subgroup within group 1, excluding TGEV, Canine enteric coronavirus (CCoV) and Feline infectious peritonitis virus (FIPV) (Figure 1). As stated above, the N-terminal region of HCoV-NL63 S protein (aa position 17-196) shows no significant similarity with any other coronavirus or cellular sequence. The origin of this insert is not known, and we might speculate that HCoV-229E lost the 5' region of its S protein, as described for PRCoV. Analysis of the M gene suggests that NL63-M is a hybrid protein, which is partially related to 229E-M and PEDV-M, although we currently cannot exclude the hypothesis of convergent evolution. One could speculate that all four viruses within the HCoV-NL63 subgroup evolved independently from a common ancestor rather than that they diverged recently.

Phylogenetic analysis of several HCoV-NL63 isolates based on the 1a gene shows the presence of viruses with different genetic markers[5,89,129]. The increasing number of strains isolated around the world and the availability of partial 1a sequences provides further support for genetic diversity within HCoV-NL63 and the presence of 2 genetic clusters (Figure 8). The close clustering of isolates that are recovered from different locations (the Netherlands, Canada, Australia and Belgium) suggests that the current evolutionary pattern of HCoV-NL63 does not correlate with geographic origin (Figure 8)[89]. Analysis of the N-terminal S sequence also shows two genotypes[5,89,129]. Since these clusters in the 1a and S genes do not match it is feasible that HCoV-NL63 strains can recombine[89]. More full-length sequences are required to characterize the degree of genetic diversity among HCoV-NL63 strains worldwide.

Conclusions

HCoV-NL63 is a recently discovered group 1 coronavirus that is a close relative of HCoV-229E and PEDV (Figure 1), viruses that cause the common cold in humans and diarrhea in porcine, respectively. HCoV-NL63 was frequently

detected in children and immunocompromised patients with acute respiratory illness. It seems unlikely that HCoV-NL63 emerged recently, and it probably has been circulating in the population for many years. The oldest diagnosed sample originated from 1988. However, the presence of multiple clusters, combined with the genetic stability of HCoV-NL63 suggest that the virus diverged a long time ago.

At the molecular level, HCoV-NL63 is clearly distinct from other group 1 coronaviruses. The N-terminal insert in the S protein and a unique cleavage site between nsp13|nsp14 of the 1a/1b gene are perhaps most remarkable. Additionally, HCoV-NL63 is unique in that it is using the same receptor as SARS-CoV, yielding a similar cell tropism.

Acknowledgments
We thank Luis Enjuanes for critical reading of the manuscript and useful comments.

References

1. Almeida, J. D. and D. A. Tyrrell. 1967. The morphology of three previously uncharacterized human respiratory viruses that grow in organ culture. J Gen Virol 1:175-178.
2. Alonso, S., A. Izeta, I. Sola, and L. Enjuanes. 2002. Transcription regulatory sequences and mRNA expression levels in the coronavirus transmissible gastroenteritis virus. J. Virol. 76:1293-1308.
3. An, S., C. J. Chen, X. Yu, J. L. Leibowitz, and S. Makino. 1999. Induction of apoptosis in murine coronavirus-infected cultured cells and demonstration of E protein as an apoptosis inducer. J. Virol. 73:7853-7859.
4. Arbour, N., R. Day, J. Newcombe, and P. J. Talbot. 2000. Neuroinvasion by human respiratory coronaviruses. J. Virol. 74:8913-8921.
5. Arden, K. E., M. D. Nissen, T. P. Sloots, and I. M. Mackay. 2005. New human coronavirus, HCoV-NL63, associated with severe lower respiratory tract disease in Australia. J. Med. Virol. 75:455-462.
6. Armstrong, J., H. Niemann, S. Smeekens, P. Rottier, and G. Warren. 1984. Sequence and topology of a model intracellular membrane protein, E1 glycoprotein, from a coronavirus. Nature 308:751-752.
7. Baker, S. C., K. Yokomori, S. Dong, R. Carlisle, A. E. Gorbalenya, E. V. Koonin, and M. M. Lai. 1993. Identification of the catalytic sites of a papain-like cysteine proteinase of murine coronavirus. J. Virol. 67:6056-6063.
8. Baranov, P. V., C. M. Henderson, C. B. Anderson, R. F. Gesteland, J. F. Atkins, and M. T. Howard. 2005. Programmed ribosomal frameshifting in decoding the SARS-CoV genome. Virology 332:498-510.
9. Baric, R. S., G. W. Nelson, J. O. Fleming, R. J. Deans, J. G. Keck, N. Casteel, and S. A. Stohlman. 1988. Interactions between coronavirus nucleocapsid protein and viral RNAs: implications for viral transcription. J. Virol. 62:4280-4287.
10. Bastien, N., K. Anderson, L. Hart, P. Van Caeseele, K. Brandt, D. Milley, T. Hatchette, E. C. Weiss, and Y. Li. 2005. Human coronavirus NL63 infection in Canada. J. Infect. Dis. 191:503-506.
11. Bendtsen, J. D., H. Nielsen, G. von Heijne, and S. Brunak. 2004. Improved prediction of signal peptides: SignalP 3.0. J. Mol. Biol. 340:783-795.
12. Bradburne, A. F., M. L. Bynoe, and D. A. Tyrrell. 1967. Effects of a "new" human respiratory virus in volunteers. Br. Med J 3:767-769.
13. Brierley, I., M. E. Boursnell, M. M. Binns, B. Bilimoria, V. C. Blok, T. D. Brown, and S. C. Inglis. 1987. An efficient ribosomal frame-shifting signal in the polymerase-encoding region of the coronavirus IBV. EMBO J. 6:3779-3785.

14. Brierley, I., P. Digard, and S. C. Inglis. 1989. Characterization of an efficient coronavirus ribosomal frameshifting signal: requirement for an RNA pseudoknot. Cell 57:537-547.
15. Britton, P., R. S. Carmenes, K. W. Page, D. J. Garwes, and F. Parra. 1988. Sequence of the nucleoprotein gene from a virulent British field isolate of transmissible gastroenteritis virus and its expression in Saccharomyces cerevisiae. Mol. Microbiol. 2:89-99.
16. Bugl, H., E. B. Fauman, B. L. Staker, F. Zheng, S. R. Kushner, M. A. Saper, J. C. Bardwell, and U. Jakob. 2000. RNA methylation under heat shock control. Mol. Cell 6:349-360.
17. Cavanagh, D. 1995. The coronavirus surface glycoprotein, p. 73-115. In S. Siddell (ed.), The Coronaviridae. Springer, New York .
18. Chambers, P., C. R. Pringle, and A. J. Easton. 1990. Heptad repeat sequences are located adjacent to hydrophobic regions in several types of virus fusion glycoproteins. J. Gen. Virol. 71 (Pt 12):3075-3080.
19. Chen, H., T. Wurm, P. Britton, G. Brooks, and J. A. Hiscox. 2002. Interaction of the coronavirus nucleoprotein with nucleolar antigens and the host cell. J. Virol. 76:5233-5250.
20. Combet, C., C. Blanchet, C. Geourjon, and G. Deleage. 2000. NPS@: network protein sequence analysis. Trends Biochem. Sci. 25:147-150.
21. Corse, E. and C. E. Machamer. 2000. Infectious bronchitis virus E protein is targeted to the Golgi complex and directs release of virus-like particles. J. Virol. 74:4319-4326.
22. Corse, E. and C. E. Machamer. 2002. The cytoplasmic tail of infectious bronchitis virus E protein directs Golgi targeting. J. Virol. 76:1273-1284.
23. Davies, H. A., R. R. Dourmashkin, and M. R. MacNaughton. 1981. Ribonucleoprotein of avian infectious bronchitis virus. J. Gen. Virol. 53:67-74.
24. de Groot, R. J., W. Luytjes, M. C. Horzinek, B. A. van der Zeijst, W. J. Spaan, and J. A. Lenstra. 1987. Evidence for a coiled-coil structure in the spike proteins of coronaviruses. J. Mol. Biol. 196:963-966.
25. de Haan, C. A., P. S. Masters, X. Shen, S. Weiss, and P. J. Rottier. 2002. The group-specific murine coronavirus genes are not essential, but their deletion, by reverse genetics, is attenuating in the natural host. Virology 296:177-189.
26. de Haan, C. A., M. Smeets, F. Vernooij, H. Vennema, and P. J. Rottier. 1999. Mapping of the coronavirus membrane protein domains involved in interaction with the spike protein. J. Virol. 73:7441-7452.
27. De, I., S. G. Sawicki, and D. L. Sawicki. 1996. Sindbis virus RNA-negative mutants that fail to convert from minus-strand to plus-strand synthesis: role of the nsP2 protein. J. Virol. 70:2706-2719.
28. Drosten, C., S. Gunther, W. Preiser, S. van der Werf, H. R. Brodt, S. Becker, H. Rabenau, M. Panning, L. Kolesnikova, R. A. Fouchier, A. Berger, A. M. Burguiere, J. Cinatl, M. Eickmann, N. Escriou, K. Grywna, S. Kramme, J. C. Manuguerra, S. Muller, V. Rickerts, M. Sturmer, S. Vieth, H. D. Klenk, A. D. Osterhaus, H. Schmitz, and H. W. Doerr. 2003. Identification of a novel coronavirus in patients with severe acute respiratory syndrome. N. Engl. J. Med. 348:1967-1976.
29. Ebihara, T., R. Endo, X. Ma, N. Ishiguro, and H. Kikuta. 2005. Detection of human coronavirus NL63 in young children with bronchiolitis. J. Med. Virol. 75:463-465.
30. Eckert, D. M. and P. S. Kim. 2001. Mechanisms of viral membrane fusion and its inhibition. Annu. Rev. Biochem. 70:777-810.
31. Enjuanes, L., D. Brian, D. Cavanagh, K. V. Holmes, M. M. C. Lai, H. Laude, P. S. Masters, P. Rottier, S. Siddell, W. Spaan, F. Taguchi, and P. Talbot. 2000. Family Coronaviridae, p. 835-849. In M. H. V. van Regenmortel, C. M. Fauquet, D. H. L. Bishop, E. B. Carstens, M. K. Estes, S. M. Lemon, J. Maniloff, M. A. Mayo, D. J. McGeoch, C. R. Pringle, and R. B. Wickner (eds.), Virus taxonomy: classification and nomenclature of viruses. Seventh report of the International Committee on Taxonomy of Viruses. Academic Press, San Diego, CA.
32. Escors, D., J. Ortego, H. Laude, and L. Enjuanes. 2001. The membrane M protein carboxy terminus binds to transmissible gastroenteritis coronavirus core and contributes to core stability. J. Virol. 75:1312-1324.
33. Esper, F., E. D. Shapiro, C. Weibel, D. Ferguson, M. L. Landry, and J. S. Kahn. 2005. Association between a novel human coronavirus and Kawasaki disease. J. Infect. Dis. 191:499-502.
34. Falquet, L., M. Pagni, P. Bucher, N. Hulo, C. J. Sigrist, K. Hofmann, and A. Bairoch. 2002. The PROSITE database, its status in 2002. Nucleic Acids Res. 30:235-238.
35. Fan, K., P. Wei, Q. Feng, S. Chen, C. Huang, L. Ma, B. Lai, J. Pei, Y. Liu, J. Chen, and L. Lai. 2004. Biosynthesis, purification, and substrate specificity of severe acute respiratory syndrome coronavirus 3C-like proteinase. J. Biol. Chem. 279:1637-1642.

36. Filipowicz, W. and V. Pogacic. 2002. Biogenesis of small nucleolar ribonucleoproteins. Curr. Opin. Cell Biol. 14:319-327.
37. Fouchier, R. A., N. G. Hartwig, T. M. Bestebroer, B. Niemeyer, J. C. de Jong, J. H. Simon, and A. D. Osterhaus. 2004. A previously undescribed coronavirus associated with respiratory disease in humans. Proc. Natl. Acad. Sci. U. S. A 101:6212-6216.
38. Fu, X. D. 1995. The superfamily of arginine/serine-rich splicing factors. RNA. 1:663-680.
39. Gallagher, T. M. and M. J. Buchmeier. 2001. Coronavirus spike proteins in viral entry and pathogenesis. Virology 279:371-374.
40. Gao, F., H. Y. Ou, L. L. Chen, W. X. Zheng, and C. T. Zhang. 2003. Prediction of proteinase cleavage sites in polyproteins of coronaviruses and its applications in analyzing SARS-CoV genomes. FEBS Lett. 553:451-456.
41. Gibbs, A. J., M. J. Gibbs, and J. S. Armstrong. 2004. The phylogeny of SARS coronavirus. Arch. Virol. 149:621-624.
42. Godeke, G. J., C. A. de Haan, J. W. Rossen, H. Vennema, and P. J. Rottier. 2000. Assembly of spikes into coronavirus particles is mediated by the carboxy-terminal domain of the spike protein. J. Virol. 74:1566-1571.
43. Gonzalez, J. M., P. Gomez-Puertas, D. Cavanagh, A. E. Gorbalenya, and L. Enjuanes. 2003. A comparative sequence analysis to revise the current taxonomy of the family Coronaviridae. Arch. Virol. 148:2207-2235.
44. Gorbalenya, A. E., E. V. Koonin, A. P. Donchenko, and V. M. Blinov. 1988. A novel superfamily of nucleoside triphosphate-binding motif containing proteins which are probably involved in duplex unwinding in DNA and RNA replication and recombination. FEBS Lett. 235:16-24.
45. Gorbalenya, A. E., E. V. Koonin, A. P. Donchenko, and V. M. Blinov. 1989. Coronavirus genome: prediction of putative functional domains in the non-structural polyprotein by comparative amino acid sequence analysis. Nucleic Acids Res. 17:4847-4861.
46. Gorbalenya, A. E., E. V. Koonin, and M. M. Lai. 1991. Putative papain-related thiol proteases of positive-strand RNA viruses. Identification of rubi- and aphthovirus proteases and delineation of a novel conserved domain associated with proteases of rubi-, alpha- and coronaviruses. FEBS Lett. 288:201-205.
47. Gorbalenya, A. E., E. J. Snijder, and W. J. Spaan. 2004. Severe acute respiratory syndrome coronavirus phylogeny: toward consensus. J. Virol. 78:7863-7866.
48. Gosert, R., A. Kanjanahaluethai, D. Egger, K. Bienz, and S. C. Baker. 2002. RNA replication of mouse hepatitis virus takes place at double-membrane vesicles. J. Virol. 76:3697-3708.
49. Guan, Y., B. J. Zheng, Y. Q. He, X. L. Liu, Z. X. Zhuang, C. L. Cheung, S. W. Luo, P. H. Li, L. J. Zhang, Y. J. Guan, K. M. Butt, K. L. Wong, K. W. Chan, W. Lim, K. F. Shortridge, K. Y. Yuen, J. S. Peiris, and L. L. Poon. 2003. Isolation and characterization of viruses related to the SARS coronavirus from animals in southern China. Science 302:276-278.
50. Guy, J. S., J. J. Breslin, B. Breuhaus, S. Vivrette, and L. G. Smith. 2000. Characterization of a coronavirus isolated from a diarrheic foal. J. Clin. Microbiol. 38:4523-4526.
51. Hamre, D. and J. J. Procknow. 1966. A new virus isolated from the human respiratory tract. Proc. Soc. Exp. Biol. Med. 121:190-193.
52. Hegyi, A., A. Friebe, A. E. Gorbalenya, and J. Ziebuhr. 2002. Mutational analysis of the active centre of coronavirus 3C-like proteases. J. Gen. Virol. 83:581-593.
53. Hegyi, A. and J. Ziebuhr. 2002. Conservation of substrate specificities among coronavirus main proteases. J. Gen. Virol. 83:595-599.
54. Hendley, J. O., H. B. Fishburne, and J. M. Gwaltney, Jr. 1972. Coronavirus infections in working adults. Eight-year study with 229 E and OC 43. Am. Rev. Respir. Dis. 105:805-811.
55. Herold, J., A. E. Gorbalenya, V. Thiel, B. Schelle, and S. G. Siddell. 1998. Proteolytic processing at the amino terminus of human coronavirus 229E gene 1-encoded polyproteins: identification of a papain-like proteinase and its substrate. J. Virol. 72:910-918.
56. Herold, J. and S. G. Siddell. 1993. An 'elaborated' pseudoknot is required for high frequency frameshifting during translation of HCV 229E polymerase mRNA. Nucleic Acids Res. 21:5838-5842.

57. Heusipp, G., U. Harms, S. G. Siddell, and J. Ziebuhr. 1997. Identification of an ATPase activity associated with a 71-kilodalton polypeptide encoded in gene 1 of the human coronavirus 229E. J. Virol. 71:5631-5634.
58. Hofmann, H., K. Pyrc, L. van der Hoek, M. Geier, B. Berkhout, and S. Pohlmann. 2005. Human coronavirus NL63 employs the severe acute respiratory syndrome coronavirus receptor for cellular entry. Proc. Natl. Acad. Sci. U. S. A 102:7988-7993.
59. Holmes, K. V. and M. M. C. Lai. 1996. Coronaviridae: The viruses and their replication, p. 1075-1093. In B. N. Fields, D. M. Knipe, P. M. Howley, and et al (eds.), Fields Virology. Lippincott-Raven Publishers, Philadelphia.
60. Homberger, F. R. 1995. Sequence analysis of the nucleoprotein genes of three enterotropic strains of murine coronavirus. Arch. Virol. 140:571-579.
61. Ito, N., E. C. Mossel, K. Narayanan, V. L. Popov, C. Huang, T. Inoue, C. J. Peters, and S. Makino. 2005. Severe acute respiratory syndrome coronavirus 3a protein is a viral structural protein. J. Virol. 79:3182-3186.
62. Ivanov, K. A., T. Hertzig, M. Rozanov, S. Bayer, V. Thiel, A. E. Gorbalenya, and J. Ziebuhr. 2004. Major genetic marker of nidoviruses encodes a replicative endoribonuclease. Proc. Natl. Acad. Sci. U. S. A 101:12694-12699.
63. Ivanov, K. A., V. Thiel, J. C. Dobbe, Y. van der Meer, E. J. Snijder, and J. Ziebuhr. 2004. Multiple enzymatic activities associated with severe acute respiratory syndrome coronavirus helicase. J. Virol. 78:5619-5632.
64. Janda, M. and P. Ahlquist. 1998. Brome mosaic virus RNA replication protein 1a dramatically increases in vivo stability but not translation of viral genomic RNA3. Proc. Natl. Acad. Sci. U. S. A 95:2227-2232.
65. Kawasaki, T., F. Kosaki, S. Okawa, I. Shigematsu, and H. Yanagawa. 1974. A new infantile acute febrile mucocutaneous lymph node syndrome (MLNS) prevailing in Japan. Pediatrics 54:271-276.
66. Kiss, T. 2001. Small nucleolar RNA-guided post-transcriptional modification of cellular RNAs. EMBO J. 20:3617-3622.
67. Koonin, E. V. and V. V. Dolja. 1993. Evolution and taxonomy of positive-strand RNA viruses: implications of comparative analysis of amino acid sequences. Crit Rev. Biochem. Mol. Biol. 28:375-430.
68. Krogh, A., B. Larsson, G. von Heijne, and E. L. Sonnhammer. 2001. Predicting transmembrane protein topology with a hidden Markov model: application to complete genomes. J. Mol. Biol. 305:567-580.
69. Ksiazek, T. G., D. Erdman, C. S. Goldsmith, S. R. Zaki, T. Peret, S. Emery, S. Tong, C. Urbani, J. A. Comer, W. Lim, P. E. Rollin, S. F. Dowell, A. E. Ling, C. D. Humphrey, W. J. Shieh, J. Guarner, C. D. Paddock, P. Rota, B. Fields, J. DeRisi, J. Y. Yang, N. Cox, J. M. Hughes, J. W. LeDuc, W. J. Bellini, and L. J. Anderson. 2003. A novel coronavirus associated with severe acute respiratory syndrome. N. Engl. J. Med. 348:1953-1966.
70. Kubo, H. and F. Taguchi. 1993. Expression of the S1 and S2 subunits of murine coronavirus JHMV spike protein by a vaccinia virus transient expression system. J. Gen. Virol. 74 (Pt 11):2373-2383.
71. Kunkel, F. and G. Herrler. 1993. Structural and functional analysis of the surface protein of human coronavirus OC43. Virology 195:195-202.
72. Kuo, L. and P. S. Masters. 2002. Genetic evidence for a structural interaction between the carboxy termini of the membrane and nucleocapsid proteins of mouse hepatitis virus. J. Virol. 76:4987-4999.
73. Lai, M. M. 2003. SARS virus: the beginning of the unraveling of a new coronavirus. J. Biomed. Sci. 10:664-675.
74. Lai, M. M. and D. Cavanagh. 1997. The molecular biology of coronaviruses. Adv. Virus Res. 48:1-100.
75. Laneve, P., F. Altieri, M. E. Fiori, A. Scaloni, I. Bozzoni, and E. Caffarelli. 2003. Purification, cloning, and characterization of XendoU, a novel endoribonuclease involved in processing of intron-encoded small nucleolar RNAs in Xenopus laevis. J. Biol. Chem. 278:13026-13032.
76. Lapps, W., B. G. Hogue, and D. A. Brian. 1987. Sequence analysis of the bovine coronavirus nucleocapsid and matrix protein genes. Virology 157:47-57.
77. Laude, H., M. Godet, S. Bernard, J. Gelfi, M. Duarte, and B. Delmas. 1995. Functional domains in the spike protein of transmissible gastroenteritis virus. Adv. Exp. Med. Biol. 380:299-304.
78. Lee, H. J., C. K. Shieh, A. E. Gorbalenya, E. V. Koonin, N. La Monica, J. Tuler, A. Bagdzhadzhyan, and M. M. Lai. 1991. The complete sequence (22 kilobases) of murine coronavirus gene 1 encoding the putative proteases and RNA polymerase. Virology 180:567-582.
79. Li, W., M. J. Moore, N. Vasilieva, J. Sui, S. K. Wong, M. A. Berne, M. Somasundaran, J. L. Sullivan, K. Luzuriaga, T. C. Greenough, H. Choe, and M. Farzan. 2003. Angiotensin-converting enzyme 2 is a functional receptor for the SARS coronavirus. Nature 426:450-454.

80. Lim, K. P. and D. X. Liu. 1998. Characterization of the two overlapping papain-like proteinase domains encoded in gene 1 of the coronavirus infectious bronchitis virus and determination of the C-terminal cleavage site of an 87-kDa protein. Virology 245:303-312.
81. Lim, K. P. and D. X. Liu. 2001. The missing link in coronavirus assembly. Retention of the avian coronavirus infectious bronchitis virus envelope protein in the pre-Golgi compartments and physical interaction between the envelope and membrane proteins. J. Biol. Chem. 276:17515-17523.
82. Luo, Z. and S. R. Weiss. 1998. Roles in cell-to-cell fusion of two conserved hydrophobic regions in the murine coronavirus spike protein. Virology 244:483-494.
83. Maeda, J., J. F. Repass, A. Maeda, and S. Makino. 2001. Membrane topology of coronavirus E protein. Virology 281:163-169.
84. Marra, M. A., S. J. Jones, C. R. Astell, R. A. Holt, A. Brooks-Wilson, Y. S. Butterfield, J. Khattra, J. K. Asano, S. A. Barber, S. Y. Chan, A. Cloutier, S. M. Coughlin, D. Freeman, N. Girn, O. L. Griffith, S. R. Leach, M. Mayo, H. McDonald, S. B. Montgomery, P. K. Pandoh, A. S. Petrescu, A. G. Robertson, J. E. Schein, A. Siddiqui, D. E. Smailus, J. M. Stott, G. S. Yang, F. Plummer, A. Andonov, H. Artsob, N. Bastien, K. Bernard, T. F. Booth, D. Bowness, M. Czub, M. Drebot, L. Fernando, R. Flick, M. Garbutt, M. Gray, A. Grolla, S. Jones, H. Feldmann, A. Meyers, A. Kabani, Y. Li, S. Normand, U. Stroher, G. A. Tipples, S. Tyler, R. Vogrig, D. Ward, B. Watson, R. C. Brunham, M. Krajden, M. Petric, D. M. Skowronski, C. Upton, and R. L. Roper. 2003. The Genome sequence of the SARS-associated coronavirus. Science 300:1399-1404.
85. Martina, B. E., B. L. Haagmans, T. Kuiken, R. A. Fouchier, G. F. Rimmelzwaan, G. van Amerongen, J. S. Peiris, W. Lim, and A. D. Osterhaus. 2003. Virology: SARS virus infection of cats and ferrets. Nature 425:915.
86. Martzen, M. R., S. M. McCraith, S. L. Spinelli, F. M. Torres, S. Fields, E. J. Grayhack, and E. M. Phizicky. 1999. A biochemical genomics approach for identifying genes by the activity of their products. Science 286:1153-1155.
87. Masters, P. S. 1992. Localization of an RNA-binding domain in the nucleocapsid protein of the coronavirus mouse hepatitis virus. Arch. Virol. 125:141-160.
88. Mathews, D. H., J. Sabina, M. Zuker, and D. H. Turner. 1999. Expanded sequence dependence of thermodynamic parameters improves prediction of RNA secondary structure. J. Mol. Biol. 288:911-940.
89. Moes, E., L. Vijgen, E. Keyaerts, K. Zlateva, S. Li, P. Maes, K. Pyrc, B. Berkhout, L. van der Hoek, and M. Van Ranst. 2005. A novel pancoronavirus RT-PCR assay: frequent detection of human coronavirus NL63 in children hospitalized with respiratory tract infections in Belgium. BMC. Infect. Dis. 5:6.
90. Mounir, S., P. Labonte, and P. J. Talbot. 1993. Characterization of the nonstructural and spike proteins of the human respiratory coronavirus OC43: comparison with bovine enteric coronavirus. Adv. Exp. Med. Biol. 342:61-67.
91. Nal, B., C. Chan, F. Kien, L. Siu, J. Tse, K. Chu, J. Kam, I. Staropoli, B. Crescenzo-Chaigne, N. Escriou, S. van der Werf, K. Y. Yuen, and R. Altmeyer. 2005. Differential maturation and subcellular localization of severe acute respiratory syndrome coronavirus surface proteins S, M and E. J. Gen. Virol. 86:1423-1434.
92. Narayanan, K., C. J. Chen, J. Maeda, and S. Makino. 2003. Nucleocapsid-independent specific viral RNA packaging via viral envelope protein and viral RNA signal. J. Virol. 77:2922-2927.
93. Narayanan, K. and S. Makino. 2001. Cooperation of an RNA packaging signal and a viral envelope protein in coronavirus RNA packaging. J. Virol. 75:9059-9067.
94. Nelson, G. W. and S. A. Stohlman. 1993. Localization of the RNA-binding domain of mouse hepatitis virus nucleocapsid protein. J. Gen. Virol. 74 (Pt 9):1975-1979.
95. Nelson, G. W., S. A. Stohlman, and S. M. Tahara. 2000. High affinity interaction between nucleocapsid protein and leader/intergenic sequence of mouse hepatitis virus RNA. J. Gen. Virol. 81:181-188.
96. Nielsen, H., J. Engelbrecht, S. Brunak, and G. von Heijne. 1997. Identification of prokaryotic and eukaryotic signal peptides and prediction of their cleavage sites. Protein Eng 10:1-6.
97. O'Reilly, E. K., N. Tang, P. Ahlquist, and C. C. Kao. 1995. Biochemical and genetic analyses of the interaction between the helicase-like and polymerase-like proteins of the brome mosaic virus. Virology 214:59-71.
98. O'Reilly, E. K., Z. Wang, R. French, and C. C. Kao. 1998. Interactions between the structural domains of the RNA replication proteins of plant-infecting RNA viruses. J. Virol. 72:7160-7169.

99. Opstelten, D. J., P. de Groote, M. C. Horzinek, and P. J. Rottier. 1994. Folding of the mouse hepatitis virus spike protein and its association with the membrane protein. Arch. Virol. Suppl 9:319-328.
100. Opstelten, D. J., M. J. Raamsman, K. Wolfs, M. C. Horzinek, and P. J. Rottier. 1995. Envelope glycoprotein interactions in coronavirus assembly. J. Cell Biol. 131:339-349.
101. Osman, T. A. and K. W. Buck. 1996. Complete replication in vitro of tobacco mosaic virus RNA by a template-dependent, membrane-bound RNA polymerase. J. Virol. 70:6227-6234.
102. Parker, M. M. and P. S. Masters. 1990. Sequence comparison of the N genes of five strains of the coronavirus mouse hepatitis virus suggests a three domain structure for the nucleocapsid protein. Virology 179:463-468.
103. Peiris, J. S., C. M. Chu, V. C. Cheng, K. S. Chan, I. F. Hung, L. L. Poon, K. I. Law, B. S. Tang, T. Y. Hon, C. S. Chan, K. H. Chan, J. S. Ng, B. J. Zheng, W. L. Ng, R. W. Lai, Y. Guan, and K. Y. Yuen. 2003. Clinical progression and viral load in a community outbreak of coronavirus-associated SARS pneumonia: a prospective study. Lancet 361:1767-1772.
104. Petty, I. T., R. French, R. W. Jones, and A. O. Jackson. 1990. Identification of barley stripe mosaic virus genes involved in viral RNA replication and systemic movement. EMBO J. 9:3453-3457.
105. Pinon, J. D., H. Teng, and S. R. Weiss. 1999. Further requirements for cleavage by the murine coronavirus 3C-like proteinase: identification of a cleavage site within ORF1b. Virology 263:471-484.
106. Poon, L. L., D. K. Chu, K. H. Chan, O. K. Wong, T. M. Ellis, Y. H. Leung, S. K. Lau, P. C. Woo, K. Y. Suen, K. Y. Yuen, Y. Guan, and J. S. Peiris. 2005. Identification of a novel coronavirus in bats. J. Virol. 79:2001-2009.
107. Pyrc, K., M. F. Jebbink, B. Berkhout, and L. van der Hoek. 2004. Genome structure and transcriptional regulation of human coronavirus NL63. Virol. J. 1:7.
108. Raamsman, M. J., J. K. Locker, A. de Hooge, A. A. de Vries, G. Griffiths, H. Vennema, and P. J. Rottier. 2000. Characterization of the coronavirus mouse hepatitis virus strain A59 small membrane protein E. J. Virol. 74:2333-2342.
109. Risco, C., I. M. Anton, L. Enjuanes, and J. L. Carrascosa. 1996. The transmissible gastroenteritis coronavirus contains a spherical core shell consisting of M and N proteins. J. Virol. 70:4773-4777.
110. Risco, C., I. M. Anton, C. Sune, A. M. Pedregosa, J. M. Martin-Alonso, F. Parra, J. L. Carrascosa, and L. Enjuanes. 1995. Membrane protein molecules of transmissible gastroenteritis coronavirus also expose the carboxy-terminal region on the external surface of the virion. J. Virol. 69:5269-5277.
111. Rota, P. A., M. S. Oberste, S. S. Monroe, W. A. Nix, R. Campagnoli, J. P. Icenogle, S. Penaranda, B. Bankamp, K. Maher, M. H. Chen, S. Tong, A. Tamin, L. Lowe, M. Frace, J. L. DeRisi, Q. Chen, D. Wang, D. D. Erdman, T. C. Peret, C. Burns, T. G. Ksiazek, P. E. Rollin, A. Sanchez, S. Liffick, B. Holloway, J. Limor, K. McCaustland, M. Olsen-Rasmussen, R. Fouchier, S. Gunther, A. D. Osterhaus, C. Drosten, M. A. Pallansch, L. J. Anderson, and W. J. Bellini. 2003. Characterization of a novel coronavirus associated with severe acute respiratory syndrome. Science 300:1394-1399.
112. Rouleau, M., R. J. Smith, J. B. Bancroft, and G. A. Mackie. 1994. Purification, properties, and subcellular localization of foxtail mosaic potexvirus 26-kDa protein. Virology 204:254-265.
113. Rowley, A. H. and S. T. Shulman. 1999. Kawasaki syndrome. Pediatr. Clin. North Am. 46:313-329.
114. Sanchez, C. M., F. Gebauer, C. Sune, A. Mendez, J. Dopazo, and L. Enjuanes. 1992. Genetic evolution and tropism of transmissible gastroenteritis coronaviruses. Virology 190:92-105.
115. Sanchez, C. M., A. Izeta, J. M. Sanchez-Morgado, S. Alonso, I. Sola, M. Balasch, J. Plana-Duran, and L. Enjuanes. 1999. Targeted recombination demonstrates that the spike gene of transmissible gastroenteritis coronavirus is a determinant of its enteric tropism and virulence. J. Virol. 73:7607-7618.
116. Sanchez, C. M., G. Jimenez, M. D. Laviada, I. Correa, C. Sune, M. Bullido, F. Gebauer, C. Smerdou, P. Callebaut, J. M. Escribano. 1990. Antigenic homology among coronaviruses related to transmissible gastroenteritis virus. Virology 174:410-417.
117. Sawicki, S. G. and D. L. Sawicki. 1998. A new model for coronavirus transcription. Adv. Exp. Med. Biol. 440:215-219.
118. Schiller, J. J., A. Kanjanahaluethai, and S. C. Baker. 1998. Processing of the coronavirus MHV-JHM polymerase polyprotein: identification of precursors and proteolytic products spanning 400 kilodaltons of ORF1a. Virology 242:288-302.
119. Seybert, A., A. Hegyi, S. G. Siddell, and J. Ziebuhr. 2000. The human coronavirus 229E superfamily 1 helicase has RNA and DNA duplex-unwinding activities with 5′-to-3′ polarity. RNA. 6:1056-1068.

120. Shi, S. T., J. J. Schiller, A. Kanjanahaluethai, S. C. Baker, J. W. Oh, and M. M. Lai. 1999. Colocalization and membrane association of murine hepatitis virus gene 1 products and De novo-synthesized viral RNA in infected cells. J. Virol. 73:5957-5969.
121. Snijder, E. J., P. J. Bredenbeek, J. C. Dobbe, V. Thiel, J. Ziebuhr, L. L. Poon, Y. Guan, M. Rozanov, W. J. Spaan, and A. E. Gorbalenya. 2003. Unique and conserved features of genome and proteome of SARS-coronavirus, an early split-off from the coronavirus group 2 lineage. J. Mol. Biol. 331:991-1004.
122. Sola, I., J. L. Moreno, S. Zuniga, S. Alonso, and L. Enjuanes. 2005. Role of nucleotides immediately flanking the transcription-regulating sequence core in coronavirus subgenomic mRNA synthesis. J. Virol. 79:2506-2516.
123. Sonnhammer, E. L., G. von Heijne, and A. Krogh. 1998. A hidden Markov model for predicting transmembrane helices in protein sequences. Proc. Int. Conf. Intell. Syst. Mol. Biol. 6:175-182.
124. Stohlman, S. A., R. S. Baric, G. N. Nelson, L. H. Soe, L. M. Welter, and R. J. Deans. 1988. Specific interaction between coronavirus leader RNA and nucleocapsid protein. J. Virol. 62:4288-4295.
125. Thiel, V., J. Herold, B. Schelle, and S. G. Siddell. 2001. Infectious RNA transcribed in vitro from a cDNA copy of the human coronavirus genome cloned in vaccinia virus. J. Gen. Virol. 82:1273-1281.
126. Thiel, V., K. A. Ivanov, A. Putics, T. Hertzig, B. Schelle, S. Bayer, B. Weissbrich, E. J. Snijder, H. Rabenau, H. W. Doerr, A. E. Gorbalenya, and J. Ziebuhr. 2003. Mechanisms and enzymes involved in SARS coronavirus genome expression. J. Gen. Virol. 84:2305-2315.
127. Tijms, M. A., L. C. van Dinten, A. E. Gorbalenya, and E. J. Snijder. 2001. A zinc finger-containing papain-like protease couples subgenomic mRNA synthesis to genome translation in a positive-stranded RNA virus. Proc. Natl. Acad. Sci. U. S. A 98:1889-1894.
128. Tyrrell, D. A. and M. L. Bynoe. 1965. Cultivation of a novel type of common-cold virus in organ cultures. Br. Med. J. 5448:1467-1470.
129. van der Hoek, L., K. Pyrc, M. F. Jebbink, W. Vermeulen-Oost, R. J. Berkhout, K. C. Wolthers, P. M. Wertheim-van Dillen, J. Kaandorp, J. Spaargaren, and B. Berkhout. 2004. Identification of a new human coronavirus. Nat. Med. 10:368-373.
130. van Dinten, L. C., H. van Tol, A. E. Gorbalenya, and E. J. Snijder. 2000. The predicted metal-binding region of the arterivirus helicase protein is involved in subgenomic mRNA synthesis, genome replication, and virion biogenesis. J. Virol. 74:5213-5223.
131. van Elden, L. J., A. M. van Loon, F. van Alphen, K. A. Hendriksen, A. I. Hoepelman, M. G. van Kraaij, J. J. Oosterheert, P. Schipper, R. Schuurman, and M. Nijhuis. 2004. Frequent detection of human coronaviruses in clinical specimens from patients with respiratory tract infection by use of a novel real-time reverse-transcriptase polymerase chain reaction. J. Infect. Dis. 189:652-657.
132. Wurm, T., H. Chen, T. Hodgson, P. Britton, G. Brooks, and J. A. Hiscox. 2001. Localization to the nucleolus is a common feature of coronavirus nucleoproteins, and the protein may disrupt host cell division. J. Virol. 75:9345-9356.
133. Xu, X., Y. Liu, S. Weiss, E. Arnold, S. G. Sarafianos, and J. Ding. 2003. Molecular model of SARS coronavirus polymerase: implications for biochemical functions and drug design. Nucleic Acids Res. 31:7117-7130.
134. Zhou, M., A. K. Williams, S. I. Chung, L. Wang, and E. W. Collisson. 1996. The infectious bronchitis virus nucleocapsid protein binds RNA sequences in the 3′ terminus of the genome. Virology 217:191-199.
135. Ziebuhr, J., G. Heusipp, A. Seybert, and S. G. Siddell. 1998. Substrate specificity of the human coronavirus 229E 3C-like proteinase. Adv. Exp. Med. Biol. 440:115-120.
136. Ziebuhr, J. and S. G. Siddell. 1999. Processing of the human coronavirus 229E replicase polyproteins by the virus-encoded 3C-like proteinase: identification of proteolytic products and cleavage sites common to pp1a and pp1ab. J. Virol. 73:177-185.
137. Ziebuhr, J., E. J. Snijder, and A. E. Gorbalenya. 2000. Virus-encoded proteinases and proteolytic processing in the Nidovirales. J. Gen. Virol. 81:853-879.
138. Ziebuhr, J., V. Thiel, and A. E. Gorbalenya. 2001. The autocatalytic release of a putative RNA virus transcription factor from its polyprotein precursor involves two paralogous papain-like proteases that cleave the same peptide bond. J. Biol. Chem. 276:33220-33232.
139. Zuker, M. 2003. Mfold web server for nucleic acid folding and hybridization prediction. Nucleic Acids Res. 31:3406-3415.

140. Zuniga, S., I. Sola, S. Alonso, and L. Enjuanes. 2004. Sequence motifs involved in the regulation of discontinuous coronavirus subgenomic RNA synthesis. J. Virol. 78:980-994.
141. Zuo, Y. and M. P. Deutscher. 2001. Exoribonuclease superfamilies: structural analysis and phylogenetic distribution. Nucleic Acids Res. 29:1017-1026.

Chapter V

Mosaic structure of human coronavirus NL63, one thousand years of evolution

Journal of Molecular Biology, December 2006, vol. 364, p. 964-973

Krzysztof Pyrc[1], Ronald Dijkman[1], Lea Deng[2], Maarten F. Jebbink[1], Howard A. Ross[2], Ben Berkhout[1] and Lia van der Hoek[1]

Laboratory of Experimental Virology, Department of Medical Microbiology, Center for Infection and Immunity Amsterdam (CINIMA), Academic Medical Center, University of Amsterdam, Meibergdreef 15, 1105 AZ, Amsterdam, The Netherlands. [2] School of Biological Sciences and Bioinformatics Institute, University of Auckland, Private Bag 92019, Auckland, New Zealand

Before the SARS outbreak only two human coronaviruses (HCoV) were known: HCoV-OC43 and HCoV-229E. With the discovery of SARS-CoV in 2003, a third family member was identified. Soon thereafter, we described the fourth human coronavirus (HCoV-NL63), a virus that has spread worldwide and is associated with croup in children. We report here the complete genome sequence of two HCoV-NL63 clinical isolates, designated Amsterdam 57 and Amsterdam 496. The genomes are 27,538 and 27,550 nucleotides long, respectively, and share the same genome organization.We identified two variable regions, one within the 1a and one within the S gene, whereas the 1b and N genes were most conserved. Phylogenetic analysis revealed that HCoV-NL63 genomes have a mosaic structure with multiple recombination sites. Additionally, employing three different algorithms, we assessed the evolutionary rate for the S gene of group Ib coronaviruses to be ~3×10^{-4} substitutions per site per year. Using this evolutionary rate we determined that HCoV-NL63 diverged in the 11th century from its closest relative HCoV-229E.

Introduction

Coronaviruses, a genus of the *Coronaviridae* family, are enveloped viruses with a large plus-strand RNA genome. The genomic RNA is 27–32 kb in size, capped and polyadenylated. Coronaviruses have been identified in bats, mice, rats, chickens, turkeys, swine, dogs, cats, rabbits, horses, cattle and humans and cause highly prevalent diseases such as respiratory, enteric, cardiovascular and neurological disorders[18,27]. Originally, coronaviruses were classified on the basis of antigenic cross-reactivity in three antigenic groups[6]. When coronavirus genome sequence data began to accumulate, the original antigenic groups were converted into genetic groups based on similarity of the nucleotide sequences.

The coronaviruses possess a characteristic genome composition. The 5′ two-thirds of a coronavirus genome encodes two polyproteins (1a and 1ab) that contain all proteins necessary for RNA replication. The 3′ one-third of a coronavirus genome encodes several structural proteins such as spike (S), envelope (E), membrane (M) and nucleocapsid (N) proteins that, among other functions, participate in the budding process and are incorporated into the virus particle. Additional accessory protein genes are located in the 3′ part of the genome in a coronavirus species-specific position.

HCoV-NL63, a recently discovered member of the *Coronaviridae* family[33,34,44], has spread worldwide, is observed most frequently in the winter season and is associated with acute respiratory illness and croup in young children, elderly and immunocompromised patients[1,8,12,45]. A recent report suggested that HCoV-NL63 is one of the pathogens underlying Kawasaki disease[14], although other studies could not confirm this association[7,13,39].

HCoV-NL63 belongs to the group I coronaviruses according to phylogenetic analyses. The highest similarity is observed with HCoV-229E and porcine epidemic diarrhoea virus (PEDV), 65% and 61%, respectively. Phylogenetic analysis based on gene 1a sequences indicates the presence of diverse HCoV-NL63 strains with distinct molecular markers[44]. The increasing number of HCoV-NL63 sequences from several locations provides further evidence for this genetic diversity and confirms the presence of two main genetic clusters[1,3,30]. However, drawing conclusions based on phylogenetic analysis of a single gene sequence and sometimes even a partial gene sequence requires caution as the true phylogeny can only be demonstrated by analyzing complete genome sequences. Full genome sequences of field isolates were, however, not available. Therefore, we sequenced the complete genomes of two HCoV-NL63 field isolates (Amsterdam 57 and Amsterdam 496) and genome fragments of 21 additional field isolates. Here, we present evidence for the in-field recombination of HCoV-NL63. Furthermore, we characterized the molecular variability of HCoV-NL63 isolates to have insight into the evolution of the virus. We observed high variability at certain genome regions and a molecular clock analysis revealed that the virus has been present in the human population for centuries.

Methods

Patient isolates

HCoV-NL63 positive patients were identified by a diagnostic nested RT-PCR as described[4] or by a real time PCR that was performed with primers NF (5′ GCGTGTTCCTACCAGAGAGGA 3′) and NR (5′ GCTGTGGAAAACCTTTGGCA 3′), and HCoV-NL63 was detected with probe NP (5′ FAM–ATGTTATTCAGTGCTTTGGTCCTCGTGAT–TAMRA 3′) as described[39]. A total of 23 NL63-positive patients were identified within the Academic Medical Center, Amsterdam. Two HCoV-NL63 isolates were selected for full genome sequencing (57 and 496) and several genome fragments were sequenced for the other 21 isolates (Table 1). Sampling dates and patient characteristics are summarized in Table 1. Sequencing was performed on an ABI 3700 machine (Perkin-Elmer Applied Biosystems) using the BigDye terminator cycle sequencing kit (version 1.1). Chromatogram sequence files were inspected and assembled with CodonCode 1.4 and further corrected manually. Several genomic regions were amplified using the following primers. For the 1a gene: sense 5′ GGTCACTATGTAGTTTATGATG 3′ and sense 5′ GGATTTTTCATAACCACTTAC 3′; antisense 5′ CTTTTGATAACGGTCACTATG 3′ and antisense 5′ CTCA TTACATAAAACATCAAACGG 3′. For the S gene: sense 5′ GGTTGTTGTTACGCAATAATGGTCGT 3′; antisense 5′ ACACGGCCATTATGTGTGGT 3′. For ORF3: sense 5′ ATTGTTTAACTTCATCAATGC 3′; antisense 5′ CCATAAAATGGAATTGAGGACAATAC 3′. For N: sense 5′ CTCTCAGGAGGGTGTTTTGTCAGAAAG 3′; antisense 5′ ATAATAAACATTCA ACTGGAATTA C 3′.

Table 1. Clinical isolates of HCoV-NL63.

Isolate name	Sampling date	Viral load in patient sample [copies/ml]	Fragments sequenced
3	n.k.	5.66×10^5	3K;
27	n.k.	2.23×10^6	3K; 21K
42	n.k.	n.d.	26K
57	08.01.2004	2.00×10^8	Full genome
63c	n.k.	n.d.	26K
72	31.12. 2002	196305	3K; 6K; 21K; 25K; 26K
111	12.01.2004	n.d.	21K
120	13.01.2004	n.d.	21K
173	n.k.	n.d.	3K
202	31.03.2003	n.d.	21K
212	01.02.2003	n.d.	21K; 25K
223	08.01.2003	n.d.	21K; 25K; 26K
242	10.02.2003	n.d.	25K; 26K
246	13.01.2003	1.80×10^4	6K; 21K; 25K; 26K
248	16.01.2003	1.98×10^6	3K; 6K; 25K; 26K
251	07.01.2003	8.34×10^7	25K
466	04.02.2003	5.36×10^5	3K; 6K; 21K; 25K; 26K
496	25.02.2003	1.70×10^6	Full genome
705	n.k.	3.30×10^6	3K; 21K
744	n.k.	7.20×10^6	3K
791	n.k.	3.70×10^6	21K
857	10.12.2003	3.50×10^7	3K; 6K; 21K; 25K; 26K
890	n.k.	7.39×10^5	3K

RT-PCR and full genome sequencing

The cDNA used for sequencing was generated with MMLV-RT, 1μg of random hexamer DNA primers, in 10mM Tris (pH 8.3), 50mM KCl, 0.1% (v/v) Triton-X100, 6mM $MgCl_2$ and 50μM dNTPs at 37°C for 90min. The cDNA was converted into double-stranded DNA in a standard PCR reaction with 1.25 units of Taq polymerase (Perkin-Elmer) per reaction and appropriate primers. Full genome

sequencing of the two field isolates of HCoV-NL63 was performed with single round RT-PCR as described above, with a set of overlapping PCR products (average size 700 bp) encompassing the entire genome. Primers were designed in regions that are conserved between the Amsterdam 1 and NL isolates of HCoV-NL63. Primer sequences used for full genome sequencing are available on request. The 5′ and 3′-terminal sequence were determined by 5′ RACE (Invitrogen) and 3′ RACE as described[44]. Each PCR fragment was sequenced on both strands and the virus isolates were amplified and sequenced on separate dates to prevent sample contamination. Each experiment contained negative extraction controls. Sequencing was performed as described above.

Sequence analysis

Multiple sequence alignments were prepared with ClustalX 1.83 and manually edited in BioEdit. Phylogenetic analyses were conducted using MEGA, version 3.1. Bootscan and similarity graphs were prepared with SimPlot 2.5 software[28]. Analysis of HCoV-NL63 variability and synonymous and non-synonymous substitutions was done with DnaSP 4.0 software. Positive selection was analyzed with PAML 3.14 software[52]. The analysis is according to the codon-based evolution models (one-ratio, neutral and selection models) developed by Nielsen and Yang[31], which allows the ratio of synonymous and non-synonymous substitution rates to vary among amino acid positions. This method uses dS and dN to denote the rates of synonymous and non-synonymous substitutions, respectively. Their ratio reflects the selection intensity at the amino acid level.

Molecular clock analysis

Evolutionary rates were estimated using three approaches: Bayesian inference in BEAST, version 1.2 (kindly made available by A. J. Drummond and A. Rambaut, University of Oxford, http://www.evolve.zoo.ox.ac.uk/beast/) and serial ML estimate and sUPGMA with PEBBLE 1.0[16]. Divergence times were estimated using Bayesian inference in BEAST, version 1.2. The Markov chain Monte Carlo (MCMC) length was 10^8 with a sample frequency of 10^3 and effective sample size of 9×10^4. The burn-in was 10^7. Convergence to stationarity was investigated using the Tracer 1.3 MCMC trace analysis tool. The molecular clock hypothesis was tested by the likelihood ratio test.

Nucleotide sequence accession numbers

The sequence of HCoV-NL63 isolate Amsterdam 57 and Amsterdam 496 described here were deposited in GenBank under accession numbers: DQ445911 and DQ445912, respectively. The partial sequences of patient isolates were deposited in GenBank under accession numbers DQ462752-DQ462792. The GenBank accession number of HCoV-NL63 isolate Amsterdam-1 is NC_005831, isolate NL is AY518894, HCoV-229E is AF304460, and PEDV (strain CV777) is AF353511. The GenBank accession numbers of the 6K region of isolates 072, 246, 248 and 466 are AY567494, AY567489, AY567493 and AY567488, respectively.

Results

HCoV-NL63 isolates

We sequenced the complete genomes of two HCoV-NL63 isolates (Amsterdam 57 and Amsterdam 496) directly from patient material. Isolate 496 was obtained from the throat swab of an eight-month old boy (February 2003) and isolate 57 was amplified from the bronchoalveolar lavage of a 57-year old woman (December 2002), both suffering from acute respiratory illness. Both isolates displayed the same basic genome structure as previously described for HCoV-NL63. Furthermore, we partially sequenced additional isolates directly from patient material to analyze the variability of HCoV-NL63 (Table 1). The regions were: 1a gene nt 3004–3888 (3K) and nt 5815–6280 (6K), S gene nt 20,497–21,003 (21K), ORF3 gene nt 24,521–25,206 (25K), and N gene nt 26,136–27,166 (26K). In some cases only a few regions were amplified because of the low virus load in some patient samples.

Genetic variability along the genome

Pair-wise sequence alignments of isolates Amsterdam 1[44], NL[15], 57 and 496 demonstrate an overall genome similarity of 99.0% between the HCoV-NL63 strains. We plotted the frequency of polymorphic nucleotides along the genome to visualize variable sites (Figure 1a) and identified two hypervariable regions, one in the 5′ part of the 1a gene encoding nsp1-nsp3 (nt 170–5000) and in the 5′ part of the spike gene (nt 20,300–22,000). The latter region encompasses the S1 region that contains a unique insert in HCoV-NL63 when compared to its closest relative HCoV-229E.

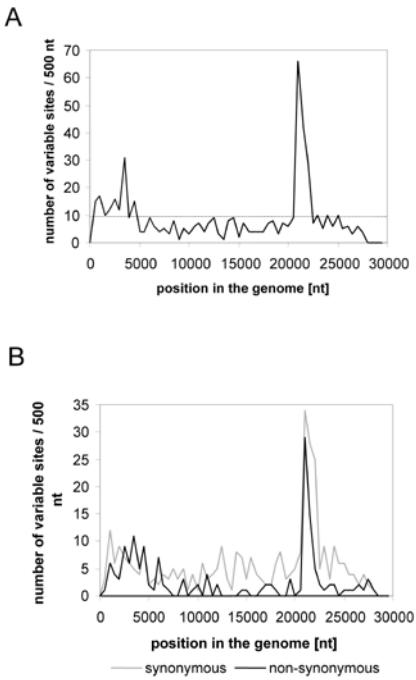


Figure 1. Molecular variability of HCoV-NL63 along the genome. (a) Frequency of polymorphic sites at the nucleotide level among four isolates of HCoV-NL63. (b) Frequency of polymorphic sites on the synonymous and non-synonymous positions among four isolates of HCoV-NL63. The analysis was done with a 500 nt non-overlapping window.

Within the variable region 1–5000 nt in the 1a gene, we identified 126 variable sites among the four full genome isolates (55 non-synonymous substitutions), which resulted in 51 variable amino acid (aa) positions. In this region, we also identified an in-frame deletion of 15nt in isolate 496 and NL (corresponding to nt 3321–3335 of Amsterdam 1). To determine the prevalence of this deletion in the virus population, we analyzed partial sequences of the 1a gene (region 3K) of additional HCoV-NL63 isolates (Table 1) and found it in three more patients (003, 890 and 248) while in eight patients no deletion was observed. The second variable region encompasses the S1 part of the S gene. Out of 175 polymorphic nucleotides (56 non-synonymous substitutions) leading to 51aa substitutions, 119 are located in the first 1200 nt (46 non-synonymous substitutions) of the spike gene leading to 41aa changes. Furthermore, we observed a 3nt deletion within the S gene (corresponding to nt 20798 and 20800 of Amsterdam 1) in isolates 496, 57 and NL. Sequencing of 12 additional patient samples identified no additional variants with this 3nt deletion.

The analysis of synonymous/non-synonymous substitutions along the genome indicates that synonymous substitutions are generally in excess over non-synonymous substitutions (Figure 1b). To determine if the high variability in the 3K and 21K regions is driven by positive selection we analyzed these regions with PAML software, which provides maximum likelihood estimates of the extent of positive selection. Likelihood ratio tests were used to assess whether a model, which included positive selection, was significantly better than one that did not. When positive selection was indicated, empirical Bayes' methods were used to identify which individual sites were under positive selection. According to the PAML analysis the 3K and 21K regions showed no significant sign of positive selection.

We analyzed the most conserved genome regions to identify suitable targets for the development of a PCR-based diagnostic assay that can detect all HCoV-NL63 isolates. The 1b polyprotein gene is highly conserved, with 25 variable nucleotides and only one aa substitution in the region nt 12401–15195 among the four isolates. This region encodes the RNA-dependent RNA polymerase (RdRp). The second most conserved region is the N protein and we confirmed the homogeneity in nine additional patient isolates. Of the 24 variable positions scored in a 1031nt region, only five were non-silent and resulted in 4 aa changes. Although it was previously mentioned that the ORF3 gene is highly variable in strain NL[15], we observed a low heterogeneity in Amsterdam 1, 57 and 496. Also among 11 patient isolates, only ten polymorphic nucleotides were observed (one non-synonymous substitution), resulting in only 1aa change in the patient isolates. A 3nt insertion and an additional 1aa change were observed only in the cultured NL isolate[15].

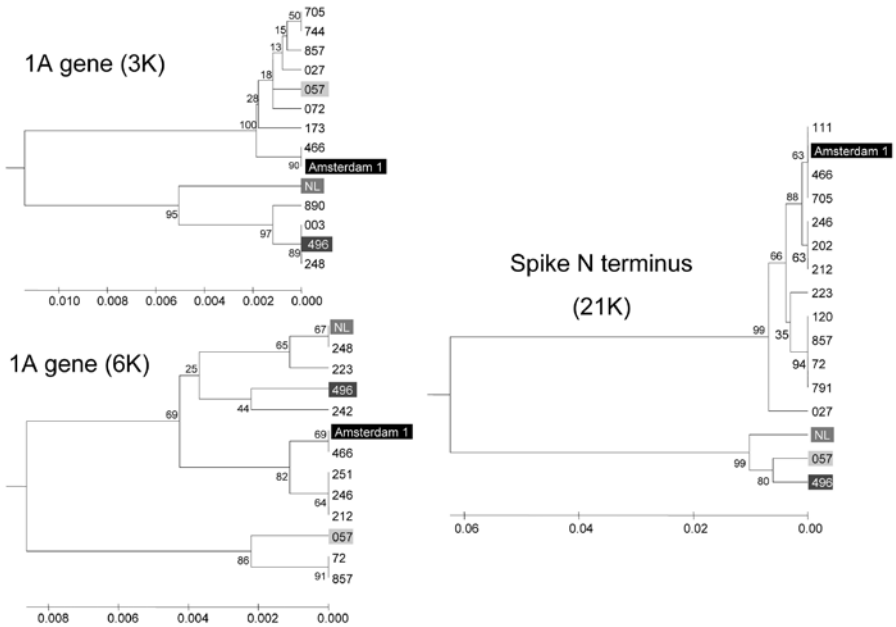


Figure 2. Discordance in phylogenetic clustering of different isolates of HCoV-NL63 at regions 3K, 6K and 21K. Phylogenetic trees were constructed as described in Materials and Methods using an UPGMA algorithm. The scale bar unit represents a 0.002 substitution per site. The trees were rooted with the sequences of it's closest relative: for 3K and 6K the HCoV-229E and for the 21K region the PEDV. Four completely sequenced isolates are marked with colored boxes, illustrating the discordance in clustering in different regions of the genome.

HCoV-NL63 recombination

We analyzed the full genome sequence of the four HCoV-NL63 isolates for possible recombination events. As the explorative bootscan analysis was not suggestive due to the low number of highly similar sequences and a stochastic noise that could not be distinguished from the real signal, we decided to analyze only the regions showing high number of informative sites. We analyzed the partial sequences of five regions (3K, 6K, 21K, 25K, and 26K) for 57, 496, NL and Amsterdam 1 isolates and nine additional patient isolates. The phylogenetic analysis confirms that in the 3K region the isolates Amsterdam 1 and 57 do cluster together in one subgroup while NL and 496 are located in the second (Figure 2 and Figure 3). Phylogenetic analysis of the 6K region of several isolates reveals that the clustering pattern changes, with isolates NL, 496 and Amsterdam 1 in one subgroup and isolate 57 being an outgroup (Figure 2 and Figure 3). In the 21K region the analysis shows that Amsterdam 1 is a single representative of one cluster, while NL, 496 and 57 are tightly clustering in the second group (Figure 2 and Figure 3). Therefore, there is clear evidence that HCoV-NL63 isolates are mosaics with multiple recombinations along the genome.

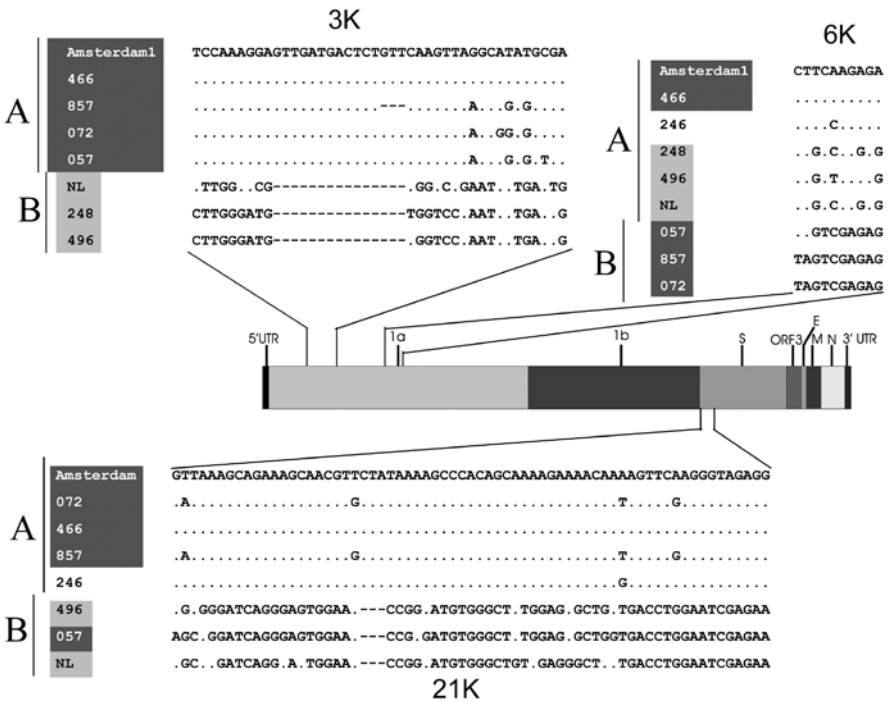


Figure 3. Discordance in clustering of different isolates of HCoV-NL63 at regions 3K, 6K and 21K. Three alignments of only variable sites subtracted from the original sequence with DnaSP 4.0 software, shows the discordance in clustering at different regions of the genome. Groups A and B were created arbitrarily to show the discordance. Group A was defined as the group that contains the Amsterdam 1 isolate.

Because in several regions the sequence was highly conserved and the analysis did not show signs of the presence of two genetic clusters it was very difficult to identify the exact location of the recombination spots. The S gene does contain enough informative sites, and we identified two spots of recombination: one between positions nt 21,072 and 21,161 and the second between positions nt 21,662 and 21,884 in the Amsterdam 1 genome (Figure 4).

Interspecies recombination

We also analyzed whether recombination within the coronavirus family can be identified. The analysis was performed with the SimPlot software by plotting the similarity between different members of the *Coronaviridae* family as well as by scanning the genome with the bootscan tool. Along the genome the similarity between HCoV-NL63 and HCoV-229E is the highest, except for one part of the M gene. The similarity graph shows that the 3′ region of the M gene has a higher nucleotide similarity to PEDV than to HCoV-229E (Figure 5a). Additionally, the bootscan analysis suggests recombination between an ancestral HCoV-NL63 strain and PEDV in that region (Figure 5b). To rule out that the observed effect

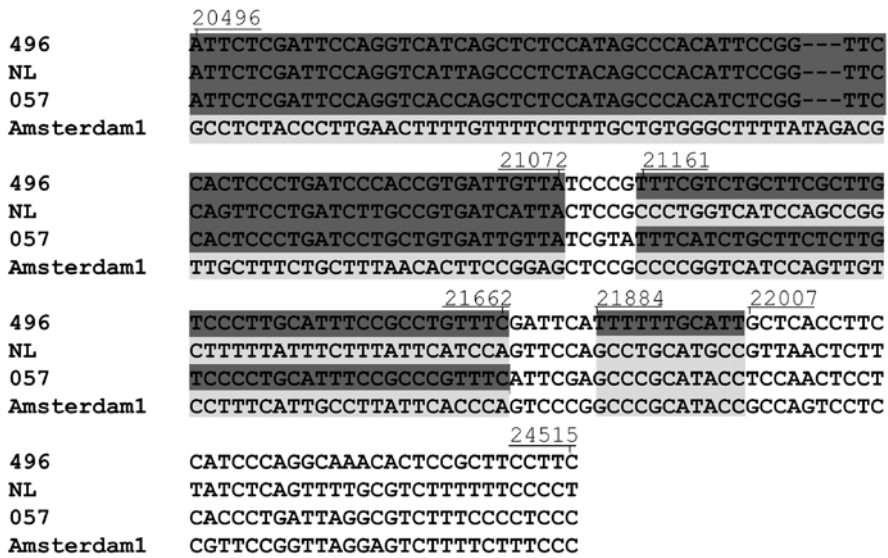


Figure 4. Identification of recombination sites in the S gene. The alignment includes only subtracted variable sites. These variable sites were subtracted with DnaSP 4.0 software. The change of color represents the alternation of genetic clustering between isolates. The numbers at the top represent the beginning of the S gene (nt 20,472 in the Amsterdam 1 isolate), coordinates of recombination spots inside the S gene (nt 21,061–21,072 and 21,575–21,576 in the Amsterdam 1 isolate) and the 3′ terminus of the S gene (nt 24,542 in the Amsterdam 1 isolate).

is the result of convergent evolution we analyzed the synonymous substitution pattern between HCoV-NL63 and HCoV-229E. It has been described that the synonymous substitution rate is increased at genome regions, which originated from another species and may be used as a marker of gene transfer from another species[37,40]. Indeed a rise in the synonymous substitution rate in the 3′ region of the M gene was observed (Figure 5c).

Molecular clock analysis

Based on the nucleotide sequence coding for the S protein (nt 20,649–22,269), a maximum-likelihood phylogenetic tree was constructed for HCoV-NL63 and several HCoV-229E strains for which the date of isolation was known (three isolates from year 1967, five isolates from year 1999 and six isolates from year 2000). Based on these sequence data, the evolutionary rate of HCoV-229E was calculated by Bayesian coalescent approach[11], serial ML estimate[9,16] and sUPGMA[10] approaches. The evolutionary rates estimated with these three approaches were of very similar magnitude and were 3.28×10^{-4} (95% confidence interval, 1.72×10^{-4} to 5.00×10^{-4}), 6.17×10^{-4} and 2.82×10^{-4} (95% confidence interval, 1.36×10^{-4} – 4.42×10^{-4}) substitutions per site per year, respectively. Assuming a constant evolutionary

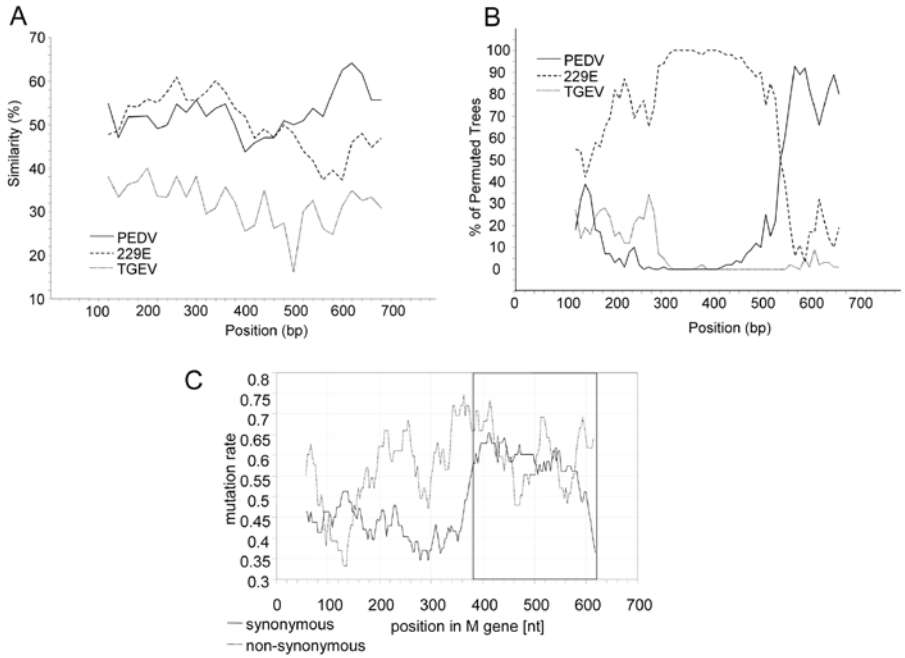


Figure 5. Signs of interspecies recombination in the M gene. Similarity plot (a) and bootscan analysis with the Kimura (two-parameter) distance model, neighbor-joining tree model and 500 bootstrap replicates (b) of the HCoV-NL63 M protein. (c) Analysis of the substitution pattern on the synonymous and non-synonymous level between the M gene of HCoV-NL63 and HCoV-229E. The window used was 40 nucleotides with a step of one nucleotide.

rate in time and between the branches for HCoV-NL63 and HCoV229E, the time to the most recent common ancestor (TMRCA) of HCoV-NL63 and HCoV-229E was dated by the Bayesian coalescent approach around the year 1053 (95% highest posterior density interval, year 966 to 1142). This estimate was highly consistent under different demographic models, including an exponential growth (TMRCA around year 1105 (95% confidence interval, 1017 to 1188)), and expansion growth (TMRCA around year 1124 (95% confidence interval, 1038 to 1206)). A likelihood ratio test indicated that the molecular clock hypothesis could not be rejected (P = 0.05). We also attempted to date back the split of two HCoV-NL63 lineages, but due to several recombination spots in the spike gene region that we sequenced (see also Figure 4) this analysis was not possible. The 3K and 6K fragments could not be used because we only know the substitution rate for the 20,649–22,269 region in the HCoV-NL63 genome.

Discussion

Homologous recombination is well known for several RNA viruses, including coronaviruses[26,29]. A "copy-choice" mechanism has been proposed, in which the RdRp, together with the nascent RNA strand, dissociates from the original

template and re-associates at the same position on another template subsequently recommencing RNA synthesis[29]. Recombination of coronavirus genomes has been observed in vitro in cell culture[2,26,29], in experimentally infected animals[23], and in embryonated eggs[24]. In the case of infectious bronchitis virus, there is evidence for homologous recombination occurring in the field[19,21,25,49]. We present evidence that recombination has occurred during the evolution of HCoV-NL63 and that viral isolates possess a mosaic genome structure. Recombination was discovered by full genome sequence analysis of HCoV-NL63 variants from clinical samples. Analysis of several genome regions showed discordance in the phylogenetic clustering along the genome, a clear sign of recombination. Because the majority of informative sites are located at non-coding positions one can exclude that related genome sequences were the result of convergent evolution due to positive selection.

HCoV-NL63 is the causative agent of up to 10% of all respiratory illnesses[1,3,4,8,12,22,41,43-45]. This high prevalence obviously increases the possibility of a recombination event through co-infection with another human or zoonotically transmitted animal coronavirus. Thus, recombination might enable highly pathogenic recombinant virus variants to arise. There is some evidence for recombination between PEDV and an ancestral HCoV-NL63 strain. Whereas HCoV-NL63 is mostly similar to HCoV-229E, a part of the HCoV-NL63 M gene shows the highest similarity to PEDV, suggesting a possible interspecies recombination event.

Coronaviruses are well equipped to adapt rapidly to changing ecological niches by the high substitution rate of their RNA genome. The average substitution rate for this family was estimated to be 10^{-4} substitutions per year per site[36,48]. HCoV-NL63 is a member of the group I coronaviruses, with highest similarity to HCoV-229E and PEDV. These three species cluster with a recently described bat coronavirus (BatCoV, strain 61)[32] in subgroup Ib. Our efforts to establish the substitution rate of HCoV-NL63 failed, as there is not enough sequence data available from isolates of past years. For this reason we decided to calculate the substitution rate for HCoV-229E, using partial sequences of the S gene from different dates. Based on this substitution rate, we dated the divergence time of HCoV-229E and HCoV-NL63 to the 11th century. The reliability of molecular dating is dependent on the validity of the molecular clock hypothesis, which assumes that the substitution rate is roughly constant. A maximum likelihood test confirmed that the molecular clock hypothesis is suitable for the coronavirus data set investigated here.

We propose that around 900 years ago the HCoV-229E and HCoV-NL63 viruses started to evolve from a common ancestor into the direction of separate species. For HCoV-OC43 it has been estimated that it emerged at the end of the 19th century or the beginning of the 20th century, implying that it has only been around for 100 years[46,47]. The SARS-CoV was introduced in humans in 2002, and

for HCoV-HKU1, this has not been investigated. The heterogeneity of HCoV-HKU1, which appears in two separate genotypes and a third genotype that is a recombinant of these two genotypes[50,51], suggests that this virus was not recently introduced into the human population, similar to the situation of HCoV-NL63. The divergence of HCoV-NL63 and HCoV-229E was followed by a separation of HCoV-NL63 into two lineages, of which we suspect that this occurred at geographically distinct locations. Subsequently the two lineages recombined during co-infection, illustrated by the fact that all four full genome sequences available thus far display a mosaic genome organization.

The variability of coronaviruses has not been studied thoroughly. Although there are several reports concerning SARS-CoV, the relatively short time that this virus was present in the human population makes a long term study impossible. The first variable region of HCoV-NL63 encodes the three proteins nsp1–nsp3. The biological function of nsp1 and nsp2 proteins is thought to be linked to virus replication[5,17]. The nsp3 protein is a coronaviral papain-like proteinase (PL^{pro}) that is expected to be a multifunctional protein with several domains that mediate various enzymatic activities[38,42]. Thus, the high variability of this region might influence the viral replication and interaction with cellular proteins. The second variable region is located in the 5′ part of the S gene. This region contains 24% of all polymorphic nucleotides, whereas it encompasses only ~4% of the genome. The coronavirus S protein is an important determinant for the host cell specificity and tissue tropism, which is largely determined by the distribution of its receptor. Recently, Hofmann *et al*. reported that HCoV-NL63 uses the angiotensin converting enzyme 2 (ACE2) molecule as a receptor[20]. The interaction of NL63-S with ACE2 is surprising, as HCoV-NL63 is closely related to HCoV-229E, which uses CD13 as a receptor. Furthermore, NL63-S shares no appreciable amino acid identity with SARS-CoV-S, which does use ACE2. The amino acid sequence of the CD13-binding site in 229E-S is 57% conserved in NL63-S, whereas the alignment of the ACE2-binding site of SARS-CoV-S with NL63-S reveals only 14% aa identity. These data suggest that NL63-S and SARS-CoV-S might have evolved different strategies to interact with ACE2. The receptor binding domain of NL63-S protein resides in the S1 region[20]. Thus, the variability that we observed may alter the ACE2-binding properties of the S protein or, alternatively, the binding to a co-receptor.

Besides the two hypervariable regions, we also identified regions with a remarkably low substitution rate. The 1b gene is extremely conserved, most prominently in the region encoding RdRp (nt 12416–15195). Analysis of the ORF3 gene shows high conservation of this gene, unlike what has been reported for HCoV-NL63[15]. This suggests a vital function of the ORF3 protein during natural infection. Further investigations on the ORF3 protein function is needed to determine its real biological relevance.

The observation of recombination within the HCoV-NL63 group indicates that two lineages, identified in previous reports in the 1a gene, cannot be treated as separate lineages. Characterization and typing of currently circulating strains should be performed with at least two assays, based on sequences derived from hypervariable regions 1–6000nt and 20,000–21,000. On the contrary, a sensitive diagnostic assay for detection of HCoV-NL63 should be designed in the regions with highest stability such as the 1b or N gene.

Acknowledgement
We thank A. de Ronde for critical reading of the manuscript. Lia van der Hoek is supported by VIDI grant 016.066.318 from Netherlands Organization for Scientific Research (NWO).

References

1. Arden, K. E., M. D. Nissen, T. P. Sloots, and I. M. Mackay. 2005. New human coronavirus, HCoV-NL63, associated with severe lower respiratory tract disease in Australia. J. Med. Virol. 75:455-462.
2. Baric, R. S., S. A. Stohlman, M. K. Razavi, and M. M. Lai. 1985. Characterization of leader-related small RNAs in coronavirus-infected cells: further evidence for leader-primed mechanism of transcription. Virus Res. 3:19-33.
3. Bastien, N., K. Anderson, L. Hart, P. Van Caeseele, K. Brandt, D. Milley, T. Hatchette, E. C. Weiss, and Y. Li. 2005. Human coronavirus NL63 infection in Canada. J. Infect. Dis. 191:503-506.
4. Bastien, N., J. L. Robinson, A. Tse, B. E. Lee, L. Hart, and Y. Li. 2005. Human coronavirus NL-63 infections in children: a 1-year study. J. Clin. Microbiol. 43:4567-4573.
5. Brockway, S. M. and M. R. Denison. 2005. Mutagenesis of the murine hepatitis virus nsp1-coding region identifies residues important for protein processing, viral RNA synthesis, and viral replication. Virology 340:209-223.
6. Cavanagh, D., D. A. Brian, M. A. Brinton, L. Enjuanes, K. V. Holmes, M. C. Horzinek, M. M. Lai, H. Laude, P. G. Plagemann and S. G. Siddell. 1993. The *Coronaviridae* now comprises two genera, coronavirus and torovirus: report of the *Coronaviridae* Study Group. Adv. Exp. Med. Biol. 342:255-257.
7. Chang, L. Y., B. L. Chiang, C. L. Kao, M. H. Wu, P. J. Chen, B. Berkhout, H. C. Yang, and L. M. Huang. 2006. Lack of association between infection with a novel human coronavirus (HCoV), HCoV-NH, and Kawasaki disease in Taiwan. J. Infect. Dis. 193:283-286.
8. Chiu, S. S., K. H. Chan, K. W. Chu, S. W. Kwan, Y. Guan, L. L. Poon, and J. S. Peiris. 2005. Human coronavirus NL63 infection and other coronavirus infections in children hospitalized with acute respiratory disease in Hong Kong, China. Clin. Infect. Dis. 40:1721-1729.
9. Drummond, A., R. Forsberg, and A. G. Rodrigo. 2001. The inference of stepwise changes in substitution rates using serial sequence samples. Mol. Biol. Evol. 18:1365-1371.
10. Drummond, A. and A. G. Rodrigo. 2000. Reconstructing genealogies of serial samples under the assumption of a molecular clock using serial-sample UPGMA. Mol. Biol. Evol. 17:1807-1815.
11. Drummond, A. J., G. K. Nicholls, A. G. Rodrigo, and W. Solomon. 2002. Estimating mutation parameters, population history and genealogy simultaneously from temporally spaced sequence data. Genetics 161:1307-1320.
12. Ebihara, T., R. Endo, X. Ma, N. Ishiguro, and H. Kikuta. 2005. Detection of human coronavirus NL63 in young children with bronchiolitis. J. Med. Virol. 75:463-465.
13. Ebihara, T., R. Endo, X. Ma, N. Ishiguro, and H. Kikuta. 2005. Lack of association between New Haven coronavirus and Kawasaki disease. J. Infect. Dis. 192:351-352.
14. Esper, F., E. D. Shapiro, C. Weibel, D. Ferguson, M. L. Landry, and J. S. Kahn. 2005. Association between a novel human coronavirus and Kawasaki disease. J. Infect. Dis. 191:499-502.

15. Fouchier, R. A., N. G. Hartwig, T. M. Bestebroer, B. Niemeyer, J. C. de Jong, J. H. Simon, and A. D. Osterhaus. 2004. A previously undescribed coronavirus associated with respiratory disease in humans. Proc. Natl. Acad. Sci. U. S. A 101:6212-6216.
16. Goode, M. and A. G. Rodrigo. 2004. Using PEBBLE for the evolutionary analysis of serially sampled molecular sequences., p. 6.8.1-6.8.26. In A. D. Baxevanis, D. B. Davison, R. D. M. Page, G. A. Petsko, L. D. Stein, and G. D. Stormo (eds.), Current Protocols in Bioinformatics. John Wiley and Sons, Inc., New York.
17. Graham, R. L., A. C. Sims, S. M. Brockway, R. S. Baric, and M. R. Denison. 2005. The nsp2 replicase proteins of murine hepatitis virus and severe acute respiratory syndrome coronavirus are dispensable for viral replication. J. Virol. 79:13399-13411.
18. Guy, J. S., J. J. Breslin, B. Breuhaus, S. Vivrette, and L. G. Smith. 2000. Characterization of a coronavirus isolated from a diarrheic foal. J. Clin. Microbiol. 38:4523-4526.
19. Herrewegh, A. A., I. Smeenk, M. C. Horzinek, P. J. Rottier, and R. J. de Groot. 1998. Feline coronavirus type II strains 79-1683 and 79-1146 originate from a double recombination between feline coronavirus type I and canine coronavirus. J. Virol. 72:4508-4514.
20. Hofmann, H., K. Pyrc, L. van der Hoek, M. Geier, B. Berkhout, and S. Pohlmann. 2005. Human coronavirus NL63 employs the severe acute respiratory syndrome coronavirus receptor for cellular entry. Proc. Natl. Acad. Sci. U. S. A 102:7988-7993.
21. Jia, W., K. Karaca, C. R. Parrish, and S. A. Naqi. 1995. A novel variant of avian infectious bronchitis virus resulting from recombination among three different strains. Arch. Virol. 140:259-271.
22. Kaiser, L., N. Regamey, H. Roiha, C. Deffernez, and U. Frey. 2005. Human coronavirus NL63 associated with lower respiratory tract symptoms in early life. Pediatr. Infect. Dis. J. 24:1015-1017.
23. Keck, J. G., G. K. Matsushima, S. Makino, J. O. Fleming, D. M. Vannier, S. A. Stohlman, and M. M. Lai. 1988. *In vivo* RNA-RNA recombination of coronavirus in mouse brain. J. Virol. 62:1810-1813.
24. Kottier, S. A., D. Cavanagh, and P. Britton. 1995. Experimental evidence of recombination in coronavirus infectious bronchitis virus. Virology 213:569-580.
25. Kusters, J. G., E. J. Jager, H. G. Niesters, and B. A. van der Zeijst. 1990. Sequence evidence for RNA recombination in field isolates of avian coronavirus infectious bronchitis virus. Vaccine 8:605-608.
26. Lai, M. M., R. S. Baric, S. Makino, J. G. Keck, J. Egbert, J. L. Leibowitz, and S. A. Stohlman. 1985. Recombination between nonsegmented RNA genomes of murine coronaviruses. J. Virol. 56:449-456.
27. Lai, M. M. C. and K. V. Holmes. 2005. *Coronaviridae* and their replication., p. 1163-1185. In P. Howley, D. Griffin, R. Lamb, M. Martin, B. Roizman, S. Straus, and D. Knipe (eds.), Fields-Virology. Lippincott Williams and Wilkins, London.
28. Lole, K. S., R. C. Bollinger, R. S. Paranjape, D. Gadkari, S. S. Kulkarni, N. G. Novak, R. Ingersoll, H. W. Sheppard, and S. C. Ray. 1999. Full-length human immunodeficiency virus type 1 genomes from subtype C-infected seroconverters in India, with evidence of intersubtype recombination. J. Virol. 73:152-160.
29. Makino, S., J. G. Keck, S. A. Stohlman, and M. M. Lai. 1986. High-frequency RNA recombination of murine coronaviruses. J. Virol. 57:729-737.
30. Moes, E., L. Vijgen, E. Keyaerts, K. Zlateva, S. Li, P. Maes, K. Pyrc, B. Berkhout, L. van der Hoek, and M. Van Ranst. 2005. A novel pancoronavirus RT-PCR assay: frequent detection of human coronavirus NL63 in children hospitalized with respiratory tract infections in Belgium. BMC. Infect. Dis. 5:6.
31. Nielsen, R. and Z. Yang. 1998. Likelihood models for detecting positively selected amino acid sites and applications to the HIV-1 envelope gene. Genetics 148:929-936.
32. Poon, L. L., D. K. Chu, K. H. Chan, O. K. Wong, T. M. Ellis, Y. H. Leung, S. K. Lau, P. C. Woo, K. Y. Suen, K. Y. Yuen, Y. Guan, and J. S. Peiris. 2005. Identification of a novel coronavirus in bats. J. Virol. 79:2001-2009.
33. Pyrc, K., B. J. Bosch, B. Berkhout, M. F. Jebbink, R. Dijkman, P. Rottier, and L. van der Hoek. 2006. Inhibition of human coronavirus NL63 infection at early stages of the replication cycle. Antimicrob. Agents Chemother. 50:2000-2008.
34. Pyrc, K., M. F. Jebbink, B. Berkhout, and L. van der Hoek. 2004. Genome structure and transcriptional regulation of human coronavirus NL63. Virol. J. 1:7.
35. Risco, C., I. M. Anton, C. Sune, A. M. Pedregosa, J. M. Martin-Alonso, F. Parra, J. L. Carrascosa, and L. Enjuanes. 1995. Membrane protein molecules of transmissible gastroenteritis coronavirus also expose the carboxy-terminal region on the external surface of the virion. J. Virol. 69:5269-5277.

36. Sanchez, C. M., F. Gebauer, C. Sune, A. Mendez, J. Dopazo, and L. Enjuanes. 1992. Genetic evolution and tropism of transmissible gastroenteritis coronaviruses. Virology 190:92-105.
37. Sharp, P. M., M. S. Rogers, and D. J. McConnell. 1984. Selection pressures on codon usage in the complete genome of bacteriophage T7. J. Mol. Evol. 21:150-160.
38. Shi, S. T., J. J. Schiller, A. Kanjanahaluethai, S. C. Baker, J. W. Oh, and M. M. Lai. 1999. Colocalization and membrane association of murine hepatitis virus gene 1 products and De novo-synthesized viral RNA in infected cells. J. Virol. 73:5957-5969.
39. Shimizu, C., H. Shike, S. C. Baker, F. Garcia, L. van der Hoek, T. W. Kuijpers, S. L. Reed, A. H. Rowley, S. T. Shulman, H. K. Talbot, J. V. Williams, and J. C. Burns. 2005. Human coronavirus NL63 is not detected in the respiratory tracts of children with acute Kawasaki disease. J. Infect. Dis. 192:1767-1771.
40. Smits, S. L., A. Lavazza, K. Matiz, M. C. Horzinek, M. P. Koopmans, and R. J. de Groot. 2003. Phylogenetic and evolutionary relationships among torovirus field variants: evidence for multiple intertypic recombination events. J. Virol. 77:9567-9577.
41. Suzuki, A., M. Okamoto, A. Ohmi, O. Watanabe, S. Miyabayashi, and H. Nishimura. 2005. Detection of human coronavirus-NL63 in children in Japan. Pediatr. Infect. Dis. J. 24:645-646.
42. Tijms, M. A., L. C. van Dinten, A. E. Gorbalenya, and E. J. Snijder. 2001. A zinc finger-containing papain-like protease couples subgenomic mRNA synthesis to genome translation in a positive-stranded RNA virus. Proc. Natl. Acad. Sci. U. S. A 98:1889-1894.
43. Vabret, A., T. Mourez, J. Dina, L. van der Hoek, S. Gouarin, J. Petitjean, J. Brouard, and F. Freymuth. 2005. Human coronavirus NL63, France. Emerg. Infect. Dis. 11:1225-1229.
44. van der Hoek, L., K. Pyrc, M. F. Jebbink, W. Vermeulen-Oost, R. J. Berkhout, K. C. Wolthers, P. M. Wertheim-van Dillen, J. Kaandorp, J. Spaargaren, and B. Berkhout. 2004. Identification of a new human coronavirus. Nat. Med. 10:368-373.
45. van der Hoek, L., K. Sure, G. Ihorst, A. Stang, K. Pyrc, M. F. Jebbink, G. Petersen, J. Forster, B. Berkhout, and K. Uberla. 2005. Croup is associated with the novel coronavirus NL63. PLoS. Med. 2:e240.
46. Vijgen, L., E. Keyaerts, P. Lemey, P. Maes, K. Van Reeth, H. Nauwynck, M. Pensaert, and M. Van Ranst. 2006. Evolutionary history of the closely related group 2 coronaviruses: porcine hemagglutinating encephalomyelitis virus, bovine coronavirus, and human coronavirus OC43. J. Virol. 80:7270-7274.
47. Vijgen, L., E. Keyaerts, E. Moes, I. Thoelen, E. Wollants, P. Lemey, A. M. Vandamme, and M. Van Ranst. 2005. Complete genomic sequence of human coronavirus OC43: molecular clock analysis suggests a relatively recent zoonotic coronavirus transmission event. J. Virol. 79:1595-1604.
48. Vijgen, L., P. Lemey, E. Keyaerts, and M. Van Ranst. 2005. Genetic variability of human respiratory coronavirus OC43. J. Virol. 79:3223-3224.
49. Wang, L., D. Junker, and E. W. Collisson. 1993. Evidence of natural recombination within the S1 gene of infectious bronchitis virus. Virology 192:710-716.
50. Woo, P. C., S. K. Lau, C. M. Chu, K. H. Chan, H. W. Tsoi, Y. Huang, B. H. Wong, R. W. Poon, J. J. Cai, W. K. Luk, L. L. Poon, S. S. Wong, Y. Guan, J. S. Peiris, and K. Y. Yuen. 2005. Characterization and complete genome sequence of a novel coronavirus, coronavirus HKU1, from patients with pneumonia. J. Virol. 79:884-895.
51. Woo, P. C., S. K. Lau, C. C. Yip, Y. Huang, H. W. Tsoi, K. H. Chan, and K. Y. Yuen. 2006. Comparative analysis of 22 coronavirus HKU1 genomes reveals a novel genotype and evidence of natural recombination in coronavirus HKU1. J. Virol. 80:7136-7145.
52. Yang, Z. 1997. PAML: a program package for phylogenetic analysis by maximum likelihood. Comput. Appl. Biosci. 13:555-556.

Chapter VI

Human coronavirus NL63 employs the severe acute respiratory syndrome coronavirus receptor for cellular entry

Proceedings of the National Acadademy of Sciences U S A, May 2005; vol. 102, p. 7988–7993.

Heike Hofmann[1], Krzysztof Pyrc[2], Lia van der Hoek[2], Martina Geier[1], Ben Berkhout[2], and Stefan Pöhlmann[1]

[1] Institute for Clinical and Molecular Virology and Nikolaus Fiebiger Center, University Erlangen–Nürnberg, 91054 Erlangen, Germany [2]Laboratory of Experimental Virology, Department of Medical Microbiology, Center for Infection and Immunity Amsterdam (CINIMA), Academic Medical Center, University of Amsterdam, Meibergdreef 15, 1105 AZ, Amsterdam, The Netherlands.

Coronavirus (CoV) infection of humans is usually not associated with severe disease. However, discovery of the severe acute respiratory syndrome (SARS) CoV revealed that highly pathogenic human CoVs (HCoVs) can evolve. The identification and characterization of new HCoVs is, therefore, an important task. Recently, a HCoV termed NL63 was discovered in patients with respiratory tract illness. Here, cell tropism and receptor usage of HCoV-NL63 were analyzed. The NL63 spike (S) protein mediated infection of different target cells compared with the closely related 229E-S protein but facilitated entry into cells known to be permissive to SARS-CoV-S-driven infection. An analysis of receptor engagement revealed that NL63-S binds angiotensin-converting enzyme (ACE) 2, the receptor for SARS-CoV, and HCoV-NL63 uses ACE2 as a receptor for infection of target cells. Potent neutralizing activity directed against NL63- but not 229E-S protein was detected in virtually all sera from patients 8 years of age or older, suggesting that HCoV-NL63 infection of humans is common and usually acquired during childhood. Here, we show that SARS-CoV shares its receptor ACE2 with HCoV-NL63. Because the two viruses differ dramatically in their ability to induce disease, analysis of HCoV-NL63 might unravel pathogenicity factors in SARS-CoV. The frequent HCoV-NL63 infection of humans suggests that highly pathogenic variants have ample opportunity to evolve, underlining the need for vaccines against HCoVs.

Introduction

Coronaviruses (CoVs) are enveloped RNA viruses that are grouped according to genome sequence and serology[21]. Human CoVs (HCoVs) 229E and OC43 are members of groups I and II, respectively, and infection with these viruses is thought to be responsible for ~30% of common-cold cases[21]. In contrast, infection with severe acute respiratory syndrome (SARS)-CoV causes a severe respiratory tract illness (RTI) that is fatal in ~10% of infected individuals[29,35]. The factors that determine the pathogenicity of CoVs are incompletely understood; however, a role for the spike (S) protein has been suggested[14]. The S proteins of CoVs, which provide virions with a corona-like appearance, mediate infection of target cells and play a central role in viral replication[14]. The interaction of CoV S proteins with specific cellular receptors determines, to a large extent, which cells can be infected[22], and the entry process is an attractive target for antiviral therapy[5].

Recently, a HCoV termed NL63 was discovered in infants and immunocompromised adults with RTI[13,38]. HCoV-NL63 is a group I CoV and is most closely related to HCoV-229E[13,30,38]. HCoV-229E employs CD13 (aminopeptidase N) as a receptor for infection of target cells[9,42]. Because the NL63- and 229E-S proteins share 56% amino acid identity[38], it is conceivable that HCoV-NL63 also engages CD13 for infectious cellular entry. However, the HCoV-NL63-S protein contains a unique, 179-aa sequence at its N terminus that does not share homology with other known CoV proteins and that might alter the receptor specificity of NL63-S relative to 229E-S[38].

In general, the functional organization of CoV S proteins is similar to that of glycoproteins from several unrelated viruses[20], such as retroviruses, and the SARS-CoV-S protein can be incorporated into the membrane of retroviral particles[33]. These so called pseudovirions ("pseudotypes") accurately mimic receptor engagement and membrane fusion of SARS-CoV and can be used to study S function[15,17,19,27,33,41]. Here, we used retroviral pseudotypes to analyze cell tropism and receptor engagement of HCoV-NL63. We report that the NL63-S protein engages the SARS-CoV receptor angiotensin-converting enzyme (ACE) 2, but not CD13, for cellular entry and that replication of HCoV-NL63 in cell lines depends on ACE2. Moreover, analysis of neutralizing activity in human sera revealed that HCoV-NL63 infection of humans is more frequent than infection with HCoV-229E and is usually acquired during childhood.

Methods

Plasmids

Eukaryotic expression vectors for murine hepatitis virus (MHV) and feline infectious peritonitis virus (FIPV) S proteins were constructed by isolation of the respective fragments from pTUG31-MHV-S and pTUG31-FIPV-S by using BamHI followed by insertion into the BglII site of pCAGGS. A pCAGGS-based plasmid for expression of the 229E-S protein was constructed by PCR amplification with a fragment comprising the 229E-S gene as template followed by insertion into pCAGGS by using KpnI and XhoI. For expression of NL63-S, RNA from HCoV-NL63-infected cells was isolated and reverse-transcribed, and the NL63-S coding region was amplified and cloned into the pCAGGS vector by using EcoRI and XhoI. The eukaryotic expression plasmid for SARS-CoV-S is described[19]. For construction of soluble Fc fusion proteins, HCoV-S1 subunits were amplified by PCR and inserted into plasmid pAB61[3].

Cell culture, infection, and reporter assays.

The lymphatic cell lines CEMx174 and B-THP were cultured in RPMI medium 1640 supplemented with 10% FCS. 293T, Huh-7, Vero E6, HOS (human osteosarcoma), MRC-5, U373, and FCWF (Felis catus) cells were maintained in Dulbecco's MEM (GIBCO/BRL) supplemented with 10% FCS; HeLa cells were cultured in MEM (GIBCO/BRL) supplemented with 5% FCS; LLC-MK2 cells were grown in a 2:1 mixture of MEM/Hanks' solution and MEM/Earle's salts (Invitrogen) with 10% FCS. HCoV-NL63 was cultured on LLC-MK2 cells as described[38]. Tissue culture 50% infectious dose was measured by cytopathic effect (CPE) development in LLC-MK2 cells after inoculation with serial dilutions of viral supernatant. HIV-based pseudotypes were produced as described[19]. Briefly, the pNL4-E—R—Luc plasmid and expression vectors for CoV-S proteins or control glycoproteins [vesicular stomatitis virus G protein (VSV-G) and murine leukemia virus glycoprotein (MLV-GP)] were cotransfected into 293T cells. The supernatant was used for infection of target cells followed by determination of luciferase activity

72 h after infection by using a commercially available kit (Promega). For analyses of receptor engagement, 293T cells were transiently transfected with expression vectors encoding murine carcinoembryonic antigen (CEACAM)-1a, human or feline CD13, human ACE1 or ACE2, seeded into 96-well plates, and infected with pseudovirions normalized for comparable infection of Huh-7 cells.

Antibodies and FACS analysis

Surface expression of ACE1 or ACE2 on transfected 293T cells was detected by FACS analysis with purified polyclonal antibodies directed against the respective proteins (R & D Systems) in combination with a FITC-labeled secondary antibody (Dianova, Hamburg, Germany). Soluble Fc fusion proteins were transiently expressed in 293T cells, concentrated from culture supernatant by using CentriconPlus ultrafilters (Millipore), and incubated for 30 min on ice with 293T cells expressing either pcDNA3 or ACE2. Bound Fc fusion proteins were subsequently detected by using an antihuman Cy5-coupled secondary antibody (Dianova).

Inhibition of S-mediated entry into target cells by soluble ACE2.

Soluble ACE2 ectodomain was concentrated from the supernatant of transiently transfected 293T cells as described[18]. For inhibition of S-mediated infection, NL63-, SARS-CoV-, or 229E-S pseudotypes standardized for equal luciferase activity upon infection of Huh-7 cells were preincubated with various dilutions of soluble ACE2 for 1h at 37°C followed by infection of Huh-7 target cells. Luciferase activity in the cell extracts was determined after 72h.

Neutralization assays

NL63-S, 229E-S, or control pseudotypes standardized for equal luciferase activity upon infection of Huh-7 cells were preincubated with a 1:50 dilution of human serum samples for 1 h at 37°C. Alternatively, cells were incubated with purified polyclonal antibodies directed against ACE1 or ACE2. Thereafter, Huh-7 target cells were infected, and luciferase activity in the cell extracts was determined after 72 h. For inhibition of HCoV-NL63 replication, LLC-MK2 or Huh-7 cells were incubated with ACE1 or ACE2 antibodies for 30 min before infection with HCoV-NL63 at a multiplicity of infection of 1.6×10^{-2} (LLC-MK2) or 3×10^{-2} (Huh-7). Virus replication in the culture was assessed on day 4 or 5 after infection by scoring development of a CPE.

Results

Cell tropism of NL63- and 229E-S-bearing pseudotypes.

We first confirmed that the pseudotyping system is, indeed, an adequate tool to analyze receptor engagement by S proteins of widely different CoVs. Retroviral pseudotypes bearing the S proteins of HCoV-229E, FIPV, and MHV were used for infection of 293T cells transiently expressing CD13 or murine CEACAM-1, the receptors for HCoV-229E, FIPV, and MHV, respectively (Figure 1A). All viruses

encode the luciferase reporter gene, which is expressed only upon successful integration of the proviral genome into the genome of host cells. Expression of human and feline CD13 rendered the cells permissive to infection driven by 229E-S and FIPV-S, respectively, and expression of CEACAM-1 allowed entry of MHV-S-bearing pseudotypes, whereas control-transfected cells were not infected (Figure 1A). Thus, receptor engagement of the pseudovirions bearing different CoV S proteins is identical to that of the CoVs from which the S proteins were derived, underlining the fact that pseudoparticles are adequate tools to determine receptor binding by CoV S proteins.

Because the sequence of the S protein of HCoV-NL63 is 56% identical to that of HCoV-229E, we first analyzed the range of target cells susceptible to infection driven by these S proteins. Viruses bearing the G protein of vesicular stomatitis virus (VSV) served as positive control, whereas pseudovirions bearing no viral glycoprotein were used as negative control. All cell lines tested were highly

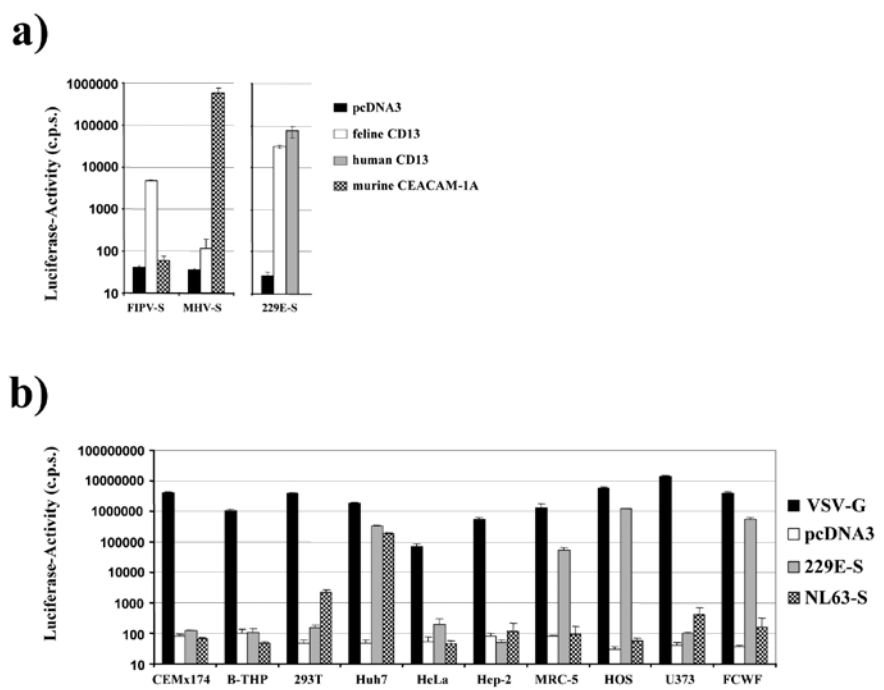


Figure 1. Cellular tropism of NL63-S- and 229E-S-bearing pseudotypes. (A) 293T cells were transfected with CoV receptors or pcDNA3 and infected with the indicated viral pseudotypes, and luciferase activities in the cell lysates were determined. c.p.s., counts per sec. A representative experiment is shown. Comparable results were obtained in an independent experiment. Error bars indicate SD. (B) Cell lines were infected with the indicated p24-normalized viral pseudotypes, and luciferase activities in the cell lysates were determined. The results were confirmed in three independent experiments. Error bars indicate SD.

susceptible to infection driven by VSV-G but were resistant to infection by control viruses bearing no glycoprotein (Figure 1B). Pseudovirions harboring the 229E-S protein infected MRC-5, HOS, and FCWF cells with appreciable efficiency, whereas none of these cells was susceptible to infection driven by NL63-S, indicating that the two S proteins interact with different cellular receptors. NL63-S mediated entry into Huh-7 and, with variable efficiency, into 293T cells (Figure 1B). These cells should, therefore, express the HCoV-NL63 receptor, and at least Huh-7 should be permissive to HCoV-NL63 entry.

The fusion activity of glycoproteins of enveloped viruses is activated by either receptor binding or protonation in endosomal vesicles[34]. Viruses that use the latter entry route can be inhibited by lysosomotropic agents such as bafilomycin A. Bafilomycin A and NH_4Cl treatment of Huh-7 cells revealed that infectious entry driven by NL63-S protein depends on the low-pH environment in intracellular vesicles (data not shown). Similar results were obtained for 229E-S-dependent infection, which is in agreement with published data[4]. Thus, the S proteins of HCoV-229E and HCoV-NL63 employ the same route of entry but likely interact with different receptors.

HCoV-NL63 engages ACE2 as a receptor for infectious cellular entry.
Comparison of the cell tropism of NL63-S-bearing pseudovirions with that documented for replication-competent SARS-CoV and SARS-CoV-S-harboring pseudotypes revealed striking similarities. Thus, Huh-7 and 293T cells are permissive to both NL63- and SARS-CoV-S-driven infection[19,33,41] and express the SARS-CoV receptor ACE2[18,24,28,39], whereas CEMx174, HeLa, and HOS cells are not permissive[19,33,41] and do not express ACE2[18,28]. We therefore determined whether ACE2 plays a role in HCoV-NL63 infection. Purified antibodies against the ectodomain of ACE1 did not modulate infection of Huh-7 cells by pseudotypes bearing 229E-, NL63-, or SARS-CoV-S (Figure 2 Left). In contrast, purified antibodies against the ectodomain of ACE2 (Figure 2 Center) or preincubation of pseudovirions with soluble ACE2 ectodomain (Figure 2 Right) potently blocked infection driven by NL63- and SARS-CoV but not 229E-S protein, indicating that NL63-S employs ACE2 for infectious cellular entry. To further investigate interactions of NL63-S with CoV receptors, CD13, ACE2, and the controls ACE1 and empty vector were overexpressed in 293T cells followed by infection with pseudotyped virions normalized for comparable infection of Huh-7 cells. Expression of CD13 rendered 293T cells highly permissive to infection driven by the S protein of HCoV-229E but not HCoV-NL63 or SARS-CoV (Figure 3A). The reverse observation was made for cells expressing ACE2 (Figure 3A), confirming that, despite the similarity between 229E- and NL63-S proteins, the latter engages ACE2 and not CD13 for cellular entry. FACS analysis employing soluble S1 domains of NL63- and SARS-CoV-S revealed binding of NL63-S1 to cells expressing ACE2 but not empty vector (Figure 3B), indicating

that ACE2 and NL63-S protein directly interact. Of note, SARS-CoV-S bound more efficiently to ACE2-expressing cells than NL63-S (Figure 3B), which could be indicative of a higher binding affinity. Finally, replication of HCoV-NL63 in LLC-MK2 and Huh-7 cells (Figure 4A), both of which express ACE2[18,41], was inhibited by antibodies against ACE2 but not ACE1 (Figure 4B), demonstrating that replication-competent HCoV-NL63 engages ACE2 as a receptor for spread in target cells. In summary, these data suggest a major role for ACE2 in HCoV-NL63 infection.

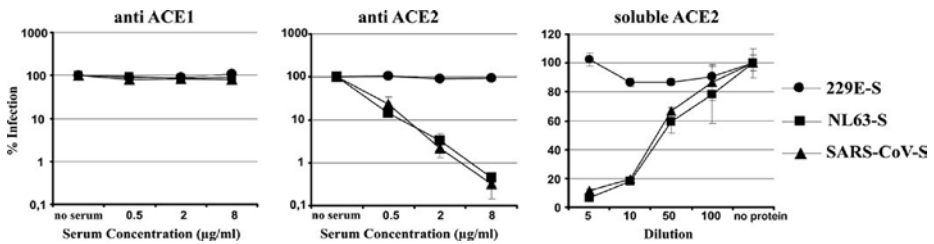


Figure 2. Inhibition of NL63-S-driven infection by ACE2-specific antibodies and soluble ACE2. Huh-7 cells were preincubated with ACE1- (Left) or ACE2- (Center) specific polyclonal antibodies, or the pseudotyped virions were preincubated with the ACE2 ectodomain (Right). Subsequently, the Huh-7 cells were infected with the indicated pseudovirions, and luciferase activities in the cell lysates were quantified. The results are shown as the percent of infection in the absence of inhibitor and were confirmed in two independent experiments. Error bars indicate SD.

Neutralizing activity directed against NL63-S is common in sera from adults.
HCoV-NL63 had initially been isolated from infants and was also detected in immunocompromised adults[13,38]. To evaluate the frequency of HCoV-NL63 in comparison with HCoV-229E infection, we first analyzed the neutralizing activity of sera obtained from adults with RTI, healthy adults, and infants between 3 and 6 months of age. Virtually all sera from adults with RTI or from healthy adults neutralized NL63-S-bearing pseudotypes with high efficiency (Figure 5A). In contrast, strong neutralization of 229E-S-harboring pseudotypes was observed with only a minority of the sera analyzed (Figure 5A), and sera from infants poorly neutralized infection driven by both NL63-S and 229E-S (Figure 5). None of the sera analyzed neutralized infection by MLV-GP-bearing pseudotypes (Figure 5B), demonstrating that the neutralization of NL63-S and 229E-S-bearing pseudotypes was, indeed, due to antibodies directed against the respective viral S proteins. Several sera strongly neutralized NL63-S-driven infection but had no effect on 229E-S-mediated infection (Figure 5A and data not shown), suggesting that a neutralizing humoral immune response directed against HCoV-NL63 does not necessarily confer protection against infection by the closely related HCoV-229E. In turn, these data also indicate that neutralization of NL63-S-dependent infection was, in most cases, not due to crossreactivity of antibodies directed against 229E-S, although the presence of crossneutralizing antibodies cannot

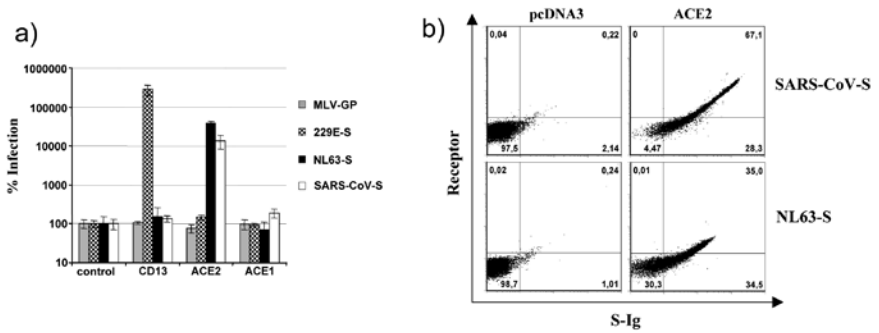


Figure 3. Expression of ACE2 potentiates NL63-S-driven infection, and soluble NL63-S protein binds to ACE2-positive cells. (A) 293T cells expressing CD13, ACE2, ACE1, or pcDNA3 were infected with the indicated pseudotypes, and luciferase activities in the cell lysates were determined. The results are shown as the percent of infection of pcDNA3-transfected cells. Similar results were obtained in three independent experiments. Error bars indicate SD. (B) ACE2 or pcDNA3 were transiently expressed on 293T cells, the cells were incubated with the S1 subunit of NL63-S or SARS-CoV-S fused to the Fc portion of human immunoglobulin, and receptor expression and S-Fc-fusion-protein binding were analyzed by FACS. Two independent experiments yielded similar results. NL63- and SARS-CoV-S binding was assessed with the same batch of transfected cells. Differences in ACE2 signal might be due to the masking of different ACE2 epitopes by the two S proteins, resulting in differential recognition of ACE2 by the polyclonal serum.

be excluded. Moreover, all sera from healthy adults recognized the N-terminal, unique sequence in NL63-S and inhibited HCoV-NL63 replication in LLC-MK2 cells (data not shown), further underlining that neutralization of NL63-S-driven infection was due to NL63-S-specific antibodies and not to crossneutralization.

Because sera from infants between 3 and 6 months of age did not modulate NL63-S-driven infection (Figure 5A), we investigated at which age a neutralizing antibody response against HCoV-NL63 becomes detectable. Analysis of sera from children of five different age groups revealed that neutralizing antibodies directed against NL63-S are first detectable in individuals with an average age of ~1.5 years and are found in most individuals with an average age of ~8 years (Figure 5B). Thus, HCoV-NL63 infection is frequent and is usually acquired during childhood.

Discussion

We demonstrated that HCoV-NL63 engages the SARS-CoV receptor ACE2 for infectious entry. Smith and colleagues independently obtained the same result (M. K. Smith, S. Tusell, B. B., L.v.d.H., and K. Holmes, unpublished data). The carboxypeptidase ACE2 is an important component of the renin–angiotensin system, which controls blood pressure[7,31], and ACE2 is required for cardiac function in mice[6]. ACE2 expression in lung and intestine[16] explains important aspects of SARS-CoV tropism, and the protein likely plays a central role in SARS-CoV

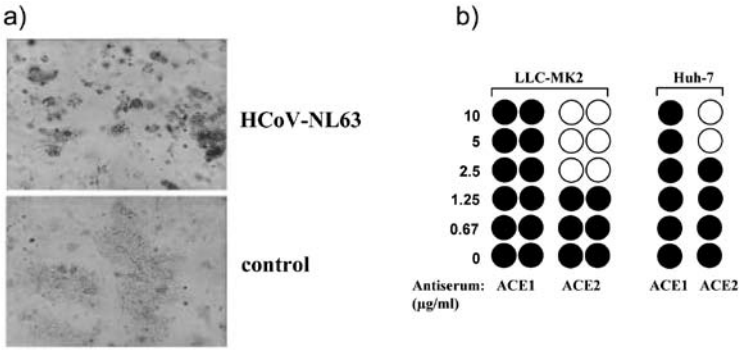


Figure 4. Inhibition of HCoV-NL63 replication by ACE2-specific antibodies. (A) Huh-7 cells were infected with HCoV-NL63 or mock infected, and CPE development was assessed 5 d after infection. Comparable results were obtained in several independent experiments. (B) LLC-MK2 and Huh-7 cells were preincubated with the indicated concentrations of ACE1- or ACE2-specific polyclonal antibodies and infected with HCoV-NL63, and the development of CPE was assessed. ●, CPE development; o, absence of CPE. Similar results were obtained in an independent experiment.

spread[20]. However, it is unclear how the virus induces disease and whether the way it engages ACE2 contributes to this process. Analysis of HCoV-NL63, a related but less pathogenic virus that shares the receptor, and thus, a major feature of its replication strategy, with SARS-CoV might yield important insights into this question.

The receptor specificity of viral glycoproteins determines, at least in part, which cell types can be infected, and the range of permissive cells has important implications for viral pathogenicity. HCoV-NL63 engages the same receptor and, consequently, infects the same target cells as SARS-CoV, but, in contrast to SARS-CoV, the virus usually induces only mild or moderate respiratory disease[2,10,12,26]. However, HCoV-NL63 was also detected in infants and immunocompromised adults with relatively severe RTI[1,13,38], suggesting that infection might have more profound pathogenic effects in individuals with reduced immune defenses. It is therefore conceivable that HCoV-NL63 lacks a specific pathogenicity factor present in SARS-CoV. Such a factor could be encoded by one or several of the accessory genes, nine of which are found in the SARS-CoV genome[25,32]. In stark contrast, the HCoV-NL63 genome harbors only a single accessory gene[13,38]. Whereas the function of the SARS-CoV accessory genes is largely unknown, the accessory genes of MHV were found to be dispensable for replication but required for full viral pathogenicity[8]. Some of the SARS-CoV accessory genes might, therefore, encode proteins that promote the development of SARS. The contribution of the accessory genes to the replication and pathogenesis of HCoV-NL63 and SARS-CoV must ultimately be assessed in infected animals. The establishment of HCoV-NL63 reverse genetics systems and small-animal models, both already described for SARS-CoV[36,43], are important prerequisites for these studies.

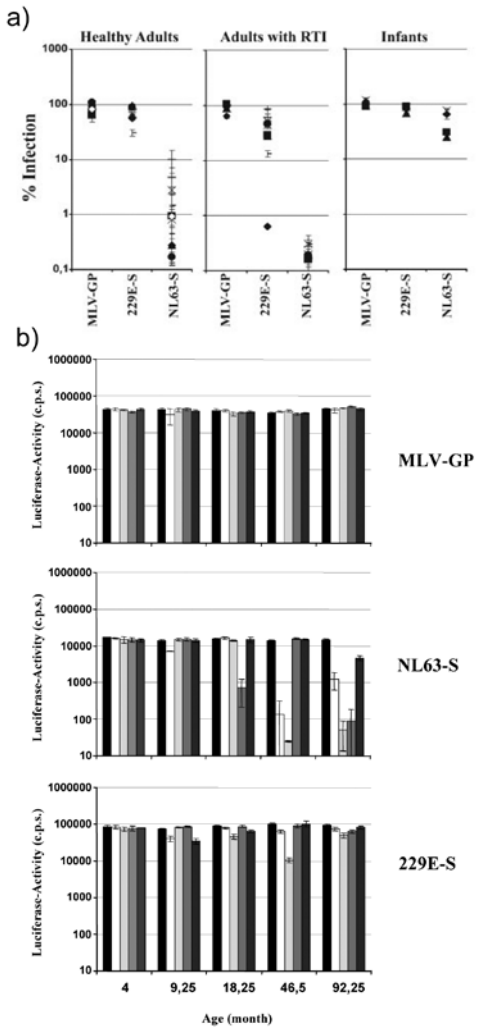


Figure 5. Neutralization of NL63-S-driven infection by human sera. (A) The indicated pseudovirions were incubated with 50-fold-diluted sera from healthy adults, adults with RTI, or infants and added onto Huh-7 cells, and luciferase activities in the cell lysates were determined. The results were confirmed in an independent experiment. Error bars indicate SD. (B) The indicated pseudovirions were incubated with 50-fold-diluted sera from a total of 25 infants of defined age groups and used for infection of Huh-7 cells as described for A. Sera from four individuals were analyzed per age group. Within age groups, bars indicate results obtained with serum from single individuals. The black bars indicate infection in the absence of patient serum. An independent experiment yielded similar results. Error bars indicate SD.

Another explanation for the apparent differences in HCoV-NL63 and SARS-CoV pathogenicity could be differences in interactions with ACE2. The SARS-CoV-S protein binds to human ACE2 with high efficiency[24], and amino acid residues in SARS-CoV-S, which are crucial for the interaction, have been identified[40]. However, the binding of SARS-CoV-S to murine ACE2 is clearly less efficient[23] and might account for the limited replication of the virus upon inoculation into mice[23,36]. Soluble NL63-S protein bound less robustly to ACE2-expressing cells compared with SARS-CoV-S, perhaps reflecting reduced affinity. If so, the S proteins might, at least partially, account for the differential pathogenicity of HCoV-NL63 and SARS-CoV. In this scenario, HCoV-NL63 variants, which

bind to ACE2 with high affinity and induce severe disease, should have ample opportunity to evolve, considering the frequent HCoV-NL63 infection of humans and high mutation rate of CoVs.

The interaction of NL63-S with ACE2 is most puzzling when taking into account that NL63-S is closely related to 229E-S, which binds CD13, but shares no appreciable amino acid identity with SARS-CoV-S, which binds ACE2. Similarly, the amino acid sequence of the CD13-binding site in 229E-S is 57% conserved in NL63-S, whereas the alignment of the ACE2-binding site of SARS-CoV-S with the most closely related sequence in NL63-S reveals only 14% amino acid identity. These data suggest that NL63- and SARS-CoV-S might have evolved different strategies to contact ACE2 or bind to different regions in ACE2. In fact, NL63-S harbors a 179-aa insertion at its N terminus[13,38], which does not share homology with any CoV sequences and which might be involved in ACE2 recognition. The latter speculation is in agreement with our observation that the bacterially purified unique region of NL63-S is recognized by human sera (data not shown), which exhibit strong neutralizing activity directed against NL63-S. Mutagenic analysis could be used to address the role of the unique region in NL63-S-mediated cellular entry. One of many possible ways to test whether SARS-CoV- and NL63-S bind to ACE2 differentially is to assess the impact of ACE2 inhibitors on SARS-CoV and HCoV-NL63 infection. Inhibitory compounds that bind to the active site in ACE2 and induce substantial conformational changes have been described[37], but their antiviral activity remains to be determined.

Analysis of the NL63-S protein interactions with ACE2 might also reveal important insights into the evolution of this virus. One could imagine that HCoV-NL63 and HCoV-229E have a common ancestor and, over time, NL63-S acquired ACE2 usage, whereas 229E-S evolved the use of CD13 as a receptor. Alternatively, HCoV-NL63 might have acquired the unique N-terminal sequence in its S protein by recombination with cellular or viral sequences, and these sequences might have conferred ACE2 binding to NL63-S. If so, this recombination event probably occurred early in HCoV-NL63 evolution because the unique sequence exhibits the same low G+C content, which is characteristic for the entire HCoV-NL63 genome[30]. However, the unique region in NL63-S does not share appreciable homology with any sequences in the database[38]. A viral or cellular donor of this sequence is, therefore, not obvious.

Infection with HCoV-229E and HCoV-OC43 is thought to be frequent and to account for a substantial amount of common-cold cases[21]. Our observation that virtually all sera from adults potently neutralized NL63-S- but not 229E-S-mediated infection suggests that HCoV-NL63 infection is more prevalent than infection with HCoV-229E. Indeed, recent reports demonstrate that HCoV-NL63 is globally distributed and that infection is associated with RTI in children[1,2,10,12,26].

Intriguingly, HCoV-NL63 infection was also found to be associated with Kawasaki disease[11], which can affect the coronary arteries and is a major cause for acquired heart disease in young children. The expression of ACE2 in coronary vessels[7] further supports a possible role of HCoV-NL63 in Kawasaki disease. In any event, diagnostic tests to detect HCoV-NL63 infection need to be developed, especially when considering the frequency of infection and the apparent similarities in HCoV-NL63 and SARS-CoV replication. In this regard, it is of interest that several patient sera potently neutralized NL63-S-driven infection but did not inhibit infection driven by 229E-S or SARS-CoV-S (data not shown), suggesting that neutralizing antibodies directed against HCoV-NL63 might not protect against infection with other HCoVs.

In summary, comparative analysis of HCoV-NL63 and SARS-CoV might reveal important aspects of SARS pathogenesis. It will be especially interesting to investigate whether the mode of ACE2 engagement by the viral S proteins impacts viral replication and pathogenesis. The establishment of reverse genetics systems and animal models for HCoV-NL63 replication are indispensable for these studies. The characterization of NL63 and SARS-CoV-S interactions with ACE2 might also have important implications for inhibitor development, because the S–ACE2 interface is a major target for therapeutic intervention. Finally, the apparent similarities between HCoV-NL63 and SARS-CoV replication and the frequent HCoV-NL63 infection of humans suggest that pathogenic HCoVs can evolve, highlighting the need for efficient vaccines against HCoVs.

Acknowledgments

We thank B. Fleckenstein and J. Behrens for constant support; B. J. Bosch and P. Rottier for plasmids encoding FIPV- and MHV-S and for discussion; G. Nabel for codon-optimized SARS-CoV-S-expression plasmid; J. Ziebuhr for a fragment encoding 229E-S; T. Gallagher for murine CEACAM-1a-expression plasmid; A. Kolb for feline CD13-encoding plasmid; P. Corvol for ACE1-encoding plasmid; F. Neipel for pAB61; B. Schmidt, H. Walter, and K. Korn for serum samples; and N. Finze for p24-ELISA. This work was supported by a grant from the Deutsche Forschungsgemeinschaft (SFB 466) to H.H., M.G., and S.P.

References

1. Arden, K. E., M. D. Nissen, T. P. Sloots, and I. M. Mackay. 2005. New human coronavirus, HCoV-NL63, associated with severe lower respiratory tract disease in Australia. J. Med. Virol. 75:455-462.
2. Bastien, N., K. Anderson, L. Hart, P. Van Caeseele, K. Brandt, D. Milley, T. Hatchette, E. C. Weiss, and Y. Li. 2005. Human coronavirus NL63 infection in Canada. J. Infect. Dis. 191:503-506.
3. Birkmann, A., K. Mahr, A. Ensser, S. Yaguboglu, F. Titgemeyer, B. Fleckenstein, and F. Neipel. 2001. Cell surface heparan sulfate is a receptor for human herpesvirus 8 and interacts with envelope glycoprotein K8.1. J. Virol. 75:11583-11593.
4. Blau, D. M. and K. V. Holmes. 2001. Human coronavirus HCoV-229E enters susceptible cells via the endocytic pathway. Adv. Exp. Med. Biol. 494:193-198.

5. Bosch, B. J., R. Van Der Zee, C. A. de Haan, and P. J. Rottier. 2003. The coronavirus spike protein is a class I virus fusion protein: structural and functional characterization of the fusion core complex. J. Virol. 77:8801-8811.
6. Crackower, M. A., R. Sarao, G. Y. Oudit, C. Yagil, I. Kozieradzki, S. E. Scanga, A. J. Oliveira-dos-Santos, J. da Costa, L. Zhang, Y. Pei, J. Scholey, C. M. Ferrario, A. S. Manoukian, M. C. Chappell, P. H. Backx, Y. Yagil, and J. M. Penninger. 2002. Angiotensin-converting enzyme 2 is an essential regulator of heart function. Nature 417:822-828.
7. Danilczyk, U., U. Eriksson, M. A. Crackower, and J. M. Penninger. 2003. A story of two ACEs. J. Mol. Med. 81:227-234.
8. de Haan, C. A., P. S. Masters, X. Shen, S. Weiss, and P. J. Rottier. 2002. The group-specific murine coronavirus genes are not essential, but their deletion, by reverse genetics, is attenuating in the natural host. Virology 296:177-189.
9. Delmas, B., J. Gelfi, R. L'Haridon, L. K. Vogel, H. Sjostrom, O. Noren, and H. Laude. 1992. Aminopeptidase N is a major receptor for the entero-pathogenic coronavirus TGEV. Nature 357:417-420.
10. Ebihara, T., R. Endo, X. Ma, N. Ishiguro, and H. Kikuta. 2005. Detection of human coronavirus NL63 in young children with bronchiolitis. J. Med. Virol. 75:463-465.
11. Esper, F., E. D. Shapiro, C. Weibel, D. Ferguson, M. L. Landry, and J. S. Kahn. 2005. Association between a novel human coronavirus and Kawasaki disease. J. Infect. Dis. 191:499-502.
12. Esper, F., C. Weibel, D. Ferguson, M. L. Landry, and J. S. Kahn. 2005. Evidence of a novel human coronavirus that is associated with respiratory tract disease in infants and young children. J. Infect. Dis. 191:492-498.
13. Fouchier, R. A., N. G. Hartwig, T. M. Bestebroer, B. Niemeyer, J. C. de Jong, J. H. Simon, and A. D. Osterhaus. 2004. A previously undescribed coronavirus associated with respiratory disease in humans. Proc. Natl. Acad. Sci. U. S. A 101:6212-6216.
14. Gallagher, T. M. and M. J. Buchmeier. 2001. Coronavirus spike proteins in viral entry and pathogenesis. Virology 279:371-374.
15. Giroglou, T., J. Cinatl, Jr., H. Rabenau, C. Drosten, H. Schwalbe, H. W. Doerr, and D. von Laer. 2004. Retroviral vectors pseudotyped with severe acute respiratory syndrome coronavirus S protein. J. Virol. 78:9007-9015.
16. Hamming, I., W. Timens, M. L. Bulthuis, A. T. Lely, G. J. Navis, and H. van Goor. 2004. Tissue distribution of ACE2 protein, the functional receptor for SARS coronavirus. A first step in understanding SARS pathogenesis. J. Pathol. 203:631-637.
17. Han, D. P., H. G. Kim, Y. B. Kim, L. L. Poon, and M. W. Cho. 2004. Development of a safe neutralization assay for SARS-CoV and characterization of S-glycoprotein. Virology 326:140-149.
18. Hofmann, H., M. Geier, A. Marzi, M. Krumbiegel, M. Peipp, G. H. Fey, T. Gramberg, and S. Pohlmann. 2004. Susceptibility to SARS coronavirus S protein-driven infection correlates with expression of angiotensin converting enzyme 2 and infection can be blocked by soluble receptor. Biochem. Biophys. Res. Commun. 319:1216-1221.
19. Hofmann, H., K. Hattermann, A. Marzi, T. Gramberg, M. Geier, M. Krumbiegel, S. Kuate, K. Uberla, M. Niedrig, and S. Pohlmann. 2004. S protein of severe acute respiratory syndrome-associated coronavirus mediates entry into hepatoma cell lines and is targeted by neutralizing antibodies in infected patients. J. Virol. 78:6134-6142.
20. Hofmann, H. and S. Pohlmann. 2004. Cellular entry of the SARS coronavirus. Trends Microbiol. 12:466-472.
21. Holmes, K. V. and M. M. C. Lai. 1996. *Coronaviridae*: The viruses and their replication, p. 1075-1093. In B. N. Fields, D. M. Knipe, P. M. Howley, and *et al* (eds.), Fields Virology. Lippincott-Raven Publishers, Philadelphia.
22. Kuo, L., G. J. Godeke, M. J. Raamsman, P. S. Masters, and P. J. Rottier. 2000. Retargeting of coronavirus by substitution of the spike glycoprotein ectodomain: crossing the host cell species barrier. J. Virol. 74:1393-1406.
23. Li, W., T. C. Greenough, M. J. Moore, N. Vasilieva, M. Somasundaran, J. L. Sullivan, M. Farzan, and H. Choe. 2004. Efficient replication of severe acute respiratory syndrome coronavirus in mouse cells is limited by murine angiotensin-converting enzyme 2. J. Virol. 78:11429-11433.

24. Li, W., M. J. Moore, N. Vasilieva, J. Sui, S. K. Wong, M. A. Berne, M. Somasundaran, J. L. Sullivan, K. Luzuriaga, T. C. Greenough, H. Choe, and M. Farzan. 2003. Angiotensin-converting enzyme 2 is a functional receptor for the SARS coronavirus. Nature 426:450-454.
25. Marra, M. A., S. J. Jones, C. R. Astell, R. A. Holt, A. Brooks-Wilson, Y. S. Butterfield, J. Khattra, J. K. Asano, S. A. Barber, S. Y. Chan, A. Cloutier, S. M. Coughlin, D. Freeman, N. Girn, O. L. Griffith, S. R. Leach, M. Mayo, H. McDonald, S. B. Montgomery, P. K. Pandoh, A. S. Petrescu, A. G. Robertson, J. E. Schein, A. Siddiqui, D. E. Smailus, J. M. Stott, G. S. Yang, F. Plummer, A. Andonov, H. Artsob, N. Bastien, K. Bernard, T. F. Booth, D. Bowness, M. Czub, M. Drebot, L. Fernando, R. Flick, M. Garbutt, M. Gray, A. Grolla, S. Jones, H. Feldmann, A. Meyers, A. Kabani, Y. Li, S. Normand, U. Stroher, G. A. Tipples, S. Tyler, R. Vogrig, D. Ward, B. Watson, R. C. Brunham, M. Krajden, M. Petric, D. M. Skowronski, C. Upton, and R. L. Roper. 2003. The Genome sequence of the SARS-associated coronavirus. Science 300:1399-1404.
26. Moes, E., L. Vijgen, E. Keyaerts, K. Zlateva, S. Li, P. Maes, K. Pyrc, B. Berkhout, L. van der Hoek, and M. Van Ranst. 2005. A novel pancoronavirus RT-PCR assay: frequent detection of human coronavirus NL63 in children hospitalized with respiratory tract infections in Belgium. BMC. Infect. Dis. 5:6.
27. Moore, M. J., T. Dorfman, W. Li, S. K. Wong, Y. Li, J. H. Kuhn, J. Coderre, N. Vasilieva, Z. Han, T. C. Greenough, M. Farzan, and H. Choe. 2004. Retroviruses pseudotyped with the severe acute respiratory syndrome coronavirus spike protein efficiently infect cells expressing angiotensin-converting enzyme 2. J. Virol. 78:10628-10635.
28. Nie, Y., P. Wang, X. Shi, G. Wang, J. Chen, A. Zheng, W. Wang, Z. Wang, X. Qu, M. Luo, L. Tan, X. Song, X. Yin, J. Chen, M. Ding, and H. Deng. 2004. Highly infectious SARS-CoV pseudotyped virus reveals the cell tropism and its correlation with receptor expression. Biochem. Biophys. Res. Commun. 321:994-1000.
29. Peiris, J. S., K. Y. Yuen, A. D. Osterhaus, and K. Stohr. 2003. The severe acute respiratory syndrome. N. Engl. J. Med. 349:2431-2441.
30. Pyrc, K., M. F. Jebbink, B. Berkhout, and L. van der Hoek. 2004. Genome structure and transcriptional regulation of human coronavirus NL63. Virol. J. 1:7.
31. Rice, G. I., D. A. Thomas, P. J. Grant, A. J. Turner, and N. M. Hooper. 2004. Evaluation of angiotensin-converting enzyme (ACE), its homologue ACE2 and neprilysin in angiotensin peptide metabolism. Biochem. J. 383:45-51.
32. Rota, P. A., M. S. Oberste, S. S. Monroe, W. A. Nix, R. Campagnoli, J. P. Icenogle, S. Penaranda, B. Bankamp, K. Maher, M. H. Chen, S. Tong, A. Tamin, L. Lowe, M. Frace, J. L. DeRisi, Q. Chen, D. Wang, D. D. Erdman, T. C. Peret, C. Burns, T. G. Ksiazek, P. E. Rollin, A. Sanchez, S. Liffick, B. Holloway, J. Limor, K. McCaustland, M. Olsen-Rasmussen, R. Fouchier, S. Gunther, A. D. Osterhaus, C. Drosten, M. A. Pallansch, L. J. Anderson, and W. J. Bellini. 2003. Characterization of a novel coronavirus associated with severe acute respiratory syndrome. Science 300:1394-1399.
33. Simmons, G., J. D. Reeves, A. J. Rennekamp, S. M. Amberg, A. J. Piefer, and P. Bates. 2004. Characterization of severe acute respiratory syndrome-associated coronavirus (SARS-CoV) spike glycoprotein-mediated viral entry. Proc. Natl. Acad. Sci. U. S. A 101:4240-4245.
34. Smith, A. E. and A. Helenius. 2004. How viruses enter animal cells. Science 304:237-242.
35. Stadler, K., V. Masignani, M. Eickmann, S. Becker, S. Abrignani, H. D. Klenk, and R. Rappuoli. 2003. SARS--beginning to understand a new virus. Nat. Rev. Microbiol. 1:209-218.
36. Subbarao, K., J. McAuliffe, L. Vogel, G. Fahle, S. Fischer, K. Tatti, M. Packard, W. J. Shieh, S. Zaki, and B. Murphy. 2004. Prior infection and passive transfer of neutralizing antibody prevent replication of severe acute respiratory syndrome coronavirus in the respiratory tract of mice. J. Virol. 78:3572-3577.
37. Towler, P., B. Staker, S. G. Prasad, S. Menon, J. Tang, T. Parsons, D. Ryan, M. Fisher, D. Williams, N. A. Dales, M. A. Patane, and M. W. Pantoliano. 2004. ACE2 X-ray structures reveal a large hinge-bending motion important for inhibitor binding and catalysis. J. Biol. Chem. 279:17996-18007.
38. van der Hoek, L., K. Pyrc, M. F. Jebbink, W. Vermeulen-Oost, R. J. Berkhout, K. C. Wolthers, P. M. Wertheim-van Dillen, J. Kaandorp, J. Spaargaren, and B. Berkhout. 2004. Identification of a new human coronavirus. Nat. Med. 10:368-373.
39. Wang, P., J. Chen, A. Zheng, Y. Nie, X. Shi, W. Wang, G. Wang, M. Luo, H. Liu, L. Tan, X. Song, Z. Wang, X. Yin, X. Qu, X. Wang, T. Qing, M. Ding, and H. Deng. 2004. Expression cloning of functional receptor used by SARS coronavirus. Biochem. Biophys. Res. Commun. 315:439-444.

40. Wong, S. K., W. Li, M. J. Moore, H. Choe, and M. Farzan. 2004. A 193-amino acid fragment of the SARS coronavirus S protein efficiently binds angiotensin-converting enzyme 2. J. Biol. Chem. 279:3197-3201.
41. Yang, Z. Y., Y. Huang, L. Ganesh, K. Leung, W. P. Kong, O. Schwartz, K. Subbarao, and G. J. Nabel. 2004. pH-dependent entry of severe acute respiratory syndrome coronavirus is mediated by the spike glycoprotein and enhanced by dendritic cell transfer through DC-SIGN. J. Virol. 78:5642-5650.
42. Yeager, C. L., R. A. Ashmun, R. K. Williams, C. B. Cardellichio, L. H. Shapiro, A. T. Look, and K. V. Holmes. 1992. Human aminopeptidase N is a receptor for human coronavirus 229E. Nature 357:420-422.
43. Yount, B., K. M. Curtis, E. A. Fritz, L. E. Hensley, P. B. Jahrling, E. Prentice, M. R. Denison, T. W. Geisbert, and R. S. Baric. 2003. Reverse genetics with a full-length infectious cDNA of severe acute respiratory syndrome coronavirus. Proc. Natl. Acad. Sci. U. S. A 100:12995-13000.

Chapter VII

Downregulation of angiotensin converting enzyme 2 protein during HCoV-NL63 infection

Unpublished

Krzysztof Pyrc, Ronald Dijkman, Maarten F. Jebbink, Ben Berkhout, Anna van der Bijl and Lia van der Hoek

Laboratory of Experimental Virology, Department of Medical Microbiology, Center for Infection and Immunity Amsterdam (CINIMA), Academic Medical Center, University of Amsterdam, Meibergdreef 15, 1105 AZ, Amsterdam, The Netherlands.

The *Coronaviridae* family is a group of positive stranded RNA viruses. The past years 3 new human coronaviruses (HCoV) were identified, HCoV-NL63, HCoV-HKU1 and SARS-CoV. The most pathogenic human coronavirus is SARS-CoV, which causes severe respiratory distress, whereas the other human coronaviruses are associated with relatively mild respiratory illness. The striking difference in pathogenesis between human coronaviruses is still puzzling, especially considering the fact that SARS-CoV and HCoV-NL63 use the same receptor – angiotensin converting enzyme 2 (ACE2) - for their cell entry. ACE2 plays a protective role during lung damage and it has been suggested that the high pathogenicity of SARS-CoV is directly linked to downregulation of ACE2 during infection. We investigated whether HCoV-NL63 infection also influences ACE2 expression. We monitored ACE2 expression at the protein and mRNA level during infection of LLC-MK2 cells. As soon as 3 days after infection we observed a steep decline in ACE2 protein expression. This coincided with a logarithmic rise in the amount of virus in the culture supernatant. At the mRNA level there was no decrease in ACE2 mRNA, indicating that the downregulation occurs at the post-transcriptional level. As HCoV-NL63 causes a decrease in ACE2 protein level similar as SARS-CoV, despite the differences in pathogenicity, the usage of the ACE2 molecule as receptor, as well as its downregulation during infection, does not necessarily cause the severe lung damage observed during SARS-CoV infection.

Introduction

Until the autumn of 2002, coronaviruses were generally considered as common cold viruses with low pathogenicity. The SARS-CoV outbreak of 2002-2003 attracted the attention to this family of viruses, resulting in the subsequent identification of additional members of the *Coronaviridae* family [18,20]. HCoV-NL63 with its worldwide spread seems to be one of the clinically most relevant coronaviruses. Studies on the incidence of HCoV-NL63 infection report a frequency of 1-10% of all respiratory infections in humans. The virus was diagnosed most frequently in children, elderly people and immunocompromised patients[1,2,5,7,10,13,16-19].

Recently, downregulation of ACE2 protein levels during SARS -CoV infection has been described[11]. ACE2 is a homologue of ACE, and functions as a negative regulator of the renin–angiotensin system that has an important role in maintaining blood pressure homeostasis, as well as fluid and salt balance[3,6,15]. ACE2 also plays a protective role in acute lung injury[9] and it has been suggested that the severity of the lung damage during SARS-CoV infection is caused by downregulation of the ACE2 protein on the airway epithelial[11].

Besides SARS-CoV, HCoV-NL63 is the only other virus that uses ACE2 to enter its target cells[8]. Considering that both viruses use the same receptor, but the clinical symptoms during infection are like poles apart, we investigated the effect of HCoV-NL63 infection on the expression of ACE2 in *in vitro* infection experiments.

Methods

Cell culture and infection

LLC-MK2 cells were cultured in minimal essential medium (MEM; 2 parts Hanks' MEM and 1 part Earle's MEM) supplemented with 3% heat-inactivated fetal calf serum (PAA Laboratories), penicillin (100U/ml), and streptomycin (100µg/ml). Cells were plated onto 6-well plates at a density of 0.3×10^6 cells / well in fresh medium (4ml per well) and cultured at 37°C with 5% CO_2.

HCoV-NL63 (isolate Amsterdam 1) was obtained from a virus culture on LLC-MK2 cells as described previously[18]. The infectious titer of the virus was determined according to the Reed and Muench formula[14] on an LLC-MK2 cell monolayer. The virus stock has a titer of 2×10^5 50 % tissue culture infectivity dose/ml.

LLC-MK2 cells were infected with HCoV-NL63 at a multiplicity of infection of 0.01 and cultured at 34°C. Culture supernatant and cells were harvested 1, 2, 3, 4, 5, 6 and 7 days after infection, together with samples from day 0. For harvesting of the cells the medium was removed, cells were washed with PBS and 5mM EDTA in PBS and detachment from the surface was achieved by 30min incubation at 37°C with 5mM EDTA in PBS. Viable cells were counted using Trypan Blue and a constant number of live cells was transferred into protein lysis buffer (62.5mM TRIS-HCl, 10% glycerol, 2% SDS, 5% β-mercaptoethanol and 0.025% bromophenol blue) for Western blot analysis. For mRNA analysis cells were lyzed with TRIzol® reagent (Invitrogen). All experiments were performed in duplo and carried out in duplicate.

RNA isolation and reverse transcription

The HCoV-NL63 RNA was isolated by Boom extraction method[4]. mRNA was isolated according to the standard TRIzol® procedure (Invitrogen). After RNA isolation samples used for ACE2 and β–actin mRNA quantification were treated with DNase (2U/ml; Ambion) for 45 minutes at 37°C and subsequently purified by phenol/chloroform extraction and ethanol precipitation. Reverse transcription was performed with Moloney murine leukemia virus reverse transcriptase (Invitrogen) (200U per reaction) and 10ng of random hexamers (Amersham Biosciences) in 10mM Tris, pH 8.3, 50mM KCl, 0.1% Triton X-100, 6mM of $MgCl_2$, and 50µM of each deoxynucleoside triphosphate at 37°C for 90min in a total volume of 40µl.

Quantitative PCR

mRNA quantification was performed with real-time PCR. Ten microliters of cDNA was amplified in 50µl 1×Platinum quantitative PCR SuperMix–uracil-DNA glycosylase (Invitrogen) with 5mM $MgCl_2$, 200nM specific probe labeled with FAM (6-carboxyfluorescein) and TAMRA (6-carboxytetramethylrhodamine), and 900nM of each primer. The following primers were used for HCoV-NL63: sense, 5'-GCGT-

GTTCCTACCAGAGAGGA-3′; antisense, 5′-GCTGTGGAAAACCTTTGGCA-3′; and probe, 5′-FAM-ATGTTATTCAGTGCTTTGGTCCTCGTGAT-TAMRA-3′. Primers and probe used for detection of Macaca Mulatta ACE2 mRNA: sense, 5′- CATGGGAGCAAGTATTGGACCTT -3′; antisense, 5′- GAACTAGTGCAT-GCCATTCTCA -3′; and probe, 5′-FAM- CTTGCAGCTGTACCAGTTCCCAG-GCA -TAMRA-3′. For the β-actin quantification, the commercially available β-actin detection kit was used (TaqMan β-actin Detection Reagents, ABI applied biosystems). All measurements were done with the ABI PRISM® 7000 Sequence Detection System (Applied Biosystems Foster City, California). Following the UDG treatment for 2min at 50°C and denaturing for 10min at 95°C, 45 cycles of amplification were performed for 15s at 95°C and 60s at 60°C.

To confirm that residual chromosomal DNA did not influence the ACE2 mRNA quantification, the isolated mRNA was analyzed for ACE2 DNA by real-time PCR. In all cases the signal was negative or at least 100 fold lower than the cDNA samples.

Protein preparation and Western blot analysis

Samples before the Western blot analysis were sheared with a syringe and needle, boiled for 5 minutes, quenched on ice and layered (10µl per lane) on 15% polyacrylamide gel for the ACE2 protein detection and β-actin detection. Dilutions of recombinant human ACE-2 (R&D systems, Minneapolis) was used as positive controls. To control the protein size, the dual color Precision Plus Protein size marker (Bio-Rad) was used. The electrophoresis was done at 30 mA. Subsequently, the gels were transferred onto Immobilon-P membrane (Millipore), by semi-dry blotting (Bio-Rad) for 1 hour, 15 Volt in buffer containing 0.38M TRIS, 0,31M glycine, 3% SDS and 20% methanol at room temperature. Unspecific binding sites were blocked with 5% skimmed milk (Fluka) in PBS-Tween (0.1%) overnight at 4°C. For detection of ACE2 protein goat derived anti-human ACE-2 ectodomain antibody (R&D systems) was used as primary antibodies and mouse derived, horseradish peroxidase labeled, anti-goat IgG (Sigma) as secondary. For the β-actin detection, monoclonal anti β-actin antibodies (Sigma) were used as primary antibodies and goat derived, horseradish peroxidase labeled, anti-mouse IgG (Sigma) as secondary. All antibodies were diluted in 1% skimmed milk in PBS-tween (0.1%). Signal was developed using the Western Lightning kit (Perkin Elmer). The signal was visualized by exposure of the membrane to an X-ray film. Pictures were analyzed with Scion Image 4 software.

Results and Discussion

We evaluated whether infection by HCoV-NL63 has an influence on the level of ACE2 protein expression. To this end we infected LLC-MK2 cells and monitored each day after infection the level of ACE2 protein by Western blot analysis. The 85kD protein can be easily detected via Western blot, and appears as a fussy band of 120kD because of glycosylation. Analysis of ACE2 expression during HCoV-NL63 infection

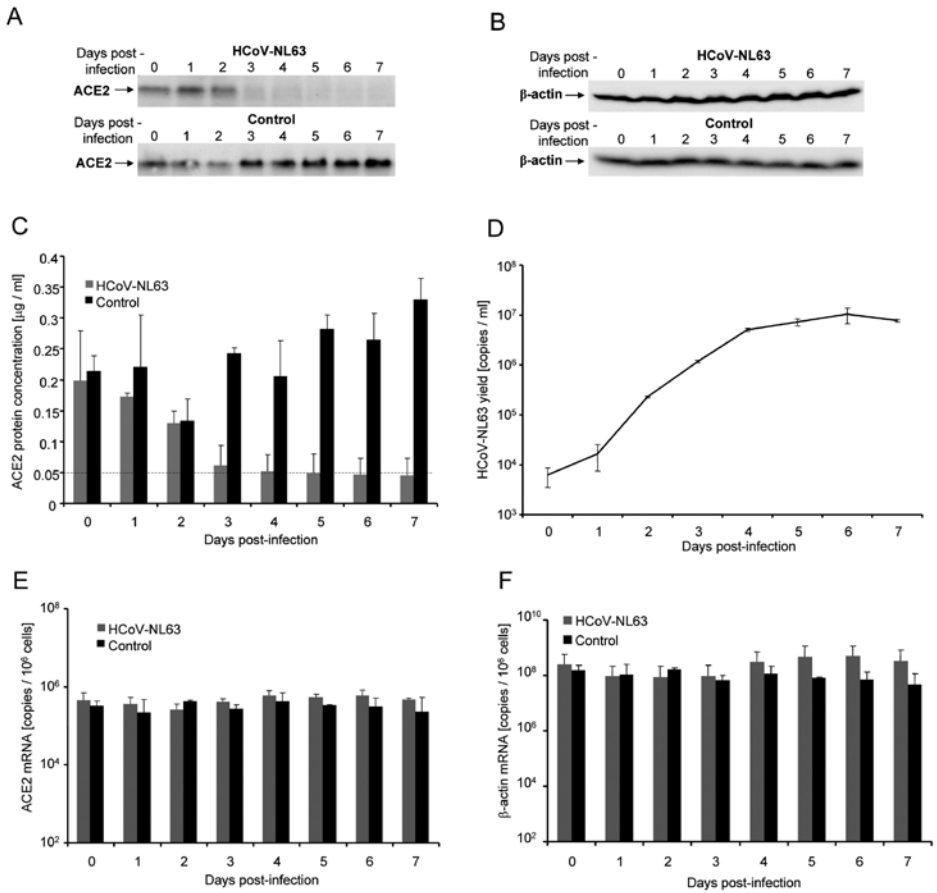


Figure 1. Downregulaion of ACE2 in HCoV-NL63 infected cells A) ACE2 protein in infected and non-infected cells. B) β-actin protein levels in infected and non-infected cells. C) Quantification of ACE2 protein levels. The dotted line represents the detection level. D) HCoV-NL63 viral yield in time. E) ACE2 mRNA in infected and non-infected cells. F) β-actin mRNA in infected and non-infected cells.

clearly shows that after 3 days of infection the level of the cellular ACE2 protein is dramatically reduced compared to non-infected control cells (Figure 1A). A β-actin control blot is shown in Figure 1B. Using serial dilutions of purified ACE2 protein we quantified the levels of ACE2 expression and the decrease during infection (Figure 1C). At day 3 the ACE2 level was decreased by 4-fold. This strong decrease in ACE2 expression coincidences with the burst of replication of HCoV-NL63. On day 3 and 4 an exponential rise of HCoV-NL63 in the culture supernatant is observed (Figure 1D). We further investigated whether the ACE2 protein decrease is regulated at the mRNA level. To this end we quantified the ACE2 mRNA level during infection. Even until day 7 no decrease in mRNA levels were observed (Figure 1E). Thus, the NL63-specific downregulation of ACE2 only affects the protein level.

HCoV-NL63 infection of LLC-MK2 cells causes a cytopathic effect (CPE). In our experiments only a very mild CPE was noticed at day 3 and 4. From day 5 onwards, massive CPE was observed with rounding of the cells and eventual cell detachment. Considering that decrease of ACE2 protein level precedes the onset of CPE, the downregulation of ACE2 cannot be explained by cell death. This is also confirmed by β-actin mRNA and protein levels. From day 0 to day 7 these levels are constant (Figure 1B, 1E and 1F).

The decrease in ACE2 protein expression is similar to what has been presented for SARS-CoV[11]. Consequently, both viruses trigger downregulation of ACE2 protein levels. This indicates that the severe pathogenesis and ARDS developed during SARS-CoV infection cannot be explained solely by the interference of SARS-CoV with the renin angiotensin system. The difference in pathogenesis of these two viruses is likely to be associated with other viral determinants: e.g. the kinetics and localization of replication, or the effects of other viral proteins on the cell metabolism. *In vivo* models can shed more light on this issue but unfortunately an animal model system for HCoV-NL63 infection is not available.

References

1. Arden, K. E., M. D. Nissen, T. P. Sloots, and I. M. Mackay. 2005. New human coronavirus, HCoV-NL63, associated with severe lower respiratory tract disease in Australia. J. Med. Virol. 75:455-462.
2. Bastien, N., J. L. Robinson, A. Tse, B. E. Lee, L. Hart, and Y. Li. 2005. Human coronavirus NL-63 infections in children: a 1-year study. J. Clin. Microbiol. 43:4567-4573.
3. Boehm, M. and E. G. Nabel. 2002. Angiotensin-converting enzyme 2--a new cardiac regulator. N. Engl. J. Med. 347:1795-1797.
4. Boom, R., C. J. Sol, M. M. Salimans, C. L. Jansen, P. M. Wertheim-van Dillen, and J. van der Noordaa. 1990. Rapid and simple method for purification of nucleic acids. J. Clin. Microbiol. 28:495-503.
5. Chiu, S. S., K. H. Chan, K. W. Chu, S. W. Kwan, Y. Guan, L. L. Poon, and J. S. Peiris. 2005. Human coronavirus NL63 infection and other coronavirus infections in children hospitalized with acute respiratory disease in Hong Kong, China. Clin. Infect. Dis. 40:1721-1729.
6. Crackower, M. A., R. Sarao, G. Y. Oudit, C. Yagil, I. Kozieradzki, S. E. Scanga, A. J. Oliveira-dos-Santos, J. da Costa, L. Zhang, Y. Pei, J. Scholey, C. M. Ferrario, A. S. Manoukian, M. C. Chappell, P. H. Backx, Y. Yagil, and J. M. Penninger. 2002. Angiotensin-converting enzyme 2 is an essential regulator of heart function. Nature 417:822-828.
7. Ebihara, T., R. Endo, X. Ma, N. Ishiguro, and H. Kikuta. 2005. Detection of human coronavirus NL63 in young children with bronchiolitis. J. Med. Virol. 75:463-465.
8. Hofmann, H., K. Pyrc, L. van der Hoek, M. Geier, B. Berkhout, and S. Pohlmann. 2005. Human coronavirus NL63 employs the severe acute respiratory syndrome coronavirus receptor for cellular entry. Proc. Natl. Acad. Sci. U. S. A 102:7988-7993.
9. Imai, Y., K. Kuba, S. Rao, Y. Huan, F. Guo, B. Guan, P. Yang, R. Sarao, T. Wada, H. Leong-Poi, M. A. Crackower, A. Fukamizu, C. C. Hui, L. Hein, S. Uhlig, A. S. Slutsky, C. Jiang, and J. M. Penninger. 2005. Angiotensin-converting enzyme 2 protects from severe acute lung failure. Nature 436:112-116.
10. Kaiser, L., N. Regamey, H. Roiha, C. Deffernez, and U. Frey. 2005. Human coronavirus NL63 associated with lower respiratory tract symptoms in early life. Pediatr. Infect. Dis. J. 24:1015-1017.
11. Kuba, K., Y. Imai, S. Rao, H. Gao, F. Guo, B. Guan, Y. Huan, P. Yang, Y. Zhang, W. Deng, L. Bao, B. Zhang, G. Liu, Z. Wang, M. Chappell, Y. Liu, D. Zheng, A. Leibbrandt, T. Wada, A. S. Slutsky, D. Liu, C. Qin, C. Jiang, and J. M. Penninger. 2005. A crucial role of angiotensin converting enzyme 2 (ACE2) in SARS coronavirus-induced lung injury. Nat. Med. 11:875-879.

12. Lee, N., D. Hui, A. Wu, P. Chan, P. Cameron, G. M. Joynt, A. Ahuja, M. Y. Yung, C. B. Leung, K. F. To, S. F. Lui, C. C. Szeto, S. Chung, and J. J. Sung. 2003. A major outbreak of severe acute respiratory syndrome in Hong Kong. N. Engl. J. Med. 348:1986-1994.
13. Moes, E., L. Vijgen, E. Keyaerts, K. Zlateva, S. Li, P. Maes, K. Pyrc, B. Berkhout, L. van der Hoek, and M. Van Ranst. 2005. A novel pancoronavirus RT-PCR assay: frequent detection of human coronavirus NL63 in children hospitalized with respiratory tract infections in Belgium. BMC. Infect. Dis. 5:6.
14. Reed, L. J. and H. Muench. 1938. A simple method of estimating fifty percent endpoints. American Journal of Hygiene 27:493-497.
15. Skeggs, L. T., F. E. Dorer, M. Levine, K. E. Lentz, and J. R. Kahn. 1980. The biochemistry of the renin-angiotensin system. Adv. Exp. Med. Biol. 130:1-27.
16. Suzuki, A., M. Okamoto, A. Ohmi, O. Watanabe, S. Miyabayashi, and H. Nishimura. 2005. Detection of human coronavirus-NL63 in children in Japan. Pediatr. Infect. Dis. J. 24:645-646.
17. Vabret, A., T. Mourez, J. Dina, L. van der Hoek, S. Gouarin, J. Petitjean, J. Brouard, and F. Freymuth. 2005. Human coronavirus NL63, France. Emerg. Infect. Dis. 11:1225-1229.
18. van der Hoek, L., K. Pyrc, M. F. Jebbink, W. Vermeulen-Oost, R. J. Berkhout, K. C. Wolthers, P. M. Wertheim-van Dillen, J. Kaandorp, J. Spaargaren, and B. Berkhout. 2004. Identification of a new human coronavirus. Nat. Med. 10:368-373.
19. van der Hoek, L., K. Sure, G. Ihorst, A. Stang, K. Pyrc, M. F. Jebbink, G. Petersen, J. Forster, B. Berkhout, and K. Uberla. 2005. Croup is associated with the novel coronavirus NL63. PLoS. Med. 2:e240.
20. Woo, P. C., S. K. Lau, C. M. Chu, K. H. Chan, H. W. Tsoi, Y. Huang, B. H. Wong, R. W. Poon, J. J. Cai, W. K. Luk, L. L. Poon, S. S. Wong, Y. Guan, J. S. Peiris, and K. Y. Yuen. 2005. Characterization and complete genome sequence of a novel coronavirus, coronavirus HKU1, from patients with pneumonia. J. Virol. 79:884-895.

Chapter VIII

HCoV-NL63 induces interleukin-6 and interleukin-8 expression

Unpublished

Krzysztof Pyrc[1], Anna van der Bijl[1], Ronald Dijkman[1], Maarten F. Jebbink[1], Mieke Snoek[2], Susan E. Burkett[3], Amy C. Sims[4], Leslie Fulcher[3], John Rossen[6], Scott Randell[3], Raymond J. Pickles[3,5], Rene Lutter[2], Ralph Baric[4,5], Ben Berkhout[1] and Lia van der Hoek[1].

Laboratory of Experimental Virology, Department of Medical Microbiology, Center for Infection and Immunity Amsterdam (CINIMA)[1] and Departments of Pulmonology[2] and Experimental Immunology[7], Academic Medical Center, University of Amsterdam, Meibergdreef 15, 1105 AZ, Amsterdam, The Netherlands.; Cystic Fibrosis/Pulmonary Research and Treatment Center[3], Departments of Epidemiology[4], Microbiology and Immunology[5], University of North Carolina at Chapel Hill, Chapel Hill, North Carolina, USA.; Eijkman-Winkler Institute, Department of Virology, University Medical Center, Utrecht, The Netherlands[6]

The pathogenesis of human coronavirus (HCoV) NL63 infection is poorly understood. HCoV-NL63 seems to cause relatively mild upper respiratory tract infections and croup. Interestingly, the cellular receptor and cell specificity is shared between HCoV-NL63 and SARS-CoV. This raises an interesting question, why are the symptoms of the latter infection so much more severe. Cytokine dysregulation has been suggested as one of the factors involved in SARS-CoV pathogenesis. We analyzed the interleukin 6 and interleukin 8 profiles during HCoV-NL63 infection in three *in vitro* systems and report increased release of both cytokines, similar to what has been described for SARS-CoV infection.

Introduction

Human coronavirus NL63 is a recently discovered human pathogen. Phylogenetic analyses have shown that it belongs to the group 1 coronaviruses, together with the other human pathogen HCoV-229E[35]. Infection with HCoV-NL63 is prevalent and associated with upper or lower respiratory tract infections, with more severe symptoms in children, elderly and immunocompromised patients[1-4,6,10,13,20,25,32,34-36].

Identification of ACE2 as the cellular receptor for HCoV-NL63 revealed that SARS-CoV and HCoV-NL63 infect the same cell type[18]. Despite that, the disease manifestations of these two infections are quite different. There are several possible explanations for that distinction, including the interaction of these viruses with the innate immune system. Cytokines play a critical role in the modulation of immune and inflammatory events[8,24,26]. For SARS-CoV it was concluded that the modulation of the innate immune response is related to the pathological changes[19,27,33]. The production of locally released cytokines during HCoV-NL63 infection has not yet been evaluated.

We chose to examine interleukin (IL) 6 and IL-8 production during HCoV-NL63 infection, as these mediators are key players in the immune system that have been shown to be clinically relevant in other viral infections. IL-8 is a major chemoattractant for neutrophils and therefore plays a major role in development of inflammation–related damage[14,22]. Production of this chemokine has been reported for some acute viral infections (SARS-CoV, RSV, parainfluenza, influenza)[27,31]. IL-6 is a pleiotropic mediator with both pro- and anti-inflammatory activities, and it is involved in the pathogenesis of several diseases. Increased release of IL-6 has been reported for various coronavirus infections[9,12], and may be involved in viral clearance by activation of acute phase response and Janus kinase/signal transducers and activators of the transcription (JAK/STAT) pathway[11,21].

We observed an increased release of IL-6 and IL-8 from *in vitro* cultured cells infected with HCoV-NL63. This increase is comparable to that described for *in vitro* RSV infection and SARS-CoV infection[27].

Methods

Cell culture

LLC-MK2 cells were maintained in a 2:1 mixture of minimal essential medium (MEM) with Hanks' salts and MEM with Earle's salts (Invitrogen) supplemented with 3% heat inactivated fetal calf serum (FCS). Diploid tertiary monkey kidney (tMK) cells (kindly provided by Berry Wilbrink, RIVM, The Netherlands) were cultured in Eagle MEM (Invitrogen).

Human tracheobronchial epithelial cells were obtained from airway specimens resected from patients undergoing surgery under University of North Carolina Institutional Review Board-approved protocols by the Cystic Fibrosis Center Tissue Culture Core. Primary cells were expanded on plastic to generate passage 1 cells and plated at a density of 2.5×10^5 cells per well on permeable Transwell-Col (12-mm-diameter) supports[15,29]. Human airway epithelium (HAE) cultures were generated by provision of an air-liquid interface for 4 to 6 weeks to form well-differentiated, polarized cultures that resemble *in vivo* pseudostratified mucociliary epithelium[29].

Virus preparation, titration, and infection

An HCoV-NL63 virus stock was prepared on LLC-MK2 cells. Cells were lysed after 6 days of infection by one freeze-thawing cycle and cell debris was removed by centrifugation. The supernatant was aliquoted and stored at -80°C. Tissue culture 50% infectious dose ($TCID_{50}$) was determined according to Reed and Muench[30]. RSV B virus stock was prepared on tMK cells in a similar manner.

Cells with 100% confluency were exposed to 800 $TCID_{50}$ of HCoV-NL63 or RSV B. A control LLC-MK2 cell lysate from mock infected cells was prepared in the same manner as the virus stock. Inactivated virus stock was prepared by exposition of a viable virus stock to ultraviolet radiation ($\lambda = 245$) for 15min. Inactivation was confirmed by a loss of *in vitro* replication. Supernatant samples that were used to measure cytokine levels were collected every 24h for seven days and stored at -80°C.

HAE cultures were infected with the virus that was inoculated at the apical surface (200µl). Prior to inoculation, the apical surfaces of HAE were rinsed three times for 30 min with phosphate-buffered saline (PBS) at 37°C. Following a 2h viral incubation at 32°C, the unbound virus was removed and HAE were maintained with an air-liquid interface for the remainder of the experiment. To generate replication curves and cytokine profiles at specific times after viral inoculation, 120µl of culture medium was applied to the apical surface of HAE and collected after 10min incubation at 32°C. All samples were stored at −80°C.

Virus detection by reverse transcription and quantitative PCR

Total RNA was extracted from the culture supernatant samples by the silica-affinity-based Boom extraction method[5]. Reverse transcription was performed with Moloney murine leukemia virus reverse transcriptase (Invitrogen) (200U per reaction) and 10ng of random hexamers (Amersham Biosciences) in 10mM Tris, pH 8.3, 50mM KCl, 0.1% Triton X-100, 5mM $MgCl_2$, and 400μM of each deoxynucleoside triphosphate at 37°C for 90min. HCoV-NL63 virus yield was determined with real-time PCR. Ten microliters of cDNA was amplified in 50 μl 1×Platinum quantitative PCR SuperMix-uracil-DNA glycosylase (Invitrogen) with 3 mM $MgCl_2$, 200nM specific probe labeled with FAM (6-carboxyfluorescein) and TAMRA (6-carboxytetramethylrhodamine), and 900nM primers. The following primers were used for HCoV-NL63: sense, 5′-GCGTGTTCCTACCAGAGAGGA-3′; antisense, 5′-GCTGTGGAAAACCTTTGGCA-3′; and probe, 5′-FAM-ATGTTATTCAGTGCTTTGGTCCTCGTGAT-TAMRA-3′. The reaction was monitored on a TaqMan 7000 machine (ABI). After 2 min 50°C and 5 min 95°C, 45 cycles of amplification were performed for 15 s at 95°C and 60 s at 60°C. RSV B virus yield was determined with real-time PCR as described before[37], in a 25μl reaction mixture containing 5μl of cDNA, 12.5μl of 2×TaqMan universal PCR master mix (PE Applied Biosystems), 300nM primers, and 66.7nM probe. The following primers were used for RSV B: sense, 5′- AAGATGCAAATCATAAATTCACAGGA -3′; antisense, 5′- TGATATCCAGCATCTTTAAGTATCTTTATAGTG -3′; and probe, 5′-FAM- TTCCCTTCCTAACCTGGACATAGCATATAACATACCT -TAMRA-3′. Amplification and detection were performed with an ABI Prism 7700 sequence detection system with the following settings: 2min at 50°C, 10min at 95°C, and 45 cycles of 15s at 95°C and 60s at 60°C.

ELISA assays

The extracellular IL-6 and IL-8 levels were determined by ELISA as described[17,38]. All values were determined in duplicate experiments. The antibodies recognize human IL-6 and IL-8 and apparently also recognize monkey IL-6 and IL-8 as serial dilution from supernatants of the monkey cells (LLC-MK2 and tMK) followed the standard curves for IL-6 and IL-8.

Protein Arrays

Initial screening of the produced cytokines was performed with a protein microarray designed to recognize several inflammatory cytokines (human inflammation antibody array III; RayBiotech, Inc.) according to the manufacturer instructions. The array includes the following cytokines: EOTAXIN, EOTAXIN-2, GCSF, GM-CSF, ICAM-1, IFN-γ, I-309, IL-1α, IL-1β, IL-2, IL-3, IL-4, IL-6, IL-6 soluble receptor, IL-7, IL-8, IL-10, IL-11, IL-12p40, IL-12p70, IL-13, IL-15, IL-16, IL-17, IP-10, MCP-1, MCP-2, M-CSF, MIG, MIP-1α, MIP-1β, MIP-1δ, RANTES, TGF-β1, TNF-α, TNF-β, soluble TNF receptor I, soluble TNF receptor II, PDGF-BB, TIMP-2. Arrays were incubated with 1 mL of undiluted cell culture supernatant

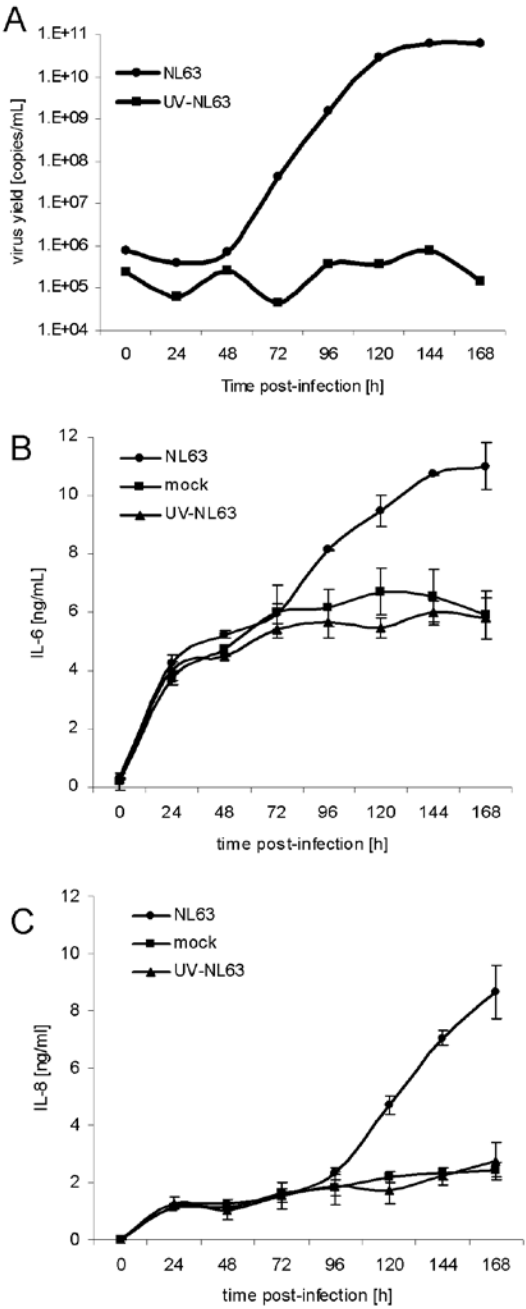


Figure 1. HCoV-NL63 driven induction of IL-6 and IL-8 on LLC-MK2 cells. A) Replication of HCoV-NL63 on LLC-MK2 cells. As a control a UV inactivated HCoV-NL63 virus stock was used. B) IL-6 levels during HCoV-NL63 infection of LLC-MK2 cells. C) IL-8 levels during HCoV-NL63 infection of LLC-MK2 cells. All measurements were performed in triplicate.

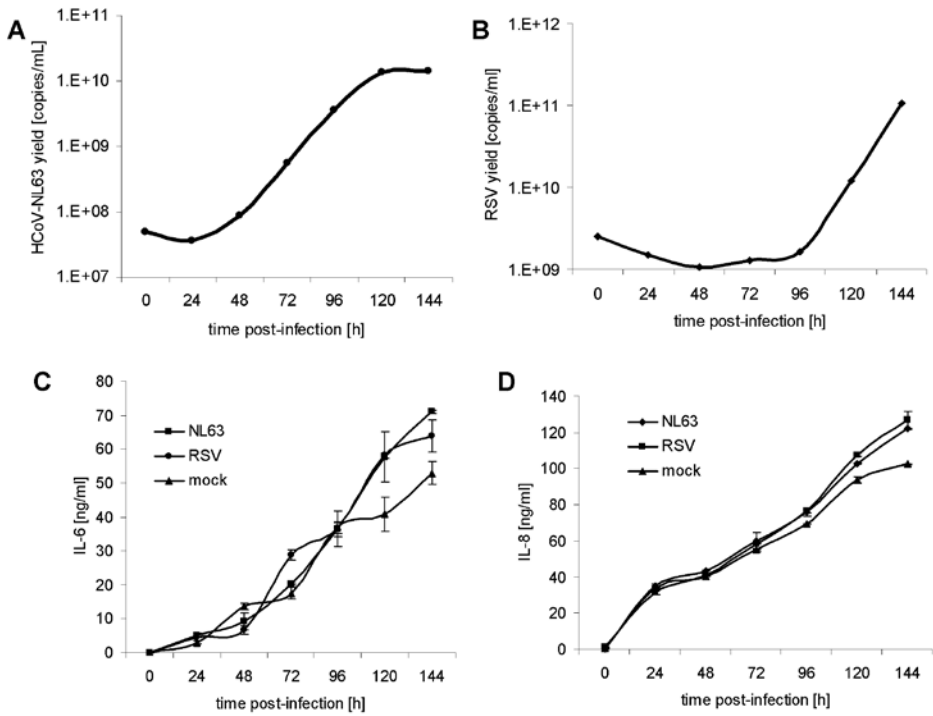


Figure 2. HCoV-NL63 and RSV B driven induction of IL-6 and IL-8 on tMK cells. Replication of HCoV-NL63 (A) and RSV B (B) on tMK cells. C) IL-6 levels during HCoV-NL63 and RSV B infection of tMK cells D) IL-8 levels during HCoV-NL63 and RSV B infection of tMK cells. All measurements were performed in triplicate and the representative graph is presented.

for LLC-MK2 cells (168h post-infection) or 1mL of 10 × diluted apical wash for HAE culture (24h and 48h post-infection) for 2 h at room temperature. Dilution of the HAE culture apical washes was needed because of the low sample volumes. After sample removal the biotinylated antibody cocktail was applied. The signal was developed with HRP-conjugated streptavidin and chemiluminescence reagents. An X-ray film was exposed to the blots, and the signal from each cytokine was assessed with ImageQuant TL software.

Statistical analysis

Data acquired by densitometry on protein arrays images were analyzed with the paired samples t-test to determine the significance levels (SPSS package version 12.02). Significance of differences between IL-6 and IL-8 scores in ELISA was analyzed with two-sample t test with unequal variances. $P<0.05$ was considered significant.

Results

HCoV-NL63 replication in monkey-derived cells and interleukin induction

After an initial lag period, HCoV-NL63 replicated efficiently in the LLC-MK2 cell line, with a significant rise in virus production 72h (3 days) post infection (Figure 1a).

We first analyzed the general cytokine profile of the HCoV-NL63 infected LLC-MK2 cells 168h (7 days) post-infection using a cytokine protein array and observed that the levels of IL-6 and IL-8 displayed the most significant rise (P=0.001 and 0.009; data not shown). The levels of other cytokines included on the protein array were either not raised markedly during HCoV-NL63 infection or that the used anti-human antibodies do not appropriately recognize monkey analogues.

To quantify IL-6 and IL-8 production during infection we used ELISA measurments. A rise of both cytokines was observed at 96h (4 days) post-infection, coinciding with viral replication (Figure 1b, 1c). UV-inactivated virus and mock infected cultures showed lower IL-6/IL-8 production, therefore HCoV-NL63 replication is the major factor triggering the IL-6 and IL-8 response (Figure 1b and 1c).

We tested whether the rise in IL-6 and IL-8 is also observed during infection of primary cells. Tertiary monkey kidney cells (tMK), that also support RSV replication, were exposed to HCoV-NL63. The HCoV-NL63 replication curve on tMK cells was similar to the one observed for LLC-MK2 cells, with a rise in virus production 72h post infection. The virus yield on the infected tMK cells was ~10^3 × lower than observed on infected LLC-MK2 cells (Figure 2a). The basal levels of IL-6 and IL-8 were high in uninfected cultures, which interferes with quantification, even though, analysis of IL-6 and IL-8 release shows that, similar to the LLC-MK2 based system, there is a marked increase in production of both cytokines, coinciding with virus replication (Figure 2c and 2d). RSV infection on tMKs showed a rise in virus yield at 120h (5 days) post infection and the IL-6 and IL-8 response was similar to the one triggered by HCoV-NL63 (Figure 2b, 2c, 2d).

Human airway epithelium cultures

The HAE *ex vivo* cultures mimic closely the differentiated human airway epithelium, thus we analyzed the cytokine content of apical washes derived from HCoV-NL63 infected HAE cultures. HCoV-NL63 infection in these cultures showed a rise in virus yield already 10h post-infection (Figure 3a). The virus was detected at 6 days post-infection only in the apical washings and not in the basolateral fraction, suggesting that the virus is released via the apical side (data not shown).

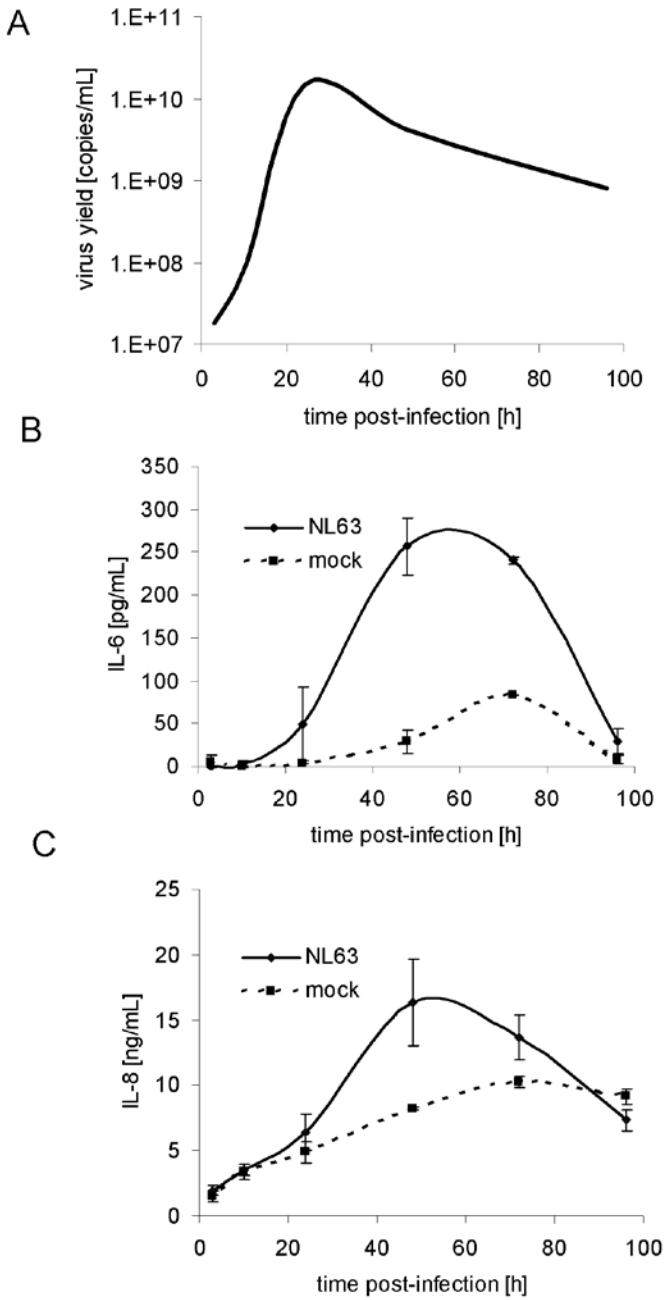


Figure 3. HCoV-NL63 driven induction of IL-6 and IL-8 on HAE cultures. A) Replication of HCoV-NL63 on HAE cultures. B) IL-6 levels during HCoV-NL63 infection of HAE cultures C) IL-8 levels during HCoV-NL63 infection of HAE cultures. The measurement was performed in duplicate and the average values are presented in the figure.

A significant rise of IL-6 and IL-8 was observed between 48h and 24h post infection, respectively ($P<0.04$), reaching its maximum after the peak in virus yield (Figure 3b, 3c). The protein array also displayed a clear upregulation of IL-6 and IL-8 production (reaching 2.5 fold and 1.5 fold, respectively, 48h post-infection), whereas no marked upregulation of other cytokine levels was observed (data not shown).

Discussion

Induction of an innate immune response is important for the control and elimination of invading pathogens. The airway epithelial cells are the primary target cells for HCoV-NL63 infection. Epithelium is not only a physical barrier, it also has the potential to synthesize a variety of cytokines and chemokines, e.g. IL-8, IL-6, granulocyte-macrophage colony-stimulating factor and transforming growth factor. In addition, chemotactic active lipid mediators for proinflammatory effector cells are also released by human airway epithelial cells[7,24].

The present study is the first to explore cytokine production by epithelial cells infected with HCoV-NL63. We showed that HCoV-NL63 infection of LLC-MK2, tMK cells and primary differentiated human airway epithelial cells increased production of IL-6 and IL-8 and that, at least for LLC-MK2 cells, it requires viral replication.

The increased IL-6 levels that we observed during the course of infection of tMK cells with HCoV-NL63 were comparable to the IL-6 upregulation observed for RSV. It was previously reported that SARS-CoV and RSV infection induce IL-6 production to a similar extent[27].

The observation of virus replication-dependent production of IL-6 and IL-8 suggest that the innate immune response may be triggered directly by the presence of HCoV-NL63 double-stranded RNA[16]. HCoV-NL63 is an RNA virus with an 27.5kb genome, and therefore it is prone to be recognized by toll-like receptor (TLR) 3 that activates transcriptional factors such as nuclear factor kappa B (NF-κB) or interferon regulatory factor (IRF)[23,28]. The further support for this theory is the preliminary observation of a correlation between the viral replication levels and the amount of produced cytokines. For the LLC-MK2 cells and HAE cultures, which support replication to much higher extent than tMK cells, the rise in both cytokines is much more pronounced than for the latter one. One would speculate that the block in viral replication observed on the HAE cultures at 48h post-infection onwards is associated with increased innate immune response triggered directly by the TLR3-HCoV-NL63 RNA interaction.

The difference in pathogenesis between HCoV-NL63 and SARS-CoV remains unexplained. A further characterization of HCoV-NL63 induced inflammatory

mediators production is needed including the involvement of TLR receptors and the negative feedback signaling molecules of the JAK/STAT pathway that are downregulated during SARS-CoV infection (e.g. SOCS3[27]). Additionally, an interesting question needs to be addressed about the difference in virus-induced sensitization to the secondary stimulus (as TNF-α)[31] during the log phase of infection between SARS-CoV and HCoV-NL63.

References

1. Arden, K. E., M. D. Nissen, T. P. Sloots, and I. M. Mackay. 2005. New human coronavirus, HCoV-NL63, associated with severe lower respiratory tract disease in Australia. J. Med. Virol. 75:455-462.
2. Bastien, N., K. Anderson, L. Hart, P. Van Caeseele, K. Brandt, D. Milley, T. Hatchette, E. C. Weiss, and Y. Li. 2005. Human coronavirus NL63 infection in Canada. J. Infect. Dis. 191:503-506.
3. Bastien, N., J. L. Robinson, A. Tse, B. E. Lee, L. Hart, and Y. Li. 2005. Human coronavirus NL-63 infections in children: a 1-year study. J. Clin. Microbiol. 43:4567-4573.
4. Boivin, G., M. Baz, S. Cote, R. Gilca, C. Deffrasnes, E. Leblanc, M. G. Bergeron, P. Dery, and G. De Serres. 2005. Infections by human coronavirus-NL in hospitalized children. Pediatr. Infect. Dis. J. 24:1045-1048.
5. Boom, R., C. J. Sol, M. M. Salimans, C. L. Jansen, P. M. Wertheim-van Dillen, and J. van der Noordaa. 1990. Rapid and simple method for purification of nucleic acids. J. Clin. Microbiol. 28:495-503.
6. Chiu, S. S., K. H. Chan, K. W. Chu, S. W. Kwan, Y. Guan, L. L. Poon, and J. S. Peiris. 2005. Human coronavirus NL63 infection and other coronavirus infections in children hospitalized with acute respiratory disease in Hong Kong, China. Clin. Infect. Dis. 40:1721-1729.
7. Chonmaitree, T., M. A. Lett-Brown, and J. A. Grant. 1991. Respiratory viruses induce production of histamine-releasing factor by mononuclear leukocytes: a possible role in the mechanism of virus-induced asthma. J. Infect. Dis. 164:592-594.
8. Cromwell, O., Q. Hamid, C. J. Corrigan, J. Barkans, Q. Meng, P. D. Collins, and A. B. Kay. 1992. Expression and generation of interleukin-8, IL-6 and granulocyte-macrophage colony-stimulating factor by bronchial epithelial cells and enhancement by IL-1 beta and tumour necrosis factor-alpha. Immunology 77:330-337.
9. Edwards, J. A., F. Denis, and P. J. Talbot. 2000. Activation of glial cells by human coronavirus OC43 infection. J. Neuroimmunol. 108:73-81.
10. Esper, F., C. Weibel, D. Ferguson, M. L. Landry, and J. S. Kahn. 2005. Evidence of a novel human coronavirus that is associated with respiratory tract disease in infants and young children. J. Infect. Dis. 191:492-498.
11. Feghali, C. A. and T. M. Wright. 1997. Cytokines in acute and chronic inflammation. Front Biosci. 2:d12-d26.
12. Foley, J. E., C. Rand, and C. Leutenegger. 2003. Inflammation and changes in cytokine levels in neurological feline infectious peritonitis. J. Feline. Med. Surg. 5:313-322.
13. Fouchier, R. A., N. G. Hartwig, T. M. Bestebroer, B. Niemeyer, J. C. de Jong, J. H. Simon, and A. D. Osterhaus. 2004. A previously undescribed coronavirus associated with respiratory disease in humans. Proc. Natl. Acad. Sci. U. S. A 101:6212-6216.
14. Fujimori, Y., M. Kataoka, S. Tada, H. Takehara, K. Matsuo, T. Miyake, M. Okahara, I. Yamadori, and M. Tanimoto. 2003. The role of interleukin-8 in interstitial pneumonia. Respirology. 8:33-40.
15. Fulcher, M. L., S. Gabriel, K. A. Burns, J. R. Yankaskas, and S. H. Randell. 2005. Well-differentiated human airway epithelial cell cultures., p. 183-206. In J. Picot (ed.), Human cell culture protocols. Humana Press, Totowa, New Jersey.
16. Guillot, L., R. Le Goffic, S. Bloch, N. Escriou, S. Akira, M. Chignard, and M. Si-Tahar. 2005. Involvement of toll-like receptor 3 in the immune response of lung epithelial cells to double-stranded RNA and influenza A virus. J Biol Chem 280:5571-5580.
17. Helle, M., L. Boeije, E. de Groot, A. de Vos, and L. Aarden. 1991. Sensitive ELISA for interleukin-6. Detection of IL-6 in biological fluids: synovial fluids and sera. J. Immunol. Methods 138:47-56.
18. Hofmann, H., K. Pyrc, L. van der Hoek, M. Geier, B. Berkhout, and S. Pohlmann. 2005. Human coronavirus NL63 employs the severe acute respiratory syndrome coronavirus receptor for cellular entry. Proc. Natl. Acad. Sci. U. S. A 102:7988-7993.

19. Huang, K. J., I. J. Su, M. Theron, Y. C. Wu, S. K. Lai, C. C. Liu, and H. Y. Lei. 2005. An interferon-gamma-related cytokine storm in SARS patients. J. Med. Virol. 75:185-194.
20. Kaiser, L., N. Regamey, H. Roiha, C. Deffernez, and U. Frey. 2005. Human coronavirus NL63 associated with lower respiratory tract symptoms in early life. Pediatr. Infect. Dis. J. 24:1015-1017.
21. Koj, A. 1996. Initiation of acute phase response and synthesis of cytokines. Biochim. Biophys. Acta 1317:84-94.
22. Kunkel, S. L., T. Standiford, K. Kasahara, and R. M. Strieter. 1991. Interleukin-8 (IL-8): the major neutrophil chemotactic factor in the lung. Exp. Lung Res. 17:17-23.
23. Le Goffic, R., V. Balloy, M. Lagranderie, L. Alexopoulou, N. Escriou, R. Flavell, M. Chignard, and M. Si-Tahar. 2006. Detrimental contribution of the Toll-like receptor (TLR)3 to influenza A virus-induced acute pneumonia. PLoS. Pathog. 2:e53.
24. McGee, D. W., K. W. Beagley, W. K. Aicher, and J. R. McGhee. 1992. Transforming growth factor-beta enhances interleukin-6 secretion by intestinal epithelial cells. Immunology 77:7-12.
25. Moes, E., L. Vijgen, E. Keyaerts, K. Zlateva, S. Li, P. Maes, K. Pyrc, B. Berkhout, L. van der Hoek, and M. Van Ranst. 2005. A novel pancoronavirus RT-PCR assay: frequent detection of human coronavirus NL63 in children hospitalized with respiratory tract infections in Belgium. BMC. Infect. Dis. 5:6.
26. Mukhopadhyay, S., J. R. Hoidal, and T. K. Mukherjee. 2006. Role of TNFalpha in pulmonary pathophysiology. Respir. Res. 7:125.
27. Okabayashi, T., H. Kariwa, S. Yokota, S. Iki, T. Indoh, N. Yokosawa, I. Takashima, H. Tsutsumi, and N. Fujii. 2006. Cytokine regulation in SARS coronavirus infection compared to other respiratory virus infections. J. Med. Virol. 78:417-424.
28. Okahira, S., F. Nishikawa, S. Nishikawa, T. Akazawa, T. Seya, and M. Matsumoto. 2005. Interferon-beta induction through toll-like receptor 3 depends on double-stranded RNA structure. DNA Cell Biol 24:614-623.
29. Pickles, R. J., D. McCarty, H. Matsui, P. J. Hart, S. H. Randell, and R. C. Boucher. 1998. Limited entry of adenovirus vectors into well-differentiated airway epithelium is responsible for inefficient gene transfer. J. Virol. 72:6014-6023.
30. Reed, L. J. and H. Muench. 1938. A simple method of estimating fifty percent endpoints. American Journal of Hygiene 27:493-497.
31. Roger, T., P. Bresser, M. Snoek, K. van der Sluijs, A. van den Berg, M. Nijhuis, H. M. Jansen, and R. Lutter. 2004. Exaggerated IL-8 and IL-6 responses to TNF-alpha by parainfluenza virus type 4-infected NCI-H292 cells. Am J Physiol Lung Cell Mol Physiol 287:L1048-L1055.
32. Suzuki, A., M. Okamoto, A. Ohmi, O. Watanabe, S. Miyabayashi, and H. Nishimura. 2005. Detection of human coronavirus-NL63 in children in Japan. Pediatr. Infect. Dis. J. 24:645-646.
33. Theron, M., K. J. Huang, Y. W. Chen, C. C. Liu, and H. Y. Lei. 2005. A probable role for IFN-gamma in the development of a lung immunopathology in SARS. Cytokine 32:30-38.
34. Vabret, A., T. Mourez, J. Dina, L. van der Hoek, S. Gouarin, J. Petitjean, J. Brouard, and F. Freymuth. 2005. Human coronavirus NL63, France. Emerg. Infect. Dis. 11:1225-1229.
35. van der Hoek, L., K. Pyrc, M. F. Jebbink, W. Vermeulen-Oost, R. J. Berkhout, K. C. Wolthers, P. M. Wertheim-van Dillen, J. Kaandorp, J. Spaargaren, and B. Berkhout. 2004. Identification of a new human coronavirus. Nat. Med. 10:368-373.
36. van der Hoek, L., K. Sure, G. Ihorst, A. Stang, K. Pyrc, M. F. Jebbink, G. Petersen, J. Forster, B. Berkhout, and K. Uberla. 2005. Croup is associated with the novel coronavirus NL63. PLoS. Med. 2:e240.
37. van Elden, L. J., A. M. van Loon, A. van der Beek, K. A. Hendriksen, A. I. Hoepelman, M. G. van Kraaij, P. Schipper, and M. Nijhuis. 2003. Applicability of a real-time quantitative PCR assay for diagnosis of respiratory syncytial virus infection in immunocompromised adults. J. Clin. Microbiol. 41:4378-4381.
38. van Wissen, M., M. Snoek, B. Smids, H. M. Jansen, and R. Lutter. 2002. IFN-gamma amplifies IL-6 and IL-8 responses by airway epithelial-like cells via indoleamine 2,3-dioxygenase. J. Immunol. 169:7039-7044.

Chapter IX

Inhibition of human coronavirus NL63 infection at early stages of the replication cycle

Antimicrobial Agents and Chemotherapy, June 2006; vol. 50, p. 2000-2008.

Krzysztof Pyrc[1], Berend Jan Bosch[2], Ben Berkhout[1], Maarten F. Jebbink[1], Ronald Dijkman[1], Peter Rottier[2], Lia van der Hoek[1].

[1]Laboratory of Experimental Virology, Department of Medical Microbiology, Center for Infection and Immunity Amsterdam (CINIMA), Academic Medical Center, University of Amsterdam, Meibergdreef 15, 1105 AZ, Amsterdam, The Netherlands. [2] Department of Infectious Diseases and Immunology, Faculty of Veterinary Medicine, and Institute of Biomembranes, Utrecht University, 3584 CL Utrecht, The Netherlands

Human coronavirus NL63 (HCoV-NL63), a recently discovered member of the *Coronaviridae* family, has spread worldwide and is associated with acute respiratory illness in young children and elderly and immunocompromised persons. Further analysis of HCoV-NL63 pathogenicity seems warranted, in particular because the virus uses the same cellular receptor as severe acute respiratory syndrome-associated coronavirus. As there is currently no HCoV-NL63-specific and effective vaccine or drug therapy available, we evaluated several existing antiviral drugs and new synthetic compounds as inhibitors of HCoV-NL63, targeting multiple stages of the replication cycle. Of the 31 compounds that we tested, 6 potently inhibited HCoV-NL63 at early steps of the replication cycle. Intravenous immunoglobulins, heptad repeat 2 peptide, small interfering RNA1 (siRNA1), siRNA2, β-d-N4-hydroxycytidine, and 6-azauridine showed 50% inhibitory concentrations of 125μg/ml, 2μM, 5nM, 3nM, 400nM, and 32nM, respectively, and low 50% cytotoxicity concentrations (>10mg/ml, >40μM, >200nM, >200nM, >100μM, and 80μM, respectively). These agents may be investigated further for the treatment of coronavirus infections.

Introduction

Coronaviruses are enveloped viruses with a positive, single-stranded RNA genome of approximately 27 to 32 kb. The 5′ two-thirds of their genome encodes a polyprotein that contains all proteins necessary for RNA replication. The 3′ one-third encodes several structural proteins, such as spike (S), envelope (E), membrane (M), and nucleocapsid (N), that, among other functions, participate in viral budding and are incorporated into the virus particle. Accessory protein genes are also present in the 3′ part of the genome, at a position and arrangement that is characteristic for each of the different coronavirus groups.

Coronavirus infection starts with the recognition of a specific receptor on the host cell surface by an S protein, followed by virus internalization, which occurs either immediately by direct fusion with the plasma membrane or after endocytosis. Fusion of the viral membrane with the cellular membrane triggers the release of the viral RNA genome into the host cell cytoplasm. Viral RNA is copied by the viral replicase in membrane-associated replication centers[14]. During the replication process, copies of the full-length genomic RNA and a nested set of subgenomic mRNAs are generated. These subgenomic mRNAs are functional templates for the translation of the structural proteins encoded in the 3′ one-third of the genome. Full-length viral RNA is encapsidated and released from the host cell as an infectious virus particle.

Human coronavirus NL63 (HCoV-NL63), a recently discovered[45,55] member of the *Coronaviridae* family, has spread worldwide, is observed most frequently in the winter season, and is associated with acute respiratory illness and croup in young children, elderly people, and immunocompromised patients[2,6,15,25,29,40,53-56].

A recent report suggested that HCoV-NL63 is the causative agent of Kawasaki disease[28], although other studies did not confirm this relationship[7,26,49]. In the developed world, Kawasaki disease is the most common cause of acquired heart disease in children[37,47]. Further analysis of HCoV-NL63 pathogenicity seems warranted, in particular because the virus uses the same cellular receptor as severe acute respiratory syndrome-associated CoV (SARS-CoV)[34].

An effective antiviral treatment is required for HCoV-NL63-infected patients who are admitted to the intensive care unit due to acute respiratory disease. To investigate the therapeutic options, we tested several potential inhibitors that target specific steps of the coronavirus life cycle, e.g., receptor binding, membrane fusion, transcription, translation, posttranslational processing, and virus release. The compounds inhibiting the early phase of HCoV-NL63 infection appeared to be the most potent antivirals.

Methods

Antiviral agents

Information about all 31 tested compounds is summarized in Table 1. The 50% inhibitory concentrations (IC_{50}s; based on the cytopathic effect [CPE] reduction assay and viral yield) and 50% cytotoxic concentrations {CC_{50}s; based on the MTS [3-(4,5-dimethylthiazol-2-yl)-5-(3-carboxymethoxyphenyl)-2-(4-sulfophenyl)-2H-tetrazolium] inner salt assay} were determined for each antiviral agent. Human sera obtained from healthy adults were inactivated by incubation for 30min at 56°C and stored at −80°C until use.

Plasmid construction, bacterial protein expression, and purification

For the production of the HR1 and HR2 peptides corresponding to amino acid residues 955 to 1064 (HR1) and 1241 to 1285 (HR2) of the HCoV-NL63 spike protein, a PCR fragment was prepared with the plasmid carrying the HCoV-NL63 spike gene[34]. The primers 5′-GCGGATCCCAAGCACGACTTAACTATG-3′ and 5′-CGAATTCAAGTAATTAATCTGTCAACTTG-3′ were used for the amplification of HR1, and the primers 5′-GCGGATCCTTTAATTTAACATATCTTAATTTG-3′ and 5′-CGAATTCACAACTTCAAATCAACATATGT-3′) were used for HR2. Bacterial expression and purification were then performed essentially as described previously[12], with a few modifications. Lysozyme (100μg/ml), dithiothreitol (DTT; 7 mM), and sarkosyl (1%) were added to phenylmethylsulfonyl fluoride (PMSF; 1 mM) prior to sonication, and Triton X-100 (2.8%) was added to the supernatant after centrifugation, prior to glutathione-Sepharose 4B purification. Production of the murine coronavirus (murine hepatitis virus [MHV] strain A59) HR2 peptide has been described previously[13].

Table 1. Antiviral agents

	agent	source	solvent
1	S-nitroso-N-acetylpenicillamine	Calbiochem	DMSO
2	2,2′-(Hydroxynitrosohydrazino)bis-ethanamine	Sigma	water
3	Calpain inhibitor VI	Calbiochem	DMSO
4	Calpain inhibitor III	Sigma	DMSO
5	Glycyrrhizin	Sigma	DMSO
6	Chloroquine phosphate	Sigma	water
7	Aurintricarboxylic acid	Calbiochem	0.1M NaOH
8	Valinomycin	Calbiochem	DMSO
9	Escin	Sigma	DMSO
10	Reserpine	Sigma	DMSO
11	Pentoxifylline	Calbiochem	water
12	2′,5-Dichloro-4′-nitrosalicylanilide	Sigma	DMSO
13	6-azauridine	Sigma	water
14	Hygromycin B	Sigma	water
15	Dipyridamole	Sigma	DMSO
16	Actinomycin D	Sigma	water
17	Ribavirin	Sigma	water
18	HR peptide 1	-	water
19	HR peptide 2	-	water
20	siRNA1	Qiagen	Buffer supplied
21	siRNA2	Qiagen	Buffer supplied
22	IVIG	Sanquin	water
23	β-D-N^4-hydroxycytidine	NIH AIDS Reagent Program	DMSO
24	Ritonavir	Abbott Laboratories	DMSO
25	Nelfinavir	Agouron pharmaceuticals	DMSO
26	Indinavir	Merck & Co	DMSO
27	Saquinavir	Roche	DMSO
28	Delavirdine	NIH AIDS Reagent Program	DMSO
29	Amprenavir	GlaxoWellcome	DMSO
30	Nevirapine	NIH AIDS Reagent Program	DMSO
31	Efavirenz	NIH AIDS Reagent Program	DMSO

Selection of siRNA sequences

The small interfering RNAs (siRNAs) were designed and synthesized by QIAGEN (QIAGEN, Benelux B.V.) with the HiPerformance design algorithm (Novartis AG) and integrated with a stringent homology analysis tool (QIAGEN). The siRNAs were synthesized using a TOM amidite chemistry process, yielding >90% purity, as determined by ion-exchange high-performance liquid chromatography analysis. Oligonucleotides were provided as annealed double-strand siRNA (Table 2). The sequence and identity of each siRNA were confirmed using matrix-assisted laser desorption ionization-time of flight spectrometric analysis. The stock and working solutions were prepared according to the manufacturer's protocol (QIAGEN). As a negative control, we used siRNA targeting Rattus norvegicus mRNA collybistin 1 (GenBank accession number AJ250425). Sequences of siRNA were BLAST analyzed (using the NCBI database "Search for short, nearly exact matches" mode) against human sequences to exclude those siRNA sequences with potential targets in the human genome.

Table 2. siRNA oligonucleotide sequence.

siRNA1-NL63[a]	
sense	r(GGA AUU AUA CGU UCU UCA A)dTdT
antisense	r(UUG AAG AAC GUA UAA UUC C)dAdG
siRNA2-NL63	
sense	r(AGG UUA AUA UAU CUC UUA A)dTdT
antisense	r(UUA AGA GAU AUA UUA ACC U)dGdG
siRNA3-control	
sense	r(GAC CAC AGU GAU UAC AGA U)dTdT
antisense	r(AUC UGU AAU CAC UGU GGU C)dTdT

[a] Coordinates of the target sequences are: nt 21980 - 22000 and nt 22384 - 22404 in the HCoV-NL63 genome for siRNA1 and siRNA2, respectively. The target for control siRNA3 is the collybistin I gene of Rattus norvegicus, nt 1190 – 1208.

Cell culture

LLC-MK2 cells were cultured in minimal essential medium (MEM; 2 parts Hanks' MEM and 1 part Earle's MEM) supplemented with 3% heat-inactivated fetal calf serum (PAA Laboratories), penicillin (100U/ml), and streptomycin (100μg/ml). Twenty-four hours prior to transfection, the cells were plated onto 96-well plates at a density of 2×10^4 cells/well in fresh medium (100μl per well) and cultured at 37°C with 5% CO_2. Twenty-four hours prior to the addition of the drug, cells were plated onto 96-well plates at a density of 4×10^4 cells/well in fresh medium (100μl per well) with 100μg of penicillin and 100μg of streptomycin and cultured at 37°C with 5% CO_2.

Cytopathic effect reduction assay
HCoV-NL63 (isolate Amsterdam 1) was obtained from a virus culture on LLC-MK2 cells as described previously[55]. The infectious titer of the virus was determined according to the Reed and Muench formula[46] on an LLC-MK2 cell monolayer. The virus stock has a titer of 2×10^5 50% tissue culture infectivity doses/ml. For the CPE reduction assay, cells were treated with serially diluted compounds and infected with HCoV-NL63 at a multiplicity of infection of 0.01. The CPE was scored visually at day 6 postinfection and confirmed with an MTS assay. Experiments were performed in quadruplicate.

Immunostaining-based HCoV-NL63 infection inhibition assay
Virus entry inhibition by the HR2 peptide was analyzed on LLC-MK2 cells in 96-well plates (4×10^4 cells per well). Cells were inoculated with HCoV-NL63 at a multiplicity of infection of 0.5 in the presence of serial dilutions of the peptides. The MHV HR2 peptide was included as a negative control. After incubation for 24h, cells were washed with phosphate-buffered saline (PBS), fixed with 3% formaldehyde for 20min, and permeabilized with 1% Triton X-100 in PBS for 5min. After they were washed twice with PBS and blocked with PBS-5% fetal calf serum, the HCoV-NL63-positive cells were detected by intracellular peroxidase staining using a human polyclonal serum (1:200) in combination with a biotinylated antihuman antibody (1:250) and the VECTASTAIN ABC kit (Vector Laboratories). The reaction mixture was developed with 3-amino-9-ethylcarbazole (AEC; Sigma) according to the manufacturer's instructions. Experiments were performed in duplicate. Infected cells were counted using a light microscope.

Drug cytotoxicity
Cytotoxicity of the compounds was determined by measuring mitochondrial activity on day 6 posttreatment with MTS (CellTiter 96 AQ_{ueous} one solution cell proliferation assay; Promega) according to the manufacturer's instructions. Cytotoxicity measurements were confirmed by determining the mRNA levels of the household gene encoding glyceraldehyde-3-phosphate dehydrogenase (GAPDH). Experiments were performed in duplicate.

Transfection of LLC-MK2 cells with siRNA
Transfection with siRNA was performed with Lipofectamine 2000 (Invitrogen) according to the manufacturer's protocol. siRNA-transfected cells were infected with HCoV-NL63 after 24 hours.

Reverse transcription-PCR and real-time quantitative PCR
Total RNA was extracted from the medium and cells by the silica-affinity-based Boom extraction method[11] and eluted in 100µl water. Reverse transcription was performed with Moloney murine leukemia virus reverse transcriptase (Invitrogen)

(200U per reaction) and 10ng of random hexamers (Amersham Biosciences) in 10mM Tris, pH 8.3, 50mM KCl, 0.1% Triton X-100, 6mM of $MgCl_2$, and 50μM of each deoxynucleoside triphosphate at 37°C for 90min in a total volume of 40μl.

Virus yield was determined with real-time PCR. Ten microliters of cDNA was amplified in 50μl 1×Platinum quantitative PCR SuperMix-uracil-DNA glycosylase (Invitrogen) with 5mM $MgCl_2$, 200nM specific probe labeled with FAM (6-carboxyfluorescein) and TAMRA (6-carboxytetramethylrhodamine), and 900nM of each primer. The following primers were used for HCoV-NL63: sense, 5′-GCGTGTTCCTACCAGAGAGGA-3′; antisense, 5′-GCTGTGGAAAACCTTTGGCA-3′; and probe, 5′-FAM-ATGTTATTCAGTGCTTTGGTCCTCGTGAT-TAMRA-3′. The reaction was carried out on a TaqMan machine (ABI). Following 2min at 50°C and 5min at 95°C, 45 cycles of amplification were performed for 15s at 95°C and 60s at 60°C.

Nucleotide sequence accession numbers

The sequence for HCoV-NL63 isolate Amsterdam 57 described in this study was deposited in GenBank under accession number DQ471450. The GenBank accession number for HCoV-NL63 isolate Amsterdam 1 is NC_005831; that for HCoV-229E is AF304460; and that for porcine epidemic diarrhea virus strain CV777 is AF353511. The sequence of the GAPDH gene (LLC-MK2 cells derived from Macaca mulatta) was deposited in GenBank under accession number DQ445913.

Results

HCoV-NL63 inhibition assay

The inhibition of HCoV-NL63 infection can be determined using several assays. The most straightforward assay is based on the reduction of CPE. Six days after infection, HCoV-NL63-infected LLC-MK2 cells exhibit evident morphological changes consisting of cell enlargement, rounding, and, eventually, detachment from the surface (Fig. 1). Thus, infecting the target cells in the presence of serially diluted candidate antiviral agents provides a means of visualizing their inhibitory activity by scoring the reduction in CPE. LLC-MK2 cells seeded on the 96-well

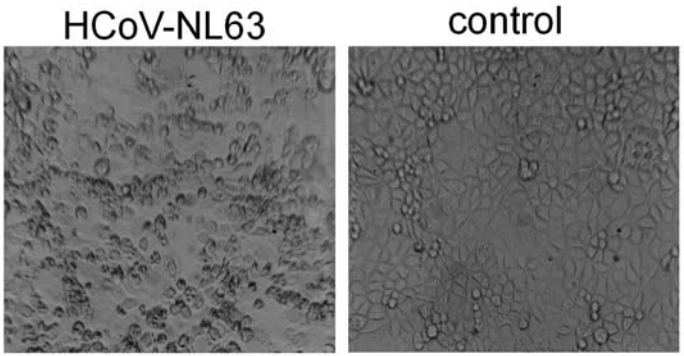


Figure 1. CPE induced by HCoV-NL63 on LLC-MK2 cells.

culture plate and subsequently infected with HCoV-NL63 in the presence of serially diluted compounds were scored for CPE using phase-contrast microscopy. Agents that showed antiviral activity in this initial assay were subsequently tested by measuring the virus yield at active concentrations of the compound.

Virus neutralization by purified human immunoglobulin G (IgG)

Sera from virtually all healthy adults contain HCoV-NL63 antibodies[34]. To determine the neutralizing potential of these antibodies, we tested 10 randomly selected human sera from healthy adults by the CPE reduction assay. All tested sera inhibited HCoV-NL63 infection at 25- to 50-fold dilutions, illustrating that the majority of adults carry neutralizing antibodies against HCoV-NL63.

To further explore the potential of neutralizing antibodies in antiviral therapy, we tested pooled purified human IgG from healthy donors (intravenous immunoglobulin [IVIG]). In fact, IVIG is part of the effective routine treatment for Kawasaki patients[43] and several immunodeficiency syndromes[23,31]. The CPE reduction assay demonstrates that this agent is very active against HCoV-NL63 infection (Fig. 2A). To confirm that CPE reduction is an accurate measurement of virus inhibition, the virus yield was determined for each serial IVIG dilution (Fig. 2B). The virus yield also allows a more precise measurement of the IC_{50} value, which was 200 μg/ml for IVIG. This concentration is ~10 times lower than the dose advised for treatment (2g/kg of body weight)[43]. The cell survival assay indicated that IVIG has a very low cytotoxicity (CC_{50}>10mg/ml), thus yielding a high selectivity index (CC_{50}/IC_{50}>50).

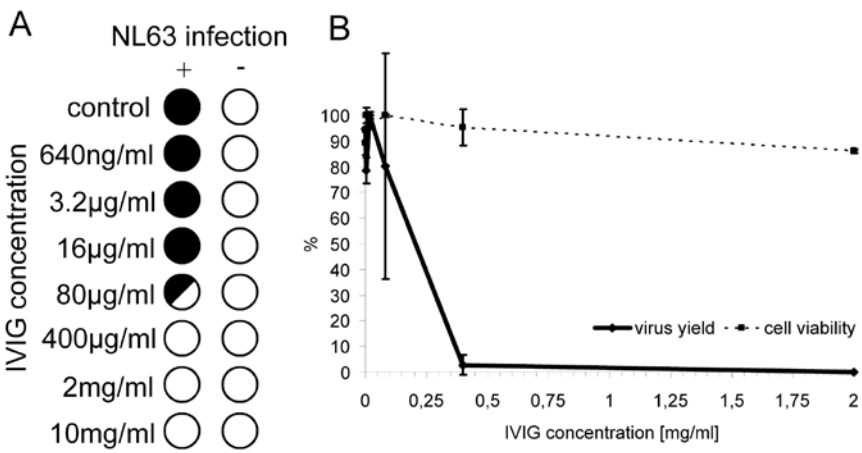


Figure 2. Inhibition of HCoV-NL63 by IVIG. A) CPE reduction mediated by IVIG. Filled circles indicate CPE development; empty circles indicate absence of CPE; half-filled circle represent the development of CPE in 50% of wells. B) Decrease in HCoV-NL63 virus yield after IVIG treatment and cell viability assay. Numbers on the Y axis represent the percentage of produced virus and percentage of viable cells.

Inhibition of cell entry

The spike protein of HCoV-NL63 is a class I fusion glycoprotein consisting of a globular S1 domain that recognizes the receptor and a rodlike S2 domain involved in membrane fusion. After receptor binding and virus internalization, the S protein undergoes a structural switch, resulting in the exposure of the fusion peptide[13,27]. The HR1 and HR2 regions in the S2 domain rearrange and interact during the structural switch. Blocking this interaction between HR1 and HR2 provides an effective antiviral strategy[12,13]. The HCoV-NL63 spike protein contains HR1 and HR2 regions with a characteristic 7-residue periodicity. HR2 is located adjacent to the transmembrane domain, and HR1 is about 170 residues away, toward the N terminus. In all coronaviruses, HR1 is consistently larger than HR2, and all group 1 coronaviruses, including HCoV-NL63, show a remarkable insertion of two heptad repeats (14 amino acids) in both HR regions[13,21].

Peptides corresponding to the HCoV-NL63 HR1 and HR2 regions were prepared with the bacterial glutathione S-transferase expression system and purified by using reverse-phase high-performance liquid chromatography. It was previously shown for SARS-CoV and MHV[12,13] that mixing HR1 and HR2 peptides leads to the assembly of an oligomeric complex that is resistant to 2% sodium dodecyl sulfate (SDS)[13]. Using the same approach, we observed that the HR1 and HR2 peptides of the HCoV-NL63 spike protein behaved in a similar manner, forming an SDS-resistant oligomeric complex in an equimolar mixture (Fig. 3A).

The HR2 peptide was subsequently tested for its inhibitory potency in the CPE reduction assay. Concentration-dependent inhibition of HCoV-NL63 infection was observed with an IC_{50} value of ~0.5μM and a CC_{50} value of >20μM (Fig. 3B and C). This effect is sequence specific, because no inhibition was seen with a corresponding peptide derived from the HR2 region of MHV (MHV-HR2) that is known to block MHV infection[13] (Fig. 3D).

Previous studies examined the antiviral activity of HR peptides (for coronaviruses) by immune peroxidase staining of infected cells after 24h. Using this method, the IC_{50} was ~0.5μM (Fig. 3D), identical to the value measured in the CPE reduction assay. NL63-HR2 exhibits the same powerful antiviral potency as the MHV-HR2 peptide against MHV infection (IC_{50} of 0.9μM[13]). The activity of NL63-HR2 is much higher than the inhibiting activity described for the corresponding SARS-CoV HR2 peptide (IC_{50} of 17μM[12]).

Targeting the viral RNA by RNA interference

siRNA-mediated degradation of the incoming full-length HCoV-NL63 genome will prevent transcription and, thus, virus production. We selected two siRNAs that target the S gene based on an algorithm for optimal siRNA design and the lack of complementarity with host gene sequences (Table 2). The siRNAs were

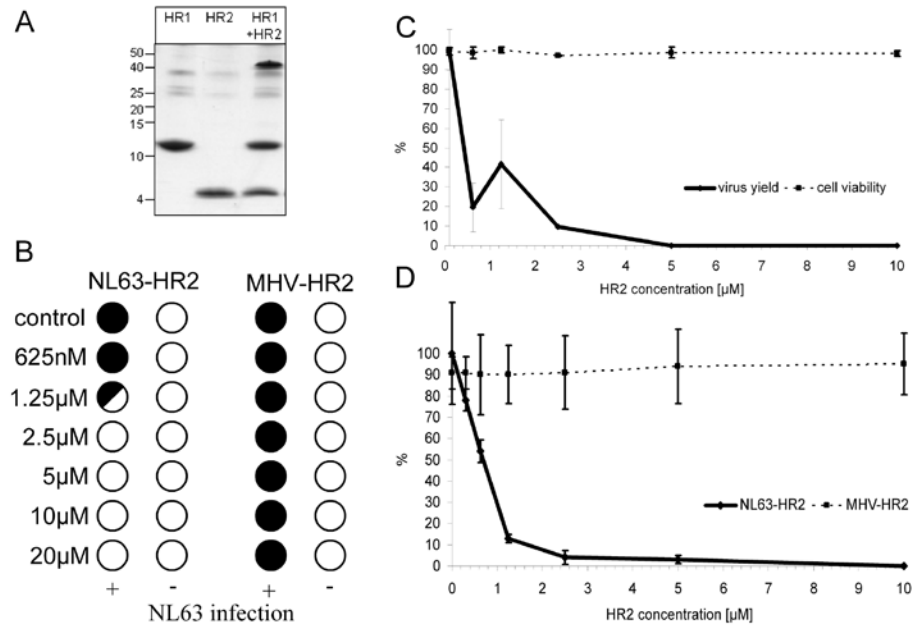


Figure 3. Inhibition of HCoV-NL63 by the HR2 peptide. A) SDS PAGE analysis of HR peptides separately and HR1/HR2 complex formation. The molecular mass of the complex corresponds to the predicted hetero hexamer. B) CPE reduction mediated by HR2 peptide. Filled circles indicate CPE development; empty circles indicate absence of CPE; half-filled circle represent the development of CPE in 50% of wells. C) Decrease in HCoV-NL63 virus yield after HR2 treatment and cell viability assay. Numbers on the Y axis represent the percentage of produced virus and percentage of viable cells. D) Immunostaining-based HCoV-NL63 infection inhibition assay. Values on the Y-axis represent the percentage of infected cells.

```
siRNA 1                          ---------- ----CTGGAA TTATACGTTC TTCAA----- ----------
HCoV-NL63 Amsterdam 1   22370   TGATTATGTT GGTACTGGAA TTATACGTTC TTCAAACCAG TCACTTGCTG
HCoV-NL63 Amsterdam 57  22370   TGATTATGTT GGTACTGGAA TTATACGTTC TTCAAACCAG TCACTTGCTG
HCoV-NL63 NL            22353   TGATTATGTT GGTACTGGAA TTATACGTTC TTCAAACCAG TCACTTGCTG
HCoV-229E               21700   TAACTTTGTT AAATTTGGCA GTGTATGTTT TTCGCTAAAG GATATACCCG
PEDV                    22368   TGATTACCTG TCTTTTAGCA AATTTTGTGT TTCAACCAGC CTTTTGGCTG

siRNA 2                          ---------- --------CC AGGTTAATAT ATCTCTTAA- ----------
HCoV-NL63 Amsterdam 1   21962   TTATGTTTGT AAACCACACC AGGTTAATAT ATCTCTTAAT GGTAACACTT
HCoV-NL63 Amsterdam 57  21962   TTATGTTTGT AAACCACACC AGGTTAATAT ATCTCTTAAT GGTAACACTT
HCoV-NL63 NL            21945   TTATGTTTGT AAACCACGCC AGGTTAATAT ATCTCTTAAT GGTAACACTT
HCoV-229E               20965   TTTGTTTAAA ACATCTTATG GTGTTGTTGT GTTTTATTGT ACCAACAACA
PEDV                    22314   TTATGTGTCT AAATCACAGG ATAGTAATTG TCCTTTCACC TTGCAATCTG
```

Figure 4. Sequence alignment illustrating conservation and specificity of siRNA target sequences in different HCoV-NL63 isolates.

designed against sequences that are conserved among HCoV-NL63 isolates, thus providing a broad antiviral activity. The target sequence is absent in other coronaviruses, as illustrated in Fig. 4, for the closest group 1 relatives, HCoV-229E and porcine epidemic diarrhea virus.

To examine the inhibitory capacity of HCoV-NL63-specific siRNA, we transfected cells with the synthetic siRNAs and subsequently infected them with HCoV-NL63. Transfection of siRNA1 and siRNA2 significantly inhibited the development of CPE, whereas transfection of the control siRNA3 did not (Fig. 5A). The latter result indicates that the transfection procedure does not interfere with CPE production and virus replication and that siRNA1 and siRNA2 inhibit HCoV-NL63 in a sequence-specific manner. The IC_{50}s are ~5nM and ~3 nM for siRNA1 and siRNA2, respectively (Fig. 5B). The CC_{50} values are higher than 200nM. These results were confirmed by real-time reverse transcription-PCR analysis of the viral RNA load in the culture medium (Fig. 5C and D).

Inhibition of HCoV-NL63 with nucleoside analogues

A rational approach to the development of drugs for the treatment of HCoV-NL63 infection in patients is to identify compounds that specifically inhibit viral RNA replication. There are several possible mechanisms of action of nucleoside analogues: chain termination resulting from incorporation into elongated RNA strands, interference of these compounds with nucleotide synthesis, or inhibition of the viral polymerase. We tested two nucleoside analogues: β-d-N4-hydroxycytidine and 6-azauridine.

6-Azauridine is a uridine analogue with a histidine-like N-3 pKa (Fig. 6A). It is used as an antineoplastic antimetabolite as it interferes with pyrimidine biosynthesis, thereby preventing the formation of cellular nucleic acids. The antiviral effect of 6-azauridine has previously been documented for several virus types *in vitro*[19,42], including coronaviruses[3,18]. This compound may thus act as a broad antiviral agent. We found that 6-azauridine is also an efficient inhibitor of HCoV-NL63 replication. The CPE reduction assay and viral yield determination indicate that the IC_{50} value is 35nM (Fig. 6B and C). The CC_{50} value determined in the MTS assay is about 80μM, a value consistent with previous reports[19]. Thus, 6-azauridine exhibits a very high selectivity index for HCoV-NL63 inhibition.

The base-modified nucleoside analogue β-d-N4-hydroxycytidine (Fig. 7A) also inhibits HCoV-NL63 replication (Fig. 7B). The virus yield measurements indicate that the IC_{50} value is ~400nM (Fig. 7C). The CC_{50} value determined in the MTS assay is about 80μM.

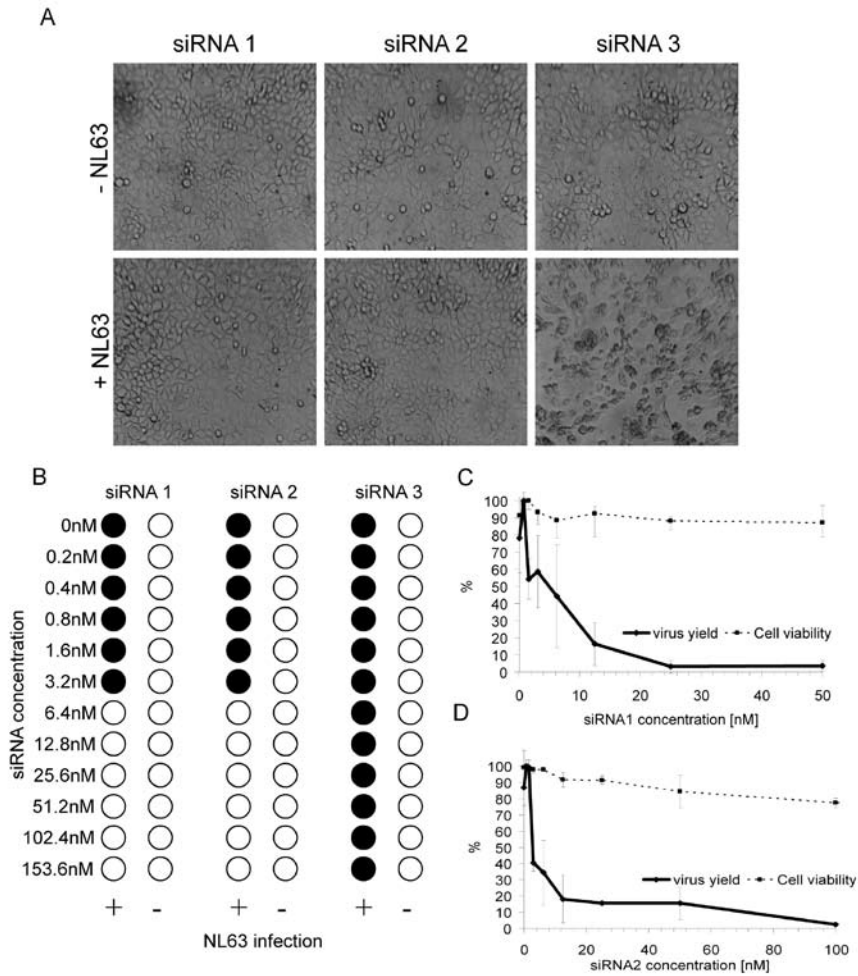


Figure 5. Inhibition of HCoV-NL63 with two specific siRNAs. A) LLC-MK2 cells transfected with 25nM siRNA1 and siRNA2 and 50nM siRNA3 and infected with HCoV-NL63. CPE was observed only in the culture transfected with control siRNA. The images were taken 6 days post-infection. B) CPE reduction mediated by siRNA1 and siRNA2. Filled circles indicate CPE development; empty circles indicate absence of CPE. C) Decrease in HCoV-NL63 virus yield after siRNA1 treatment and cell viability assay. Numbers on the Y axis represent the percentage of produced virus and percentage of viable cells. D) Decrease in HCoV-NL63 virus yield after siRNA2 treatment and cell viability assay. Numbers on the Y axis represent the percentage of produced virus and percentage of viable cells.

Agents with low inhibitory activity against HCoV-NL63
Several other compounds were tested. We observed weak antiviral activity with ritonavir[16], the human immunodeficiency virus type 1 (HIV-1) protease inhibitor, at a concentration of 20μM but with a very low selectivity index (CC_{50} ~80μM) (Table 3). Other HIV-1 protease inhibitors (nelfinavir, indinavir, amprenavir, or saquinavir) did not show any anti-HCoV-NL63 activity. We observed inhibition of HCoV-NL63 with aurintricarboxylic acid[32,36], an RNase and polymerase inhibitor[22,30], at a concentration of ~60μM, but we could not exclude the possibility that the effect was the result of an increased pH of the medium (Table 3). We measured no anti-HCoV-NL63 activity in the following compounds: calpain inhibitors VI and III, glycyrrhizin, valinomycin, escin, ribavirin, dipyridamole, actinomycin D, and pentoxifylline. These compounds have been reported to inhibit other coronaviruses[3,4,8,18,38,41,58,].

Discussion
The CPE reduction assay of HCoV-NL63-infected LLC-MK2 cells provides an easy and reproducible method for the evaluation of candidate antiviral compounds. We selected antiviral compounds that potentially target different stages of the HCoV-NL63 life cycle. Of the 31 compounds tested, we identified 6 compounds that effectively inhibit HCoV-NL63 replication. These compounds interfere at an early stage of virus replication: receptor binding, virus-cell membrane fusion, cytoplasmic stability of viral RNA, and transcription (Table 3).

All of the serum samples tested for the presence of neutralizing antibodies against HCoV-NL63 were positive. Thus, it is not surprising that we also measured potent inhibition with IVIG, which is consisting for 95% of pooled human IgGs isolated from the sera of healthy donors. IVIG is approved as an intravenously delivered drug by the Food and Drug Administration and is successfully used to treat several diseases, mostly primary immune deficiencies and autoimmune neuromuscular disorders but also respiratory diseases (e.g., respiratory syncytial virus)[33] and Kawasaki disease[50]. The effectiveness of IVIG therapy for Kawasaki disease supports the recent claim that HCoV-NL63 is the causative agent of this disease[28], although it does not provide independent evidence for such a correlation, especially because there is accumulating evidence against such an association[7,26,49]. IVIG treatment may be applied to severe HCoV-NL63-related diseases, as the *in vitro* inhibitory concentration is about 10 times lower than the therapeutic dose advised for treatment.

The spike proteins of coronaviruses are class I fusion proteins that exhibit a characteristic membrane fusion mechanism that is driven by conformational changes in the spike protein. The association of the HR1 and HR2 domains brings the fusion peptide that is located near the N terminus of HR1 in close proximity

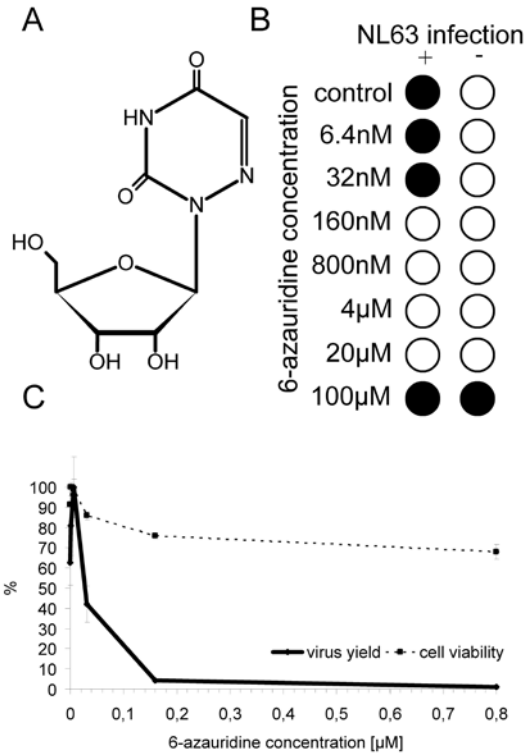


Figure 6. Inhibition of HCoV-NL63 with 6-azauridine. A) Structure of 6-azauridine. B) CPE reduction mediated by 6-azauridine. Filled circles indicate CPE development; empty circles indicate absence of CPE. C) Decrease in HCoV-NL63 virus yield after treatment with 6-azauridine and cell viability assay. Numbers on the Y axis represent the percentage of produced virus and percentage of viable cells.

Table 3. HCoV-NL63 inhibiting compounds.

Antiviral agent	IC_{50}	CC_{50}	Decrease in virus yield[a]	Selectivity index (CC_{50}/IC_{50})
IVIG	125μg/ml	>10mg/ml	3.42×10^3	>80
Heptad repeat peptide	2μM	>40μM	5.75×10^3	>20
siRNA1	5nM	>200nM	6.54×10^1	>40
siRNA2	3nM	>200nM	9.12×10^1	>66
β-D-N^4-hydroxycytidine	400nM	>100μM	3.73×10^3	>250
6-azauridine	32nM	80μM	1.59×10^3	2500
Aurintricarboxylic acid	65μM	300μM	nd[b]	>4.6
Ritonavir	20μM	80μM	nd	4

[a] with > 50% of cells viable
[b] nd = not determined

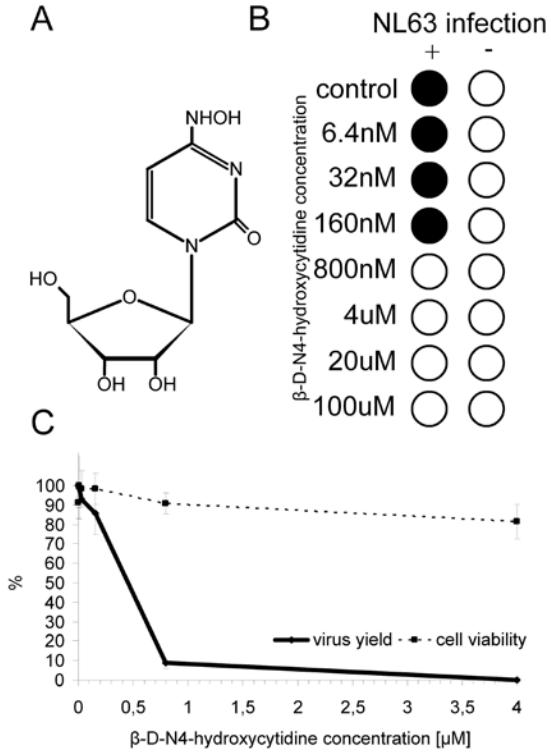


Figure 7. Inhibition of HCoV-NL63 with β-D-N4-hydroxycytidine. A) Structureofβ-D-N4-hydroxycytidine. B) CPE reduction mediated by β-D-N4-hydroxycytidine. Filled circles indicate CPE development; empty circles indicate absence of CPE. C) Decrease in HCoV-NL63 virus yield after treatment with β-D-N4-hydroxycytidine and cell viability assay. Numbers on the Y-axis represent the percentage of produced virus and percentage of viable cells.

to the transmembrane domain, thereby facilitating membrane fusion. Peptides corresponding to the HR1 and HR2 domains were found to associate tightly with the prefusion complex, thus blocking the conformational switch, as has been observed previously for retrovirus and paramyxovirus fusion proteins[10,24]. An NL63-HR2 peptide was able to inhibit HCoV-NL63 infection of LLC-MK2 cells in a concentration-dependent manner. The effect is supposedly mediated by the competitive binding of NL63-HR2 to the HR1 region of the HCoV-NL63 spike protein, thus blocking the conformational switch and, consequently, the close apposition of the fusion peptide and transmembrane domain and, hence, membrane fusion. The NL63-HR2 peptide shows an antiviral potency against HCoV-NL63 similar to that of an MHV-directed HR2 peptide against MHV[13] but is more potent than the SARS-HR2 peptide[12] (IC_{50} values of 0.5, 0.9, and 17.0μM, respectively). We present the first report that HR regions present in the S protein of group 1 coronaviruses, which typically contain a 14-amino-acid insert compared to group 2 coronaviruses, associate into complexes and function similarly to group 2 HR peptides[12,13]. The success of the antiviral T20 peptide against HIV-1 demonstrates the clinical potential of this class of new antivirals.

Following fusion with the host cellular membrane, viral RNA is released into the cytoplasm of the host cell. We found that targeting HCoV-NL63 RNA by employing the RNA interference machinery and transfection of cells with two siRNAs specific for HCoV-NL63 resulted in a profound inhibition of viral replication. The targeted RNA encodes the S glycoprotein, which initiates entry of the virus into susceptible cells; entry is medicated by binding to the cellular receptor, which leads to membrane fusion. The choice of the S gene as a target was also based on the theoretical sequence requirements for an effective siRNA. To avoid the possibility that sequence variation among different HCoV-NL63 strains might restrict the inhibitory effect, we chose well-conserved target sequences in the S gene. The effectiveness of siRNA against respiratory tract diseases in a therapeutic setting was demonstrated recently by the intranasal administration of siRNA targeting respiratory syncytial virus, parainfluenzavirus, and SARS-CoV, with or without transfection reagents, in mouse and monkey models[9,39,59]. Inhaled siRNA in low doses may offer a fast, potent, and easily administered antiviral tool against HCoV-NL63 infection in humans.

The HCoV-NL63 positive-strand RNA is copied by the viral-RNA-dependent RNA polymerase via a negative-strand intermediate. We tested two pyrimidine nucleoside analogues that could potentially interfere with transcription: β-d-N4-hydroxycytidine and 6-azauridine. Nucleoside analogues may be incorporated in the new nascent strand during transcription and cause chain termination. Several pyrimidine ribonucleoside analogs, including 6-azauridine[44,57], act as antimetabolites, exerting pharmacological effects in their monophosphate forms by inhibiting UMP synthase[17] and thereby interfering with UTP metabolism. Additionally, incorporation of the nucleoside analogues may change the processivity and fidelity of transcription. This change results in an increased mutagenicity rate that forces the replicon into "error catastrophe," as described previously for ribavirin[1,20]. Nucleoside analogues are known for their inhibition of several types of viruses, including HIV, pestivirus, hepacivirus, flaviviruses, hepatitis C virus, West Nile virus, feline infectious peritonitis virus, and SARS-CoV[4,5,35,42,48,51,52]. Both compounds show very potent antiviral activities, with IC_{50} values of 35 and 400nM for β-d-N4-hydroxycytidine and 6-azauridine, respectively. Relatively high cytotoxicity is compensated for by low IC_{50} values and thus a high selectivity index.

Recent data indicate that HCoV-NL63 is the most prevalent human coronavirus that is associated with acute respiratory diseases, croup, and possibly Kawasaki disease in children. The lack of an effective vaccine or drug motivated us to design and evaluate therapeutic agents that could inhibit viral replication and thus provide a potential therapy for treating acute respiratory illness of children and immunocompromised patients. Combined with fast diagnostic tools to recognize HCoV-NL63 infection, these antivirals may provide a more appropriate therapy than the routine treatments with steroids, adrenaline, and antibiotics. The agents

described in this report may be used in a mono- or multidrug therapy setting, thereby inhibiting viral infection at different stages of the replication cycle.

Acknowledgments

We thank Joost Haasnoot for helpful comments and Wim van Est for photographic support.

References

1. Anderson, J. P., R. Daifuku, and L. A. Loeb. 2004. Viral error catastrophe by mutagenic nucleosides. Annu. Rev. Microbiol. 58:183-205.
2. Arden, K. E., M. D. Nissen, T. P. Sloots, and I. M. Mackay. 2005. New human coronavirus, HCoV-NL63, associated with severe lower respiratory tract disease in Australia. J. Med. Virol. 75:455-462.
3. Barlough, J. E. and B. L. Shacklett. 1994. Antiviral studies of feline infectious peritonitis virus in vitro. Vet. Rec. 135:177-179.
4. Barnard, D. L., V. D. Hubbard, J. Burton, D. F. Smee, J. D. Morrey, M. J. Otto, and R. W. Sidwell. 2004. Inhibition of severe acute respiratory syndrome-associated coronavirus (SARSCoV) by calpain inhibitors and beta-D-N4-hydroxycytidine. Antivir. Chem. Chemother. 15:15-22.
5. Barreiro, P., T. Garcia-Benayas, A. Rendon, S. Rodriguez-Novoa, and V. Soriano. 2004. Combinations of nucleoside/nucleotide analogues for HIV therapy. AIDS Rev. 6:234-243.
6. Bastien, N., K. Anderson, L. Hart, P. Van Caeseele, K. Brandt, D. Milley, T. Hatchette, E. C. Weiss, and Y. Li. 2005. Human coronavirus NL63 infection in Canada. J. Infect. Dis. 191:503-506.
7. Belay, E. D., D. D. Erdman, L. J. Anderson, T. C. Peret, S. J. Schrag, B. S. Fields, J. C. Burns, and L. B. Schonberger. 2005. Kawasaki disease and human coronavirus. J. Infect. Dis. 192:352-353.
8. Bermejo Martin, J. F., J. L. Jimenez, and A. Munoz-Fernandez. 2003. Pentoxifylline and severe acute respiratory syndrome (SARS): a drug to be considered. Med. Sci. Monit. 9:SR29-SR34.
9. Bitko, V., A. Musiyenko, O. Shulyayeva, and S. Barik. 2005. Inhibition of respiratory viruses by nasally administered siRNA. Nat. Med. 11:50-55.
10. Blacklow, S. C., M. Lu, and P. S. Kim. 1995. A trimeric subdomain of the simian immunodeficiency virus envelope glycoprotein. Biochemistry 34:14955-14962.
11. Boom, R., C. J. Sol, M. M. Salimans, C. L. Jansen, P. M. Wertheim-van Dillen, and J. van der Noordaa. 1990. Rapid and simple method for purification of nucleic acids. J. Clin. Microbiol. 28:495-503.
12. Bosch, B. J., B. E. Martina, R. Van Der Zee, J. Lepault, B. J. Haijema, C. Versluis, A. J. Heck, R. De Groot, A. D. Osterhaus, and P. J. Rottier. 2004. Severe acute respiratory syndrome coronavirus (SARS-CoV) infection inhibition using spike protein heptad repeat-derived peptides. Proc. Natl. Acad. Sci. U. S. A 101:8455-8460.
13. Bosch, B. J., R. Van Der Zee, C. A. de Haan, and P. J. Rottier. 2003. The coronavirus spike protein is a class I virus fusion protein: structural and functional characterization of the fusion core complex. J. Virol. 77:8801-8811.
14. Brockway, S. M., C. T. Clay, X. T. Lu, and M. R. Denison. 2003. Characterization of the expression, intracellular localization, and replication complex association of the putative mouse hepatitis virus RNA-dependent RNA polymerase. J. Virol. 77:10515-10527.
15. Chiu, S. S., K. H. Chan, K. W. Chu, S. W. Kwan, Y. Guan, L. L. Poon, and J. S. Peiris. 2005. Human coronavirus NL63 infection and other coronavirus infections in children hospitalized with acute respiratory disease in Hong Kong, China. Clin. Infect. Dis. 40:1721-1729.
16. Chu, C. M., V. C. Cheng, I. F. Hung, M. M. Wong, K. H. Chan, K. S. Chan, R. Y. Kao, L. L. Poon, C. L. Wong, Y. Guan, J. S. Peiris, and K. Y. Yuen. 2004. Role of lopinavir/ritonavir in the treatment of SARS: initial virological and clinical findings. Thorax 59:252-256.
17. Cihak, A. and B. Rada. 1976. Uridine kinase: properties, biological significance and chemotherapeutic aspects (a review). Neoplasma 23:233-257.
18. Cinatl, J., B. Morgenstern, G. Bauer, P. Chandra, H. Rabenau, and H. W. Doerr. 2003. Glycyrrhizin, an active component of liquorice roots, and replication of SARS-associated coronavirus. Lancet 361:2045-2046.

19. Crance, J. M., N. Scaramozzino, A. Jouan, and D. Garin. 2003. Interferon, ribavirin, 6-azauridine and glycyrrhizin: antiviral compounds active against pathogenic flaviviruses. Antiviral Res. 58:73-79.
20. Crotty, S., C. E. Cameron, and R. Andino. 2001. RNA virus error catastrophe: direct molecular test by using ribavirin. Proc. Natl. Acad. Sci. U. S. A 98:6895-6900.
21. de Groot, R. J., W. Luytjes, M. C. Horzinek, B. A. van der Zeijst, W. J. Spaan, and J. A. Lenstra. 1987. Evidence for a coiled-coil structure in the spike proteins of coronaviruses. J. Mol. Biol. 196:963-966.
22. Dreyer, C. and P. Hausen. 1978. Inhibition of mammalian RNA polymerase by 5,6-dichlororibofuranosylbenzimidazole (DRB) and DRB triphosphate. Nucleic Acids Res. 5:3325-3335.
23. Durandy, A., V. Wahn, S. Petteway, and E. W. Gelfand. 2005. Immunoglobulin replacement therapy in primary antibody deficiency diseases--maximizing success. Int. Arch. Allergy Immunol. 136:217-229.
24. Dutch, R. E., S. B. Joshi, and R. A. Lamb. 1998. Membrane fusion promoted by increasing surface densities of the paramyxovirus F and HN proteins: comparison of fusion reactions mediated by simian virus 5 F, human parainfluenza virus type 3 F, and influenza virus HA. J. Virol. 72:7745-7753.
25. Ebihara, T., R. Endo, X. Ma, N. Ishiguro, and H. Kikuta. 2005. Detection of human coronavirus NL63 in young children with bronchiolitis. J. Med. Virol. 75:463-465.
26. Ebihara, T., R. Endo, X. Ma, N. Ishiguro, and H. Kikuta. 2005. Lack of association between New Haven coronavirus and Kawasaki disease. J. Infect. Dis. 192:351-352.
27. Eckert, D. M. and P. S. Kim. 2001. Mechanisms of viral membrane fusion and its inhibition. Annu. Rev. Biochem. 70:777-810.
28. Esper, F., E. D. Shapiro, C. Weibel, D. Ferguson, M. L. Landry, and J. S. Kahn. 2005. Association between a novel human coronavirus and Kawasaki disease. J. Infect. Dis. 191:499-502.
29. Fouchier, R. A., N. G. Hartwig, T. M. Bestebroer, B. Niemeyer, J. C. de Jong, J. H. Simon, and A. D. Osterhaus. 2004. A previously undescribed coronavirus associated with respiratory disease in humans. Proc. Natl. Acad. Sci. U. S. A 101:6212-6216.
30. Hallick, R. B., B. K. Chelm, P. W. Gray, and E. M. Orozco, Jr. 1977. Use of aurintricarboxylic acid as an inhibitor of nucleases during nucleic acid isolation. Nucleic Acids Res. 4:3055-3064.
31. Hanson, L. A., J. Bjorkander, C. Wadsworth, and B. Bake. 1982. Intravenous immunoglobulin in antibody deficiency syndromes. Lancet 1:396.
32. He, R., A. Adonov, M. Traykova-Adonova, J. Cao, T. Cutts, E. Grudesky, Y. Deschambaul, J. Berry, M. Drebot, and X. Li. 2004. Potent and selective inhibition of SARS coronavirus replication by aurintricarboxylic acid. Biochem. Biophys. Res. Commun. 320:1199-1203.
33. Hemming, V. G., W. Rodriguez, H. W. Kim, C. D. Brandt, R. H. Parrott, B. Burch, G. A. Prince, P. A. Baron, R. J. Fink, and G. Reaman. 1987. Intravenous immunoglobulin treatment of respiratory syncytial virus infections in infants and young children. Antimicrob. Agents Chemother. 31:1882-1886.
34. Hofmann, H., K. Pyrc, L. van der Hoek, M. Geier, B. Berkhout, and S. Pohlmann. 2005. Human coronavirus NL63 employs the severe acute respiratory syndrome coronavirus receptor for cellular entry. Proc. Natl. Acad. Sci. U. S. A 102:7988-7993.
35. Hollecker, L., H. Choo, Y. Chong, C. K. Chu, S. Lostia, T. R. McBrayer, L. J. Stuyver, J. C. Mason, J. Du, S. Rachakonda, J. Shi, R. F. Schinazi, and K. A. Watanabe. 2004. Synthesis of beta-enantiomers of N4-hydroxy-3'-deoxypyrimidine nucleosides and their evaluation against bovine viral diarrhoea virus and hepatitis C virus in cell culture. Antivir. Chem. Chemother. 15:43-55.
36. Hunt, D. M. and R. R. Wagner. 1975. Inhibition by aurintricarboxylic acid and polyethylene sulfonate of RNA transcription of vesicular stomatitis virus. J. Virol. 16:1146-1153.
37. Kawasaki, T., F. Kosaki, S. Okawa, I. Shigematsu, and H. Yanagawa. 1974. A new infantile acute febrile mucocutaneous lymph node syndrome (MLNS) prevailing in Japan. Pediatrics 54:271-276.
38. Lewis, E. L., D. A. Harbour, J. E. Beringer, and J. Grinsted. 1992. Differential in vitro inhibition of feline enteric coronavirus and feline infectious peritonitis virus by actinomycin D. J. Gen. Virol. 73 (Pt 12):3285-3288.
39. Li, B. J., Q. Tang, D. Cheng, C. Qin, F. Y. Xie, Q. Wei, J. Xu, Y. Liu, B. J. Zheng, M. C. Woodle, N. Zhong, and P. Y. Lu. 2005. Using siRNA in prophylactic and therapeutic regimens against SARS coronavirus in Rhesus macaque. Nat. Med. 11:944-951.

40. Moes, E., L. Vijgen, E. Keyaerts, K. Zlateva, S. Li, P. Maes, K. Pyrc, B. Berkhout, L. van der Hoek, and M. Van Ranst. 2005. A novel pancoronavirus RT-PCR assay: frequent detection of human coronavirus NL63 in children hospitalized with respiratory tract infections in Belgium. BMC. Infect. Dis. 5:6.
41. Morgenstern, B., M. Michaelis, P. C. Baer, H. W. Doerr, and J. Cinatl, Jr. 2005. Ribavirin and interferon-beta synergistically inhibit SARS-associated coronavirus replication in animal and human cell lines. Biochem. Biophys. Res. Commun. 326:905-908.
42. Morrey, J. D., D. F. Smee, R. W. Sidwell, and C. Tseng. 2002. Identification of active antiviral compounds against a New York isolate of West Nile virus. Antiviral Res. 55:107-116.
43. Oates-Whitehead, R. M., J. H. Baumer, L. Haines, S. Love, I. K. Maconochie, A. Gupta, K. Roman, J. S. Dua, and I. Flynn. 2003. Intravenous immunoglobulin for the treatment of Kawasaki disease in children. Cochrane. Database. Syst. Rev. 4: doi:10.1002/14651858.CD004000.
44. Pasternak, C. A., G. A. Fischer, and R. E. Handschumacher. 1961. Alterations in pyrimidine metabolism in L5178Y leukemia cells resistant to 6-azauridine. Cancer Res. 21:110-117.
45. Pyrc, K., M. F. Jebbink, B. Berkhout, and L. van der Hoek. 2004. Genome structure and transcriptional regulation of human coronavirus NL63. Virol. J. 1:7.
46. Reed, L. J. and H. Muench. 1938. A simple method of estimating fifty percent endpoints. American Journal of Hygiene 27:493-497.
47. Rowley, A. H. and S. T. Shulman. 1999. Kawasaki syndrome. Pediatr. Clin. North Am. 46:313-329.
48. Schinazi, R. F., J. Mellors, H. Bazmi, S. Diamond, S. Garber, K. Gallagher, R. Geleziunas, R. Klabe, M. Pierce, M. Rayner, J. T. Wu, H. Zhang, J. Hammond, L. Bacheler, D. J. Manion, M. J. Otto, L. Stuyver, G. Trainor, D. C. Liotta, and S. Erickson-Viitanen. 2002. DPC 817: a cytidine nucleoside analog with activity against zidovudine- and lamivudine-resistant viral variants. Antimicrob. Agents Chemother. 46:1394-1401.
49. Shimizu, C., H. Shike, S. C. Baker, F. Garcia, L. van der Hoek, T. W. Kuijpers, S. L. Reed, A. H. Rowley, S. T. Shulman, H. K. Talbot, J. V. Williams, and J. C. Burns. 2005. Human coronavirus NL63 is not detected in the respiratory tracts of children with acute Kawasaki disease. J. Infect. Dis. 192:1767-1771.
50. Stiehm, E. R., E. Ashida, K. S. Kim, D. J. Winston, A. Haas, and R. P. Gale. 1987. Intravenous immunoglobulins as therapeutic agents. Ann. Intern. Med. 107:367-382.
51. Stuyver, L. J., S. Lostia, M. Adams, J. S. Mathew, B. S. Pai, J. Grier, P. M. Tharnish, Y. Choi, Y. Chong, H. Choo, C. K. Chu, M. J. Otto, and R. F. Schinazi. 2002. Antiviral activities and cellular toxicities of modified 2',3'-dideoxy-2',3'-didehydrocytidine analogues. Antimicrob. Agents Chemother. 46:3854-3860.
52. Stuyver, L. J., T. Whitaker, T. R. McBrayer, B. I. Hernandez-Santiago, S. Lostia, P. M. Tharnish, M. Ramesh, C. K. Chu, R. Jordan, J. Shi, S. Rachakonda, K. A. Watanabe, M. J. Otto, and R. F. Schinazi. 2003. Ribonucleoside analogue that blocks replication of bovine viral diarrhea and hepatitis C viruses in culture. Antimicrob. Agents Chemother. 47:244-254.
53. Suzuki, A., M. Okamoto, A. Ohmi, O. Watanabe, S. Miyabayashi, and H. Nishimura. 2005. Detection of human coronavirus-NL63 in children in Japan. Pediatr. Infect. Dis. J. 24:645-646.
54. Vabret, A., T. Mourez, J. Dina, L. van der Hoek, S. Gouarin, J. Petitjean, J. Brouard, and F. Freymuth. 2005. Human coronavirus NL63, France. Emerg. Infect. Dis. 11:1225-1229.
55. van der Hoek, L., K. Pyrc, M. F. Jebbink, W. Vermeulen-Oost, R. J. Berkhout, K. C. Wolthers, P. M. Wertheim-van Dillen, J. Kaandorp, J. Spaargaren, and B. Berkhout. 2004. Identification of a new human coronavirus. Nat. Med. 10:368-373.
56. van der Hoek, L., K. Sure, G. Ihorst, A. Stang, K. Pyrc, M. F. Jebbink, G. Petersen, J. Forster, B. Berkhout, and K. Uberla. 2005. Croup is associated with the novel coronavirus NL63. PLoS. Med. 2:e240.
57. Vesely, J. and A. Cihak. 1973. Resistance of mammalian tumour cells toward pyrimidine analogues. A review. Oncology 28:204-226.
58. Wu, C. Y., J. T. Jan, S. H. Ma, C. J. Kuo, H. F. Juan, Y. S. Cheng, H. H. Hsu, H. C. Huang, D. Wu, A. Brik, F. S. Liang, R. S. Liu, J. M. Fang, S. T. Chen, P. H. Liang, and C. H. Wong. 2004. Small molecules targeting severe acute respiratory syndrome human coronavirus. Proc. Natl. Acad. Sci. U. S. A 101:10012-10017.
59. Zhang, W., H. Yang, X. Kong, S. Mohapatra, H. Juan-Vergara, G. Hellermann, S. Behera, R. Singam, R. F. Lockey, and S. S. Mohapatra. 2005. Inhibition of respiratory syncytial virus infection with intranasal siRNA nanoparticles targeting the viral NS1 gene. Nat. Med. 11:56-62.

Chapter X

Antiviral strategies against human coronaviruses

Infectious Disorders - Drug Targets, March 2007, vol. 7, p. 59 - 66

Krzysztof Pyrc, Ben Berkhout and Lia van der Hoek

Laboratory of Experimental Virology, Department of Medical Microbiology, Center for Infection and Immunity Amsterdam (CINIMA), Academic Medical Center, University of Amsterdam, Meibergdreef 15, 1105 AZ, Amsterdam, The Netherlands.

Since the mid 60's the human coronaviruses (HCoV), represented by HCoV-OC43 and HCoV229E, were generally considered relatively harmless viruses. This status changed dramatically with the emergence of SARS-CoV in 2002/2003. The SARS-CoV pandemic took 774 lives around the globe and infected more than 8000 people in 29 countries. SARS-CoV is believed to be of zoonotic origin, transmitted from its natural reservoir in bats through several animal species (e.g., civet cats, raccoon dogs sold for human consumption in markets in southern China). The epidemic was halted in 2003 by a highly effective global public health response, and SARS-CoV is currently not circulating in humans. The outbreak of SARS-CoV and the danger of its re-introduction into the human population, as well as the danger of the emergence of other zoonotic coronaviral infections triggered an intense survey for an efficient treatment that resulted in the evaluation of several anticoronaviral compounds.

HCoV-NL63 and HCoV-HKU1 were identified shortly after the SARS-CoV outbreak. The 4 human coronaviruses HCoV-229E, HCoV-OC43, HCoV-NL63 and HCoV-HKU1 cause mild respiratory illnesses when compared to SARS, but these infections are involved in 10 – 20% of hospitalizations of young children and immunocompromised adults with respiratory tract illness. Therefore, there is an urgent need for a successful therapy to prevent disease induction or a vaccine to prevent new infections. This review summarizes the current status of anticoronaviral strategies.

Coronaviruses

Coronaviruses, a genus of the *Coronaviridae* family, are enveloped viruses with a plus-strand RNA genome. The genomic RNA is 27–32kb in size, capped and polyadenylated. Coronaviruses have been identified in bats, mice, rats, chickens, turkeys, swine, dogs, cats, rabbits, horses, cattle and humans and cause highly prevalent diseases such as respiratory, enteric, cardiovascular and neurological disorders. Originally, coronaviruses were classified on the basis of antigenic cross-reactivity, and three antigenic groups were recognized. When coronavirus genome sequences began to accumulate, the original antigenic groups were converted into genetic groups based on similarity of the nucleotide sequences[64,84].

Clinical manifestation

Human coronaviruses received relatively little attention as human pathogens, as they were considered to be common cold viruses. Inoculation of HCoV-229E and HCoV-OC43 in healthy volunteers revealed that infection with these viruses causes common cold, but more severe lower respiratory tract infections (LRTI) were observed in infants and immunocompromized persons[5,7,16,37,38,57,63,100,121,141,142,172,191,220,221,223,230]. Coryza occurs more often in patient with HCoV-229E infection, while HCoV-OC43 positive patients frequently have sore throat manifestations[172]. The SARS epidemic started in the Guandong

province of China in 2003. At first it was suggested that known viruses were involved, but soon thereafter SARS-CoV was identified as the responsible pathogen[53,112,161]. SARS-CoV probably originated from a wild animal reservoir, most likely bats, and was transmitted in a zoonotic event to humans via civet cats that are traded as food in China[120]. The short but wide-spread epidemic was terminated at the end of 2003 and has not returned thereafter[160]. The last two viruses: HCoV-NL63 and HCoV-HKU1 were identified in 2004 and 2005, respectively[222,229]. Infection by these viruses probably displays a spectrum of diseases similar to HCoV-229E and HCoV-OC43 infection. A clear link between HCoV-NL63 and croup has been observed. Of the children with HCoV-NL63 infection, 45% had laryngotracheitis (croup) compared to only 6% in the control group[223]. The respiratory symptoms accompanying an HCoV-HKU1 infection are usually rhinorrhoea, fever, cough, febrile seizure and wheezing, and disease manifestations like bronchiolitis and pneumonia[191]. It has been suggested that HCoV-HKU1 might also trigger gastrointestinal disease[221].

Genome structure

The coronaviral genome encompasses 27-32kb and contains at least seven open reading frames (ORF) and untranslated regions at the 5′ and 3′ ends. The two large 5′ terminal ORFs 1a and 1ab encode non-structural proteins that are required for viral replication. The remaining ORF's in the 3′ part of the genome encode the four structural proteins spike (S), envelope (E), membrane (M) and nucleocapsid (N) for group I coronaviruses and an additional haemaglutinin esterase (HE) protein for group II coronaviruses. Between the structural protein genes several accessory ORF's are located. The position and order of these ORF's varies between species[222]. Recent studies have shown that some of the accessory proteins of SARS-CoV are structural proteins that are incorporated in the virion[87,88,182].

Replication cycle

Coronavirus infection starts with the recognition of a specific receptor on the host cell surface by the coronaviral S protein, followed by internalization of the virion core either by direct fusion of the viral membrane with the plasma membrane or via endocytosis[19,111]. Viral RNA is released into the cytoplasm and "cap-dependent" initiation of translation results in the immediate expression of viral proteins and subsequent RNA replication[115]. Full-length genomic RNA and a nested set of subgenomic mRNAs (sg mRNA) are generated in the membrane-associated replication centers (double membrane vesicles, DMV's)[26]. These sg mRNAs are functional templates for translation of structural proteins. Full-length viral RNA which is bound to the N protein is encapsidated in newly assembled virion particles that are released from the host cell via exocytosis or apoptosis.

Antiviral agents targeting different steps of the viral replication cycle

Cell entry

The coronavirus S protein is a 180–200kDa type I membrane glycoprotein, incorporated in a virion as a surface protein. The S protein is composed of a short C-terminal tail inside the virion, a single transmembrane domain, and a rod - like domain (S2) with a globular "head" (S1). The main function of the S protein is binding to the cellular receptor by the receptor binding site (RBS) on the S1 domain, resulting in fusion with the cellular membrane. Group II coronavirus S proteins contain a furin cleavage site between S1 and S2, and cleavage of the S protein is critical to reach an active conformation[47,189]. The receptor specificity varies between species, especially for group II viruses: MHV uses CEACAM-1[228], HCoV-OC43 and BCoV use O-acetylated sialic acid[225] and SARS-CoV uses angiotensin converting enzyme 2 (ACE2)[127]. All group I coronaviruses use CD13 (also known as aminopeptidase N) as receptor[51,156,215,239], except HCoV-NL63 which uses ACE2 as receptor[80].

After binding of S to the receptor enveloped viruses employ two different strategies to enter their target cells. One involves fusion of viral / cellular membrances on the cell surface while the second strategy uses endocytosis and subsequent acidification of the environment, which is needed directly or indirectly (by pH dependent activation of endosomal proteinases) for fusion.

Inhibition of cell attachment

The S protein of coronaviruses is highly glycosylated. This carbohydrate shield may be used as a target for compounds specifically binding to sugar moieties, e.g. lectins, thus coating the protein and blocking the interaction with the receptor. Plant lectins are known to inhibit the infection of viruses that contain a glycosylated envelope such as human immunodeficiency virus type 1, cytomegalovirus and human T-cell leukemia virus type I[12,194,235]. The mannose-specific plant lectins derived from Galanthus nivalis (Common Snowdrop), Hippeastrum hybrid (Amaryllis) and Allium porrum (leek) inhibit replication of SARS-CoV and feline coronavirus[13,224]. These lectins indeed block the S - receptor interaction as inhibition is observed at a very early stage of replication[13].

A more specific inhibitory approach is provided by specific monoclonal or polyclonal antibodies directed to the RBS of the S protein or the domain of the cellular receptor that is recognized by the S protein. Several reports describe RBS - specific antibodies that efficiently inhibit receptor binding[69,75,90,203,217]. These antibodies can be generated by immunization of laboratory animals with proteins[69,75,76,203] or complete viruses[39,217] and subsequent purification of specific antibodies. Alternatively, *in vitro* generation of human antibodies is possible based on antibody phage display library screening[56,128,210]. The CR304 human monoclonal antibody (mAb) and 80R mAb immunoglobulin IgG1 are potent

SARS-CoV-RBS binders that block the S – ACE2 interaction[203,210]. These mAbs can limit SARS-CoV infection below the detection levels in an *in vivo* mouse and ferret model[202,204,210]. A broader protection is provided by polyclonal antibodies, as the possible selection of viral escape mutants is less likely[170,211].

Only few studies have tested monoclonal and polyclonal antibodies against the other human coronaviruses. Inhibition of HCoV-229E infection can be achieved *in vitro* by polyclonal antibodies directed to complete virus or the RBS, and also a monoclonal antibody directed to the HCoV-229E receptor, aminopeptidase N, inhibits HCoV-229E replication[21]. HCoV-NL63 can be neutralized by pooled immunoglobulins (IVIG)[170].

Small-molecular-weight inhibitors interacting with the viral receptor provide another therapeutic option, e.g. N-(2-aminoethyl)-1 aziridine-ethanamine (NAAE), which binds to the ACE2 protein[214].

Another approach to influence coronavirus entry is to induce downregulation of the receptor on the cell surface. Treatment of Vero E6 cells with interleukin 4 and interferon γ decreases the expression of ACE2 at the transcriptional level, thus limiting the susceptibility of the cells to SARS-CoV infection[49]. Although these results were presented only for SARS-CoV, it might be expected that HCoV-NL63 infection will also be restricted since this virus uses the same receptor. The clinical consequences of such a treatment are currently not known. ACE2 together with ACE are involved in regulation of the renin–angiotensin system and have an important role in maintaining blood pressure homeostasis, as well as fluid and salt balance[20,43,190]. Moreover, ACE2 is involved in protection against lung damage[93,113], and decreasing ACE2 levels or inactivating ACE2 can therefore have serious adverse effects.

Inhibition of virus – cell fusion

A second step of coronavirus cell entry is the virion fusion with the host cell membrane and release of the virion core with the RNA genome into the cytoplasm. Depending on the virus species, the fusion can occur directly on the cell surface or may require internalization into the endosome[189]. Treatment with inhibitors of vacuolar acidification like ammonium chloride, chloroquine (an anti malaric drug, approved for use in humans) or bafilomycin A, demonstrated that HCoV-229E and SARS-CoV require the endosomal pathway for entry[19,89]. HCoV-NL63 may engage a different route for entry since vacuolar acidification inhibitors have only limited influence[81,89]. Thus, inhibition of the fusion process with chloroquine has limitations and may be applied only for some coronaviruses[19,89,170].

The S proteins of coronaviruses exhibit a characteristic membrane fusion mechanism that is driven by conformational changes in the S protein, involving

rearrangement and interaction of heptad repeat regions (HR1 and HR2) located in the S2 domain. Association of the HR1 and HR2 domains into a 6-helix bundle triggers membrane fusion. Characteristic for group I viruses is the insertion of 14 additional amino acid in both HR regions, when compared to group II viruses[25]. Several reports showed that treatment with synthetic peptides corresponding to the HR1 and HR2 regions results in profound inhibition of SARS-CoV replication[24,241,246]. For non-SARS human coronaviruses such a study was performed only for HCoV-NL63 and a clear inhibition was observed *in vitro* with a synthetic HR2 peptide, illustrating that group I coronaviruses use the same fusion mechanism as group II viruses[170]. Such an antiviral approach is not a novelty, as it was presented for several other viruses, including the T20 peptide that has been approved as anti-HIV-1 drug[117]. Besides inhibition by HR-derived peptides, the association between HR1 and HR2 can also be blocked by HR-specific antibodies[105,116,133,216].

Furthermore, Sainz *et al* developed peptide fusion inhibitors based on non-HR regions of S2. Five regions within the SARS-CoV S2 subunit with a high propensity to interact with the lipid interface of membranes were identified and peptides analogous to these regions are effective inhibitors of SARS-CoV[176].

Coronaviral transcription

Coronavirus replication is a complex, not yet fully understood process[179,180]. The 5' end of coronavirus genomic RNA contains the untranslated leader sequence that ends with the Transcription Regulation Sequence (TRS) element. These sequence elements are also present upstream of each ORF (body TRSs). During transcription the RNA-dependent RNA-polymerase (RdRp) has been proposed to pause once one of the body TRS is copied during minus strand synthesis. Subsequent strand transfer to the leader TRS adds a common leader sequence to each minus strand sg mRNA[193]. This discontinuous transcription mechanism is based on base-pairing of the nascent minus strand copy RNA with the plus strand leader TRS[48,82,109,184].

Polymerase inhibitors

All coronaviruses encode their own RdRp. The RdRp gene is located partially in the 1a ORF and mostly in the 1b ORF[122]. The polymerase is the most conserved protein among coronaviral species, providing a convenient target for broad anti-coronaviral drugs. Unfortunately, no RdRp specific inhibitors have been developed according to our knowledge.

In silico molecular docking studies to identify potential inhibitors have been performed for the aurintricarboxylic acid (ATA) and RdRp protein, showing a possible interaction[238]. *In vitro* experiments with ATA indeed showed inhibition of SARS-CoV and HCoV-NL63, but *in vitro* studies with the purified enzyme have not been performed[74,170].

Nucleoside analogues

As mentioned above, the coronaviral positive-strand RNA is copied by the viral RdRp via a negative-strand intermediate. Nucleoside analogues can inhibit virus replication by interference with various processes, e.g. they can be incorporated in the new strand and cause chain termination[114] or decrease the processivity and fidelity of transcription, resulting in an "error catastrophy"[45]. Furthermore, several pyrimidine ribonucleoside analogs can also act as antimetabolites, inhibiting UMP synthase and thereby interfering with the UTP metabolism[40]. Nucleoside analogues are known for their inhibition of several types of viruses, including HIV, pestivirus, hepacivirus, flaviviruses, hepatitis C virus and West Nile virus[15,83,145,183,200,201]. Only a few nucleoside inhibitors can in fact inhibit the replication of coronaviruses. The most promising drug candidates are β-D-N4-hydroxycytidine and 6-azauridine that can inhibit SARS-CoV and HCoV-NL63 replication *in vitro*[14,42,170].

Ribavirin, a purine analogue, was incorporated in clinical practice during the SARS-CoV outbreak because of its broad antiviral activity against numerous RNA viruses. However, the anti-coronaviral activity of this compound is rather poor[4,36,45]. *In vitro* inhibition of SARS-CoV indicated that the IC_{50} value is relatively high, whereas no inhibitory action was observed on HCoV-NL63[42,170,175,199]. Also experimental therapy of SARS patients with this compound showed no positive effect[36]. Another widely known compound, the imidazole nucleoside analogue mizoribine[70,85,91,147,148,158,234], exhibits only marginal anti - coronavirus activity[175].

Helicase inhibitors

The coronaviral helicase protein is enzymatically active and efficiently unwinds ds DNA and ds RNA[94,212]. The helicase domain is encoded in ORF1b by the nsp13 gene, which is located downstream of the RdRp gene. Coronaviral helicase shares sequence similarity with the superfamily 1 helicases. This enzyme family is common among viruses, being encoded by e.g. alphaviruses, rubiviruses, hepatitis E viruses and arteriviruses[65,66]. Biochemical and genetic data suggest a role of these proteins in diverse aspects of viral replication: transcription, RNA stability, cell-to-cell movement and virus biogenesis[50,95,154,155,157,166,174]. Adamantane-derived bananins are potent inhibitors of SARS-CoV helicase activity and replication. Six bananin derivatives have been tested in an ATPase assay: bananin, iodobananin, adeninobananin, vanillinbananin, eubananin, and ansabananin. Iodobananin and vanillinbananin appeared to be the most effective SARS-CoV helicase inhibitors. Unfortunately, only bananin was tested against SARS-CoV replication *in vitro* and exhibited a reasonable inhibitory potency in the micromolar range[208].

Small interfering RNA and antisense phosphorodiamidate morpholino oligomers

RNA interference (RNAi) is a mechanism for sequence-specific mRNA degradation by dsRNA molecules. Long dsRNA molecules are recognized

and cleaved into short 21-24nt fragments by an endogenous DICER enzyme with RNase III activity. The resulting small interfering (si) RNA molecules are incorporated into the RNA-induced silencing complex (RISC), which degrades mRNA molecules with perfect sequence complementarity to the siRNA. Antiviral RNAi can be induced by synthetic siRNA that is incorporated directly into RISC[197]. Several groups developed effective siRNA's, against different regions of a coronavirus genome, including the 5' leader genome sequence[126,231], TRS region[231], nsp1 gene[151], nsp12 gene[125], RdRp gene[137,227], S gene[73,125,170,171,242], E[73,185], M[73,185], N gene[73,185,209,243] and 3' UTR[231]. The effectiveness of siRNAs against respiratory tract diseases in a therapeutic setting was demonstrated recently by the intranasal administration of siRNA targeting respiratory syncytial virus, parainfluenzavirus, and SARS-CoV, with or without transfection reagents, in mouse and monkey models[9, 39, 59]. An inhaled siRNA coctail in low doses may offer a fast, potent, and easily administered antiviral tool to control coronaviral infection in humans. Although the field is moving fast, to date no RNAi therapy is approved for use in humans[96,110,198].

A similar approach, targeting directly the viral RNA, employs antisense phosphorodiamidate morpholino oligomers (PMO). While RNAi is based on degradation of the viral RNA, PMO's bind to complementary sequences and form a steric block[205]. PMO's that efficiently inhibit SARS-CoV replication *in vitro* target the ORF 1a initiation codon, ORF 1a/1b pseudoknot structure, TRS, S2M motif, 3'-UTR pseudoknot structure, and 3' UTR[149].

Agents targeting translation and protein processing

During replication of coronaviruses, several structural and non-structural proteins are produced. Translation of coronaviral proteins is a rather difficult target for therapy, as it employs a cellular mechanism[140]. In contrast, a therapeutic window is presented by the post-translational processing of the 1a / 1ab polyprotein, which is performed exclusively by viral proteinases. This proteolytic processing is a key regulatory mechanism in the expression of the replicative proteins. Three proteinases are encoded by the N-terminal part of the 1a/1ab polyprotein. Two papain-like proteinase domains ($PL1^{pro}$ and $PL2^{pro}$) are encoded by the nsp3 gene and process 3 cleavage sites, including an autoproteolytic release[62]. The second proteinase is named chymotrypsin-like proteinase or "main proteinase" (M^{pro}) to stress its dominant function. M^{pro} is encoded by nsp5 and recognizes 11 cleavage sites in the 1ab polyprotein.

Main proteinase inhibitors

The coronaviral M^{pro} displays very low amino acid variability between coronavirus species and is therefore a convenient target for broad range inhibitors. Several studies have described potent inhibition of the M^{pro} enzyme by different compounds[2,6,18,28-30,32,52,54,55,61,86,99,102,103,124,131,135,136,138,139,187,218,232,233,236,237].

As the crystal structure is solved for SARS-CoV M^{pro} [3], the most popular method for de novo identification of inhibitors is computer-based docking of existing drugs and compounds, followed by an *in vitro* M^{pro} activity assay[29,30,99,138]. Furthermore, there are several computational methods that allow an efficient in silico structure-based screening. Despite the power of these methods, only a few agents identified this way were able to inhibit SARS-CoV M^{pro} in the micromolar range[29,61,188].

Agents inhibiting M^{pro} are either peptide-based inhibitors or small non-peptide compounds, both binding (reversibly or irreversibly) to the catalytic site of M^{pro} and thus inhibiting its activity. Unfortunately, most studies have focused exclusively on SARS-CoV, while these proteinase inhibitors may have the capacity to inhibit all coronaviruses. As an exception, a broad approach was presented by Yang *et al*, who described several M^{pro} inhibitors targeting all group I and II human coronaviruses[236].

Papain – like proteinase inhibitors

The papain-like proteinase (PL^{pro}) consists of two domains: $PL1^{pro}$ and $PL2^{pro}$, of which in most cases both have catalytic activity except for SARS-CoV and IBV, which lack the $PL1^{pro}$ [8,22,67,78,101,130,134,212,250]. PL^{pro}s cut between two small amino acids with short uncharged side chains [129,247-249].

Coronaviral PL^{pro} is a multi-functional protein with catalytic domains that mediate different enzymatic activities. The PL^{pro} protein is a more difficult target for antiviral agents because of its high variability. One study describes that zinc ion and its conjugates can act as inhibitors of the SARS-CoV Cys-His catalytic dyad activity[71]. No such assays have been performed for other coronaviruses.

Antiviral agents with unspecified mode of action

Steroids

Proinflammatory cytokines released by stimulated macrophages in the alveoli play a prominent role in SARS pathogenesis, resulting in cytokine dysregulation[97,152]. During the SARS-CoV outbreak in 2003 several patients received anti-inflammatory corticosteroids that may reduce the damaging effect of the local inflammatory response[17]. Steroids inhibit cytokine, chemokine and adhesion molecule production and antagonize the action of proinflammatory cytokines by interfering with the Jak/STAT intracellular signalling pathways. In several studies early use of high-dose steroids (methylprednisolone) resulted in improvement of clinical symptoms, decreased incidence of acute respiratory distress syndrome and mortality[192,206,244]. However, other studies show lack of direct effect of steroid treatment in SARS patients[23,41,97]. It is also worth mentioning that immunosupression caused by steroid treatment may increase the danger of secondary infections, in fact occasionally increasing the mortality in SARS patients[226].

Interferons

Interferons (IFN) play a key role in the antiviral defense by activation of the innate immune system in response to the presence of dsRNA. There are several hundreds of genes transcriptionally regulated by IFNs in response to viral invasion. Additionally, type I IFNs (α and β) upregulate surface expression of MHC class I and II molecules, enhancing the presentation of viral antigens[58,164,165].

The employment of exogenous IFN as an antiviral agent has been described for animal coronaviruses[60,98,159,195] and the first study on human coronaviruses appeared already in 1983[79]. An antiviral effect of recombinant human leukocyte IFN-α was observed in healthy volunteers challenged with HCoV-229E. The percentage of individuals that developed respiratory illness was significantly lower for the group treated with IFN (5.7%) compared to the control group (37.0%). Another study presented the inhibitory effect of IFN-α delivered intranasally. The majority of the placebo recipients (73%) developed a cold, whereas only 41% of interferon recipients developed disease[219]. The same effect of type I IFNs has been observed for SARS-CoV both *in vitro* and *in vivo*[46,77,196,199,207], but type II IFN (IFN-γ) is a poor inhibitor of SARS-CoV replication[245]. Although IFN-γ by itself appeared to have little inhibitory effect, it acted synergistically in combination with IFN β[177,181]. A similar synergistic effect was observed during treatment with IFN-β and ribavirin[27,144].

Still, the *in vivo* data is limited. Prophylactic treatment of SARS-CoV infected macaques with pegylated IFN-α significantly reduced viral replication, excretion and pulmonary damage, but post-infection treatment yielded only intermediate protection. Moreover, treatment with IFN-α during the SARS-CoV outbreak showed no benefit[244].

Nitric oxide

Nitric oxide (NO) is an important cell-to-cell signalling molecule and is involved in a wide range of biological processes[92]. It also plays a key role in the host defence against bacteria, protozoa, and tumour cells. Antiviral activity of NO has been described for several viruses[119,168,173,213], but the antiviral mechanism is not known. Several NO donors (DETA NONOate, SNAP) can inhibit SARS-CoV, but not HCoV-NL63[42,107,170]. It has been suggested that IFN-γ activity against SARS-CoV is partially due to its stimulatory effects on inducible NO synthase (iNOS) expression[1]. Clinical trials in Beijing during the SARS-CoV epidemic suggested that inhalation of NO gas may improve the patient's outcome[31].

Calpain inhibitors

Calpains are mammalian intracellular calcium-dependent cystein proteinases[163]. Calpain plays a regulatory role in membrane and cytoskeletal remodeling, including mitosis and apoptosis regulation[150]. It was demonstrated that two

commercially available calpain inhibitors (calpain inhibitor III and VI) inhibit SARS-CoV replication in cell culture[14], but they failed to inhibit HCoV-NL63 replication[170].

Herbs

Several compounds of herbal origin have strong anti-coronaviral activity. Glycyrrhizin is a bioactive compound isolated from the liqorice root[9]. It exhibits anti-tumoural, anti-inflammatory and antiviral properties[44,118,132,167,178,186]. The mechanism of glycyrrhizin's activity against SARS-CoV[27,42] is unclear as the compound affects many cellular signalling pathways[35,72,123,153]. One possible mode of action includes stimulation of iNOS expression and subsequent increase of the NO concentration in treated cells[240]. The advantage of glycyrrhizin treatment is that it has been approved as an intravenous drug and it is commercially available as SNMC (Stronger Neo-Minophagen C)[143]. Glycyrrhizin is inactive against HCoV-NL63[170].

There are several other examples of plant-derived compounds that can inhibit coronavirus replication. Baicalin is a flavonoid compound derived from Scutellaria baicalensis that inhibits SARS-CoV *in vitro*[27]. Escin, active against SARS-CoV but not HCoV-NL63, is an approved drug derived from the horse chestnut tree[170,232]. Reserpine, a naturally occurring alkaloid produced by several members of the Rauwolfia genus, also inhibits SARS-CoV replication[232]. Several other plant compounds have been mentioned in other sections e.g. quercetine, isatin and mannose binding lectins, illustrating the potency of this natural reservoir.

Antibiotics

Glycopeptide antibiotics are commonly used for treatment of bacterial infections. They alter the cell wall characteristics and interfere with DNA and RNA synthesis. But these compounds can also inhibit several animal and human viruses by inhibiting virus replication or interfering with proper glycosylation of viral proteins, e.g. bleomycin for Rauscher murine leukemia virus[146], tunicamycin for herpex simplex virus[104] and teicoplanin, DA40 and DMDA40, vancomycin, eremomycin and their derivatives for HIV-1 and HIV-2[11,169]. Two compounds – eremomycin and vancomycin - also display anti SARS-CoV activity[10].

Another antibiotic, actinomycin D, the first antibiotic shown to have anti-cancer activity, can inhibit replication of HCoV-229[106]. However, the high cytotoxicity of the compound limits its usability as an anticoronaviral drug. Valinomycin, a cyclododecadepsipeptide antibiotic that is a natural product of Streptomyces[162], possesses antifungal, insecticidal-nematocidal, and antibacterial activities. It was recently demonstrated to exhibit *in vitro* anti SARS-CoV activity[34,232]. No inhibitory effect of actinomycin D or valinomycin was observed for HCoV-NL63[170].

Future directions

The outbreak of SARS-CoV in 2003 brought the coronaviruses back in the spotlight. The sudden appearance of SARS-CoV and the subsequent SARS epidemic met us unprepared. The current status of the anticoronaviral drugs has improved, but the majority of studies focus exclusively on compounds that target SARS-CoV. Realizing that many undiscovered coronaviruses may reside in animal reservoirs, this approach seems too restricted, leaving us unprepared for a future strike by another coronavirus species. Broadly active anticoronaviral compounds should be designed to quickly respond to new zoonotic epidemics of pathogenic coronaviruses. The antivirals should be potent, but some toxicity may be allowed.

Future studies on anticoronavirals should also focused on a preventive therapy for known coronaviral pathogens and quick-response drugs with specificity and broad activity. The major requirement for these drugs is lack of toxicity or side effects, considering the fact that these infections are relatively mild and very common. Of special interest are the natural compounds used for several years in folk medicine (e.g. leek, lucretia, garlic extracts, Chinese herbs). Unfortunately, there is no coherent study on activity of these compounds against different coronaviruses. Another option is the development of a broad siRNA cocktail against variety of respiratory viruses delivered by inhalation.

References

1. Akerstrom, S., M. Mousavi-Jazi, J. Klingstrom, M. Leijon, A. Lundkvist, and A. Mirazimi. 2005. Nitric oxide inhibits the replication cycle of severe acute respiratory syndrome coronavirus. J. Virol. 79:1966-1969.
2. Al Gharabli, S. I., S. T. Shah, S. Weik, M. F. Schmidt, J. R. Mesters, D. Kuhn, G. Klebe, R. Hilgenfeld, and J. Rademann. 2006. An efficient method for the synthesis of peptide aldehyde libraries employed in the discovery of reversible SARS coronavirus main protease (SARS-CoV M^{pro}) inhibitors. Chembiochem. 7:1048-1055.
3. Anand, K., J. Ziebuhr, P. Wadhwani, J. R. Mesters, and R. Hilgenfeld. 2003. Coronavirus main proteinase (3CLpro) structure: basis for design of anti-SARS drugs. Science 300:1763-1767.
4. Anderson, J. P., R. Daifuku, and L. A. Loeb. 2004. Viral error catastrophe by mutagenic nucleosides. Annu. Rev. Microbiol. 58:183-205.
5. Arden, K. E., M. D. Nissen, T. P. Sloots, and I. M. Mackay. 2005. New human coronavirus, HCoV-NL63, associated with severe lower respiratory tract disease in Australia. J. Med. Virol. 75:455-462.
6. Bacha, U., J. Barrila, A. Velazquez-Campoy, S. A. Leavitt, and E. Freire. 2004. Identification of novel inhibitors of the SARS coronavirus main protease 3CLpro. Biochemistry 43:4906-4912.
7. Baker, S. C. 2004. Coronaviruses: from common colds to severe acute respiratory syndrome. Pediatr. Infect. Dis. J. 23:1049-1050.
8. Baker, S. C., C. K. Shieh, L. H. Soe, M. F. Chang, D. M. Vannier, and M. M. Lai. 1989. Identification of a domain required for autoproteolytic cleavage of murine coronavirus gene A polyprotein. J. Virol. 63:3693-3699.
9. Baltina, L. A. 2003. Chemical modification of glycyrrhizic acid as a route to new bioactive compounds for medicine. Curr. Med. Chem. 10:155-171.
10. Balzarini, J., E. Keyaerts, L. Vijgen, H. Egberink, E. De Clercq, M. Van Ranst, S. S. Printsevskaya, E. N. Olsufyeva, S. E. Solovieva, and M. N. Preobrazhenskaya. 2006. Inhibition of feline (FIPV) and human (SARS) coronavirus by semisynthetic derivatives of glycopeptide antibiotics. Antiviral Res. 72:20-33.

11. Balzarini, J., C. Pannecouque, E. De Clercq, A. Y. Pavlov, S. S. Printsevskaya, O. V. Miroshnikova, M. I. Reznikova, and M. N. Preobrazhenskaya. 2003. Antiretroviral activity of semisynthetic derivatives of glycopeptide antibiotics. J. Med. Chem. 46:2755-2764.
12. Balzarini, J., D. Schols, J. Neyts, E. Van Damme, W. Peumans, and E. De Clercq. 1991. Alpha-(1-3)- and alpha-(1-6)-D-mannose-specific plant lectins are markedly inhibitory to human immunodeficiency virus and cytomegalovirus infections *in vitro*. Antimicrob. Agents Chemother. 35:410-416.
13. Balzarini, J., L. Vijgen, E. Keyaerts, E. Van Damme, W. Peumans, E. De Clercq, H. Egberink, and M. Van Ranst. 2004. Mannose-Specific Plant Lectins are Potent Inhibitors of Coronavirus Infection Including the Virus Causing SARS., p. A27-90. Abstracts of the 17th International Conference on Antiviral Research. Antiviral Research, Tucson, USA.
14. Barnard, D. L., V. D. Hubbard, J. Burton, D. F. Smee, J. D. Morrey, M. J. Otto, and R. W. Sidwell. 2004. Inhibition of severe acute respiratory syndrome-associated coronavirus (SARSCoV) by calpain inhibitors and beta-D-N4-hydroxycytidine. Antivir. Chem. Chemother. 15:15-22.
15. Barreiro, P., T. Garcia-Benayas, A. Rendon, S. Rodriguez-Novoa, and V. Soriano. 2004. Combinations of nucleoside/nucleotide analogues for HIV therapy. AIDS Rev. 6:234-243.
16. Bastien, N., J. L. Robinson, A. Tse, B. E. Lee, L. Hart, and Y. Li. 2005. Human coronavirus NL-63 infections in children: a 1-year study. J. Clin. Microbiol. 43:4567-4573.
17. Bianchi, M., C. Meng, and L. B. Ivashkiv. 2000. Inhibition of IL-2-induced Jak-STAT signaling by glucocorticoids. Proc. Natl. Acad. Sci. U. S. A 97:9573-9578.
18. Blanchard, J. E., N. H. Elowe, C. Huitema, P. D. Fortin, J. D. Cechetto, L. D. Eltis, and E. D. Brown. 2004. High-throughput screening identifies inhibitors of the SARS coronavirus main proteinase. Chem. Biol. 11:1445-1453.
19. Blau, D. M. and K. V. Holmes. 2001. Human coronavirus HCoV-229E enters susceptible cells via the endocytic pathway. Adv. Exp. Med. Biol. 494:193-198.
20. Boehm, M. and E. G. Nabel. 2002. Angiotensin-converting enzyme 2--a new cardiac regulator. N. Engl. J. Med. 347:1795-1797.
21. Bonavia, A., B. D. Zelus, D. E. Wentworth, P. J. Talbot, and K. V. Holmes. 2003. Identification of a receptor-binding domain of the spike glycoprotein of human coronavirus HCoV-229E. J. Virol. 77:2530-2538.
22. Bonilla, P. J., S. A. Hughes, and S. R. Weiss. 1997. Characterization of a second cleavage site and demonstration of activity in trans by the papain-like proteinase of the murine coronavirus mouse hepatitis virus strain A59. J. Virol. 71:900-909.
23. Booth, C. M., L. M. Matukas, G. A. Tomlinson, A. R. Rachlis, D. B. Rose, H. A. Dwosh, S. L. Walmsley, T. Mazzulli, M. Avendano, P. Derkach, I. E. Ephtimios, I. Kitai, B. D. Mederski, S. B. Shadowitz, W. L. Gold, L. A. Hawryluck, E. Rea, J. S. Chenkin, D. W. Cescon, S. M. Poutanen, and A. S. Detsky. 2003. Clinical features and short-term outcomes of 144 patients with SARS in the greater Toronto area. JAMA 289:2801-2809.
24. Bosch, B. J., B. E. Martina, R. Van Der Zee, J. Lepault, B. J. Haijema, C. Versluis, A. J. Heck, R. De Groot, A. D. Osterhaus, and P. J. Rottier. 2004. Severe acute respiratory syndrome coronavirus (SARS-CoV) infection inhibition using spike protein heptad repeat-derived peptides. Proc. Natl. Acad. Sci. U. S. A 101:8455-8460.
25. Bosch, B. J., R. Van Der Zee, C. A. de Haan, and P. J. Rottier. 2003. The coronavirus spike protein is a class I virus fusion protein: structural and functional characterization of the fusion core complex. J. Virol. 77:8801-8811.
26. Brockway, S. M., C. T. Clay, X. T. Lu, and M. R. Denison. 2003. Characterization of the expression, intracellular localization, and replication complex association of the putative mouse hepatitis virus RNA-dependent RNA polymerase. J. Virol. 77:10515-10527.
27. Chen, F., K. H. Chan, Y. Jiang, R. Y. Kao, H. T. Lu, K. W. Fan, V. C. Cheng, W. H. Tsui, I. F. Hung, T. S. Lee, Y. Guan, J. S. Peiris, and K. Y. Yuen. 2004. *In vitro* susceptibility of 10 clinical isolates of SARS coronavirus to selected antiviral compounds. J. Clin. Virol. 31:69-75.
28. Chen, L., S. Chen, C. Gui, J. Shen, X. Shen, and H. Jiang. 2006. Discovering Severe Acute Respiratory Syndrome Coronavirus 3CL Protease Inhibitors: Virtual Screening, Surface Plasmon Resonance, and Fluorescence Resonance Energy Transfer Assays. J Biomol. Screen.

29. Chen, L., C. Gui, X. Luo, Q. Yang, S. Gunther, E. Scandella, C. Drosten, D. Bai, X. He, B. Ludewig, J. Chen, H. Luo, Y. Yang, Y. Yang, J. Zou, V. Thiel, K. Chen, J. Shen, X. Shen, and H. Jiang. 2005. Cinanserin is an inhibitor of the 3C-like proteinase of severe acute respiratory syndrome coronavirus and strongly reduces virus replication *in vitro*. J. Virol. 79:7095-7103.
30. Chen, L., J. Li, C. Luo, H. Liu, W. Xu, G. Chen, O. W. Liew, W. Zhu, C. M. Puah, X. Shen, and H. Jiang. 2006. Binding interaction of quercetin-3-beta-galactoside and its synthetic derivatives with SARS-CoV 3CL(pro): Structure-activity relationship studies reveal salient pharmacophore features. Bioorg. Med. Chem.
31. Chen, L., P. Liu, H. Gao, B. Sun, D. Chao, F. Wang, Y. Zhu, G. Hedenstierna, and C. G. Wang. 2004. Inhalation of nitric oxide in the treatment of severe acute respiratory syndrome: a rescue trial in Beijing. Clin. Infect. Dis. 39:1531-1535.
32. Chen, L. R., Y. C. Wang, Y. W. Lin, S. Y. Chou, S. F. Chen, L. T. Liu, Y. T. Wu, C. J. Kuo, T. S. Chen, and S. H. Juang. 2005. Synthesis and evaluation of isatin derivatives as effective SARS coronavirus 3CL protease inhibitors. Bioorg. Med. Chem. Lett. 15:3058-3062.
33. Cheng, A., W. Zhang, Y. Xie, W. Jiang, E. Arnold, S. G. Sarafianos, and J. Ding. 2005. Expression, purification, and characterization of SARS coronavirus RNA polymerase. Virology 335:165-176.
34. Cheng, Y. Q. 2006. Deciphering the biosynthetic codes for the potent anti-SARS-CoV cyclodepsipeptide valinomycin in Streptomyces tsusimaensis ATCC 15141. Chembiochem. 7:471-477.
35. Cherng, J. M., H. J. Lin, Y. H. Hsu, M. S. Hung, and J. C. Lin. 2004. A quantitative bioassay for HIV-1 gene expression based on UV activation: effect of glycyrrhizic acid. Antiviral Res. 62:27-36.
36. Chiou, H. E., C. L. Liu, M. J. Buttrey, H. P. Kuo, H. W. Liu, H. T. Kuo, and Y. T. Lu. 2005. Adverse effects of ribavirin and outcome in severe acute respiratory syndrome: experience in two medical centers. Chest 128:263-272.
37. Chiu, S. S., K. H. Chan, K. W. Chu, S. W. Kwan, Y. Guan, L. L. Poon, and J. S. Peiris. 2005. Human coronavirus NL63 infection and other coronavirus infections in children hospitalized with acute respiratory disease in Hong Kong, China. Clin. Infect. Dis. 40:1721-1729.
38. Choi, E. H., H. J. Lee, S. J. Kim, B. W. Eun, N. H. Kim, J. A. Lee, J. H. Lee, E. K. Song, S. H. Kim, J. Y. Park, and J. Y. Sung. 2006. The association of newly identified respiratory viruses with lower respiratory tract infections in Korean children, 2000-2005. Clin. Infect. Dis. 43:585-592.
39. Chou, T. H., S. Wang, P. V. Sakhatskyy, I. Mboudjeka, J. M. Lawrence, S. Huang, S. Coley, B. Yang, J. Li, Q. Zhu, and S. Lu. 2005. Epitope mapping and biological function analysis of antibodies produced by immunization of mice with an inactivated Chinese isolate of severe acute respiratory syndrome-associated coronavirus (SARS-CoV). Virology 334:134-143.
40. Cihak, A. and B. Rada. 1976. Uridine kinase: properties, biological significance and chemotherapeutic aspects (a review). Neoplasma 23:233-257.
41. Cinatl, J., Jr., M. Michaelis, B. Morgenstern, and H. W. Doerr. 2005. High-dose hydrocortisone reduces expression of the pro-inflammatory chemokines CXCL8 and CXCL10 in SARS coronavirus-infected intestinal cells. Int. J. Mol. Med. 15:323-327.
42. Cinatl, J., B. Morgenstern, G. Bauer, P. Chandra, H. Rabenau, and H. W. Doerr. 2003. Glycyrrhizin, an active component of liquorice roots, and replication of SARS-associated coronavirus. Lancet 361:2045-2046.
43. Crackower, M. A., R. Sarao, G. Y. Oudit, C. Yagil, I. Kozieradzki, S. E. Scanga, A. J. Oliveira-dos-Santos, J. da Costa, L. Zhang, Y. Pei, J. Scholey, C. M. Ferrario, A. S. Manoukian, M. C. Chappell, P. H. Backx, Y. Yagil, and J. M. Penninger. 2002. Angiotensin-converting enzyme 2 is an essential regulator of heart function. Nature 417:822-828.
44. Crance, J. M., N. Scaramozzino, A. Jouan, and D. Garin. 2003. Interferon, ribavirin, 6-azauridine and glycyrrhizin: antiviral compounds active against pathogenic flaviviruses. Antiviral Res. 58:73-79.
45. Crotty, S., C. E. Cameron, and R. Andino. 2001. RNA virus error catastrophe: direct molecular test by using ribavirin. Proc. Natl. Acad. Sci. U. S. A 98:6895-6900.
46. Dahl, H., A. Linde, and O. Strannegard. 2004. *In vitro* inhibition of SARS virus replication by human interferons. Scand. J. Infect. Dis. 36:829-831.
47. de Haan, C. A., K. Stadler, G. J. Godeke, B. J. Bosch, and P. J. Rottier. 2004. Cleavage inhibition of the murine coronavirus spike protein by a furin-like enzyme affects cell-cell but not virus-cell fusion. J. Virol. 78:6048-6054.

48. de Haan, C. A., L. van Genne, J. N. Stoop, H. Volders, and P. J. Rottier. 2003. Coronaviruses as vectors: position dependence of foreign gene expression. J. Virol. 77:11312-11323.
49. de Lang, A., A. D. Osterhaus, and B. L. Haagmans. 2006. Interferon-gamma and interleukin-4 downregulate expression of the SARS coronavirus receptor ACE2 in Vero E6 cells. Virology.
50. De, I., S. G. Sawicki, and D. L. Sawicki. 1996. Sindbis virus RNA-negative mutants that fail to convert from minus-strand to plus-strand synthesis: role of the nsP2 protein. J. Virol. 70:2706-2719.
51. Delmas, B., J. Gelfi, R. L'Haridon, L. K. Vogel, H. Sjostrom, O. Noren, and H. Laude. 1992. Aminopeptidase N is a major receptor for the entero-pathogenic coronavirus TGEV. Nature 357:417-420.
52. Dooley, A. J., N. Shindo, B. Taggart, J. G. Park, and Y. P. Pang. 2006. From genome to drug lead: identification of a small-molecule inhibitor of the SARS virus. Bioorg. Med. Chem. Lett. 16:830-833.
53. Drosten, C., S. Gunther, W. Preiser, S. van der Werf, H. R. Brodt, S. Becker, H. Rabenau, M. Panning, L. Kolesnikova, R. A. Fouchier, A. Berger, A. M. Burguiere, J. Cinatl, M. Eickmann, N. Escriou, K. Grywna, S. Kramme, J. C. Manuguerra, S. Muller, V. Rickerts, M. Sturmer, S. Vieth, H. D. Klenk, A. D. Osterhaus, H. Schmitz, and H. W. Doerr. 2003. Identification of a novel coronavirus in patients with severe acute respiratory syndrome. N. Engl. J. Med. 348:1967-1976.
54. Du, Q., S. Wang, D. Wei, S. Sirois, and K. C. Chou. 2005. Molecular modeling and chemical modification for finding peptide inhibitor against severe acute respiratory syndrome coronavirus main proteinase. Anal. Biochem. 337:262-270.
55. Du, Q. S., S. Q. Wang, Y. Zhu, D. Q. Wei, H. Guo, S. Sirois, and K. C. Chou. 2004. Polyprotein cleavage mechanism of SARS CoV M^{pro} and chemical modification of the octapeptide. Peptides 25:1857-1864.
56. Duan, J., X. Ji, J. Feng, W. Han, P. Zhang, W. Cao, X. Guo, C. Qi, D. Yang, G. Jin, G. Gao, and X. Yan. 2006. A human neutralizing antibody against a conformational epitope shared by oligomeric SARS S1 protein. Antivir. Ther. 11:117-123.
57. Ebihara, T., R. Endo, X. Ma, N. Ishiguro, and H. Kikuta. 2005. Detection of human coronavirus NL63 in young children with bronchiolitis. J. Med. Virol. 75:463-465.
58. Faltynek, C. R. and H. F. Kung. 1988. The biochemical mechanisms of action of the interferons. Biofactors 1:227-235.
59. Forster, J., G. Ihorst, C. H. Rieger, V. Stephan, H. D. Frank, H. Gurth, R. Berner, A. Rohwedder, H. Werchau, M. Schumacher, T. Tsai, and G. Petersen. 2004. Prospective population-based study of viral lower respiratory tract infections in children under 3 years of age (the PRI.DE study). Eur. J. Pediatr. 163:709-716.
60. Fuchizaki, U., S. Kaneko, Y. Nakamoto, Y. Sugiyama, K. Imagawa, M. Kikuchi, and K. Kobayashi. 2003. Synergistic antiviral effect of a combination of mouse interferon-alpha and interferon-gamma on mouse hepatitis virus. J. Med. Virol. 69:188-194.
61. Gan, Y. R., H. Huang, Y. D. Huang, C. M. Rao, Y. Zhao, J. S. Liu, L. Wu, and D. Q. Wei. 2006. Synthesis and activity of an octapeptide inhibitor designed for SARS coronavirus main proteinase. Peptides 27:622-625.
62. Gao, F., H. Y. Ou, L. L. Chen, W. X. Zheng, and C. T. Zhang. 2003. Prediction of proteinase cleavage sites in polyproteins of coronaviruses and its applications in analyzing SARS-CoV genomes. FEBS Lett. 553:451-456.
63. Garbino, J., S. Crespo, J. D. Aubert, T. Rochat, B. Ninet, C. Deffernez, W. Wunderli, J. C. Pache, P. M. Soccal, and L. Kaiser. 2006. A prospective hospital-based study of the clinical impact of non-severe acute respiratory syndrome (Non-SARS)-related human coronavirus infection. Clin. Infect. Dis. 43:1009-1015.
64. Gonzalez, J. M., P. Gomez-Puertas, D. Cavanagh, A. E. Gorbalenya, and L. Enjuanes. 2003. A comparative sequence analysis to revise the current taxonomy of the family *Coronaviridae*. Arch. Virol. 148:2207-2235.
65. Gorbalenya, A. E., E. V. Koonin, A. P. Donchenko, and V. M. Blinov. 1988. A novel superfamily of nucleoside triphosphate-binding motif containing proteins which are probably involved in duplex unwinding in DNA and RNA replication and recombination. FEBS Lett. 235:16-24.
66. Gorbalenya, A. E., E. V. Koonin, A. P. Donchenko, and V. M. Blinov. 1989. Coronavirus genome: prediction of putative functional domains in the non-structural polyprotein by comparative amino acid sequence analysis. Nucleic Acids Res. 17:4847-4861.

67. Gorbalenya, A. E., E. V. Koonin, and M. M. Lai. 1991. Putative papain-related thiol proteases of positive-strand RNA viruses. Identification of rubi- and aphthovirus proteases and delineation of a novel conserved domain associated with proteases of rubi-, alpha- and coronaviruses. FEBS Lett. 288:201-205.
68. Gosert, R., A. Kanjanahaluethai, D. Egger, K. Bienz, and S. C. Baker. 2002. RNA replication of mouse hepatitis virus takes place at double-membrane vesicles. J. Virol. 76:3697-3708.
69. Greenough, T. C., G. J. Babcock, A. Roberts, H. J. Hernandez, W. D. Thomas, Jr., J. A. Coccia, R. F. Graziano, M. Srinivasan, I. Lowy, R. W. Finberg, K. Subbarao, L. Vogel, M. Somasundaran, K. Luzuriaga, J. L. Sullivan, and D. M. Ambrosino. 2005. Development and characterization of a severe acute respiratory syndrome-associated coronavirus-neutralizing human monoclonal antibody that provides effective immunoprophylaxis in mice. J. Infect. Dis. 191:507-514.
70. Hamaguchi, M., Y. Kawahito, Y. Tsubouchi, M. Kohno, A. Yamamoto, H. Ishino, M. Wada, and T. Yoshikawa. 2006. Combination therapy of prednisolone and mizoribine improves cryoglobulinemic vasculitis with purpura and skin ulcers. Clin. Rheumatol.
71. Han, Y. S., G. G. Chang, C. G. Juo, H. J. Lee, S. H. Yeh, J. T. Hsu, and X. Chen. 2005. Papain-like protease 2 (PLP2) from severe acute respiratory syndrome coronavirus (SARS-CoV): expression, purification, characterization, and inhibition. Biochemistry 44:10349-10359.
72. Harada, S., A. Karino, Y. Shimoyama, F. Shamsa, and K. Ohtsuki. 1996. Identification of glycyrrhizin-binding protein kinase as casein kinase II and characterization of its associated phosphate acceptors in mouse liver. Biochem. Biophys. Res. Commun. 227:102-109.
73. He, M. L., B. J. Zheng, Y. Chen, K. L. Wong, J. D. Huang, M. C. Lin, Y. Peng, K. Y. Yuen, J. J. Sung, and H. F. Kung. 2006. Kinetics and synergistic effects of siRNAs targeting structural and replicase genes of SARS-associated coronavirus. FEBS Lett. 580:2414-2420.
74. He, R., A. Adonov, M. Traykova-Adonova, J. Cao, T. Cutts, E. Grudesky, Y. Deschambaul, J. Berry, M. Drebot, and X. Li. 2004. Potent and selective inhibition of SARS coronavirus replication by aurintricarboxylic acid. Biochem. Biophys. Res. Commun. 320:1199-1203.
75. He, Y., H. Lu, P. Siddiqui, Y. Zhou, and S. Jiang. 2005. Receptor-binding domain of severe acute respiratory syndrome coronavirus spike protein contains multiple conformation-dependent epitopes that induce highly potent neutralizing antibodies. J. Immunol. 174:4908-4915.
76. He, Y., Y. Zhou, S. Liu, Z. Kou, W. Li, M. Farzan, and S. Jiang. 2004. Receptor-binding domain of SARS-CoV spike protein induces highly potent neutralizing antibodies: implication for developing subunit vaccine. Biochem. Biophys. Res. Commun. 324:773-781.
77. Hensley, L. E., L. E. Fritz, P. B. Jahrling, C. L. Karp, J. W. Huggins, and T. W. Geisbert. 2004. Interferon-beta 1a and SARS coronavirus replication. Emerg. Infect. Dis. 10:317-319.
78. Herold, J., A. E. Gorbalenya, V. Thiel, B. Schelle, and S. G. Siddell. 1998. Proteolytic processing at the amino terminus of human coronavirus 229E gene 1-encoded polyproteins: identification of a papain-like proteinase and its substrate. J. Virol. 72:910-918.
79. Higgins, P. G., R. J. Phillpotts, G. M. Scott, J. Wallace, L. L. Bernhardt, and D. A. Tyrrell. 1983. Intranasal interferon as protection against experimental respiratory coronavirus infection in volunteers. Antimicrob. Agents Chemother. 24:713-715.
80. Hofmann, H., K. Pyrc, L. van der Hoek, M. Geier, B. Berkhout, and S. Pohlmann. 2005. Human coronavirus NL63 employs the severe acute respiratory syndrome coronavirus receptor for cellular entry. Proc. Natl. Acad. Sci. U. S. A 102:7988-7993.
81. Hofmann, H., G. Simmons, A. J. Rennekamp, C. Chaipan, T. Gramberg, E. Heck, M. Geier, A. Wegele, A. Marzi, P. Bates, and S. Pohlmann. 2006. Highly conserved regions within the spike proteins of human coronaviruses 229E and NL63 determine recognition of their respective cellular receptors. J. Virol. 80:8639-8652.
82. Hofmann, M. A., R. Y. Chang, S. Ku, and D. A. Brian. 1993. Leader-mRNA junction sequences are unique for each subgenomic mRNA species in the bovine coronavirus and remain so throughout persistent infection. Virology 196:163-171.
83. Hollecker, L., H. Choo, Y. Chong, C. K. Chu, S. Lostia, T. R. McBrayer, L. J. Stuyver, J. C. Mason, J. Du, S. Rachakonda, J. Shi, R. F. Schinazi, and K. A. Watanabe. 2004. Synthesis of beta-enantiomers of N4-hydroxy-3'-deoxypyrimidine nucleosides and their evaluation against bovine viral diarrhoea virus and hepatitis C virus in cell culture. Antivir. Chem. Chemother. 15:43-55.

84. Holmes, K. V. and M. M. C. Lai. 1996. *Coronaviridae*: The viruses and their replication, p. 1075-1093. In B. N. Fields, D. M. Knipe, P. M. Howley, and *et al* (eds.), Fields Virology. Lippincott-Raven Publishers, Philadelphia.
85. Hosoya, M., S. Shigeta, T. Ishii, H. Suzuki, and E. De Clercq. 1993. Comparative inhibitory effects of various nucleoside and nonnucleoside analogues on replication of influenza virus types A and B *in vitro* and in ovo. J. Infect. Dis. 168:641-646.
86. Hsu, J. T., C. J. Kuo, H. P. Hsieh, Y. C. Wang, K. K. Huang, C. P. Lin, P. F. Huang, X. Chen, and P. H. Liang. 2004. Evaluation of metal-conjugated compounds as inhibitors of 3CL protease of SARS-CoV. FEBS Lett. 574:116-120.
87. Huang, C., N. Ito, C. T. Tseng, and S. Makino. 2006. Severe acute respiratory syndrome coronavirus 7a accessory protein is a viral structural protein. J. Virol. 80:7287-7294.
88. Huang, C., K. Narayanan, N. Ito, C. J. Peters, and S. Makino. 2006. Severe acute respiratory syndrome coronavirus 3a protein is released in membranous structures from 3a protein-expressing cells and infected cells. J. Virol. 80:210-217.
89. Huang, I. C., B. J. Bosch, F. Li, W. Li, K. H. Lee, S. Ghiran, N. Vasilieva, T. S. Dermody, S. C. Harrison, P. R. Dormitzer, M. Farzan, P. J. Rottier, and H. Choe. 2006. SARS coronavirus, but not human coronavirus NL63, utilizes cathepsin L to infect ACE2-expressing cells. J. Biol. Chem. 281:3198-3203.
90. Hwang, W. C., Y. Lin, E. Santelli, J. Sui, L. Jaroszewski, B. Stec, M. Farzan, W. A. Marasco, and R. C. Liddington. 2006. Structural Basis of Neutralization by a Human Anti-severe Acute Respiratory Syndrome Spike Protein Antibody, 80R. J. Biol. Chem. 281:34610-34616.
91. Ichikawa, Y., M. Kyo, T. Hanafusa, T. Kohro, H. Kishikawa, T. Fukunishi, S. Nagano, and Y. Shinji. 1998. A 20-year case study of a kidney transplant recipient with chronic active hepatitis C: clinical course and successful treatment for late acute rejection induced by interferon therapy. Transplantation 65:134-138.
92. Ignarro, L. J. 1999. Nitric oxide: a unique endogenous signaling molecule in vascular biology. Biosci. Rep. 19:51-71.
93. Imai, Y., K. Kuba, S. Rao, Y. Huan, F. Guo, B. Guan, P. Yang, R. Sarao, T. Wada, H. Leong-Poi, M. A. Crackower, A. Fukamizu, C. C. Hui, L. Hein, S. Uhlig, A. S. Slutsky, C. Jiang, and J. M. Penninger. 2005. Angiotensin-converting enzyme 2 protects from severe acute lung failure. Nature 436:112-116.
94. Ivanov, K. A., V. Thiel, J. C. Dobbe, Y. van der Meer, E. J. Snijder, and J. Ziebuhr. 2004. Multiple enzymatic activities associated with severe acute respiratory syndrome coronavirus helicase. J. Virol. 78:5619-5632.
95. Janda, M. and P. Ahlquist. 1998. Brome mosaic virus RNA replication protein 1a dramatically increases *in vivo* stability but not translation of viral genomic RNA3. Proc. Natl. Acad. Sci. U. S. A 95:2227-2232.
96. Jia, F., Y. Z. Zhang, and C. M. Liu. 2006. Stable inhibition of hepatitis B virus expression and replication in HepG2.2.15 cells by RNA interference based on retrovirus delivery. J. Biotechnol.
97. Jones, B. M., E. S. Ma, J. S. Peiris, P. C. Wong, J. C. Ho, B. Lam, K. N. Lai, and K. W. Tsang. 2004. Prolonged disturbances of *in vitro* cytokine production in patients with severe acute respiratory syndrome (SARS) treated with ribavirin and steroids. Clin. Exp. Immunol. 135:467-473.
98. Jordan, L. T. and J. B. Derbyshire. 1995. Antiviral action of interferon-alpha against porcine transmissible gastroenteritis virus. Vet. Microbiol. 45:59-70.
99. Kaeppler, U., N. Stiefl, M. Schiller, R. Vicik, A. Breuning, W. Schmitz, D. Rupprecht, C. Schmuck, K. Baumann, J. Ziebuhr, and T. Schirmeister. 2005. A new lead for nonpeptidic active-site-directed inhibitors of the severe acute respiratory syndrome coronavirus main protease discovered by a combination of screening and docking methods. J. Med. Chem. 48:6832-6842.
100. Kaiser, L., N. Regamey, H. Roiha, C. Deffernez, and U. Frey. 2005. Human coronavirus NL63 associated with lower respiratory tract symptoms in early life. Pediatr. Infect. Dis. J. 24:1015-1017.
101. Kanjanahaluethai, A. and S. C. Baker. 2000. Identification of mouse hepatitis virus papain-like proteinase 2 activity. J. Virol. 74:7911-7921.
102. Kao, R. Y., A. P. To, L. W. Ng, W. H. Tsui, T. S. Lee, H. W. Tsoi, and K. Y. Yuen. 2004. Characterization of SARS-CoV main protease and identification of biologically active small molecule inhibitors using a continuous fluorescence-based assay. FEBS Lett. 576:325-330.

103. Kao, R. Y., W. H. Tsui, T. S. Lee, J. A. Tanner, R. M. Watt, J. D. Huang, L. Hu, G. Chen, Z. Chen, L. Zhang, T. He, K. H. Chan, H. Tse, A. P. To, L. W. Ng, B. C. Wong, H. W. Tsoi, D. Yang, D. D. Ho, and K. Y. Yuen. 2004. Identification of novel small-molecule inhibitors of severe acute respiratory syndrome-associated coronavirus by chemical genetics. Chem. Biol. 11:1293-1299.
104. Katz, E., E. Margalith, and D. Duksin. 1980. Antiviral activity of tunicamycin on herpes simplex virus. Antimicrob. Agents Chemother. 17:1014-1022.
105. Keng, C. T., A. Zhang, S. Shen, K. M. Lip, B. C. Fielding, T. H. Tan, C. F. Chou, C. B. Loh, S. Wang, J. Fu, X. Yang, S. G. Lim, W. Hong, and Y. J. Tan. 2005. Amino acids 1055 to 1192 in the S2 region of severe acute respiratory syndrome coronavirus S protein induce neutralizing antibodies: implications for the development of vaccines and antiviral agents. J. Virol. 79:3289-3296.
106. Kennedy, D. A. and C. M. Johnson-Lussenburg. 1979. Inhibition of coronavirus 229E replication by actinomycin D. J. Virol. 29:401-404.
107. Keyaerts, E., L. Vijgen, L. Chen, P. Maes, G. Hedenstierna, and M. Van Ranst. 2004. Inhibition of SARS-coronavirus infection *in vitro* by S-nitroso-N-acetylpenicillamine, a nitric oxide donor compound. Int. J. Infect. Dis. 8:223-226.
108. Konig, B., W. Konig, R. Arnold, H. Werchau, G. Ihorst, and J. Forster. 2004. Prospective study of human metapneumovirus infection in children less than 3 years of age. J. Clin. Microbiol. 42:4632-4635.
109. Konings, D. A., P. J. Bredenbeek, J. F. Noten, P. Hogeweg, and W. J. Spaan. 1988. Differential premature termination of transcription as a proposed mechanism for the regulation of coronavirus gene expression. Nucleic Acids Res. 16:10849-10860.
110. Konstantinova, P., W. de Vries, J. Haasnoot, O. Ter Brake, P. de Haan, and B. Berkhout. 2006. Inhibition of human immunodeficiency virus type 1 by RNA interference using long-hairpin RNA. Gene Ther. 13:1403-1413.
111. Kooi, C., M. Cervin, and R. Anderson. 1991. Differentiation of acid-pH-dependent and -nondependent entry pathways for mouse hepatitis virus. Virology 180:108-119.
112. Ksiazek, T. G., D. Erdman, C. S. Goldsmith, S. R. Zaki, T. Peret, S. Emery, S. Tong, C. Urbani, J. A. Comer, W. Lim, P. E. Rollin, S. F. Dowell, A. E. Ling, C. D. Humphrey, W. J. Shieh, J. Guarner, C. D. Paddock, P. Rota, B. Fields, J. DeRisi, J. Y. Yang, N. Cox, J. M. Hughes, J. W. LeDuc, W. J. Bellini, and L. J. Anderson. 2003. A novel coronavirus associated with severe acute respiratory syndrome. N. Engl. J. Med. 348:1953-1966.
113. Kuba, K., Y. Imai, S. Rao, H. Gao, F. Guo, B. Guan, Y. Huan, P. Yang, Y. Zhang, W. Deng, L. Bao, B. Zhang, G. Liu, Z. Wang, M. Chappell, Y. Liu, D. Zheng, A. Leibbrandt, T. Wada, A. S. Slutsky, D. Liu, C. Qin, C. Jiang, and J. M. Penninger. 2005. A crucial role of angiotensin converting enzyme 2 (ACE2) in SARS coronavirus-induced lung injury. Nat. Med. 11:875-879.
114. Lai, C. L. and M. F. Yuen. 2000. Profound suppression of hepatitis B virus replication with lamivudine. J. Med. Virol. 61:367-373.
115. Lai, M. M. and D. Cavanagh. 1997. The molecular biology of coronaviruses. Adv. Virus Res. 48:1-100.
116. Lai, S. C., P. C. Chong, C. T. Yeh, L. S. Liu, J. T. Jan, H. Y. Chi, H. W. Liu, A. Chen, and Y. C. Wang. 2005. Characterization of neutralizing monoclonal antibodies recognizing a 15-residues epitope on the spike protein HR2 region of severe acute respiratory syndrome coronavirus (SARS-CoV). J. Biomed. Sci. 12:711-727.
117. Lambert, D. M., S. Barney, A. L. Lambert, K. Guthrie, R. Medinas, D. E. Davis, T. Bucy, J. Erickson, G. Merutka, and S. R. Petteway, Jr. 1996. Peptides from conserved regions of paramyxovirus fusion (F) proteins are potent inhibitors of viral fusion. Proc. Natl. Acad. Sci. U. S. A 93:2186-2191.
118. Lampi, G., D. Deidda, M. Pinza, and R. Pompei. 2001. Enhancement of anti-herpetic activity of glycyrrhizic acid by physiological proteins. Antivir. Chem. Chemother. 12:125-131.
119. Lane, T. E., A. D. Paoletti, and M. J. Buchmeier. 1997. Disassociation between the *in vitro* and *in vivo* effects of nitric oxide on a neurotropic murine coronavirus. J. Virol. 71:2202-2210.
120. Lau, S. K., P. C. Woo, K. S. Li, Y. Huang, H. W. Tsoi, B. H. Wong, S. S. Wong, S. Y. Leung, K. H. Chan, and K. Y. Yuen. 2005. Severe acute respiratory syndrome coronavirus-like virus in Chinese horseshoe bats. Proc. Natl. Acad. Sci. U. S. A 102:14040-14045.

121. Lau, S. K., P. C. Woo, C. C. Yip, H. Tse, H. W. Tsoi, V. C. Cheng, P. Lee, B. S. Tang, C. H. Cheung, R. A. Lee, L. Y. So, Y. L. Lau, K. H. Chan, and K. Y. Yuen. 2006. Coronavirus HKU1 and other coronavirus infections in Hong Kong. J. Clin. Microbiol. 44:2063-2071.
122. Lee, H. J., C. K. Shieh, A. E. Gorbalenya, E. V. Koonin, N. La Monica, J. Tuler, A. Bagdzhadzhyan, and M. M. Lai. 1991. The complete sequence (22 kilobases) of murine coronavirus gene 1 encoding the putative proteases and RNA polymerase. Virology 180:567-582.
123. Lee, J., E. Jung, J. Park, K. Jung, E. Park, J. Kim, S. Hong, J. Park, S. Park, S. Lee, and D. Park. 2005. Glycyrrhizin induces melanogenesis by elevating a cAMP level in b16 melanoma cells. J. Invest Dermatol. 124:405-411.
124. Lee, T. W., M. M. Cherney, C. Huitema, J. Liu, K. E. James, J. C. Powers, L. D. Eltis, and M. N. James. 2005. Crystal structures of the main peptidase from the SARS coronavirus inhibited by a substrate-like aza-peptide epoxide. J. Mol. Biol. 353:1137-1151.
125. Li, B. J., Q. Tang, D. Cheng, C. Qin, F. Y. Xie, Q. Wei, J. Xu, Y. Liu, B. J. Zheng, M. C. Woodle, N. Zhong, and P. Y. Lu. 2005. Using siRNA in prophylactic and therapeutic regimens against SARS coronavirus in Rhesus macaque. Nat. Med. 11:944-951.
126. Li, T., Y. Zhang, L. Fu, C. Yu, X. Li, Y. Li, X. Zhang, Z. Rong, Y. Wang, H. Ning, R. Liang, W. Chen, L. A. Babiuk, and Z. Chang. 2005. siRNA targeting the leader sequence of SARS-CoV inhibits virus replication. Gene Ther. 12:751-761.
127. Li, W., M. J. Moore, N. Vasilieva, J. Sui, S. K. Wong, M. A. Berne, M. Somasundaran, J. L. Sullivan, K. Luzuriaga, T. C. Greenough, H. Choe, and M. Farzan. 2003. Angiotensin-converting enzyme 2 is a functional receptor for the SARS coronavirus. Nature 426:450-454.
128. Liang, M. F., R. L. Du, J. Z. Liu, C. Li, Q. F. Zhang, L. L. Han, J. S. Yu, S. M. Duan, X. F. Wang, K. X. Wu, Z. H. Xiong, Q. Jin, and D. X. Li. 2005. SARS patients-derived human recombinant antibodies to S and M proteins efficiently neutralize SARS-coronavirus infectivity. Biomed. Environ. Sci. 18:363-374.
129. Lim, K. P. and D. X. Liu. 1998. Characterization of the two overlapping papain-like proteinase domains encoded in gene 1 of the coronavirus infectious bronchitis virus and determination of the C-terminal cleavage site of an 87-kDa protein. Virology 245:303-312.
130. Lim, K. P., L. F. Ng, and D. X. Liu. 2000. Identification of a novel cleavage activity of the first papain-like proteinase domain encoded by open reading frame 1a of the coronavirus Avian infectious bronchitis virus and characterization of the cleavage products. J. Virol. 74:1674-1685.
131. Lin, C. W., F. J. Tsai, C. H. Tsai, C. C. Lai, L. Wan, T. Y. Ho, C. C. Hsieh, and P. D. Chao. 2005. Anti-SARS coronavirus 3C-like protease effects of Isatis indigotica root and plant-derived phenolic compounds. Antiviral Res. 68:36-42.
132. Lin, J. C. 2003. Mechanism of action of glycyrrhizic acid in inhibition of Epstein-Barr virus replication *in vitro*. Antiviral Res. 59:41-47.
133. Lip, K. M., S. Shen, X. Yang, C. T. Keng, A. Zhang, H. L. Oh, Z. H. Li, L. A. Hwang, C. F. Chou, B. C. Fielding, T. H. Tan, J. Mayrhofer, F. G. Falkner, J. Fu, S. G. Lim, W. Hong, and Y. J. Tan. 2006. Monoclonal antibodies targeting the HR2 domain and the region immediately upstream of the HR2 of the S protein neutralize *in vitro* infection of severe acute respiratory syndrome coronavirus. J. Virol. 80:941-950.
134. Liu, D. X., K. W. Tibbles, D. Cavanagh, T. D. Brown, and I. Brierley. 1995. Involvement of viral and cellular factors in processing of polyprotein encoded by ORF1a of the coronavirus IBV. Adv. Exp. Med. Biol. 380:413-421.
135. Liu, Y. C., V. Huang, T. C. Chao, C. D. Hsiao, A. Lin, M. F. Chang, and L. P. Chow. 2005. Screening of drugs by FRET analysis identifies inhibitors of SARS-CoV 3CL protease. Biochem. Biophys. Res. Commun. 333:194-199.
136. Liu, Z., C. Huang, K. Fan, P. Wei, H. Chen, S. Liu, J. Pei, L. Shi, B. Li, K. Yang, Y. Liu, and L. Lai. 2005. Virtual screening of novel noncovalent inhibitors for SARS-CoV 3C-like proteinase. J. Chem. Inf. Model. 45:10-17.
137. Lu, A., H. Zhang, X. Zhang, H. Wang, Q. Hu, L. Shen, B. S. Schaffhausen, W. Hou, and L. Li. 2004. Attenuation of SARS coronavirus by a short hairpin RNA expression plasmid targeting RNA-dependent RNA polymerase. Virology 324:84-89.

138. Lu, I. L., N. Mahindroo, P. H. Liang, Y. H. Peng, C. J. Kuo, K. C. Tsai, H. P. Hsieh, Y. S. Chao, and S. Y. Wu. 2006. Structure-based drug design and structural biology study of novel nonpeptide inhibitors of severe acute respiratory syndrome coronavirus main protease. J. Med. Chem. 49:5154-5161.
139. Martina, E., N. Stiefl, B. Degel, F. Schulz, A. Breuning, M. Schiller, R. Vicik, K. Baumann, J. Ziebuhr, and T. Schirmeister. 2005. Screening of electrophilic compounds yields an aziridinyl peptide as new active-site directed SARS-CoV main protease inhibitor. Bioorg. Med. Chem. Lett. 15:5365-5369.
140. Masters, P. S. 2006. The molecular biology of coronaviruses. Adv. Virus Res. 66:193-292.
141. McIntosh, K. 2005. Coronaviruses in the limelight. J. Infect. Dis. 191:489-491.
142. McIntosh, K., R. K. Chao, H. E. Krause, R. Wasil, H. E. Mocega, and M. A. Mufson. 1974. Coronavirus infection in acute lower respiratory tract disease of infants. J. Infect. Dis. 130:502-507.
143. Miyake, K., T. Tango, Y. Ota, K. Mitamura, M. Yoshiba, M. Kako, S. Hayashi, Y. Ikeda, N. Hayashida, S. Iwabuchi, Y. Sato, T. Tomi, N. Funaki, N. Hashimoto, T. Umeda, J. Miyazaki, K. Tanaka, Y. Endo, and H. Suzuki. 2002. Efficacy of Stronger Neo-Minophagen C compared between two doses administered three times a week on patients with chronic viral hepatitis. J. Gastroenterol. Hepatol. 17:1198-1204.
144. Morgenstern, B., M. Michaelis, P. C. Baer, H. W. Doerr, and J. Cinatl, Jr. 2005. Ribavirin and interferon-beta synergistically inhibit SARS-associated coronavirus replication in animal and human cell lines. Biochem. Biophys. Res. Commun. 326:905-908.
145. Morrey, J. D., D. F. Smee, R. W. Sidwell, and C. Tseng. 2002. Identification of active antiviral compounds against a New York isolate of West Nile virus. Antiviral Res. 55:107-116.
146. Muller, W. E., Z. I. Yamazaki, and R. K. Zahn. 1972. Bleomycin, a selective inhibitor of DNA-dependent DNA polymerase from oncogenic RNA viruses. Biochem. Biophys. Res. Commun. 46:1667-1673.
147. Naka, K., M. Ikeda, K. Abe, H. Dansako, and N. Kato. 2005. Mizoribine inhibits hepatitis C virus RNA replication: effect of combination with interferon-alpha. Biochem. Biophys. Res. Commun. 330:871-879.
148. Nakagawa, M., K. Nakahara, Y. Maruyama, M. Kawabata, I. Higuchi, H. Kubota, S. Izumo, K. Arimura, and M. Osame. 1996. Therapeutic trials in 200 patients with HTLV-I-associated myelopathy/ tropical spastic paraparesis. J. Neurovirol. 2:345-355.
149. Neuman, B. W., D. A. Stein, A. D. Kroeker, M. J. Churchill, A. M. Kim, P. Kuhn, P. Dawson, H. M. Moulton, R. K. Bestwick, P. L. Iversen, and M. J. Buchmeier. 2005. Inhibition, escape, and attenuated growth of severe acute respiratory syndrome coronavirus treated with antisense morpholino oligomers. J. Virol. 79:9665-9676.
150. Neumar, R. W., Y. A. Xu, H. Gada, R. P. Guttmann, and R. Siman. 2003. Cross-talk between calpain and caspase proteolytic systems during neuronal apoptosis. J. Biol. Chem. 278:14162-14167.
151. Ni, B., X. Shi, Y. Li, W. Gao, X. Wang, and Y. Wu. 2005. Inhibition of replication and infection of severe acute respiratory syndrome-associated coronavirus with plasmid-mediated interference RNA. Antivir. Ther. 10:527-533.
152. Nicholls, J. M., L. L. Poon, K. C. Lee, W. F. Ng, S. T. Lai, C. Y. Leung, C. M. Chu, P. K. Hui, K. L. Mak, W. Lim, K. W. Yan, K. H. Chan, N. C. Tsang, Y. Guan, K. Y. Yuen, and J. S. Peiris. 2003. Lung pathology of fatal severe acute respiratory syndrome. Lancet 361:1773-1778.
153. O'Brian, C. A., N. E. Ward, and V. G. Vogel. 1990. Inhibition of protein kinase C by the 12-O-tetradecanoylphorbol-13-acetate antagonist glycyrrhetic acid. Cancer Lett. 49:9-12.
154. O'Reilly, E. K., N. Tang, P. Ahlquist, and C. C. Kao. 1995. Biochemical and genetic analyses of the interaction between the helicase-like and polymerase-like proteins of the brome mosaic virus. Virology 214:59-71.
155. O'Reilly, E. K., Z. Wang, R. French, and C. C. Kao. 1998. Interactions between the structural domains of the RNA replication proteins of plant-infecting RNA viruses. J. Virol. 72:7160-7169.
156. Oh, J. S., D. S. Song, and B. K. Park. 2003. Identification of a putative cellular receptor 150 kDa polypeptide for porcine epidemic diarrhea virus in porcine enterocytes. J. Vet. Sci. 4:269-275.
157. Osman, T. A. and K. W. Buck. 1996. Complete replication *in vitro* of tobacco mosaic virus RNA by a template-dependent, membrane-bound RNA polymerase. J. Virol. 70:6227-6234.
158. Pancheva, S., D. Dundarova, and M. Remichkova. 2002. Potentiating effect of mizoribine on the anti-herpes virus activity of acyclovir. Z. Naturforsch. [C.] 57:902-904.
159. Pei, J., M. J. Sekellick, P. I. Marcus, I. S. Choi, and E. W. Collisson. 2001. Chicken interferon type I inhibits infectious bronchitis virus replication and associated respiratory illness. J. Interferon Cytokine Res. 21:1071-1077.

160. Peiris, J. S., Y. Guan, and K. Y. Yuen. 2004. Severe acute respiratory syndrome. Nat. Med. 10:S88-S97.
161. Peiris, J. S., S. T. Lai, L. L. Poon, Y. Guan, L. Y. Yam, W. Lim, J. Nicholls, W. K. Yee, W. W. Yan, M. T. Cheung, V. C. Cheng, K. H. Chan, D. N. Tsang, R. W. Yung, T. K. Ng, and K. Y. Yuen. 2003. Coronavirus as a possible cause of severe acute respiratory syndrome. Lancet 361:1319-1325.
162. Perkins, J. B., S. K. Guterman, C. L. Howitt, V. E. Williams, and J. Pero. 1990. Streptomyces genes involved in biosynthesis of the peptide antibiotic valinomycin. J. Bacteriol. 172:3108-3116.
163. Perrin, B. J. and A. Huttenlocher. 2002. Calpain. Int. J. Biochem. Cell Biol. 34:722-725.
164. Pestka, S. 2000. The human interferon alpha species and receptors. Biopolymers 55:254-287.
165. Pestka, S., S. V. Kotenko, G. Muthukumaran, L. S. Izotova, J. R. Cook, and G. Garotta. 1997. The interferon gamma (IFN-gamma) receptor: a paradigm for the multichain cytokine receptor. Cytokine Growth Factor Rev. 8:189-206.
166. Petty, I. T., R. French, R. W. Jones, and A. O. Jackson. 1990. Identification of barley stripe mosaic virus genes involved in viral RNA replication and systemic movement. EMBO J. 9:3453-3457.
167. Pompei, R., O. Flore, M. A. Marccialis, A. Pani, and B. Loddo. 1979. Glycyrrhizic acid inhibits virus growth and inactivates virus particles. Nature 281:689-690.
168. Pope, M., P. A. Marsden, E. Cole, S. Sloan, L. S. Fung, Q. Ning, J. W. Ding, J. L. Leibowitz, M. J. Phillips, and G. A. Levy. 1998. Resistance to murine hepatitis virus strain 3 is dependent on production of nitric oxide. J. Virol. 72:7084-7090.
169. Preobrazhenskaya, M. N. and E. N. Olsufyeva. 2006. Polycyclic peptide and glycopeptide antibiotics and their derivatives as inhibitors of HIV entry. Antiviral Res. 71:227-236.
170. Pyrc, K., B. J. Bosch, B. Berkhout, M. F. Jebbink, R. Dijkman, P. Rottier, and L. van der Hoek. 2006. Inhibition of human coronavirus NL63 infection at early stages of the replication cycle. Antimicrob. Agents Chemother. 50:2000-2008.
171. Qin, Z. L., P. Zhao, X. L. Zhang, J. G. Yu, M. M. Cao, L. J. Zhao, J. Luan, and Z. T. Qi. 2004. Silencing of SARS-CoV spike gene by small interfering RNA in HEK 293T cells. Biochem. Biophys. Res. Commun. 324:1186-1193.
172. Reed, S. E. 1984. The behaviour of recent isolates of human respiratory coronavirus *in vitro* and in volunteers: evidence of heterogeneity among 229E-related strains. J. Med. Virol. 13:179-192.
173. Reiss, C. S. and T. Komatsu. 1998. Does nitric oxide play a critical role in viral infections? J. Virol. 72:4547-4551.
174. Rouleau, M., R. J. Smith, J. B. Bancroft, and G. A. Mackie. 1994. Purification, properties, and subcellular localization of foxtail mosaic potexvirus 26-kDa protein. Virology 204:254-265.
175. Saijo, M., S. Morikawa, S. Fukushi, T. Mizutani, H. Hasegawa, N. Nagata, N. Iwata, and I. Kurane. 2005. Inhibitory effect of mizoribine and ribavirin on the replication of severe acute respiratory syndrome (SARS)-associated coronavirus. Antiviral Res. 66:159-163.
176. Sainz, B., Jr., E. C. Mossel, W. R. Gallaher, W. C. Wimley, C. J. Peters, R. B. Wilson, and R. F. Garry. 2006. Inhibition of severe acute respiratory syndrome-associated coronavirus (SARS-CoV) infectivity by peptides analogous to the viral spike protein. Virus Res. 120:146-155.
177. Sainz, B., Jr., E. C. Mossel, C. J. Peters, and R. F. Garry. 2004. Interferon-beta and interferon-gamma synergistically inhibit the replication of severe acute respiratory syndrome-associated coronavirus (SARS-CoV). Virology 329:11-17.
178. Sasaki, H., M. Takei, M. Kobayashi, R. B. Pollard, and F. Suzuki. 2002. Effect of glycyrrhizin, an active component of licorice roots, on HIV replication in cultures of peripheral blood mononuclear cells from HIV-seropositive patients. Pathobiology 70:229-236.
179. Sawicki, S. G. and D. L. Sawicki. 1990. Coronavirus transcription: subgenomic mouse hepatitis virus replicative intermediates function in RNA synthesis. J. Virol. 64:1050-1056.
180. Sawicki, S. G. and D. L. Sawicki. 1998. A new model for coronavirus transcription. Adv. Exp. Med. Biol. 440:215-219.
181. Scagnolari, C., E. Vicenzi, F. Bellomi, M. G. Stillitano, D. Pinna, G. Poli, M. Clementi, F. Dianzani, and G. Antonelli. 2004. Increased sensitivity of SARS-coronavirus to a combination of human type I and type II interferons. Antivir. Ther. 9:1003-1011.
182. Schaecher, S. R., J. M. Mackenzie, and A. Pekosz. 2006. The ORF7b protein of SARS-CoV is expressed in virus-infected cells and incorporated into SARS-CoV particles. J. Virol.

183. Schinazi, R. F., J. Mellors, H. Bazmi, S. Diamond, S. Garber, K. Gallagher, R. Geleziunas, R. Klabe, M. Pierce, M. Rayner, J. T. Wu, H. Zhang, J. Hammond, L. Bacheler, D. J. Manion, M. J. Otto, L. Stuyver, G. Trainor, D. C. Liotta, and S. Erickson-Viitanen. 2002. DPC 817: a cytidine nucleoside analog with activity against zidovudine- and lamivudine-resistant viral variants. Antimicrob. Agents Chemother. 46:1394-1401.
184. Sethna, P. B., S. L. Hung, and D. A. Brian. 1989. Coronavirus subgenomic minus-strand RNAs and the potential for mRNA replicons. Proc. Natl. Acad. Sci. U. S. A 86:5626-5630.
185. Shi, Y., D. H. Yang, J. Xiong, J. Jia, B. Huang, and Y. X. Jin. 2005. Inhibition of genes expression of SARS coronavirus by synthetic small interfering RNAs. Cell Res. 15:193-200.
186. Shibata, S. 2000. A drug over the millennia: pharmacognosy, chemistry, and pharmacology of licorice. Yakugaku Zasshi 120:849-862.
187. Shie, J. J., J. M. Fang, C. J. Kuo, T. H. Kuo, P. H. Liang, H. J. Huang, W. B. Yang, C. H. Lin, J. L. Chen, Y. T. Wu, and C. H. Wong. 2005. Discovery of potent anilide inhibitors against the severe acute respiratory syndrome 3CL protease. J. Med. Chem. 48:4469-4473.
188. Shie, J. J., J. M. Fang, T. H. Kuo, C. J. Kuo, P. H. Liang, H. J. Huang, Y. T. Wu, J. T. Jan, Y. S. Cheng, and C. H. Wong. 2005. Inhibition of the severe acute respiratory syndrome 3CL protease by peptidomimetic alpha,beta-unsaturated esters. Bioorg. Med. Chem. 13:5240-5252.
189. Simmons, G., D. N. Gosalia, A. J. Rennekamp, J. D. Reeves, S. L. Diamond, and P. Bates. 2005. Inhibitors of cathepsin L prevent severe acute respiratory syndrome coronavirus entry. Proc. Natl. Acad. Sci. U. S. A 102:11876-11881.
190. Skeggs, L. T., F. E. Dorer, M. Levine, K. E. Lentz, and J. R. Kahn. 1980. The biochemistry of the renin-angiotensin system. Adv. Exp. Med. Biol. 130:1-27.
191. Sloots, T. P., P. McErlean, D. J. Speicher, K. E. Arden, M. D. Nissen, and I. M. Mackay. 2006. Evidence of human coronavirus HKU1 and human bocavirus in Australian children. J. Clin. Virol. 35:99-102.
192. So, L. K., A. C. Lau, L. Y. Yam, T. M. Cheung, E. Poon, R. W. Yung, and K. Y. Yuen. 2003. Development of a standard treatment protocol for severe acute respiratory syndrome. Lancet 361:1615-1617.
193. Spaan, W., H. Delius, M. Skinner, J. Armstrong, P. Rottier, S. Smeekens, B. A. van der Zeijst, and S. G. Siddell. 1983. Coronavirus mRNA synthesis involves fusion of non-contiguous sequences. EMBO J. 2:1839-1844.
194. Spear, G. T., M. R. Zariffard, J. Xin, and M. Saifuddin. 2003. Inhibition of DC-SIGN-mediated trans infection of T cells by mannose-binding lectin. Immunology 110:80-85.
195. Sperber, S. J. and F. G. Hayden. 1989. Comparative susceptibility of respiratory viruses to recombinant interferons-alpha 2b and -beta. J. Interferon Res. 9:285-293.
196. Spiegel, M., A. Pichlmair, E. Muhlberger, O. Haller, and F. Weber. 2004. The antiviral effect of interferon-beta against SARS-coronavirus is not mediated by MxA protein. J. Clin. Virol. 30:211-213.
197. Stevenson, M. 2004. Therapeutic potential of RNA interference. N. Engl. J. Med. 351:1772-1777.
198. Stram, Y. and L. Kuzntzova. 2006. Inhibition of viruses by RNA interference. Virus Genes 32:299-306.
199. Stroher, U., A. DiCaro, Y. Li, J. E. Strong, F. Aoki, F. Plummer, S. M. Jones, and H. Feldmann. 2004. Severe acute respiratory syndrome-related coronavirus is inhibited by interferon- alpha. J. Infect. Dis. 189:1164-1167.
200. Stuyver, L. J., S. Lostia, M. Adams, J. S. Mathew, B. S. Pai, J. Grier, P. M. Tharnish, Y. Choi, Y. Chong, H. Choo, C. K. Chu, M. J. Otto, and R. F. Schinazi. 2002. Antiviral activities and cellular toxicities of modified 2',3'-dideoxy-2',3'-didehydrocytidine analogues. Antimicrob. Agents Chemother. 46:3854-3860.
201. Stuyver, L. J., T. Whitaker, T. R. McBrayer, B. I. Hernandez-Santiago, S. Lostia, P. M. Tharnish, M. Ramesh, C. K. Chu, R. Jordan, J. Shi, S. Rachakonda, K. A. Watanabe, M. J. Otto, and R. F. Schinazi. 2003. Ribonucleoside analogue that blocks replication of bovine viral diarrhea and hepatitis C viruses in culture. Antimicrob. Agents Chemother. 47:244-254.
202. Subbarao, K., J. McAuliffe, L. Vogel, G. Fahle, S. Fischer, K. Tatti, M. Packard, W. J. Shieh, S. Zaki, and B. Murphy. 2004. Prior infection and passive transfer of neutralizing antibody prevent replication of severe acute respiratory syndrome coronavirus in the respiratory tract of mice. J. Virol. 78:3572-3577.
203. Sui, J., W. Li, A. Murakami, A. Tamin, L. J. Matthews, S. K. Wong, M. J. Moore, A. S. Tallarico, M. Olurinde, H. Choe, L. J. Anderson, W. J. Bellini, M. Farzan, and W. A. Marasco. 2004. Potent neutralization of severe acute respiratory syndrome (SARS) coronavirus by a human mAb to S1 protein that blocks receptor association. Proc. Natl. Acad. Sci. U. S. A 101:2536-2541.

204. Sui, J., W. Li, A. Roberts, L. J. Matthews, A. Murakami, L. Vogel, S. K. Wong, K. Subbarao, M. Farzan, and W. A. Marasco. 2005. Evaluation of human monoclonal antibody 80R for immunoprophylaxis of severe acute respiratory syndrome by an animal study, epitope mapping, and analysis of spike variants. J. Virol. 79:5900-5906.
205. Summerton, J. 1999. Morpholino antisense oligomers: the case for an RNase H-independent structural type. Biochim. Biophys. Acta 1489:141-158.
206. Sung, J. J., A. Wu, G. M. Joynt, K. Y. Yuen, N. Lee, P. K. Chan, C. S. Cockram, A. T. Ahuja, L. M. Yu, V. W. Wong, and D. S. Hui. 2004. Severe acute respiratory syndrome: report of treatment and outcome after a major outbreak. Thorax 59:414-420.
207. Tan, E. L., E. E. Ooi, C. Y. Lin, H. C. Tan, A. E. Ling, B. Lim, and L. W. Stanton. 2004. Inhibition of SARS coronavirus infection *in vitro* with clinically approved antiviral drugs. Emerg. Infect. Dis. 10:581-586.
208. Tanner, J. A., B. J. Zheng, J. Zhou, R. M. Watt, J. Q. Jiang, K. L. Wong, Y. P. Lin, L. Y. Lu, M. L. He, H. F. Kung, A. J. Kesel, and J. D. Huang. 2005. The adamantane-derived bananins are potent inhibitors of the helicase activities and replication of SARS coronavirus. Chem. Biol. 12:303-311.
209. Tao, P., J. Zhang, N. Tang, B. Q. Zhang, T. C. He, and A. L. Huang. 2005. Potent and specific inhibition of SARS-CoV antigen expression by RNA interference. Chin Med. J. (Engl.) 118:714-719.
210. Ter Meulen, J., A. B. Bakker, E. N. van den Brink, G. J. Weverling, B. E. Martina, B. L. Haagmans, T. Kuiken, J. de Kruif, W. Preiser, W. Spaan, H. R. Gelderblom, J. Goudsmit, and A. D. Osterhaus. 2004. Human monoclonal antibody as prophylaxis for SARS coronavirus infection in ferrets. Lancet 363:2139-2141.
211. Ter Meulen, J., E. N. van den Brink, L. L. Poon, W. E. Marissen, C. S. Leung, F. Cox, C. Y. Cheung, A. Q. Bakker, J. A. Bogaards, E. van Deventer, W. Preiser, H. W. Doerr, V. T. Chow, J. de Kruif, J. S. Peiris, and J. Goudsmit. 2006. Human Monoclonal Antibody Combination against SARS Coronavirus: Synergy and Coverage of Escape Mutants. PLoS. Med. 3:e237.
212. Thiel, V., K. A. Ivanov, A. Putics, T. Hertzig, B. Schelle, S. Bayer, B. Weissbrich, E. J. Snijder, H. Rabenau, H. W. Doerr, A. E. Gorbalenya, and J. Ziebuhr. 2003. Mechanisms and enzymes involved in SARS coronavirus genome expression. J. Gen. Virol. 84:2305-2315.
213. Torre, D., A. Pugliese, and F. Speranza. 2002. Role of nitric oxide in HIV-1 infection: friend or foe? Lancet Infect. Dis. 2:273-280.
214. Towler, P., B. Staker, S. G. Prasad, S. Menon, J. Tang, T. Parsons, D. Ryan, M. Fisher, D. Williams, N. A. Dales, M. A. Patane, and M. W. Pantoliano. 2004. ACE2 X-ray structures reveal a large hinge-bending motion important for inhibitor binding and catalysis. J. Biol. Chem. 279:17996-18007.
215. Tresnan, D. B., R. Levis, and K. V. Holmes. 1996. Feline aminopeptidase N serves as a receptor for feline, canine, porcine, and human coronaviruses in serogroup I. J. Virol. 70:8669-8674.
216. Tripet, B., D. J. Kao, S. A. Jeffers, K. V. Holmes, and R. S. Hodges. 2006. Template-based coiled-coil antigens elicit neutralizing antibodies to the SARS-coronavirus. J. Struct. Biol. 155:176-194.
217. Tripp, R. A., L. M. Haynes, D. Moore, B. Anderson, A. Tamin, B. H. Harcourt, L. P. Jones, M. Yilla, G. J. Babcock, T. Greenough, D. M. Ambrosino, R. Alvarez, J. Callaway, S. Cavitt, K. Kamrud, H. Alterson, J. Smith, J. L. Harcourt, C. Miao, R. Razdan, J. A. Comer, P. E. Rollin, T. G. Ksiazek, A. Sanchez, P. A. Rota, W. J. Bellini, and L. J. Anderson. 2005. Monoclonal antibodies to SARS-associated coronavirus (SARS-CoV): identification of neutralizing and antibodies reactive to S, N, M and E viral proteins. J. Virol. Methods 128:21-28.
218. Tsai, K. C., S. Y. Chen, P. H. Liang, I. L. Lu, N. Mahindroo, H. P. Hsieh, Y. S. Chao, L. Liu, D. Liu, W. Lien, T. H. Lin, and S. Y. Wu. 2006. Discovery of a novel family of SARS-CoV protease inhibitors by virtual screening and 3D-QSAR studies. J. Med. Chem. 49:3485-3495.
219. Turner, R. B., A. Felton, K. Kosak, D. K. Kelsey, and C. K. Meschievitz. 1986. Prevention of experimental coronavirus colds with intranasal alpha-2b interferon. J. Infect. Dis. 154:443-447.
220. Tyrrell, D. A. and M. L. Bynoe. 1965. Cultivation of a novel type of common-cold virus in organ cultures. Br. Med. J. 5448:1467-1470.
221. Vabret, A., J. Dina, S. Gouarin, J. Petitjean, S. Corbet, and F. Freymuth. 2006. Detection of the new human coronavirus HKU1: a report of 6 cases. Clin. Infect. Dis. 42:634-639.
222. van der Hoek, L., K. Pyrc, M. F. Jebbink, W. Vermeulen-Oost, R. J. Berkhout, K. C. Wolthers, P. M. Wertheim-van Dillen, J. Kaandorp, J. Spaargaren, and B. Berkhout. 2004. Identification of a new human coronavirus. Nat. Med. 10:368-373.

223. van der Hoek, L., K. Sure, G. Ihorst, A. Stang, K. Pyrc, M. F. Jebbink, G. Petersen, J. Forster, B. Berkhout, and K. Uberla. 2005. Croup is associated with the novel coronavirus NL63. PLoS. Med. 2:e240.
224. Vijgen, L., B. Keyaerts, E. Van Damme, W. Peumans, E. De Clercq, J. Balzarini, and M. Van Ranst. 2004. Antiviral effect of plant compounds of the Alliaceae family against the SARS coronavirus. 17th International Conference on Antiviral Research. Antiviral Research 123:A76.
225. Vlasak, R., W. Luytjes, W. Spaan, and P. Palese. 1988. Human and bovine coronaviruses recognize sialic acid-containing receptors similar to those of influenza C viruses. Proc. Natl. Acad. Sci. U. S. A 85:4526-4529.
226. Wang, H., Y. Ding, X. Li, L. Yang, W. Zhang, and W. Kang. 2003. Fatal aspergillosis in a patient with SARS who was treated with corticosteroids. N. Engl. J. Med. 349:507-508.
227. Wang, Z., L. Ren, X. Zhao, T. Hung, A. Meng, J. Wang, and Y. G. Chen. 2004. Inhibition of severe acute respiratory syndrome virus replication by small interfering RNAs in mammalian cells. J. Virol. 78:7523-7527.
228. Williams, R. K., G. S. Jiang, and K. V. Holmes. 1991. Receptor for mouse hepatitis virus is a member of the carcinoembryonic antigen family of glycoproteins. Proc. Natl. Acad. Sci. U. S. A 88:5533-5536.
229. Woo, P. C., S. K. Lau, C. M. Chu, K. H. Chan, H. W. Tsoi, Y. Huang, B. H. Wong, R. W. Poon, J. J. Cai, W. K. Luk, L. L. Poon, S. S. Wong, Y. Guan, J. S. Peiris, and K. Y. Yuen. 2005. Characterization and complete genome sequence of a novel coronavirus, coronavirus HKU1, from patients with pneumonia. J. Virol. 79:884-895.
230. Woo, P. C., S. K. Lau, H. W. Tsoi, Y. Huang, R. W. Poon, C. M. Chu, R. A. Lee, W. K. Luk, G. K. Wong, B. H. Wong, V. C. Cheng, B. S. Tang, A. K. Wu, R. W. Yung, H. Chen, Y. Guan, K. H. Chan, and K. Y. Yuen. 2005. Clinical and molecular epidemiological features of coronavirus HKU1-associated community-acquired pneumonia. J. Infect. Dis. 192:1898-1907.
231. Wu, C. J., H. W. Huang, C. Y. Liu, C. F. Hong, and Y. L. Chan. 2005. Inhibition of SARS-CoV replication by siRNA. Antiviral Res. 65:45-48.
232. Wu, C. Y., J. T. Jan, S. H. Ma, C. J. Kuo, H. F. Juan, Y. S. Cheng, H. H. Hsu, H. C. Huang, D. Wu, A. Brik, F. S. Liang, R. S. Liu, J. M. Fang, S. T. Chen, P. H. Liang, and C. H. Wong. 2004. Small molecules targeting severe acute respiratory syndrome human coronavirus. Proc. Natl. Acad. Sci. U. S. A 101:10012-10017.
233. Wu, C. Y., K. Y. King, C. J. Kuo, J. M. Fang, Y. T. Wu, M. Y. Ho, C. L. Liao, J. J. Shie, P. H. Liang, and C. H. Wong. 2006. Stable benzotriazole esters as mechanism-based inactivators of the severe acute respiratory syndrome 3CL protease. Chem. Biol. 13:261-268.
234. Yanagida, K., C. Baba, and M. Baba. 2004. Inhibition of bovine viral diarrhea virus (BVDV) by mizoribine: synergistic effect of combination with interferon-alpha. Antiviral Res. 64:195-201.
235. Yang, D., Y. Haraguchi, H. Iwai, A. Handa, N. Shimizu, and H. Hoshino. 1994. Inhibition of adsorption of human T-cell-leukemia virus type 1 by a plant lectin, wheat-germ agglutinin. Int. J. Cancer 56:100-105.
236. Yang, H., W. Xie, X. Xue, K. Yang, J. Ma, W. Liang, Q. Zhao, Z. Zhou, D. Pei, J. Ziebuhr, R. Hilgenfeld, K. Y. Yuen, L. Wong, G. Gao, S. Chen, Z. Chen, D. Ma, M. Bartlam, and Z. Rao. 2005. Design of wide-spectrum inhibitors targeting coronavirus main proteases. PLoS. Biol. 3:e324.
237. Yang, S., S. J. Chen, M. F. Hsu, J. D. Wu, C. T. Tseng, Y. F. Liu, H. C. Chen, C. W. Kuo, C. S. Wu, L. W. Chang, W. C. Chen, S. Y. Liao, T. Y. Chang, H. H. Hung, H. L. Shr, C. Y. Liu, Y. A. Huang, L. Y. Chang, J. C. Hsu, C. J. Peters, A. H. Wang, and M. C. Hsu. 2006. Synthesis, crystal structure, structure-activity relationships, and antiviral activity of a potent SARS coronavirus 3CL protease inhibitor. J. Med. Chem. 49:4971-4980.
238. Yap, Y., X. Zhang, A. Andonov, and R. He. 2005. Structural analysis of inhibition mechanisms of aurintricarboxylic acid on SARS-CoV polymerase and other proteins. Comput. Biol. Chem. 29:212-219.
239. Yeager, C. L., R. A. Ashmun, R. K. Williams, C. B. Cardellichio, L. H. Shapiro, A. T. Look, and K. V. Holmes. 1992. Human aminopeptidase N is a receptor for human coronavirus 229E. Nature 357:420-422.
240. Yi, H., I. Nakashima, and K. Isobe. 1996. Enhancement of nitric oxide production from activated macrophages by glycyrrhizin. Am. J. Chin Med. 24:271-278.
241. Yuan, K., L. Yi, J. Chen, X. Qu, T. Qing, X. Rao, P. Jiang, J. Hu, Z. Xiong, Y. Nie, X. Shi, W. Wang, C. Ling, X. Yin, K. Fan, L. Lai, M. Ding, and H. Deng. 2004. Suppression of SARS-CoV entry by peptides corresponding to heptad regions on spike glycoprotein. Biochem. Biophys. Res. Commun. 319:746-752.

242. Zhang, Y., T. Li, L. Fu, C. Yu, Y. Li, X. Xu, Y. Wang, H. Ning, S. Zhang, W. Chen, L. A. Babiuk, and Z. Chang. 2004. Silencing SARS-CoV Spike protein expression in cultured cells by RNA interference. FEBS Lett. 560:141-146.
243. Zhao, P., Z. L. Qin, J. S. Ke, Y. Lu, M. Liu, W. Pan, L. J. Zhao, J. Cao, and Z. T. Qi. 2005. Small interfering RNA inhibits SARS-CoV nucleocapsid gene expression in cultured cells and mouse muscles. FEBS Lett. 579:2404-2410.
244. Zhao, Z., F. Zhang, M. Xu, K. Huang, W. Zhong, W. Cai, Z. Yin, S. Huang, Z. Deng, M. Wei, J. Xiong, and P. M. Hawkey. 2003. Description and clinical treatment of an early outbreak of severe acute respiratory syndrome (SARS) in Guangzhou, PR China. J. Med. Microbiol. 52:715-720.
245. Zheng, B., M. L. He, K. L. Wong, C. T. Lum, L. L. Poon, Y. Peng, Y. Guan, M. C. Lin, and H. F. Kung. 2004. Potent inhibition of SARS-associated coronavirus (SCOV) infection and replication by type I interferons (IFN-alpha/beta) but not by type II interferon (IFN-gamma). J. Interferon Cytokine Res. 24:388-390.
246. Zhu, J., G. Xiao, Y. Xu, F. Yuan, C. Zheng, Y. Liu, H. Yan, D. K. Cole, J. I. Bell, Z. Rao, P. Tien, and G. F. Gao. 2004. Following the rule: formation of the 6-helix bundle of the fusion core from severe acute respiratory syndrome coronavirus spike protein and identification of potent peptide inhibitors. Biochem. Biophys. Res. Commun. 319:283-288.
247. Ziebuhr, J., G. Heusipp, A. Seybert, and S. G. Siddell. 1998. Substrate specificity of the human coronavirus 229E 3C-like proteinase. Adv. Exp. Med. Biol. 440:115-120.
248. Ziebuhr, J. and S. G. Siddell. 1999. Processing of the human coronavirus 229E replicase polyproteins by the virus-encoded 3C-like proteinase: identification of proteolytic products and cleavage sites common to pp1a and pp1ab. J. Virol. 73:177-185.
249. Ziebuhr, J., E. J. Snijder, and A. E. Gorbalenya. 2000. Virus-encoded proteinases and proteolytic processing in the Nidovirales. J. Gen. Virol. 81:853-879.
250. Ziebuhr, J., V. Thiel, and A. E. Gorbalenya. 2001. The autocatalytic release of a putative RNA virus transcription factor from its polyprotein precursor involves two paralogous papain-like proteases that cleave the same peptide bond. J. Biol. Chem. 276:33220-33232.

Chapter XI

Identification of new human coronaviruses

Expert Review of Anti-infective Therapy, April 2007, vol. 5, p. 245 - 253

Krzysztof Pyrc, Ben Berkhout and Lia van der Hoek

Laboratory of Experimental Virology, Department of Medical Microbiology, Center for Infection and Immunity Amsterdam (CINIMA), Academic Medical Center, University of Amsterdam, Meibergdreef 15, 1105 AZ, Amsterdam, The Netherlands.

To date, there are still a variety of human infections with unknown etiology. Identification of previously unrecognized viral agents in patient samples is of great medical interest, but remains a major technical challenge. Acute respiratory tract infections are responsible for considerable morbidity and mortality in humans and animals. A variety of viruses, bacteria, and fungi are associated with respiratory tract illness. Most of the respiratory viruses belong to the families of *Paramyxoviridae*, *Orthomyxoviridae*, *Picornaviridae*, *Adenoviridae*, and *Coronaviridae*. No pathogens can be detected in a relatively large proportion of patients with respiratory disease. Partially due to limitations of current diagnostic assays, but also because some infections are caused by yet unknown pathogens. In this review we will focus on human coronaviruses. In the mid-1960's two human coronaviruses were identified that cause the common cold: HCoV-229E and HCoV-OC43. The recent outbreak of SARS-CoV and subsequent identification of two additional human coronaviruses (HCoV-NL63 and HCoV-HKU1) has drawn the attention to this virus family. This manuscript summarizes the knowledge of the human coronaviruses and describes their discovery. Furthermore, the current methodology to identify novel coronavirus species will be presented.

Human coronaviruses

Coronaviruses are positive strand RNA viruses with one of the largest viral genomes among the RNA viruses (27-33 kb). The virus particles are enveloped and carry extended spike proteins on the membrane surface. Currently, several coronaviral species are known to infect mammals and birds. These species were first divided into three groups based on serological relationship[19,23]. As the number of species increased and molecular biology tools became available, the serologic groups have been converted into three phylogenetic clusters based on genome sequence analysis. The group III viruses are found exclusively in birds, whereas members of the group I and II can infect mammals.

The genome organization of coronaviruses is conserved between species, with the 5' two-third of the genome encompassing the large 1a and 1b open reading frames (ORFs) encoding non-structural, replicase proteins and the 3' terminal part encoding structural proteins. Accessory protein genes are located between the structural genes, but they differ in number and size between viral species[8]. The coronaviruses can cause a variety of diseases in animals including gastroenteritis and respiratory tract disease. In humans, currently identified coronaviruses are exclusively associated with respiratory tract illnesses. At present, there are five human coronaviruses known: HCoV-229E, HCoV-OC43, SARS-CoV, HCoV-NL63 and HCoV-HKU1 (Table 1).

HCoV-229E and HCoV-OC43 were first described in the mid-1960's and were believed for over forty years to be the only representatives of human

Table 1. Human coronaviruses

Coronavirus	Year of identification	Detection method	Reference
HCoV-229E	1966	Tissue cultures, healthy adult volunteers inoculation	Hamre Procknow 1966[21]
HCoV-OC43 (– like viruses)	1965 / 1967	Organ cultures, healthy adult volunteers inoculation, electron microscopy	Tyrrell and Bynoe 1965[43]; McIntosh et al 1967[31].
SARS-CoV	2003	Cell culture, electron microscopy, consensus primers, random RT-PCR	Peiris et al 2003[34]; Drosten et al 2003[10]; Ksiazek et al 2003[25]
HCoV-NL63	2004	Cell culture, VIDISCA, electron microscopy, RAP-PCR	van der Hoek et al 2004[45]; Fouchier et al 2004[16].
HCoV-HKU1	2005	Consensus primers	Woo et al 2005[50].

coronaviruses. Inoculation of healthy adult volunteers revealed that infection causes common cold symptoms. Coryza occurs often in persons infected with HCoV-229E, while HCoV-OC43 positive patients frequently have sore throat manifestations[36]. The SARS epidemic started in 2003 in the Guandong province of China. At first, it was suspected that known viral pathogens were involved, but soon SARS-CoV was identified as the responsible pathogen[10,25,34]. The SARS-CoV probably originated from a wild animal reservoir, most likely bats, and was transmitted in a zoonotic event to humans via civet cats that are traded as food in China[26]. The exploding epidemic was controlled at the end of 2003 by quarantine measures[33]. HCoV-NL63 and HCoV-HKU1 were identified in 2004 and 2005, respectively. Both viruses were not recently introduced in humans, but were previously unrecognized. They have spread worldwide and display a spectrum of disease similar to the ones described for HCoV-229E and HCoV-OC43. The four currently circulating human coronaviruses can probably all be classified as common cold viruses, but a more severe lower respiratory tract infection is frequently observed in young children, patients with underlying disease and elderly persons[5,7,9,15,17,30,37,44,46].

Current techniques for coronavirus discovery

Currently, there are several techniques for discovery of novel coronaviruses. Here we provide an overview of the methods that have successfully been used for coronavirus detection and identification, e.g. electron microscopy, consensus primer PCR amplification, VIDISCA, random PCR or microarrays.

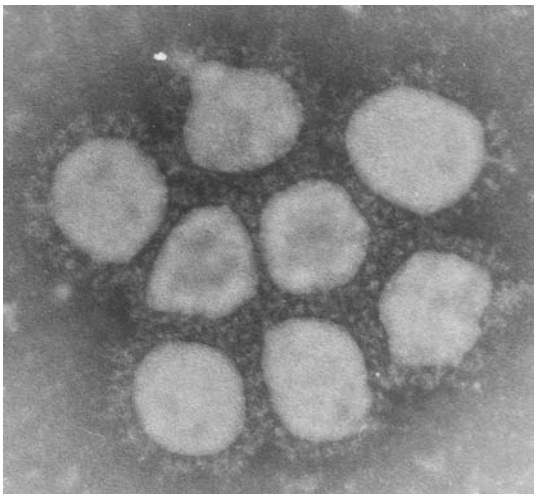


Figure 1. Negatively stained electron micrograph of HCoV-NL63. Courtesy of Dr Bermingham and Dr Hoschler and the EM unit of the Health Protection Agency, Colindale, London.

Electron microscopy

Coronaviruses are named after their shape (corona = crown) under the electron microscopy. The virus particles (50-150nm diameter) are easily recognizable because of their potato-like shape, surrounded by the "crown" consisting of the extended surface spike proteins (Figure 1). The first identification of a virus occurs frequently by electron microscopy. It was used for identification of SARS-CoV, HCoV-229E, HCoV-OC43 and HCoV-NL63[10,16,21,25,29]. The main disadvantage of this method is the need for a high-titer virus stock. Obviously, this physical technique on itself does not provide detailed information on the virus type, but combined with serology and molecular biology methods it remains a powerful instrument for virus discovery.

PCR amplification based on universal coronavirus primers

The most specific method for identification of coronaviruses in clinical samples is a PCR amplification based method that uses primers that can amplify any member of the coronavirus family. Besides quick screening for several pathogens in a single assay, it provides the opportunity to identify previously unknown coronaviruses. The ideal target for primers is a conserved gene, which is preferably identical in all known coronaviral species. If such a "perfect target" is not available, degenerate primers that mimic the natural sequence diversity form an alternative. For coronaviruses, conserved regions of the 1a / 1b open reading frames (ORF) constitute a convienient target for the design of universal coronavirus primers. The encoded RNA-dependent RNA polymerase is the most conserved gene and several broad PCR assays have been described based on this region[1,25,32,39,50] (Table 2). The simplicity and time effectiveness of the method are counterbalanced by some limitations. Assays designed before the identification of SARS-CoV, HCoV-NL63 and HCoV-HKU1, were later on demonstrated to be unable to efficiently amplify these coronaviruses. Optimized universal

Table 2. Consensus primers developed for coronaviruses

	Primer sequences	Targeted gene	Species included for primer design [b].	Virus identified	reference
1	5'-TGATGATGS[a]NGTTGTNTGYTAYAA-3' 5'-GCATWGTRTGYTGNGARCARAATTC-3'	1b gene	SARS-CoV, HCoV-229E and HCoV-OC43, HCoV-NL63 & HCoV-HKU1	-	Escutenaire et al 2006[12].
2	5'-GGTTGGGACTATCCTAAGTGTGA-3' 5'-CCATCATCAGATAGAATCATCATA-3'	1b gene	SARS-CoV, HCoV-229E, HCoV-OC43 & HCoV-NL63	HCoV-HKU1	Woo et al 2005[50].
3	5'-ACWCARHTVAAYYTNAARTAYGC-3' 5'-TCRCAYTTDGGRTARTCCCA-3'	1b gene	SARS-CoV, HCoV-229E, HCoV-OC43 & HCoV-NL63	-	Moes et al 2005[32].
4	5'-SGCAAAATAATGAATTAATGCC -3' 5'-GACGCACCACCATATGAATCCTG -3'	1a gene	SARS-CoV & HCoV-229E	-	Esper et al 2005[14].
5	5'-TGATGGGTTGGGACTATCCTAAATGTGA-3' 5'-GTAGTTGCATCACCGGAAGTTGTGCCACC-3'	1b gene	SARS-CoV, HCoV-229E & HCoV-OC43	-	Adachi et al 2004[1].
6	5'-GGGTT-GGGACTATCCTAAGTGTGA-3' 5'-TAACACACAACICCATCATCA-3'	1b gene	HCoV-229E & HCoV-OC43	SARS-CoV	Ksiazek et al 2003[25].
7	5'-ACTCARWTRAATYTNAAATAYGC-3' 5'-TCACAYTTWGGATARTCCCA-3'	1b gene	HCoV-229E & HCoV-OC43	-	Stephensen et al 1999[39].

[a] The degenerated positions are underlined.

[b] The human coronaviruses included in the multiple alignment used for design of universal

primers should therefore not only target all sequences of known members of the coronavirus family, but ideally have broader specificity. Such an effect can be obtained by including outgroup sequences (e.g. another virus family members from the order of *Nidovirales*) in the multiple sequence alignment used for primer design. Unfortunately, this approach often results in highly degenerate primers that lack specificity and therefore produce many false positive signals.

Serology

The coronavirus family was initially divided into three distinct groups based on serology[19,23]. The shared immunogenic epitopes might be employed for broad detection of coronaviral proteins, even from species not identified previously. It was shown that coronaviruses from one serologic group are generally recognized by the sera raised by any member of that serogroup[18,24,35]. In fact, coronaviruses that belong to different serological groups also possesses common epitopes that can give cross-reactivity in an immunoassay[22,40]. Thus, the development of coronavirus specific, broadly reactive sera – as known for *Picornaviridae* species - might be used as an introductory assay for the detection of a coronavirus in cell culture[47].

Sequence - independent amplification

There are several techniques that allow the amplification of a viral genome without prior sequence information. These methods vary considerably in approach and use ligated adaptors to allow amplification, random primer PCR, differential display and shotgun sequencing.

VIDISCA

The VIDISCA (Virus Discovery based on cDNA AFLP) method is based on the cDNA-AFLP technique[6,45]. In this protocol, RNA is reverse transcribed into cDNA using random hexamer oligonucleotides, followed by second strand synthesis. The dsDNA is digested with two frequently cutting restriction enzymes (HinP1-I and Mse-I) of which the recognition sequence is likely to be present in every viral target. HinP1-I and Mse-I anchors are ligated to the digested DNA. Because the restriction enzymes have not been inactivated before the ligation step, they will digest fragment concatamers. However, the proper DNA-anchor hybrids are protected from restriction because a defective restriction enzyme recognition site is created upon ligation. The target is subsequently PCR-amplified based on the flanking anchor sequences. The second round of amplification is performed in 16 reactions with 5′ and 3′ primers extended with one nucleotide (G, A, T or C) to improve sensitivity and selectivity. A reproducible PCR pattern is generated that should ideally be compared to a negative control.

Random RT-PCR

The random PCR protocol uses primers with a random 3′ hexanucleotide sequence that can anneal to nearly any RNA or ssDNA. The 5′ 20 nucleotides of the primer (tail) contain a unique sequence that serves as a template for subsequent PCR primer annealing. The primer that is annealed to the RNA template is extended by reverse transcriptase with an RNase H activity that allows the re-attachment of the enzyme and insertion of the tailed random primer on both 3′ and 5′ sides. The cDNA product is PCR amplified using the unique region of the initial primer. In the random PCR method, the ligation step is omitted, what may significantly increase the sensitivity.

A similar approach is RNA arbitrarily primed PCR (RAP-PCR), where arbitrarily chosen oligonucleotides are used for priming. Competition between the annealing events during the initial low-stringency cycles results in the reproducible and semiquantitative amplification of many discrete DNA fragments during the subsequent high stringency cycles[16].

Differential display

Differential display is a method that has primarily been developed to identify and isolate genes differentially expressed in various cells or under altered conditions[27]. The method can also be used for identification of RNA viruses with a poly-A tail. The key step is the use of an oligo-dT with a 3′ terminal G, C or A to prime reverse transcription. The subsequent PCR amplification uses a specific tail sequence of the oligo-dT primer for primer annealing, together with a random oligonucleotide as a 5′ primer. The addition of radiolabelled dNTPs to the reaction allows the precise gel visualization of the products. With multiple primer sets, reproducible patterns of amplified cDNA fragments can be obtained[28].

Microarrays

The usage of microarrays for virus discovery is a relatively new application[48,49]. A virus-broad microarray system, consisting of 70-mer nucleotides that represent the conserved regions of virtually all known viral species (more than 1000 viruses represented on a single array), was described recently[49]. Key features of this approach are the cross-hybridization of viral material to highly conserved sequence motifs, and direct recovery of hybridized material from the microarray. This method provides a rapid route for obtaining sequences of novel viruses. For SARS-CoV, Wang retrospectively stated to be able to ascertain that a novel coronavirus was present in the unknown sample within 24 h. They also show that novel viruses with limited homology to known viruses can be successfully detected by this method[49]. In light of the continuous threat of emerging infectious diseases, this powerful approach will greatly help in the rapid identification and characterization of novel viruses.

Enrichment of viral nucleic acids

Cell culture

Most viruses are discovered upon culturing in susceptible cells, rather than directly in clinical specimens. It is obvious that active virus replication will provide a dramatic enrichment of the viral genome compared to background DNA/RNA from cells. Unfortunately, not all viruses replicate in cell culture, e.g. HCoV-HKU1 does not replicate *in vitro*. Organ cultures or airway epithelial cultures may provide a powerful ex vivo extension to the standard cell line based *in vitro* cultures.

Removal of cells and mitochondria

All samples derived from patients or from cell culture contain cells, mitochondria, cell debris, mucus and other contaminants. All these components might contain cellular DNA / RNA. A centrifugation step is a very simple, but potent purification method. Only 10 minutes centrifugation with 14000×g significantly improves the sample quality and purity[45]. Another option is sample filtration through a 0.22μm filter[2]. Although the latter method is also very simple, the limiting factor is the large volume of sample that is needed. While centrifugation of a 110μl specimen results in loss of 10μl, which is discarded together with the pellet, relatively large sample losses are encountered upon filtration.

DNase and RNase pre-treatment

As mentioned above, contaminating RNA / DNA can interfere with the virus detection process. The cellular nucleic acids originate mostly from cells killed by the virus infection or from cells that are lysed during sample collection and preparation. To overcome this problem, a sample can be treated with nucleases before extraction of the RNA genome from virus particles. The general assumption

is that the viral genetic material is protected inside the virus particle and that the DNase/RNase treatment will affect only the free, unprotected molecules. Although this seems to be true for DNase, an RNase treatment can also decrease the viral RNA virus yield[2,45] (Unpublished observation, Lia van der Hoek).

Other methods and possible applications

Except for the methods for enrichment of viral nucleic acids that were already used for coronaviruses, there are several alternative methods to increase the concentration of viral nucleic acid. One basic technique is ultracentrifugation that allows the concentration of virus particles[3]. Endoh suggested an additional interesting approach for selective amplification of viral nucleic acids. The enrichment takes place during the reverse transcription step, by using specific random hexamers that rarely prime ribosomal RNAs but that can anneal to all known mammalian viruses listed in public databases[11]. Alternatively, especially for samples with a very low virus yield, a sequence independent pre-amplification step may be included, e.g. with the random PCR technique described above. Inclusion of this assay before the universal coronavirus primer PCR amplification may significantly increase the sensitivity of a virus search.

Five members of the coronavirus family - Identification

HCoV-229E and HCoV-OC43

The first report about coronaviral infection in humans was presented by Tyrrell and Bynoe in 1965[43]. The infectious material was recovered from the nasal wash of a boy with a typical common cold. The sample was obtained at the peak of disease symptoms, and was subsequently inoculated in healthy volunteers who developed colds afterwards. The material obtained in subsequent infections was negative for the human pathogens known in 1960's (influenza A, B and C, para-influenza 1,2,3,4, respiratory syncytial virus, herpes simplex virus, enteroviruses, rhinoviruses, mycoplasma and adenoviruses). Laboratory experiments indicated that the pathogen is sensitive to ether, but resistant to antibiotics. Furthermore, the pathogen could cross a bacteria-tight filter, indicating that the isolated pathogen was an enveloped virus. The virus did not grow in cell culture using different cell lines and primary cells, but it replicated on human trachea organ cultures. Replication was measured by the ability of the culture supernatant to induce common cold in volunteers. The initially described strain was called B814[43]. One year later, Hamre and Procknow described the isolation and propagation in cell culture of another unknown respiratory virus. The infectious material was obtained from students at the University of Chicago with respiratory illness of unknown origin. The virus was propagated on primary human kidney cells and subsequently inoculated onto diploid human embryonic lung cells (HEL) and human fetal lung-derived, fibroblast-like cells (WI-38). The infection resulted in slow development of cytophatic effects (CPE) first detected after 6 days. The pathogen (HCoV-

229E) was shown to be ether-labile, to consist of particles approximately about 89nm in diameter, and to contain RNA as genetic material[21]. The 229E virus isolate from Chicago became the prototype strain for the HCoV-229E species. Electron microscopical analysis revealed that both B814 and 229E are similar in morphology to infectious bronchitis virus (IBV), an avian coronavirus[4,42]. A subsequent study from McIntosh *et al* describes the isolation of several human IBV-like viruses, among which HCoV-OC43. The virus samples were obtained from persons with common cold and inoculated in human embryonic trachea organ cultures (OC). None of these patients developed a significant antibody response to the 229E strain, providing the first evidence that OC-strains, including the initial B814 isolate are serologically unrelated to HCoV-229E[31]. Unfortunately, the B814 sample and most of the OC isolates (except for OC43) were lost over time. It is therefore impossible to determine whether these strains represent one of the known coronaviruses. The OC43 isolate was further propagated and is now the prototype strain for the HCoV-OC43 species.

The full genome sequences of HCoV-229E and HCoV-OC43 were obtained recently, in 2000 and 2004, respectively[38,41]. The sequence analysis confirms that HCoV-229E and HCoV-OC43 belong to separate coronavirus groups, I and II, respectively.

SARS-CoV

After the identification of SARS as a new infectious human disease, several groups made an effort to identify the responsible pathogen. It was initially suspected that the disease might be caused by chlamydia, rhinoviruses or paramyxoviruses, but these results could not be confirmed by other groups[10,25,34]. A new coronavirus was identified as the infectious agent linked to SARS by three independent research groups[10,25,34]. All three groups started their search by cell culture analysis, inoculating several cell lines that are used in routine diagnostics with patient specimens. A group from Hong Kong[34] was the first to observe CPE after inoculating a lung biopsy specimen and a nasopharyngeal aspirate sample on fetal rhesus kidney cells (FRhK-4). The initial CPE of rounded refractile cells appeared 2–4 days after sample inoculation, but reappeared within 24 hours after subsequent passage. Furthermore, the infected cells stained positive in an immunostaining assay with sera derived from patients with SARS, but not with healthy blood donor sera. The infected cells did not react with the routine panel of immunological reagents used to identify virus isolates (influenza A, B, parainfluenza types 1, 2, and 3, adenovirus, and RSV) nor in RT-PCR assays (influenza A and human metapneumovirus, mycoplasma). The virus was ether-sensitive and electron microscopy showed the presence of pleomorphic enveloped virus particles of approximately 80–90nm in diameter, with surface morphology characteristic for coronaviruses.

Two other groups obtained similar results with Vero cells, including the description of coronavirus-like particles by electron microscopy[10,25]. Based on that finding, Ksiazek *et al* designed universal coronavirus primers based on the sequence of RNA dependent RNA polymerase gene of several coronaviruses.
At the same time, Drosten *et al* and Peiris *et al* amplified the virus from their cell culture supernatants with random RT-PCR techniques. The group of Peiris *et al* applied differential display primers and cloned the RT-PCR fragments[34], while Drosten *et al* utilized degenerated primers under low-stringency conditions[10]. All studies revealed that a novel viral agent was present, constituting a new species within the genus *Coronaviridae*[10]. Full genome sequencing showed that the virus is not a recombinant of known coronavirus species, but a distinct member of the group II coronaviruses.

HCoV-NL63
In January 2003, a 7-month child was admitted to a hospital in Amsterdam with coryza, conjunctivitis, bronchiolitis and fever[45]. A nasopharyngeal aspirate sample was collected five days after the onset of disease and subsequently tested for known respiratory pathogens. Diagnostic tests for respiratory syncytial virus, adenovirus, influenza viruses A and B, rhinovirus, enterovirus, HCoV-229E and HCoV-OC43 were negative. The clinical sample (NL63) was inoculated in cell culture (human fetal lung fibroblasts, tertiary monkey kidney cells (tMK; Cynomolgus monkey) and HeLa cells). CPE was detected on tMK cells at day eight after inoculation. The observed CPE was diffuse, with a refractive appearance followed by cell detachment. CPE was more pronounced when the virus was passaged onto a monkey kidney cell line (LLC-MK2). Acid lability and chloroform sensitivity tests indicated that the virus was most likely enveloped. The sample was analyzed with the VIDISCA method, followed by full-length genome sequencing, which revealed that HCoV-NL63 is a previously unknown group I coronavirus.

Soon after the first publication another group from the Netherlands reported the same human coronavirus[16]. This study described the isolation of an unidentifiable virus from a nose swab sample collected from an 8 months old boy suffering from pneumonia in the Netherlands in April 1988. The virus was inoculated on tMK cells, in which it caused CPE after 7 days, affecting about 50% of the cells after 13 days. The virus was subsequently passaged, which resulted in CPE development on tMK and Vero cells. Supernatants of infected tMK and Vero E6 cells were used for negative contrast electron microscopy analysis, revealing the presence of coronavirus-like particles with an average diameter of 140nm and average envelope projections of 20nm. The cell cultures appeared negative for HCoV-OC43 and HCoV-229E. Subsequently, the sample was analysed with RAP-PCR and RT-PCR with primers specific for the coronavirus family.

Remarkably, one year after the publications of both Dutch groups the team of Kahn described the identification of essentially the same virus, which was given a novel name: New Haven (NH) coronavirus[13,14]. Clinical respiratory specimens were screened for coronaviruses using universal primers based on the conserved regions of the 1a replicase gene of groups I, II, and III. The screening was performed on pooled samples (5–10 specimens per pool) and 17 out of 80 pools yielded an expected amplicon of approximately 550 bp. Most samples (15 of 17) contained the known coronaviruses HCoV-OC43 or HCoV-229E or human DNA but 2 pool samples contained the NH coronavirus. The sequences of these 550 bp fragments are very similar to the isolates of the Netherlands (94% - 100% at nucleotide level), and represent the same species. Considering that the publication appeared 10 months after the first HCoV-NL63 report, this study cannot be regarded as the one discovering this viral species.

In 2005, the coronavirus study group of the International Committee on Taxonomy of Viruses (ICTV) executive committee advised the use of HCoV-NL63 as the proper species name for all related viruses.

HCoV-HKU1

The index patient for HCoV-HKU1 was a 71-year-old Chinese man who was admitted to the hospital in January 2004 because of fever and productive cough with purulent sputum for 2 days[50]. A chest radiograph showed patchy infiltrates over the left lower zone. A nasopharyngeal aspirate was used for direct antigen detection of several respiratory viruses and RT-PCR assays for influenza A virus, human metapneumovirus and SARS-CoV. All tests were negative. Additionally, the ability of the virus to grow in cell culture was assayed. The nasopharyngeal aspirate was inoculated on several cell lines: RD (human rhabdomyosarcoma), I13.35 (murine macrophage), L929 (murine fibroblast), HRT-18 (colorectal adenocarcinoma), and B95a (marmoset B-lymblastoid) and a mixed neuron-glia culture. No CPE was observed. Since no known microbiological agent could be identified, research was initiated to identify novel agents. An RT-PCR amplification with universal coronavirus primers resulted in a 440 bp product of which the sequence clusters with the *Coronaviridae* in phylogenetic analysis. Full-length sequencing revealed that HCoV-HKU1 is a previously unknown group II coronavirus[50].

Summary

The main technical problem during the search for novel coronaviruses is the low virus yield in clinical samples. This precludes the selective, but sequence non-specific amplification of viral RNA. Most human coronaviruses have been identified after cell culture enrichment[10,16,25,34,45,]. Once the virus can be efficiently propagated in cell culture, any of the molecular biology tools developed for virus discovery can be used to identify the pathogen. This is nicely illustrated by the discovery of SARS-CoV. Once the virus was cultured, it was identified by a

variety of methods: random PCR, differential display random amplification and universal primers[10,25,34]. The identification of a new coronavirus directly from patient material is however significantly more difficult. The only approach that resulted in successful identification of a novel coronavirus directly from the clinical specimens is the universal coronavirus primer PCR[50]. Enrichment of viral nucleic acids is a prerequisite for the use of sequence-independent amplification strategies like VIDISCA and random PCR. This can be achieved by selective purification e.g. by ultracentrifugation or centrifugation/filtration, or by selective amplification of viral RNA, e.g. by using non-ribosomal random hexamer primers[2,45,11].

Expert commentary

Given the recent explosion in the number of newly identified human coronaviruses (2003 – SARS-CoV, 2004 – HCoV-NL63, 2005 – HCoV-HKU1), one wonders whether we currently know the complete arsenal of coronaviral pathogens. The SARS case demonstrated that new invaders can come from the animal kingdom via a zoonotic transfer. There are 25 known animal coronavirus species, including mammals and birds, of which 10 were identified in the last year. This means that the count is not finished yet, and we should be aware of new introductions. A curious aspect of coronavirus pathology is the almost exclusive link to respiratory diseases in humans, whereas coronaviruses can also cause enteric, cardiovascular and neurological disorders in animals[20,23]. Thus, one should keep an open eye for such symptoms and disease correlations in humans. Finally, coronaviruses are commonly addressed as common cold viruses except for SARS-CoV. This neglects the disease course frequently seen in young children, which can be much more serious, although usually not life-threatening. This necessitates the further improvement of diagnostic tools and warrants the development of antiviral drugs.

Five-year view

Significant progress in the field of human coronaviruses has been made within the last 3 years. This includes the identification of three novel coronaviruses, of which two (HCoV-NL63 and HCoV-HKU1) have been circulating in humans for many years, whereas the third one (SARS-CoV) was recently introduced from an animal reservoir. As the search is in progress, we might expect the identification of more, previously unknown human coronaviruses in the coming years. It would be important to perform a broad virus search of clinical samples derived from different tissues, e.g. gastrointestinal tract or the central nervous system. The further improvement of nucleic acid purification and amplification methods will accelerate virus discovery programs and might result in the identification of new viral species that are characterized by a low virus load, e.g. in chronically infected patients.

Several reports have described broad anti-coronaviral drugs, but at present there are no commercially available wide spectrum agents. To prepare for a possible zoonotic transfer of animal coronaviruses, emphasis should be put on the identification and commercialization of such compounds.

References

1. Adachi, D., G. Johnson, R. Draker, M. Ayers, T. Mazzulli, P. J. Talbot, and R. Tellier. 2004. Comprehensive detection and identification of human coronaviruses, including the SARS-associated coronavirus, with a single RT-PCR assay. J. Virol. Methods 122:29-36.
2. Allander, T., S. U. Emerson, R. E. Engle, R. H. Purcell, and J. Bukh. 2001. A virus discovery method incorporating DNase treatment and its application to the identification of two bovine parvovirus species. Proc Natl Acad Sci U S A 98:11609-11614.
3. Allander, T., M. T. Tammi, M. Eriksson, A. Bjerkner, A. Tiveljung-Lindell, and B. Andersson. 2005. Cloning of a human parvovirus by molecular screening of respiratory tract samples. Proc. Natl. Acad. Sci. U. S. A 102:12891-12896.
4. Almeida, J. D. and D. A. Tyrrell. 1967. The morphology of three previously uncharacterized human respiratory viruses that grow in organ culture. J Gen Virol 1:175-178.
5. Arden, K. E., M. D. Nissen, T. P. Sloots, and I. M. Mackay. 2005. New human coronavirus, HCoV-NL63, associated with severe lower respiratory tract disease in Australia. J. Med. Virol. 75:455-462.
6. Bachem, C. W., R. S. van der Hoeven, S. M. de Bruijn, D. Vreugdenhil, M. Zabeau, and R. G. Visser. 1996. Visualization of differential gene expression using a novel method of RNA fingerprinting based on AFLP: analysis of gene expression during potato tuber development. Plant J 9:745-753.
7. Boivin, G., M. Baz, S. Cote, R. Gilca, C. Deffrasnes, E. Leblanc, M. G. Bergeron, P. Dery, and G. De Serres. 2005. Infections by human coronavirus-NL in hospitalized children. Pediatr. Infect. Dis. J. 24:1045-1048.
8. Brian, D. A. and R. S. Baric. 2005. Coronavirus genome structure and replication. Curr. Top. Microbiol. Immunol. 287:1-30.
9. Chiu, S. S., K. H. Chan, K. W. Chu, S. W. Kwan, Y. Guan, L. L. Poon, and J. S. Peiris. 2005. Human coronavirus NL63 infection and other coronavirus infections in children hospitalized with acute respiratory disease in Hong Kong, China. Clin. Infect. Dis. 40:1721-1729.
10. Drosten, C., S. Gunther, W. Preiser, S. van der Werf, H. R. Brodt, S. Becker, H. Rabenau, M. Panning, L. Kolesnikova, R. A. Fouchier, A. Berger, A. M. Burguiere, J. Cinatl, M. Eickmann, N. Escriou, K. Grywna, S. Kramme, J. C. Manuguerra, S. Muller, V. Rickerts, M. Sturmer, S. Vieth, H. D. Klenk, A. D. Osterhaus, H. Schmitz, and H. W. Doerr. 2003. Identification of a novel coronavirus in patients with severe acute respiratory syndrome. N. Engl. J. Med. 348:1967-1976.
11. Endoh, D., T. Mizutani, R. Kirisawa, Y. Maki, H. Saito, Y. Kon, S. Morikawa, and M. Hayashi. 2005. Species-independent detection of RNA virus by representational difference analysis using non-ribosomal hexanucleotides for reverse transcription. Nucleic Acids Res. 33:e65.
12. Escutenaire, S., N. Mohamed, M. Isaksson, P. Thoren, B. Klingeborn, S. Belak, M. Berg, and J. Blomberg. 2006. SYBR Green real-time reverse transcription-polymerase chain reaction assay for the generic detection of coronaviruses. Arch. Virol.
13. Esper, F., E. D. Shapiro, C. Weibel, D. Ferguson, M. L. Landry, and J. S. Kahn. 2005. Association between a novel human coronavirus and Kawasaki disease. J. Infect. Dis. 191:499-502.
14. Esper, F., C. Weibel, D. Ferguson, M. L. Landry, and J. S. Kahn. 2005. Evidence of a novel human coronavirus that is associated with respiratory tract disease in infants and young children. J. Infect. Dis. 191:492-498.
15. Esper, F., C. Weibel, D. Ferguson, M. L. Landry, and J. S. Kahn. 2006. Coronavirus HKU1 infection in the United States. Emerg. Infect. Dis. 12:775-779.
16. Fouchier, R. A., N. G. Hartwig, T. M. Bestebroer, B. Niemeyer, J. C. de Jong, J. H. Simon, and A. D. Osterhaus. 2004. A previously undescribed coronavirus associated with respiratory disease in humans. Proc. Natl. Acad. Sci. U. S. A 101:6212-6216.

17. Gerna, G., G. Campanini, F. Rovida, E. Percivalle, A. Sarasini, A. Marchi, and F. Baldanti. 2006. Genetic variability of human coronavirus OC43-, 229E-, and NL63-like strains and their association with lower respiratory tract infections of hospitalized infants and immunocompromised patients. J. Med. Virol. 78:938-949.
18. Gerna, G., P. M. Cereda, M. G. Revello, E. Cattaneo, M. Battaglia, and M. T. Gerna. 1981. Antigenic and biological relationships between human coronavirus OC43 and neonatal calf diarrhoea coronavirus. J. Gen. Virol. 54:91-102.
19. Gonzalez, J. M., P. Gomez-Puertas, D. Cavanagh, A. E. Gorbalenya, and L. Enjuanes. 2003. A comparative sequence analysis to revise the current taxonomy of the family *Coronaviridae*. Arch. Virol. 148:2207-2235.
20. Guy, J. S., J. J. Breslin, B. Breuhaus, S. Vivrette, and L. G. Smith. 2000. Characterization of a coronavirus isolated from a diarrheic foal. J. Clin. Microbiol. 38:4523-4526.
21. Hamre, D. and J. J. Procknow. 1966. A new virus isolated from the human respiratory tract. Proc. Soc. Exp. Biol. Med. 121:190-193.
22. Hasony, H. J. and M. R. MacNaughton. 1982. Serological relationships of the subcomponents of human coronavirus strain 229E and mouse hepatitis virus strain 3. J. Gen. Virol. 58:449-452.
23. Holmes, K. V. and M. M. C. Lai. 1996. *Coronaviridae*: The viruses and their replication, p. 1075-1093. In B. N. Fields, D. M. Knipe, P. M. Howley, and et al (eds.), Fields Virology. Lippincott-Raven Publishers, Philadelphia.
24. Horzinek, M. C., H. Lutz, and N. C. Pedersen. 1982. Antigenic relationships among homologous structural polypeptides of porcine, feline, and canine coronaviruses. Infect. Immun. 37:1148-1155.
25. Ksiazek, T. G., D. Erdman, C. S. Goldsmith, S. R. Zaki, T. Peret, S. Emery, S. Tong, C. Urbani, J. A. Comer, W. Lim, P. E. Rollin, S. F. Dowell, A. E. Ling, C. D. Humphrey, W. J. Shieh, J. Guarner, C. D. Paddock, P. Rota, B. Fields, J. DeRisi, J. Y. Yang, N. Cox, J. M. Hughes, J. W. LeDuc, W. J. Bellini, and L. J. Anderson. 2003. A novel coronavirus associated with severe acute respiratory syndrome. N. Engl. J. Med. 348:1953-1966.
26. Lau, S. K., P. C. Woo, K. S. Li, Y. Huang, H. W. Tsoi, B. H. Wong, S. S. Wong, S. Y. Leung, K. H. Chan, and K. Y. Yuen. 2005. Severe acute respiratory syndrome coronavirus-like virus in Chinese horseshoe bats. Proc. Natl. Acad. Sci. U. S. A 102:14040-14045.
27. Liang, P. and A. B. Pardee. 1992. Differential display of eukaryotic messenger RNA by means of the polymerase chain reaction. Science 257:967-971.
28. Lu, Y., S. Y. Wang, and J. M. Lotz. 2004. The use of differential display to isolate viral genomic sequence for rapid development of PCR-based detection methods. A test case using Taura syndrome virus. J Virol Methods 121:107-114.
29. McIntosh, K., W. B. Becker, and R. M. Chanock. 1967. Growth in suckling-mouse brain of "IBV-like" viruses from patients with upper respiratory tract disease. Proc. Natl. Acad. Sci. U. S. A 58:2268-2273.
30. McIntosh, K., R. K. Chao, H. E. Krause, R. Wasil, H. E. Mocega, and M. A. Mufson. 1974. Coronavirus infection in acute lower respiratory tract disease of infants. J. Infect. Dis. 130:502-507.
31. McIntosh, K., J. H. Dees, W. B. Becker, A. Z. Kapikian, and R. M. Chanock. 1967. Recovery in tracheal organ cultures of novel viruses from patients with respiratory disease. Proc Natl Acad Sci U S A 57:933-940.
32. Moes, E., L. Vijgen, E. Keyaerts, K. Zlateva, S. Li, P. Maes, K. Pyrc, B. Berkhout, L. van der Hoek, and M. Van Ranst. 2005. A novel pancoronavirus RT-PCR assay: frequent detection of human coronavirus NL63 in children hospitalized with respiratory tract infections in Belgium. BMC. Infect. Dis. 5:6.
33. Peiris, J. S., Y. Guan, and K. Y. Yuen. 2004. Severe acute respiratory syndrome. Nat. Med. 10:S88-S97.
34. Peiris, J. S., S. T. Lai, L. L. Poon, Y. Guan, L. Y. Yam, W. Lim, J. Nicholls, W. K. Yee, W. W. Yan, M. T. Cheung, V. C. Cheng, K. H. Chan, D. N. Tsang, R. W. Yung, T. K. Ng, and K. Y. Yuen. 2003. Coronavirus as a possible cause of severe acute respiratory syndrome. Lancet 361:1319-1325.
35. Pensaert, M. B., P. Debouck, and D. J. Reynolds. 1981. An immunoelectron microscopic and immunofluorescent study on the antigenic relationship between the coronavirus-like agent, CV 777, and several coronaviruses. Arch. Virol. 68:45-52.
36. Reed, S. E. 1984. The behaviour of recent isolates of human respiratory coronavirus *in vitro* and in volunteers: evidence of heterogeneity among 229E-related strains. J. Med. Virol. 13:179-192.

37. Sloots, T. P., P. McErlean, D. J. Speicher, K. E. Arden, M. D. Nissen, and I. M. Mackay. 2006. Evidence of human coronavirus HKU1 and human bocavirus in Australian children. J. Clin. Virol. 35:99-102.
38. St Jean, J. R., H. Jacomy, M. Desforges, A. Vabret, F. Freymuth, and P. J. Talbot. 2004. Human respiratory coronavirus OC43: genetic stability and neuroinvasion. J. Virol. 78:8824-8834.
39. Stephensen, C. B., D. B. Casebolt, and N. N. Gangopadhyay. 1999. Phylogenetic analysis of a highly conserved region of the polymerase gene from 11 coronaviruses and development of a consensus polymerase chain reaction assay. Virus Res. 60:181-189.
40. Sun, Z. F. and X. J. Meng. 2004. Antigenic cross-reactivity between the nucleocapsid protein of severe acute respiratory syndrome (SARS) coronavirus and polyclonal antisera of antigenic group I animal coronaviruses: implication for SARS diagnosis. J. Clin. Microbiol. 42:2351-2352.
41. Thiel, V., J. Herold, B. Schelle, and S. G. Siddell. 2001. Infectious RNA transcribed *in vitro* from a cDNA copy of the human coronavirus genome cloned in vaccinia virus. J. Gen. Virol. 82:1273-1281.
42. Tyrrell, D. A. and J. D. Almeida. 1967. Direct electron-microscopy of organ culture for the detection and characterization of viruses. Arch. Gesamte Virusforsch. 22:417-425.
43. Tyrrell, D. A. and M. L. Bynoe. 1965. Cultivation of a novel type of common-cold virus in organ cultures. Br. Med. J. 5448:1467-1470.
44. Vabret, A., J. Dina, S. Gouarin, J. Petitjean, S. Corbet, and F. Freymuth. 2006. Detection of the new human coronavirus HKU1: a report of 6 cases. Clin. Infect. Dis. 42:634-639.
45. van der Hoek, L., K. Pyrc, M. F. Jebbink, W. Vermeulen-Oost, R. J. Berkhout, K. C. Wolthers, P. M. Wertheim-van Dillen, J. Kaandorp, J. Spaargaren, and B. Berkhout. 2004. Identification of a new human coronavirus. Nat. Med. 10:368-373.
46. van der Hoek, L., K. Sure, G. Ihorst, A. Stang, K. Pyrc, M. F. Jebbink, G. Petersen, J. Forster, B. Berkhout, and K. Uberla. 2005. Croup is associated with the novel coronavirus NL63. PLoS. Med. 2:e240.
47. van Doornum, G. J. and J. C. de Jong. 1998. Rapid shell vial culture technique for detection of enteroviruses and adenoviruses in fecal specimens: comparison with conventional virus isolation method. J Clin Microbiol. 36:2865-2868.
48. Wang, D., L. Coscoy, M. Zylberberg, P. C. Avila, H. A. Boushey, D. Ganem, and J. L. DeRisi. 2002. Microarray-based detection and genotyping of viral pathogens. Proc Natl Acad Sci U S A 99:15687-15692.
49. Wang, D., A. Urisman, Y. T. Liu, M. Springer, T. G. Ksiazek, D. D. Erdman, E. R. Mardis, M. Hickenbotham, V. Magrini, J. Eldred, J. P. Latreille, R. K. Wilson, D. Ganem, and J. L. DeRisi. 2003. Viral discovery and sequence recovery using DNA microarrays. PLoS. Biol. 1:E2.
50. Woo, P. C., S. K. Lau, C. M. Chu, K. H. Chan, H. W. Tsoi, Y. Huang, B. H. Wong, R. W. Poon, J. J. Cai, W. K. Luk, L. L. Poon, S. S. Wong, Y. Guan, J. S. Peiris, and K. Y. Yuen. 2005. Characterization and complete genome sequence of a novel coronavirus, coronavirus HKU1, from patients with pneumonia. J. Virol. 79:884-895.

Chapter XII

VIDISCA analyses of untypable picornaviruses reveals two novel human type B enteroviruses and one novel rhinovirus

Submitted for Publication

Krzysztof Pyrc[1], Ron Berkhout[2], Wilma Vermeulen-Oost[2], Ronald Dijkman[1], Maarten F. Jebbink[1], Sylvia Bruisten[2], Ben Berkhout[1], Paul Gruteke[2] and Lia van der Hoek[1]

[1]Laboratory of Experimental Virology, Department of Medical Microbiology, Center of Infection and Immunity Amsterdam (CINIMA), Academic Medical Center, University of Amsterdam, Meibergdreef 15, 1105 AZ, Amsterdam, The Netherlands. [2] Public Health Laboratory, Municipal Health Service, Nieuwe Achtergracht 100, 1018 WT, Amsterdam, The Netherlands.

The quality and sensitivity of diagnostic assays for the identification of viral infection are constantly improving. Nevertheless, several viruses are still missed during the standard diagnostic screening process and there is a need for a broad range virus detection assay. Previously, we developed the VIDISCA method and demonstrated its potency for identification of known and new virus species. In this study, cell culture combined with VIDISCA led to the identification of three novel human pathogens in samples from patients suffering from illness with unknown etiology. All three viruses belong to the *Picornaviridae* family and a detailed study including serotyping and phylogenetic sequence analysis indicates that they constitute previously unknown types. The identified viruses were named human rhinovirus (HRV) AMS323, and the two human echoviruses (EV) AMS573 and AMS721. This report shows that the VIDISCA method is a valuable tool for the detection and typing of pathogens that could not be typed by conventional diagnostic methods.

Introduction

To date, there remain a variety of human diseases with unknown etiology, including chronic diseases like amyotrophic lateral sclerosis (ALS) and multiple sclerosis (MS), but also acute infections like Kawasaki disease and several respiratory diseases[8,10]. A viral origin has been suggested for many of these diseases, emphasizing the importance of a continuous search for new viruses.

Previously, we identified the novel pathogen human coronavirus NL63 using the VIDISCA method (Virus Discovery based on cDNA-AFLP)[5,34]. We developed this technique to identify unknown viral pathogens in samples derived from infected individuals (e.g. in serum, plasma, respiratory washes, urine) or virus culture supernatant. The main advantage of VIDISCA is that prior knowledge of the nucleotide sequence of the viral genome is not required as the presence of frequently occurring restriction enzyme sites is sufficient to guarantee PCR amplification[34].

The *Picornaviridae* family is comprised of icosahedral, non-enveloped viruses with a positive stranded RNA genome. Picornaviruses are among the most diverse species (more than 200 types) and the family is classified into six genera: rhinoviruses, enteroviruses, aphthoviruses, cardioviruses, hepatoviruses and parechoviruses. The picornaviral RNA genome ranges in size from 7.2kb (human rhinovirus 14) to 8.5kb (foot and mouth disease virus). The genome has several characteristic and conserved features, including a single open reading frame encoding the polyprotein (2100 – 2400 amino acids (aa)) and extended untranslated regions on both termini. The 5′ end of the genomic RNA is protected by the covalently attached small, basic protein VPg and the 3′ end is polyadenylated[9,19,21]. The picornaviral polyprotein encompasses four capsid proteins (VP1 to VP4) and seven non-structural proteins, including polymerase (3D), proteases (3C and 2A) and the genome-linked VPg protein (3B), which are released from the polyprotein

by co- and post-translational cleavage by the viral proteases[1,2]. Here we report the identification of three novel types of picornaviruses: rhinovirus AMS323 and echoviruses AMS573 and AMS721.

Methods

Patient samples

Clinical samples from hospitals were referred to the Municipal Public Health Laboratory Amsterdam. Fecal and throat swab samples were stored at 4°C in vials before being transported to the laboratory at ambient temperature. The nasopharyngeal lavage specimens were transported in virus transport medium containing Eagle minimum essential medium (MEM) in Hanks balanced salt solution (BSS) with antibiotics (20,000 U/ml penicillin; 20,000 μl/ml streptomycin).

In case of respiratory symptoms, the patient's material was tested for the presence of RSV, adenovirus, influenza A and B virus, and parainfluenza virus type 1, 2 and 3 using the Virus Respiratory Kit (Bartels: Trinity Biotech plc, Wicklow Ireland) and additionally for RSV with ImagenTM RSV (DakoCytomation). Furthermore, PCR tests for rhinoviruses, enterovirus (HEV) and metapneumovirus were performed as described[13].

Nasopharyngeal lavage specimen S323 was diluted 1:1 with Hanks BSS with 5% gelatin. Throat swab sample S721 was inoculated on cells without pre-treatment. Approximately 2 to 3 g of feces sample S573 was suspended in 10 ml of Eagle MEM in Hanks BSS with 5% gelatin. The sample was shaken vigorously with glass pearls (about 10% volume of the sample) to promote fragmentation. After centrifugation at 700g for 5min at 25°C, supernatants were filtered (pore diameter, 0.20μm) and inoculated on a cell monolayer.

Cell culture infections

Respiratory samples S323 and S721 were inoculated on human fetal lung fibroblasts (HFL), tertiary Cynomolgus monkey kidney cells (tMK; RIVM, Bilthoven, the Netherlands), epithelial monkey kidney cell line (LLC-MK2), epithelial canine kidney cell line (MDCK) and a modified human cervical carcinoma cell line (RHeLa). All cultures were incubated at 34°C, but a duplicate HFL culture was also incubated at 37°C. Fecal sample S573 was inoculated onto HFL cells, tMK cells, colorectal adenocarcinoma epithelial cell lines (CaCo2 and HT-29) and rhabdomyosarcoma (Rd) cell line. Culturing was performed at 37°C and the medium was replenished every 3 to 4 days.

Prior to specimen inoculation, medium was removed from the cells and 0.4ml of the specimen was inoculated in duplicate cell cultures. Fresh medium was added after 2h of infection and the cultures were kept in a rollerdrum at 34°C or 37°C and inspected for cytopathic effect (CPE) every 3 to 4 days.

Two types of medium were used: Optimem 1 (Invitrogen, Breda, The Netherlands) for the MDCK, LLC-MK2 and tMK cells. In all other cultures MEM Hank's / Earle's (2:1) medium (Invitrogen, Breda, The Netherlands) with 3% inactivated fetal bovine serum (FBS; Cambrex Bio Science, Verviers, Belgium). Both media were supplemented with vancomycin (0.1mg/ml) and streptomycin (0.1mg/ml) (Duchefa Biochemie, Haarlem, the Netherlands).

Diagnostic assays and picornavirus typing

Shell vial cell cultures infected with S323 and S721 were analyzed by direct staining with pools of fluorescent-labeled mouse antibodies against RSV (RHeLa culture; ImagenTM RSV, DakoCytomation, Ely, UK) and influenza type A/B viruses (tMK cell culture; ImagenTM Influenza virus, DakoCytomation). Indirect staining was performed for parainfluenza 1/2/3 viruses (tMK cell culture; monoclonal mouse anti-parainfluenza 1/2/3, Chemicon International, Temecula, USA, in combination with polyclonal rabbit anti-mouse Ig/FITC, DakoCytomation), CMV virus (HFL culture; monoclonal mouse anti-CMV, DakoCytomation in combination with polyclonal rabbit anti-mouse Ig/FITC, DakoCytomation) and adenovirus (RheLa cell culture; monoclonal mouse anti-adenovirus, Chemicon International, in combination with polyclonal rabbit anti-mouse Ig/FITC, DakoCytomation). S573 infected tMK shell vial culture was analyzed by direct staining for adenovirus (ImagenTM Adenovirus, DakoCytomation) and by indirect staining for enteroviruses (Monoclonal mouse anti-enterovirus, DakoCytomation in combination with polyclonal rabbit anti-mouse Ig/FITC, DakoCytomation).

Acid liability testing was performed to distinguish between enterovirus and rhinovirus[17]. Typing of the enteroviruses was performed with chloroform-treated isolates by neutralization tests with antiserum pools obtained from National Institute of Public Health and the Environment (RIVM, Bilthoven, The Netherlands) for the identification of poliovirus type 1, 2, or 3, echoviruses 1-7, 9, 11-14, 20, 21 - 22, 25, 27, 29, 30, and 33, coxsackievirus B types 1 – 6, as described before[20]. The rhinovirus and enterovirus diagnostic PCR assay was performed as described previously[3,13].

VIDISCA method

VIDISCA of samples S323, S573 and S721 used the culture supernatants from HFL cells, tMK cells and RD cells, respectively. A negative control supernatant from corresponding mock-infected cells was included. VIDISCA was performed as described previously[34]. In short, samples were prepared using one-round centrifugation (14000×g, 10 minutes) and DNase treatment for 45 minutes at 37°C (Ambion; 2U/ml). After this step the sample was lysed in L6 solution (10 minutes at room temperature) and total nucleic acids were isolated using the Boom extraction method[7]. Single stranded RNA was converted to cDNA with reverse transcriptase (MMLV-RT; Invitrogen) using random hexamer DNA primers

(Amersham Biosciences) and the second DNA strand was generated with Sequenase 2.0 (Amersham Biosystems). Double-stranded (ds) cDNA was digested with the MseI and HinP1I restriction enzymes and dsDNA anchors (HinP1-I anchor: 5′-GACGATGAGTCCTGAC-3′ and 5′-CGGTCAGGACTCAT-3′. Mse I anchor: 5′-CTCGTAGACTGCGTACC-3′ and 5′-TAGGTACGCAGTC-3′.) were ligated to the fragments (Ligase; Invitrogen) as described previously[34]. Further amplification was performed with the anchor-specific primers (First PCR primer set: HinP1-I standard primer 5′-GACGATGAGTCCTGACCGC-3′ and Mse I standard primer 5′-CTCGTAGACTGCGTACCTAA-3′. Second PCR primerset: HinP1-I-A: 5′-GACGATGAGTCCTGACCGCA-3′; HinP1-I-T: 5′-GACGATGAGTCCTGACCGCT-3′; HinP1-I-C: 5′-GACGATGAGTCCTGACCGCC-3′; HinP1-I-G: 5′-GACGATGAGTCCTGACCGCG-3′; MseI-A: 5′-CTCGTAGACTGCGTACCTAAA-3′; MseI-T: 5′-CTCGTAGACTGCGTACCTAAT-3′; MseI-C: 5′-CTCGTAGACTGCGTACCTAAC-3′; MseI-G: 5′-CTCGTAGACTGCGTACCTAAG-3′.) in a two-step PCR amplification[34]. PCR fragments present in the infected sample, but not the control sample, were subsequently sequenced.

cDNA libraries and complete genome sequencing

cDNA libraries were generated as described by Marra *et al*[28] with minor modifications. Random hexamer primers instead of the oligo-dT primer were used for reverse transcription and the amplified cDNA was cloned into the PCR2.1-TOPO TA cloning vector (Invitrogen). Transformed bacterial colonies were collected and suspended in LB medium, which was used as input for PCR amplification with vector-specific primers (T7 and M13RP). The PCR products were subsequently sequenced. Sequencing was performed on an ABI 3700 machine (Perkin-Elmer Applied Biosystems) using the BigDye terminator cycle sequencing kit (version 1.1) and T7 and M13RP primers. Chromatogram sequence files were inspected and assembled with CodonCode 1.4 and further corrected manually.

Sequence analysis

Sequences of the PCR-amplified fragments were compared to sequences deposited in the GenBank database using the BLAST tool (NCBI; http://www.ncbi.nlm.nih.gov/blast). Sequences were aligned using the ClustalX software[32,33] package with the following settings: gap opening penalties: 10.00; gap extension penalty 0.20; delay divergent sequences switch at 30% and transition weight 0.5[32]. Phylogenetic analysis was carried out using the neighbor-joining method of the MEGA program[22]. The nucleotide distance matrix was generated by Kimura's 2 parameter estimation. Bootstrap resampling (1000 replicates) was employed to place approximate confidence limits on individual branches. The similarity analysis on the full genome scale was performed with the SimPlot 2.5 software[25] using Kimura 2-parameter distance model. The window used was 200 nt, with a step size of 20nt. The coding regions in the genomes were identified using the ZCURVE_V tool (http://tubic.tju.edu.cn/Zcurve_V/)[14]. The potential cleavage

sites in the picornaviral polyprotein were identified with the NetPicoRNA 1.0 server available at: http://www.cbs.dtu.dk/services/NetPicoRNA/ and the results were verified by multiple sequence alignment as described previously[6].

Nucleotide sequence accession numbers

The full genome sequences of rhinovirus AMS323, echovirus AMS573 and AMS721 described in this study were deposited in GenBank under accession numbers: EF155421, EF155423 and EF155422, respectively. The accession numbers of the picornaviruses used in the phylogenetic analysis are: AF152253; AY355181 - AY355183; AY355188 - AY355194; AY355196; AY355197; AY355199 - AY355206; AY355209 - AY355215; AY355217; AY355219 - AY355222; AY355224 - AY355228; AY355230 - AY355232; AY355234 - AY355249; AY355252; AY355254 - AY355259; AY355261 - AY355263; AY355266; AY355269; AY355270; AY355271; AY355275 - AY355277; AY355279; AY355281; AF029859; AF039205; AF081485; AF083069; AF114383; AF162711; AF230973; AF233852; AF241360; AF268065; AF311939; AF317694; AJ245864; AJ493062; AY208120; AY302539-AY302560; AY556057; AY556070; AY843297-AY843308; D00627; M16560; M88483; X79047; X80059; X84981

Results

Index patients and microbiological tests

Sample S323 is a nasopharyncheal lavage from a 6-week old boy hospitalized because of stridor, coughing, shortness of breath, and rhinitis. The boy quickly recovered and he was discharged after one day. Sample S573 is the feces of a 4 year and 9 month old boy that experienced stomach aches and vomiting for several months. The patient was subsequently followed in the outpatient clinic and recovered within a month. Sample S721 is a throat swab obtained from a 6 year and 7 month old boy with petechiae and fever that was admitted to the hospital. The patient was treated with intravenous antibiotics and recovered within 4 days. These three cases have in common that all standard diagnostic tests for viral pathogens remained negative.

The three samples were inoculated on different conventional cell cultures depending on the nature of the sample. Sub-culturing of the viral isolates was performed and the replication characteristics of these three isolates on the various cells are summarized in table 1. The cell culture analysis displayed the presence of a viral pathogen, with typical enterovirus / rhinovirus cell tropism and CPE.

Picornavirus typing

None of the tested samples displayed decreased infectivity after chloroform treatment, suggesting the presence of a virus without a lipid envelope. Additionally, the acid stability of samples S573 and S721 is suggestive for enterovirus, while S323 was acid sensitive and thus may be identified as a rhinovirus. S573 and S721 were tested in neutralization assays with antiserum pools directed against poliovirus type

1-3, echovirus 1-7, 9, 11-14, 20-22, 25, 27, 29, 30, 33, coxsackievirus B types 1-6. No virus neutralization was observed with any of the pools.

Identification of a novel type of picornavirus

The VIDISCA method was performed on the three positive cell culture supernatants. As a negative control the supernatants from corresponding uninfected cell cultures were used. Analysis of the PCR products revealed the presence of several sample-specific PCR fragments for all three positive cultures, as presented in figure 1 for the S323 sample on HFL cells. Sequence analysis revealed that the amplified regions share some similarity with known rhinoviruses or enteroviruses, but with relatively low similarity scores. The identified pathogens therefore constitute unknown types of the rhinovirus A group (S323) and the enterovirus B group (S573 and S721). Viruses were named provisionally: HRV-AMS323, EV-AMS573 and EV-AMS721.

Analysis of full-length genome sequences

To further characterize the viruses, we determined the complete genome sequence of the viruses by constructing and sequencing a cDNA library. The three genomes all have the characteristic picornavirus organization, encoding a single polyprotein (HRV-AMS323: 2165aa; EV-AMS573: 2194aa; EV-AMS721: 2196aa) that is predicted to be further cleaved into mature proteins by two proteases ($2A^{pro}$ and CD^{pro}). The polyprotein is divided into three domains: P1, P2, and P3. The P1 domain contains the viral capsid protein and the P2 and P3 domains encode proteins that are involved in protein processing and replication. The predicted cleavage sites and protein organization have been summarized for all three viruses in table 2.

Table 1. Replication characteristics of novel picornaviruses

	EV-AMS721	EV-AMS573	HRV-AMS323
tertiary monkey kidney (tMK)	Rapid non-focal swelling of cells followed by complete detachment within a few days	Slow non-focal swelling of cells *not* followed by complete detachment within a week[a]	Slow non-focal vacuolation of cells not followed by complete detachment within a few days
human foetal lung fibroblasts (HFL)	Non-focal disruption of cells and complete disruption within a week	Non-focal disruption of cells and complete disruption within a week	Focal rhinovirus-like "pearly" rounding of cells followed by complete disruption of cells within a week[a]
CaCo2	No CPE	Slow focal swelling of cells *not* followed by complete detachment within a week	Not tested
HT29	Slow non-focal swelling of cells *not* followed by complete detachment within a week	Rapid non-focal swelling of cells followed by complete detachment within a few days	Not tested
Rhabdomyosarcoma	Rapid non-focal detachment of cells[a]	No CPE	No CPE

[a] VIDISCA was performed on these cultures.

Typing of picornaviruses is generally performed on the sequence of the VP1 / VP2 regions[24] and phylogenetic analysis of the VP1 nucleotide sequence of all three viruses is presented in figure 2. It is not possible to do a comparative analysis of the complete HRV-AMS323 genome, as the complete genome sequence of its closest relative (HRV-65) is not available. Analysis of the VP1 region of HRV-AMS323 is presented in table 3. The distance between HRV-AMS323 and its closest relative HRV-65 in the VP1 region is 84%, which is similar to the distance between known rhinovirus types such as HRV-20 and HRV-68 (85%) and HRV-46 and HRV-80 (82%). Thus, HRV-AMS323 represents a new rhinovirus type.

The distances between the identified enteroviruses and their closest relatives (EV-AMS573 versus EV-21 and EV-AMS721 versus EV-16; 78% and 81% nucleotide similarity, respectively) are of similar magnitude as for established group members (e.g. HEV-96 versus EV-4, HEV-77 versus HEV-84 and swine vesicular disease virus versus coxackievirus 5; 79%; 79% and 80% nucleotide similarity, respectively).

To further analyze the similarity of EV-AMS573 and EV-AMS721 to their closest relatives (EV 21, 25, 30 and 5, 14, 16, respectively) and to show that the new isolates do not represent recombinants, we inspected the full-length genomes using the similarity plot (Figure 3). This analysis demonstrates that both enteroviruses are clearly distinct along the genome from previously described types.

The fact that EV-AMS573 was not neutralized by sera raised against EV-21 further confirms that it represents a novel enterovirus serotype. An antiserum against EV-16 is not included in the routine neutralization assay. To confirm that EV-AMS721 also represents a new serotype, we used a specific EV-16 (strain Harrington) serum (kindly provided by Harrie van der Avoort, RIVM, Bilthoven, The Netherlands). No inhibition of infection was observed, confirming that EV-AMS721 is a novel serotype.

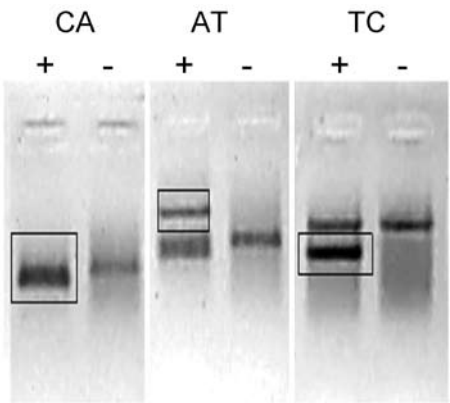


Figure 1. VIDISCA amplification products. Representative DNA fragments resulting from the VIDISCA analysis of the AMS323 sample. The CA, AT and TC marks represent the PCR fragments generated with nested VIDISCA primer combinations (e.g. HinP1 I-C and Mse1-A primers for CA). The '+' and '-' marks represent the infected and control samples, respectively. PCR fragments of viral origin are boxed.

Table 2. Polyprotein organization of HRV-AMS323, EV-AMS573 and EV-AMS721

Resulting protein	Position in the polyprotein			Length [aa]			Protease	Predicted cleavage site		
	323	573	721	323	573	721		323	573	721
VP4	1	1	1	69	69	69	autocl.	GVPTLQ|SPSVE	SLPALN|SPTVE	SMPALN|SPSAE
VP2	70	70	70	262	261	262	$3C^{pro}$	QSVKQ|GLPV	LAGHQ|GLPV	STQHQ|GLPV
VP3	332	331	332	238	238	239	$3C^{pro}$	VNITQ|NPVE	DALYQ|NDPA	DAELQ|GEPG
VP1	570	569	571	296	292	292	2Apro	IKIVNV|GPSDM	TPIRTM|GVFGQ	HNLRTA|GVFGQ
2A	866	861	863	143	150	150	$3C^{pro}$	VADTQ|GITD	DAMEQ|GVKD	DAMEQ|GVKD
2B	1009	1011	1013	95	99	99	$3C^{pro}$	YIHKE|SDGW	MAERQ|NNGW	MAERQ|NNGW
2C	1104	1110	1112	321	329	329	$3C^{pro}$	QAIFQ|GPID	EALFQ|GPPV	EALFQ|GPPV
3A	1425	1439	1441	78	89	89	$3C^{pro}$	FCSLQ|GPYS	FAGFQ|GAYT	FAGFQ|GAYT
3B	1503	1528	1530	21	22	22	$3C^{pro}$	RVVTQ|GPQE	QAKVQ|GPAF	QAKVQ|GPAF
3C	1524	1550	1552	183	183	183	$3C^{pro}$	FNEQQ|GQIV	FNDEQ|GEIE	FNEEQ|GEIE
3D	1707	1733	1735	459	462	462	$3C^{pro}$	-	-	-

Diagnostic assays

The failure of the diagnostic PCR to detect the rhinovirus and enterovirus isolates on the original patient material was further investigated. In table 4 the primers used in the diagnostic assay are presented. The genome sequences to which they anneal were inspected for mismatches. HRV-AMS323 contains several mismatches with the rhinovirus primers (n=3), but we think that this would not explain a negative PCR result. We subsequently tested the culture supernatant in the rhinovirus RT-PCR, and could indeed detect the virus with these primers (data not shown). EV-AMS573 and EV-AMS721 did not display mismatches with the enterovirus consensus primers (table 4), and the enterovirus PCR should be able to amplify the genome of both viruses. Indeed, the EV-AMS573 positive culture yielded a positive PCR product, but EV-AMS721 produced only a faint signal (data not shown). We hypothesize that a low copy number of the viruses in the original patient material, in case of HRV-AMS323 and EV-AMS573, explains the negative result in the initial diagnostic screen, but we have no explanation for the weak amplification of EV-AMS721.

Discussion

We report the characterization and complete genome sequence of three novel picornaviruses detected in a nasopharyngeal aspirate (S323), throat swab (S721) and feces (S573) of hospitalized patients. All three samples remained negative in the standard diagnostic assays for the detection of enteroviruses and rhinoviruses, but the cell culture revealed a development of characteristic viral CPE. Therefore, the samples were included in the VIDISCA analysis and the recovered PCR fragments displayed similarity to *Picornaviridae* family members.

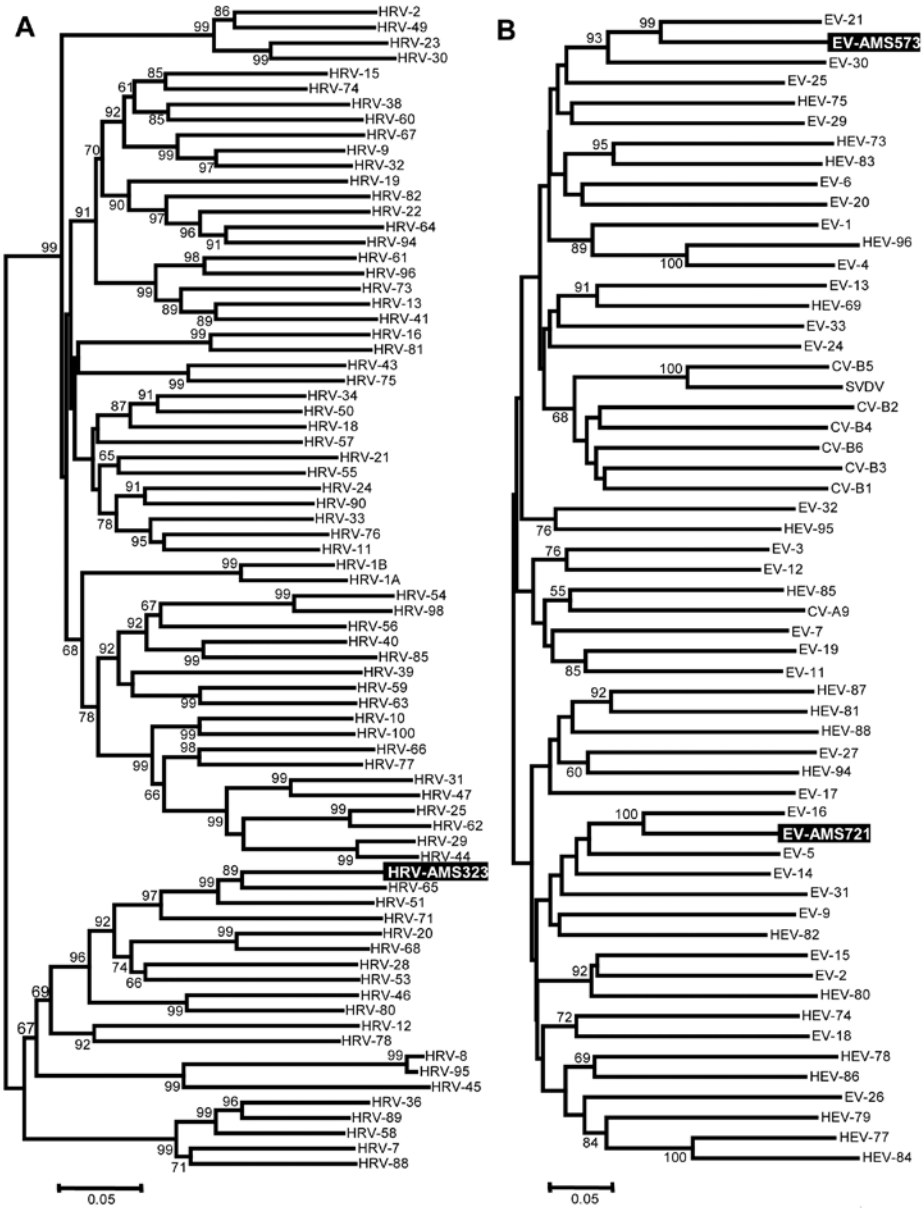


Figure 2. Phylogenetic analysis of the nucleotide sequence of the VP1 region of HRV-AMS323, EV-AMS573 and EV-AMS721. A) Rhinovirus A phylogenetic tree. B) Enterovirus B phylogenetic tree. Phylogenetic trees were constructed as described in the materials and methods. The scale bar unit is equivalent to 0.05 substitutions per site.

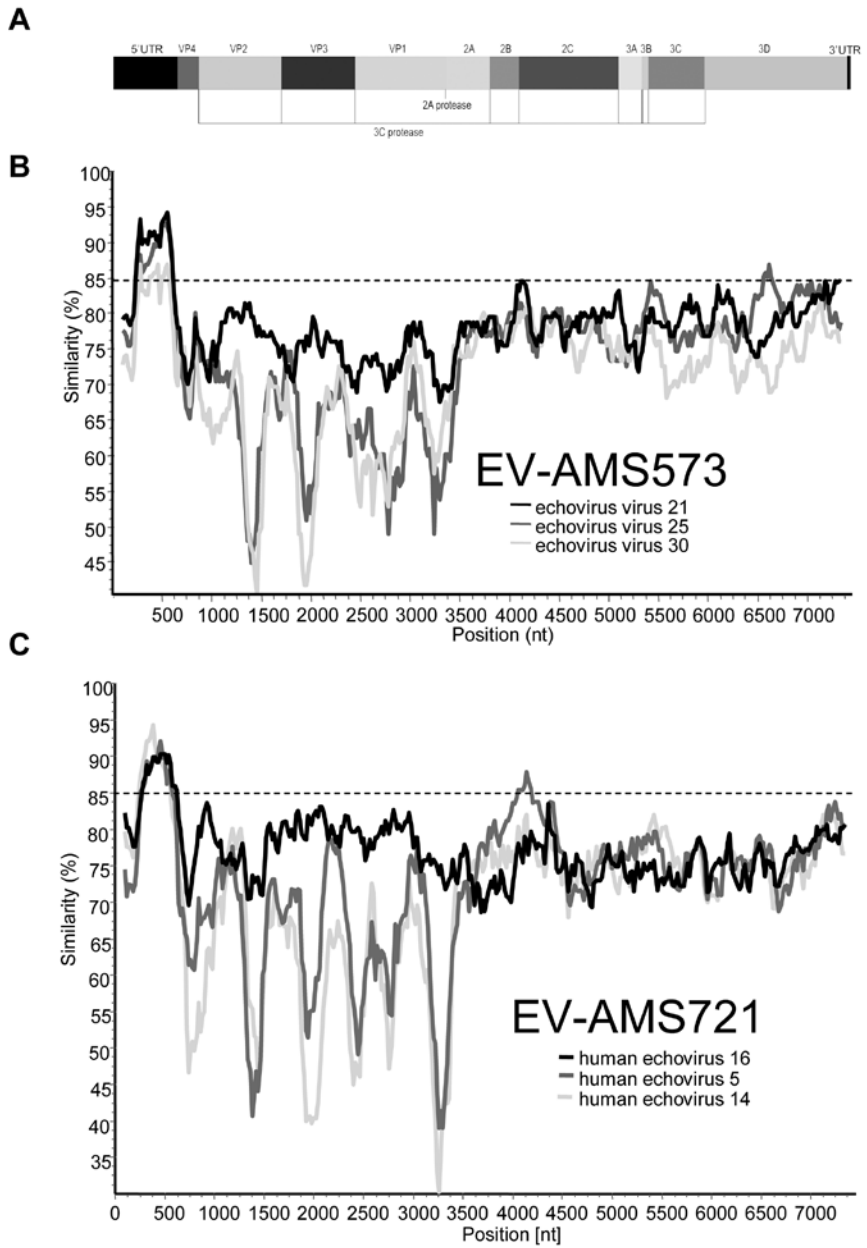


Figure 3. Genome similarity scan of EV-AMS573 and EV-AMS721. A) Genome organization of EV-AMS573. The genome organization of HRV-AMS323 and EV-AMS721 is very similar, the exact characteristics are summarized in Table 3. The vertical lines represent the cleavage sites of the 3C or 2A proteases. B) Similarity plot of EV-AMS573 with the closest relatives EV-21, EV-25 and EV-30. C) Similarity plot of EV-AMS721 with the closest relatives EV-5, EV-14 and EV-16. The analysis was performed with a 200 nt window and 20 nt steps.

Table 3. Nucleotide sequence similarity of HRV-AMS323 VP1 region to other rhinoviruses.

	HRV-AMS323	HRV-65	HRV-51	HRV-71	HRV-68
HRV-AMS323	-	-	-	-	-
HRV-65	84%	-	-	-	-
HRV-51	81%	80%	-	-	-
HRV-71	76%	76%	75%	-	-
HRV-68	72%	72%	72%	71%	-
HRV-20	71%	70%	71%	71%	85%

Table 4. Consensus rhinovirus and enterovirs primers versus HRV-AMS323, EV-AMS573 and EV-AMS721

Primer	Target	Sequence
NCR1outse	Consensus rhinovirus	CGGTAATTTTGTACGCCAGTTT
	HRV-AMS323[a]	CGGTATGTTTGCACGCCAGTTT
NCR2outse	Consensus rhinovirus	GAAACACGGACACCCAAAGTAGT
	HRV-AMS323	GAAACACGGACACCCAAAGTAGT
NCR3innse	Consensus rhinovirus	CAAGCACTTCTGTTTCCCCGG
	HRV-AMS323	CAAGCACTTCTGTTACCCCGG
NCR4innse	Consensus rhinovirus	CATTCAGGGGCCGGAGGA
	HRV-AMS323	CATTCAGGGGCCGGAGGA
Fox AB out se	Consensus enterovirus	GGTGYGAAGAGYCTAYTGAGCT
	EV-AMS573	GGTGCGAAGAGTCTATTGAGCT
	EV-AMS721	GGTGTGAAGAGTCTATTGAGCT
Srent 2 out as	Consensus enterovirus	CACCGGATGGCCAATCCA
	EV-AMS573	CACCGGATGGCCAATCCA
	EV-AMS721	CACCGGATGGCCAATCCA
Srent 3 inn se	Consensus enterovirus	CCCCTGAATGCGGCTAAT
	EV-AMS573	CCCCTGAATGCGGCTAAT
	EV-AMS721	CCCCTGAATGCGGCTAAT
Srent 4 inn as	Consensus enterovirus	ATTGTCACCATAAGCAGCCA
	EV-AMS573	ATTGTCACCATAAGCAGCCA
	EV-AMS721	ATTGTCACCATAAGCAGCCA

[a] Mismatches of consensus primers with HRV-AMS323 sequence are marked with black boxes.

The clinical significance of these viruses remains unknown, but the absence of other known pathogens may cautiously link these viruses to the symptoms that caused hospitalization. For HRV-AMS323, we identified an additional infected patient (data not shown) illustrating that infection is not rare and that the virus is circulating in the human population.

The group of enteroviruses comprise a large group of over 70 serotypes that are ubiquitous in nature, infecting different hosts and causing a wide range of diseases. Human enteroviruses are classified into five species, human enterovirus A–D and poliovirus. Enterovirus typing is traditionally carried out by neutralisation with antiserum pools and verified by individual type-specific antisera. The lack of EV-AMS573 and EV-AMS721 neutralization with antisera that are specific for the closest phylogenetic relatives, echovirus 21 and echovirus 16, respectively, indicates that these two pathogens constitute new serotypes. Recently, molecular typing has become more common as a tool for enterovirus typing[16,18,29]. This approach is based on sequencing of the capsid-encoding VP1 genome region[29,31]. The phylogenetic analysis of echoviruses AMS573 and AMS721 confirms that both viruses are clearly distinct from their closest relatives.

Enteroviruses cause a wide range of clinical manifestations. Fever is noted, although some infants also develop irritability, lethargy, poor feeding, vomiting, diarrhea, exanthema, or signs of upper respiratory tract infection[12,27]. Furthermore, enteroviruses can cause severe neurological disorders e.g. meningitis[23], foot-hand-and-mouth disease[15], acute haemorrhagic conjunctivitis[11], multisystem haemorrhagic disease of newborns, uveitis[26], myalgia, myocarditis[4] and type I diabetes[30]. The patients infected with EV-AMS573 and EV-AMS721 exhibited normal, relatively mild enteroviral infection symptoms.

The group of rhinoviruses comprises 105 serotypes. These viruses show optimal replication at 33°C, reflecting the temperature of the upper airways, and they cause the common cold. The typing of rhinoviruses is generally based on sequence analysis. As presented in figure 2A and table 3, the genetic distance between HRV-AMS323 and its closest relative HRV-65 is sufficiently high to name the virus a new type. Human rhinovirus AMS323 was found in respiratory material of a child with upper respiratory illness, and as no second pathogen was detected, it is likely that HRV-AMS323 infection caused this illness.

Identification of three new members of the *Picornaviridae* family shows the potency of conventional virus culture combined with the recently developed VIDISCA method. VIDISCA provides a quick and efficient method for the identification of unknown pathogens.

References

1. Ambros, V. and D. Baltimore. 1980. Purification and properties of a HeLa cell enzyme able to remove the 5′-terminal protein from poliovirus RNA. J Biol Chem 255:6739-6744.
2. Ambros, V., R. F. Pettersson, and D. Baltimore. 1978. An enzymatic activity in uninfected cells that cleaves the linkage between poliovirion RNA and the 5′ terminal protein. Cell 15:1439-1446.
3. Andeweg, A. C., T. M. Bestebroer, M. Huybreghs, T. G. Kimman, and J. C. de Jong. 1999. Improved detection of rhinoviruses in clinical samples by using a newly developed nested reverse transcription-PCR assay. J Clin Microbiol. 37:524-530.
4. Archard, L. C., P. J. Richardson, E. G. Olsen, V. Dubowitz, C. Sewry, and N. E. Bowles. 1987. The role of Coxsackie B viruses in the pathogenesis of myocarditis, dilated cardiomyopathy and inflammatory muscle disease. Biochem. Soc. Symp. 53:51-62.
5. Bachem, C. W., R. S. van der Hoeven, S. M. de Bruijn, D. Vreugdenhil, M. Zabeau, and R. G. Visser. 1996. Visualization of differential gene expression using a novel method of RNA fingerprinting based on AFLP: analysis of gene expression during potato tuber development. Plant J 9:745-753.
6. Blom, N., J. Hansen, D. Blaas, and S. Brunak. 1996. Cleavage site analysis in picornaviral polyproteins: discovering cellular targets by neural networks. Protein Sci. 5:2203-2216.
7. Boom, R., C. J. Sol, M. M. Salimans, C. L. Jansen, P. M. Wertheim-van Dillen, and J. van der Noordaa. 1990. Rapid and simple method for purification of nucleic acids. J. Clin. Microbiol. 28:495-503.
8. Burgner, D. and A. Harnden. 2005. Kawasaki disease: what is the epidemiology telling us about the etiology? Int. J. Infect. Dis. 9:185-194.
9. Flanegan, J. B., R. F. Petterson, V. Ambros, N. J. Hewlett, and D. Baltimore. 1977. Covalent linkage of a protein to a defined nucleotide sequence at the 5′-terminus of virion and replicative intermediate RNAs of poliovirus. Proc Natl Acad Sci U S A 74:961-965.
10. Fujinami, R. S., M. G. von Herrath, U. Christen, and J. L. Whitton. 2006. Molecular mimicry, bystander activation, or viral persistence: infections and autoimmune disease. Clin. Microbiol. Rev. 19:80-94.
11. Goh, K. T., P. L. Ooi, K. Miyamura, T. Ogino, and S. Yamazaki. 1990. Acute haemorrhagic conjunctivitis: seroepidemiology of coxsackievirus A24 variant and enterovirus 70 in Singapore. J. Med. Virol. 31:245-247.
12. Grist, N. R., E. J. Bell, and F. Assaad. 1978. Enteroviruses in human disease. Prog. Med Virol 24:114-157.
13. Gruteke, P., A. S. Glas, M. Dierdorp, W. B. Vreede, J. W. Pilon, and S. M. Bruisten. 2004. Practical implementation of a multiplex PCR for acute respiratory tract infections in children. J. Clin. Microbiol. 42:5596-5603.
14. Guo, F. B. and C. T. Zhang. 2006. ZCURVE_V: a new self-training system for recognizing protein-coding genes in viral and phage genomes. BMC. Bioinformatics. 7:9.
15. Higgins, P. G. and R. P. Warin. 1967. Hand, foot, and mouth disease. A clinically recognizable virus infection seen mainly in children. Clin. Pediatr. (Phila) 6:373-376.
16. Hughes, A. L. 2004. Phylogeny of the *Picornaviridae* and differential evolutionary divergence of picornavirus proteins. Infect. Genet. Evol. 4:143-152.
17. Hughes, J. H., S. Chema, N. Lin, R. M. Conant, and V. V. Hamparian. 1974. Acid lability of rhinoviruses: loss of C and D antigenicity after treatment at pH 3.0. J Immunol 112:919-925.
18. Ishiko, H., Y. Shimada, M. Yonaha, O. Hashimoto, A. Hayashi, K. Sakae, and N. Takeda. 2002. Molecular diagnosis of human enteroviruses by phylogeny-based classification by use of the VP4 sequence. J. Infect. Dis. 185:744-754.
19. Kapsenberg, J. G. 2006. *Picornaviridae*: The Enteroviruses (Polioviruses, Coxsackieviruses, Echoviruses)., p. 692-722. In P. H. E. H. Lennette and F. A. Murphy (eds.), Laboratory Diagnosis of Infectious Diseases. Principles and Practice, vol. II, Viral, Rickettsial and Chlamydial Diseases. Springer-Verlag, New York.
20. Kitamura, N., B. L. Semler, P. G. Rothberg, G. R. Larsen, C. J. Adler, A. J. Dorner, E. A. Emini, R. Hanecak, J. J. Lee, S. van der Werf, C. W. Anderson, and E. Wimmer. 1981. Primary structure, gene organization and polypeptide expression of poliovirus RNA. Nature 291:547-553.
21. Kumar, S., K. Tamura, and M. Nei. 2004. MEGA3: Integrated software for Molecular Evolutionary Genetics Analysis and sequence alignment. Brief. Bioinform. 5:150-163.

22. Kupila, L., T. Vuorinen, R. Vainionpaa, V. Hukkanen, R. J. Marttila, and P. Kotilainen. 2006. Etiology of aseptic meningitis and encephalitis in an adult population. Neurology 66:75-80.
23. Ledford, R. M., N. R. Patel, T. M. Demenczuk, A. Watanyar, T. Herbertz, M. S. Collett, and D. C. Pevear. 2004. VP1 sequencing of all human rhinovirus serotypes: insights into genus phylogeny and susceptibility to antiviral capsid-binding compounds. J Virol 78:3663-3674.
24. Lee, Y. F., A. Nomoto, B. M. Detjen, and E. Wimmer. 1977. A protein covalently linked to poliovirus genome RNA. Proc Natl Acad Sci U S A 74:59-63.
25. Lole, K. S., R. C. Bollinger, R. S. Paranjape, D. Gadkari, S. S. Kulkarni, N. G. Novak, R. Ingersoll, H. W. Sheppard, and S. C. Ray. 1999. Full-length human immunodeficiency virus type 1 genomes from subtype C-infected seroconverters in India, with evidence of intersubtype recombination. J. Virol. 73:152-160.
26. Lukashev, A. N., V. A. Lashkevich, G. A. Koroleva, J. Ilonen, G. G. Karganova, V. I. Reznik, and A. E. Hinkkanen. 2003. Molecular epidemiology of enteroviruses causing uveitis and multisystem hemorrhagic disease of infants. Virology 307:45-53.
27. Makela, M. J., T. Puhakka, O. Ruuskanen, M. Leinonen, P. Saikku, M. Kimpimaki, S. Blomqvist, T. Hyypia, and P. Arstila. 1998. Viruses and bacteria in the etiology of the common cold. J. Clin. Microbiol. 36:539-542.
28. Marra, M. A., S. J. Jones, C. R. Astell, R. A. Holt, A. Brooks-Wilson, Y. S. Butterfield, J. Khattra, J. K. Asano, S. A. Barber, S. Y. Chan, A. Cloutier, S. M. Coughlin, D. Freeman, N. Girn, O. L. Griffith, S. R. Leach, M. Mayo, H. McDonald, S. B. Montgomery, P. K. Pandoh, A. S. Petrescu, A. G. Robertson, J. E. Schein, A. Siddiqui, D. E. Smailus, J. M. Stott, G. S. Yang, F. Plummer, A. Andonov, H. Artsob, N. Bastien, K. Bernard, T. F. Booth, D. Bowness, M. Czub, M. Drebot, L. Fernando, R. Flick, M. Garbutt, M. Gray, A. Grolla, S. Jones, H. Feldmann, A. Meyers, A. Kabani, Y. Li, S. Normand, U. Stroher, G. A. Tipples, S. Tyler, R. Vogrig, D. Ward, B. Watson, R. C. Brunham, M. Krajden, M. Petric, D. M. Skowronski, C. Upton, and R. L. Roper. 2003. The Genome sequence of the SARS-associated coronavirus. Science 300:1399-1404.
29. Palacios, G., I. Casas, A. Tenorio, and C. Freire. 2002. Molecular identification of enterovirus by analyzing a partial VP1 genomic region with different methods. J. Clin. Microbiol. 40:182-192.
30. Roivainen, M. 2006. Enteroviruses: new findings on the role of enteroviruses in type 1 diabetes. Int. J. Biochem. Cell Biol. 38:721-725.
31. Santti, J., R. Vainionpaa, and T. Hyypia. 1999. Molecular detection and typing of human picornaviruses. Virus Res. 62:177-183.
32. Thompson, J. D., T. J. Gibson, F. Plewniak, F. Jeanmougin, and D. G. Higgins. 1997. The CLUSTAL_ X windows interface: flexible strategies for multiple sequence alignment aided by quality analysis tools. Nucleic Acids Res 25:4876-4882.
33. Thompson, J. D., D. G. Higgins, and T. J. Gibson. 1994. CLUSTAL W: improving the sensitivity of progressive multiple sequence alignment through sequence weighting, position-specific gap penalties and weight matrix choice. Nucleic Acids Res 22:4673-4680.
34. van der Hoek, L., K. Pyrc, M. F. Jebbink, W. Vermeulen-Oost, R. J. Berkhout, K. C. Wolthers, P. M. Wertheim-van Dillen, J. Kaandorp, J. Spaargaren, and B. Berkhout. 2004. Identification of a new human coronavirus. Nat. Med. 10:368-373.

Chapter XIII

Epilogue

Adapted from: Human Coronavirus NL63, a long lost brother
Coronaviruses: Molecular and Cellular Biology, August 2007, p. 295 - 315

Krzysztof Pyrc and Lia van der Hoek.

Laboratory of Experimental Virology, Department of Medical Microbiology, Center for Infection and Immunity Amsterdam (CINIMA), Academic Medical Center, University of Amsterdam, Meibergdreef 15, 1105 AZ, Amsterdam, The Netherlands.

Given the recent explosion in the number of newly identified human viruses (e.g. SARS-CoV, HCoV-NL63, HCoV-HKU1, bocavirus, human metapneumovirus), one wonders whether we currently know the complete arsenal of viral pathogens[1,26,43,61,78,79,86]. Even if most viruses currently circulating in humans are already discovered, the SARS case demonstrated that new invaders can come from the animal kingdom via a zoonotic transfer. This necessitates the further improvement of diagnostic tools.

Currently, several promising methods are available, including the random RT-PCR, differential display and microarrays technology[50,53,82,83]. We developed a novel method VIDISCA based on the common presence of restriction sites in nucleic acids (Chapter II and Appendix A). Identification of four novel viruses (three novel members of the *Picornaviridae* family and a coronavirus) shows the potency of conventional virus culture combined with the VIDISCA method (Chapter II and XII). This technique can be used not only for identification of completely novel pathogens, but also to improve the diagnosis of new virus variants that belong to known virus families.

Generally, the available techniques can be sorted into two groups. One includes techniques that allow sequence independent amplification (VIDISCA, SISPA, random RT-PCR, differential display) and the second group of methods is based on utilization of conserved nucleic acid stretches among viral genomes (microarrays, universal primers). Both approaches have their pros and cons. The weak point of the former group, including VIDISCA, is the low sensitivity. The lower detection cutoff is around 10^5 – 10^6 copies per mL, which is caused by the low efficiency of ligation, which is indispensable for amplification. The random RT-PCR and differential display methods do not employ a ligation procedure, but unfortunately they result in a non-specific and non-reproducible amplification pattern. Therefore, they require extensive cloning and sequencing of multiple samples which should ideally represent the complete set of nucleic acids present in the input sample. The methods that belong to the latter group are more sensitive, but capable only of detecting pathogens that are very similar to the ones previously characterized. This is illustrated by the universal PCR primers described for coronaviruses before identification of SARS-CoV, HCoV-NL63 and HCoV-HKU1. The "old" universal primers have limited capacity to detect these new viruses[71,79]. The microarray technology is facing similar problem, as it is based on hybridization of viral nucleic acids with synthetic oligomers designed in conserved regions of known virus families[82,83]. Therefore, further improvements of nucleic acid purification and amplification methods are needed to accelerate virus discovery programs and to identify new viral species that are present at a low viral load, e.g. in chronic diseases.

The three new picornaviruses described in this thesis (Chapter XII) were identified very recently. Follow-up studies, e.g. on the disease association and prevalence of infection are not available yet. The picture is different for HCoV-NL63. This virus was identified in 2004 (Chapter II), and we managed to study this virus in detail in the subsequent years. The current knowledge on HCoV-NL63 is reviewed in this chapter.

Identification of HCoV-NL63

The first report describing identification of HCoV-NL63 origins from Amsterdam, the Netherlands[79]. The virus was isolated from a nasopharyngeal aspirate, obtained from a 7-month child suffering from coryza, conjunctivitis and fever. All diagnostic tests failed to identify the underlying pathogen, but a cytopathic effect (CPE) was observed on the tertiary monkey kidney cells inoculated with the clinical sample. Furthermore, once the isolate was introduced in an in vitro culture system on the tMK cells, it also produced CPE on LLC-MK2 cells. As all the standard tools failed to identify a pathogen, the cell culture supernatant from LLC-MK2 cells was tested using the VIDISCA method, which revealed presence of nucleic acids displaying sequence similarity to known members of Coronaviridae family. Full genome sequencing and phylogenetic analysis confirmed that the untyped pathogen was a coronavirus constituting a novel species - HCoV-NL63 (Chapter II). Shortly thereafter, a second group from the Netherlands reported the discovery of the same human coronavirus[31]. This latter report describes identification of the virus in a cell culture inoculated with a nose swab collected in 1988 from an 8-month boy suffering from pneumonia. The clinical sample, similar as in the first report, was inoculated on tMK cells and resulted in CPE onset on day 7. After initial isolation on tMK cells, the virus replicated in Vero cells. An electron microscopy study revealed the presence of coronavirus-like particles with an average size of 140nm and average envelope projections of 20nm. Amplification by RAP-PCR yielded HCoV-NL63 PCR fragments.

Interestingly, one year after the publications of both Dutch groups the team of J. Kahn described the identification of essentially the same virus, but with a novel name: New Haven (NH) coronavirus[29]. However, the partial sequences deposited in GenBank show 94% - 100% similarity between the prototype HCoV-NL63 strain and isolates from New Haven. In 2005 HCoV-NL63 was advised as the proper species name by the coronavirus study group of the International Committee on Taxonomy of Viruses (ICTV) executive committee.

Analysis of early coronavirus reports suggests that HCoV-NL63 might have been observed previously. The research on human coronaviruses started in 1965 when B814 coronavirus was isolated from an adult with respiratory illness[76]. In subsequent reports from the 1960's several additional coronavirus isolates were obtained that could be propagated in human embryonic tracheal organ culture.

Of these, only HCoV-229E and HCoV-OC43 were studied during the last decades, whereas the other isolates were lost for follow-up studies (B814, HCoV-OC16, HCoV-OC37, and HCoV-OC48[56,76]). Some of them might have been HCoV-NL63 isolates. Furthermore, in the early 1980's various isolates of human coronaviruses were described that were obtained by cell culture or organ culture (HCoV strains AD, PA, LP, KI, PR, TO, RO, GI, and HO)[45,54,64]. Some of these isolates were termed group II isolates because they were serologically related to HCoV-OC43 (strains RO, GI and HO), whereas others were assigned group I isolates (strains AD, PA, LP, KI, PR, and TO). Of these group I viruses, LP, KI, PR and TO could be cultured in MRC5 continuous cells, but strains AD and PA could only be cultured in human foetal tracheal and nasal organ cultures. This difference in culture characteristics resembles the difference in cell tropism also noticed for HCoV-229E and HCoV-NL63 (Chapter VI). This raises the possibility that some of these group I strains were in fact HCoV-NL63 isolates. Unfortunately, isolates AD and PA were also lost for further study (Phil Minor, personal communication). Therefore, the earliest HCoV-NL63 isolate remains the NL-strain that was obtained from a patient in 1988[31].

Molecular Biology of HCoV-NL63

The HCoV-NL63 genome

The RNA genome encompasses 27535 to 27553 nucleotides (depending on the virus strain). It is predicted to contain seven functional open reading frames and untranslated regions at its 5′ and 3′ ends. The two large 5′ terminal ORFs 1a and 1b encode non-structural proteins that are required for viral replication. The remaining ORFs in the 3′ part of the genome encode the four structural proteins S-E-M-N and one accessory ORF3 protein (Chapter III).

Phylogenetic analysis

HCoV-NL63 is closely related to group I coronaviruses according to phylogenetic analyses (Figure 1). Similarity is the highest with HCoV-229E and porcine epidemic diarrhea virus (PEDV), 65% and 61%, respectively. These three viruses cluster with a recently described bat coronavirus[63] in a subgroup within group I (Ib), excluding transmissible gastroenteritis virus (TGEV), canine enteric coronavirus (CCoV) and feline infectious peritonitis virus (FIPV). But also within the HCoV-NL63 species different phylogenetic subgroups can be identified in the ORF 1a and S (Chapter II). This clustering does not correlate with the geographic location of the patients (Chapter IV). For those patients of which both viral genome regions have been sequenced, a discordant clustering was found[57] indicating recombination between HCoV-NL63 isolates. At present four full genome sequences of HCoV-NL63 are available (Amsterdam 1, NL, A57 and A496). They share ~99% similarity on the nucleotide level. The 5′ region of the 1a gene and the 5′ part of the S gene are the most variable among the different isolates (Chapter V). Analyses of the full-length sequences further supports the

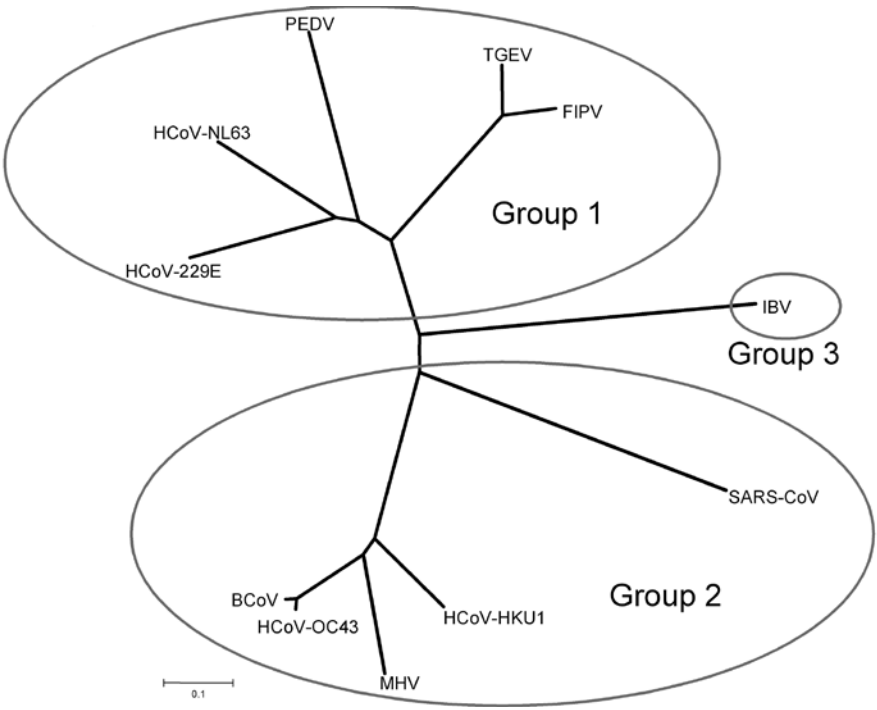


Figure 1. Phylogenetic analysis of the *Coronaviridae* **family.** In the analysis full genome sequences were employed and analysis was done with the Neighbour-joining method and Kimura 2-parameter model.

theory that recombination between HCoV-NL63 isolates occurs (Chapter V). Another region with a unique feature is the M gene. Analysis of the sequence suggests that HCoV-NL63 M is a hybrid protein, which is partially related to 229E M (N-terminus) and partially to PEDV M (C-terminus). This may suggest that even interspecies recombination has taken place (Chapter V).

Transcription

Coronavirus replication is a complex, not yet fully understood mechanism[65,66]. The 5′ end of the HCoV-NL63 genomic RNA contains the untranslated leader sequence of 72 nucleotides that ends with the leader Transcription Regulation Sequence (TRS) element. This leader TRS is very similar to sequences that can be found upstream of each ORF (body TRSs). The RNA-dependent RNA polymerase (RdRp) has been proposed to pause after a body TRS of a particular gene is copied during minus strand synthesis, subsequently switching to the leader TRS and thus adding a common leader sequence to each minus strand subgenomic (sg) mRNA. This discontinuous transcription mechanism is based on base-pairing of the nascent minus strand copy RNA with the plus strand leader TRS. Inspection of sg mRNA junctions of HCoV-NL63 shows that they are composed of the part of the HCoV-NL63 genome that is directly downstream of a particular body TRS,

and a 5′ end derived from the leader sequence. The most conserved TRS region of HCoV-NL63 was defined by multiple sequence alignment as AACUAAA (Chapter III). This core sequence is conserved in almost all sg mRNA. The only exception is the E gene sg mRNA that contains the sub-optimal TRS core AACUAUA. A 13-nucleotide sequence upstream of the E gene core sequence harbours perfect homology to the leader sequence and it was suggested that the upstream sequence compensates for the absence of an optimal TRS core during discontinuous (-) strand synthesis. HCoV-NL63 generates five distinct sg mRNAs during HCoV-NL63 replication, encoding S, ORF3 protein, E, M and N. The 1a/ab polyprotein is supposed to be translated from the genomic RNA. Northern blot analysis revealed that the transcription levels of sg mRNAs of HCoV-NL63 are inversely related to the distance between the body TRS and the 3′ end of the genome (Chapter III).

Translation

The sg mRNAs of S, E, M, N and ORF3 protein are monocistronic, so they encode a single protein. A completely different situation is observed for the large replicase gene. This gene encodes the polyproteins 1a and 1ab. Expression of polyprotein 1ab requires ribosomal frameshifting. Ribosomal frameshifting in coronaviruses was the first described non-retroviral example of translational frameshifting in higher eukaryotes[11]. It is a mechanism of translational regulation in which a directed change of translational reading frame allows the synthesis of a single protein from two overlapping ORFs. In coronaviruses, frameshifting is thought to regulate the level of replicative proteins[10,11]. Coronaviral ribosomal frameshifting is induced by a complex RNA structure called a pseudoknot, consisting of a hairpin of which the loop interacts with a sequence further downstream, and a slippery site upstream of the hairpin[11]. The pseudoknot structure in HCoV-NL63 possesses an extended structure and was therefore called an “elaborated” pseudoknot, similarly to the structure found in HCoV-229E, PEDV and TGEV[3,36,55]. In the HCoV-NL63 genome, the ribosomal frameshift site is located inside the RNA-dependent RNA-polymerase gene. The predicted “elaborated” pseudoknot consists of a hairpin with a highly conserved 11 basepair stem, and a loop of 8 nucleotides that interacts with a sequence 167 nucleotides downstream (with 5 nucleotides basepairing) that is presented on a hairpin structure. The heptanucleotide slippery UUUAAAC sequence is present just upstream of the first hairpin at position nt 12433 (Chapter IV).

Posttranslational modification

Similar to all other coronaviruses, HCoV-NL63 is supposed to employ post-translational proteolytic processing as a key regulatory mechanism in the expression of its replicative proteins[22]. In the genome of HCoV-NL63 three proteinases can be predicted in the 5′ region of the 1a/1ab polyproteins. First, two papain-like proteinases (PL^{pro}s) are encoded in non-structural protein (nsp) 3 (Chapter IV). Analysis of the HCoV-NL63 cleavage sites indicates that HCoV-

NL63-PL^{pro}s cut between two small amino acids with short uncharged side chains, similar to homologous enzymes from other species from the *Coronaviridae* family[51].

The second proteinase of HCoV-NL63 resides in nsp5. It has a predicted serine-like proteinase activity and is designated chymotrypsin-like proteinase or "the main proteinase" (M^{pro}) to stress its dominant function. Analysis of the cleavage sites of HCoV-NL63 M^{pro} reveals an interesting cleavage site change between nsp13 and nsp14. In contrast to most coronaviruses, this cleavage site of HCoV-NL63 contains a histidine residue at position P1 instead of glutamine[30,34,90]. This was observed in four different HCoV-NL63 isolates (Amsterdam 1, A57, A496 and NL), and might suggest altered substrate specificity or the absence of the cleavage site (Chapter IV). For instance, alteration of the consensus M^{pro} cleavage sequence LQ|(A,S,G) for M^{pro} derived from other coronaviruses resulted in significantly reduced cleavage efficiencies in most cases[30,33,90]. Surprisingly, a recent report about HCoV-HKU1 suggest that the HCoV-HKU1 genome harbours the same alteration in nsp13|nsp14 cleavage site[85]. However, HCoV-HKU1 also has a standard cleavage site with the regular glutamine at the P1 position for nsp13/nsp14. This standard site is recognized by the ZCurve_CoV 2.0 software and is located 24 residues amino-terminal of the histidine-containing cleavage site. Future experiments should resolve which site is cleaved by HKU1-M^{pro}.

Entry to the target cell

Cell tropism and receptor usage

The S protein of a coronavirus is a type I membrane glycoprotein that is incorporated into the virion as a surface protein. It mediates attachment and entry into host cells[13] and is synthesized as a 180- to 200kDa protein. The protein can be cleaved by host-derived proteases (e.g. furin)[20,39,70] into two, noncovalently associated subunits S1 and S2. The HCoV-NL63 S protein resembles other group I viral fusion proteins, with its short C-terminal tail inside the virion, single transmembrane domain, rod-like S2 domain and located on top of the S2 domain a globular head consisting of the S1 region (Chapter IV). Receptor binding is mediated by the S1 subunit, while the membrane-anchored S2 portion is required for fusion of viral and cellular membranes.

The HCoV-NL63 S contains a unique N-terminal region (aa position 17-196). This region shows no significant similarity with any other coronavirus or cellular sequence (Chapter II). The origin of the insert is not known, and one might speculate that HCoV-229E lost the 5' region of its S protein, similar to what has been described for porcine respiratory coronavirus and TGEV[46]. This region is also most diverse between HCoV-NL63 isolates on both nucleotide and amino acid level. Furthermore, it contains many glycosylation sites and is immunodominant. Its exact function in virus replication is however unknown.

The receptor specificity among coronaviruses varies between species. This variability is especially visible among group II viruses: MHV uses CAECAM-1[84], HCoV-OC43 and BCoV use O-acetylated sialic acid[81] and SARS-CoV uses angiotensin converting enzyme 2 (ACE2)[49]. Before the discovery of HCoV-NL63 it was generally thought that all group I coronaviruses use CD13 (also known as aminopeptidase N) as receptor, because the representatives of that group (HCoV-229E, porcine, feline and canine coronaviruses) engage CD13 for cell entry[6,21,59,60,75,88]. Studies on HCoV-NL63 cell tropism revealed that the virus, unlike its closest relative HCoV-229E, can be propagated on LLC-MK2, Vero-E6 and Huh-7 cells (Chapter II and Chapter VI)[31,67]. These cells all express ACE2, suggesting that HCoV-NL63 and SARS-CoV might use the same receptor. Further analysis with the retroviral pseudotyping system confirmed that HCoV-NL63 does not use CD13, but indeed uses ACE2 as the receptor for cell entry (Chapter VI).

The receptor binding site of HCoV-NL63 has been mapped to position 232 to 684[38]. This region does not exhibit significant homology to SARS-CoV but is more related to the S-protein of HCoV-229E, which enters target cells by engaging CD13. Therefore it is hypothesized that HCoV-NL63 and SARS-CoV have independently gained the capacity to use ACE2 to enter their target cells[38].

The ACE2 molecule was first identified as a homolog of angiotensin-converting enzyme with zinc metalloproteinase activity[74]. The activity of ACE2 differs from ACE1[9], but both enzymes are key players of the renin-angiotensin system, thereby regulating cardiac and vascular functions[18]. There is now an increasing body of evidence supporting the role for the renin-angiotensin system in acute lung injury. It is thought that ACE2 influences the vascular permeability, air-vessel interface and pneumocyte viability and indeed, increased levels of ACE2 in the respiratory tract were found in patients with an acute respiratory distress syndrome (ARDS)[40]. ACE2 acts in the opposite way and protects against lung injury. It was suggested that binding of SARS-CoV to ACE2 downregulates ACE2 levels, thus aggravating the lung injury and produce lung edema during infection[44]. HCoV-NL63 also binds to ACE2 and induces its downregulation similar to SARS-CoV (Chapter VII). But unlike SARS-CoV, HCoV-NL63 infection is generally not associated with ARDS. Therefore the use of ACE2 as a viral receptor by itself does not invariably result in aggravating acute lung injury.

Cell entry

Enveloped viruses employ two strategies to enter their target cells. One involves glycoprotein mediated engagement of receptors on the cell surface, which triggers fusion of the viral and cellular membranes[23]. Alternatively, receptor binding can trigger endocytosis followed by transport into an endocytic compartment, where the acid pH triggers the fusion[69]. Inhibitors of vacuolar acidification are well-

established tools to assess if the fusion of the membranes is pH dependent[24,25,62]. Bafilomycin A is an inhibitor of vacuolar proton pumps[9] and in chapter VI it is shown that treatment with this compound reduces HCoV-NL63 entry to a similar level as for HCoV-229E, indicating that the virus is using the endosomal entry pathway. However, subsequent studies demonstrated that HCoV-NL63 S-mediated infection of hepatocytes (Huh-7 cells) depends on low pH (50% inhibition), but to a lower extent than SARS-CoV (97% inhibition)[38]. I-Chueh Huang *et al* showed that treatment with NH_4Cl poorly inhibits HCoV-NL63, compared to a strong inhibition of SARS-CoV[39], suggesting that the entry into an acidified environment of the endosome is not essential for HCoV-NL63. These results suggest that HCoV-NL63 may use the same route of entry as MHV, via direct fusion of the membranes. Additionally, HCoV-NL63 does not require cathepsin L (an endosomal proteinase) activity for infection of LLC-MK2 cells unlike SARS-CoV [39]. The entry pathway and S protein intracellular processing of HCoV-NL63 obviously needs further study.

The spike proteins of coronaviruses exhibit a characteristic membrane fusion mechanism that is driven by conformational changes in the S protein, with rearrangements and interactions of heptad repeat regions (HR1 and HR2) located in the S2 domain. Association of the HR1 and HR2 domains into a hetero-hexamer brings the fusion peptide that is located near the N-terminus of HR1 in close proximity to the transmembrane domain, thereby facilitating membrane fusion. HCoV-NL63 S also contains the HR1 and HR2 regions with typical seven-residue periodicity. Characteristic for group I viruses are the two additional repeats in both HR regions and also HCoV-NL63 contains these additional repeats. HR2 of HCoV-NL63 is located adjacent to the transmembrane domain, and HR1 is about 170 amino acids towards the N-terminus. These regions associate tightly into the hetero-hexamer which is essential for HCoV-NL63 entry (Chapter IX).

Infection

Prevalence and disease association

In chapter II it was demonstrated that infection by HCoV-NL63 is not a rare event. Among 614 respiratory specimens collected between December 2002 and April 2003, 7 individuals were positive for HCoV-NL63 with an incidence in the winter months up to 7%. All individuals that were HCoV-NL63 positive had upper or lower respiratory tract disease (URTI and LRTI) or both. The report from Fouchier *et al* describes HCoV-NL63 in a clinical sample derived from 1988 and four additional samples out of 139 respiratory specimens (2.9%) collected from November 2000 to January 2002[31]. Since then, several groups reported HCoV-NL63 in patients suffering from respiratory tract disease (Figure 2)[2,4,5,5,8,8,41,57,72,77]. HCoV-NL63 was detected in Hong Kong in 15 of 587 children (2.6%)[16]. These Hong Kong children participated in a prospective clinical and virological study on children under the age of 18 with acute respiratory tract infection. The study group represented the population, such

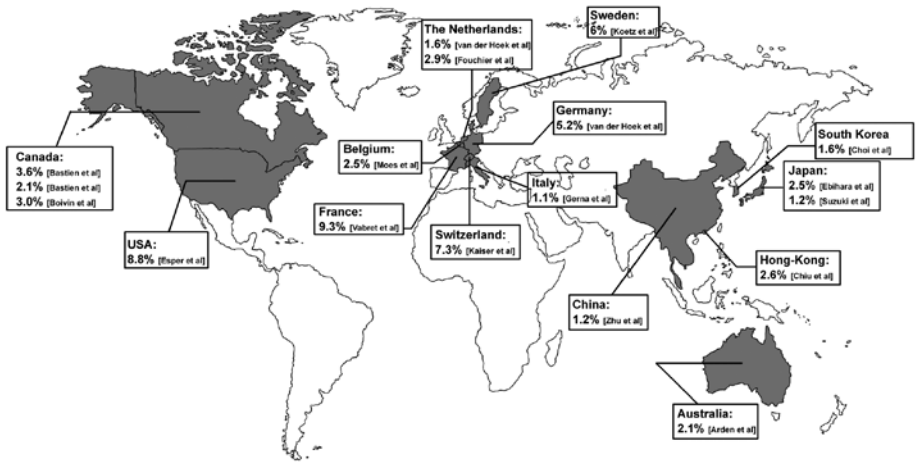


Figure 2. The worldwide distribution of HCoV-NL63. Countries with documented HCoV-NL63 infections are indicated in grey. Blank regions represent countries that did not search for HCoV-NL63 infection. There are no reports on the absence of HCoV-NL63 in certain countries. In the boxes the frequency of HCoV-NL63 infection is indicated.

that it could be estimated that HCoV-NL63 infection causes more than 200 hospital admissions each year per 100,000 children under the age of 6 in Hong Kong. A similar study was performed on the PRI.DE cohort, which is a population-based retrospective German multicentre study on paediatric respiratory infections[80]. The study included young children from paediatric practices and hospitals with clinical signs of laryngotracheitis (croup), bronchitis, bronchiolitis, pneumonia, or apnoea. Of the 949 PRI.DE samples, 49 (5.2%) were positive for HCoV-NL63. Various clinical diagnoses of lower respiratory tract disease were observed for the HCoV-NL63-positive patients, including croup, bronchitis, bronchiolitis, and pneumonia. A high frequency of co-infections in HCoV-NL63-positive samples (59%) was observed. However, in children with no other pathogen the incidence of croup was high whereas in the HCoV-NL63-negative children croup was rarely diagnosed. This suggests that HCoV-NL63 is one of the major pathogens causing croup in early childhood. Croup is an inflammation of the trachea and is characterized by a loud barking cough that usually worsens at night.

Respiratory coronavirus infections occur more often in winter and spring than in the summer and fall. Already in the first report about HCoV-NL63 the winter preference of HCoV-NL63 was presented (Chapter II). Additional studies from several countries with moderate climate (Belgium, Australia, Japan, Canada, Germany and France) confirmed that observation (Figure 3). Only in Hong Kong, HCoV-NL63 showed a spring-summer peak of activity, whereas in the same study HCoV-OC43 was mostly found in the winter season. This indicates that the seasonality of HCoV-NL63 in tropical and subtropical regions is not restricted to the winter season.

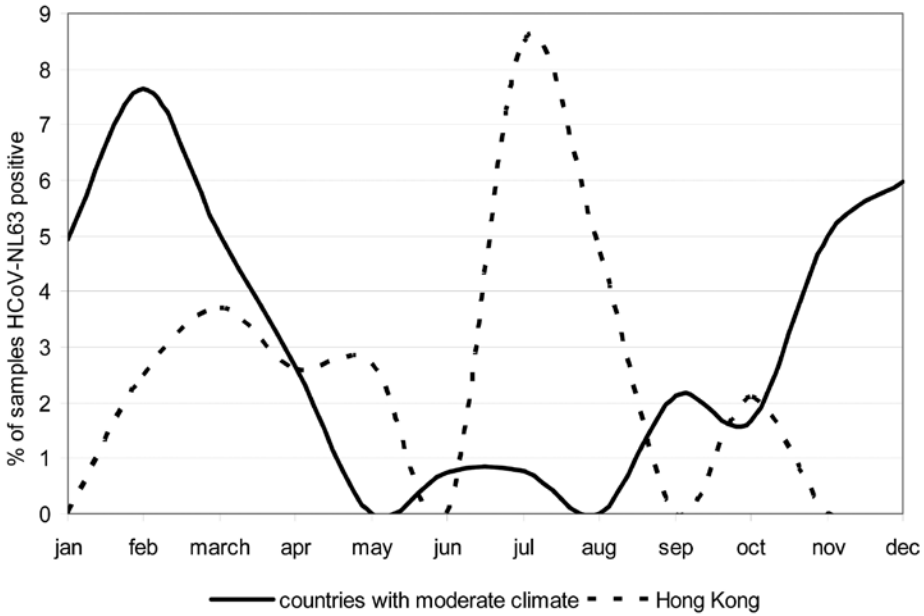


Figure 3. Seasonality of HCoV-NL63 infection. Studies in moderate climate (Germany, Canada, Belgium, France) and sub-tropical climate (Hong Kong) were included. The values on the Y axis represent the percentage of HCoV-NL63 positive samples.

HCoV-NL63 versus other coronaviruses, frequency of infection

Until recently only HCoV-229E and HCoV-OC43 were thoroughly studied. The third human coronavirus, SARS-CoV, was identified during the 2002–2003 outbreak of severe acute respiratory syndrome (SARS). Although SARS-CoV is the most pathogenic human coronavirus and responsible for ~800 fatal cases (10% mortality), the further spread of this zoonotic infection in humans was halted within one season due to a highly effective global public health response. To compare the burden of disease caused by the non-SARS-CoV coronaviruses, the frequency of HCoV-NL63 infection was compared with the frequency of HCoV-229E and HCoV-OC43 infection. The screening of a Belgian sample collection led to identification of 7 patients with HCoV-NL63 infection (2.3%), 7 patients with HCoV-OC43 infection (2.3%) and one patient with HCoV-229E infection (0.3%). Similar results were obtained in Amsterdam for patients with respiratory disease that were diagnosed in the Public Health Laboratory at the Municipal Health Service. Of the 63 respiratory samples that were tested for the 3 human coronaviruses in the winter of 2002-2003, 3 samples were positive for HCoV-NL63 (4.7%), 3 for HCoV-OC43 (4.7%) and no HCoV-229E detected (M. van Zon, S. Bruisten, J. Spaargaren and L. van der Hoek unpublished results). A population based study in Hong Kong identified 26 children with coronaviral infection (4.4% of 587 patients). Of them 15 were infected with HCoV-NL63 (2.6%), 9 by HCoV-OC43 (1.5%) and HCoV-229E was found in only 2 patients (0.3%) [16]. In a French study

HCoV-NL63 was detected in 9.3% of 300 patients, while HCoV-OC43 was detected in 1.2% of samples and no HCoV-229E positive sample was identified [77]. A Swiss study on coronavirus infection detected 13 positive patients (17%)[41]. Among these, 6 samples were positive for HCoV-NL63 (7.3%), 5 samples were HCoV-OC43 positive (6%) and HCoV-229E was found in 3 cases (3.7%). Combining these results suggests that the frequency of infection with different coronaviruses follows the ranking order: HCoV-NL63 ≥HCoVOC43 > HCoV-229E.

Co-infection with a second respiratory virus

Several studies showed that HCoV-NL63 infection is often combined with a second respiratory virus. The frequency of co-infection might reach even 75% (Table 1). In the PRI.DE cohort, double infections of HCoV-NL63 and a second respiratory virus was apparent in 29 of the 49 HCoV-NL63 positive samples (59%), with the highest co-infection frequency with RSV-A (41%), followed by PIV3 (10%) and RSV-B (8%). On the contrary, the other population based study from Hong-Kong reported 15 HCoV-NL63 positive patients but double infection was rather rare (20%) and the most common second respiratory virus was influenza A. These data suggest that there is no preference for the second pathogen, but that the frequency of co-infection with a specific agent correlates with pathogen's co-seasonality. Several other reports also show that HCoV-NL63 is frequently present with a second virus, although the numbers are not representative because these studies made a selection of samples that are negative for other viral pathogens was performed. The direct impact of co-infection with other respiratory viruses on disease severity is not known, but doubly infected patients are more often hospitalized then single HCoV-NL63 infected patients[80]. The viral load of HCoV-NL63 is significantly lower in co-infected versus singly infected patients, which may illustrate the influence of innate immune responses triggered by one virus on the replication of HCoV-NL63[16,80].

Virus shedding

The study of Chiu *et al* shows that the HCoV-NL63 load in respiratory specimens correlates inversely with the time after onset of symptoms[16]. While the mean viral load on day zero of infection was estimated to be ~2×10^8 copies/ml, it decreased linearly to the level of 3×10^4 copies/ml on day 3. Although it is known that a coronavirus infection is generally cleared within a week it has been reported that coronaviruses can also be shed for a long period[37,52]. For HCoV-NL63 the situation does not seem much different. Three weeks after an initial HCoV-NL63 infection, the virus was still detectable in 50% of the respiratory specimens. All children were free of symptoms at this time [41]. This prolonged shedding may explain HCoV-NL63 detection in symptom-free control persons[8].

Sero-prevalence

Coronaviruses are responsible for 10 to 30% of common cold cases each winter season. This means that during a lifetime virtually everybody will experience an

Table 1. Overview of clinical symptoms of HCoV-NL63 infected patients

		Clinical symptoms					
Country of origin	No. of samples	Fever	Cough	Running nose	URTI	LRTI	Co-infection
The Netherlands[31]	4	100%	100%	100%	N.D.	N.D.	N.A.[a]
The Netherlands[79]	8	N.D.	N.D.	N.D.	38%	38%	25%
Belgium[57]	7	86%	57%	29%	43%	57%	N.A.
Switzerland[41]	6	83%	100%	100%	67%	100%	33%
Germany[80]	49	43%	N.D.	N.D.	0%	100%	59%
France[77]	28	61%	N.D.	39%	22%	39%	N.A.
USA[29]	79	48%	64%	61%	N.D.	N.D.	12%
Canada[4]	19	53%	47%	11%	26%	21%	N.A.
Canada[5]	26	31%	54%	31%	42%	58%	4%
Canada[7]	12	58%	100%	100%	17%	83%	75%
Japan[27]	3	100%	100%	100%	33%	100%	N.A.
Japan[72]	5	100%	80%	80%	80%	20%	N.A.
Hong Kong[16]	15	20%	67%	60%	27%	20%	33%
Australia[2]	16	69%	81%	56%	19%	81%	38%

[a] Not applicable because all or part of the clinical samples were selected for absence of other respiratory virus.

infection with these viruses, and everybody will consequently carry antibodies against these viruses. This is also true for HCoV-NL63. Adults carry neutralizing antibodies that can inhibit HCoV-NL63 spike protein-mediated infection (Chapter VI and chapter IX). In contrast, strong neutralization of HCoV-229E S was observed with only a minority of adult sera. Sera from infants poorly neutralized infection driven by both HCoV-NL63 S and HCoV-229E S (Chapter VI), indicating that the first infection by HCoV-NL63 occurs during childhood. Screening of a larger number of samples with an HCoV-NL63-specific-ELISA will allow a more precise determination of the average age at which HCoV-NL63 antibodies are acquired.

HCoV-NL63 and Kawasaki disease

In 2005 an association between HCoV-NL63 infection and Kawasaki disease was reported[28]. Kawasaki disease is a systemic vasculitis in childhood that may result in aneurysms of the coronary arteries. In the developed world, Kawasaki disease is the most common cause of acquired heart disease in children. The evidence that Kawasaki disease is linked with an infectious agent includes temporal clustering and marked seasonality, geographic clustering[12,14] and age distribution[14]. Previously, various infectious agents have been suggested, including bacteria, allergens and some viruses[17,58,73]. Coronary complications can be reduced significantly by the use of intravenous immunoglobulin (IVIG) therapy combined with oral aspirin[42,47].

The study on coronavirus infection included 11 children with Kawasaki disease and 22 control children that were sampled in the same week. Eight children with Kawasaki disease were infected by HCoV-NL63 (73%), while in the control group of 22 children only one single HCoV-NL63 positive patient was identified (4.5%). Soon thereafter several groups reported a lack of association between HCoV-NL63 infection and Kawasaki disease[15,27,68]. To solve this matter, a sensitive immunological assay is needed to investigate whether seroconversion to HCoV-NL63 occurs during Kawasaki disease.

Treatment strategies

All published data point to HCoV-NL63 as being one of the most prevalent human coronaviruses, associated with acute respiratory disease and croup in children. The development of therapeutic agents that are able to efficiently inhibit viral replication, and supply a useful therapy for acute respiratory illness of children and immunocompromised patients is thus important. Combined with fast diagnostic tools to identify HCoV-NL63 infection, the viral inhibitors would provide an alternative to the regular treatment with steroids and antibiotics. Several inhibitors are known to reduce replication of coronaviruses (Chapter X). These inhibitors act at various steps of the coronavirus replication cycle, e.g. receptor binding, membrane fusion, transcription and post-translational processing. Unfortunately, up to date there is no animal model for HCoV-NL63 available validate these findings *in vivo*.

As mentioned above, virtually all sera from adults with RTI or from healthy adults carry neutralizing antibodies. Thus, it is not surprising that intravenous immunoglobulins (IVIG), consisting for 95% of pooled human IgG's isolated from serum of healthy donors, inhibit HCoV-NL63 replication (Chapter IX). IVIG is approved as an intravenously delivered drug by the Food and Drug Administration and is successfull in the treatment of several diseases, mostly primary immune deficiencies and autoimmune neuromuscular disorders, but also respiratory diseases[35] and Kawasaki disease[32,47]. The mode of action of this agent in HCoV-NL63 infection is most probably based on its ability to neutralize the virus. The anti-HCoV-NL63 potential, low cytotoxicity and availability makes IVIG a perfect candidate for human trials. A second target for inhibition of HCoV-NL63 replication targets the process of membrane fusion. The S proteins of coronaviruses are class I fusion proteins and membrane fusion follows a characteristic path. The peptide corresponding to the HCoV-NL63 HR2 domain associates tightly with HR1 (Chapter IX). Addition of HR2 peptide during infection of LLC-MK2 cells efficiently blocks replication, illustrating that the peptide interferes with the natural HR1-HR2 interaction during membrane fusion and that HCoV-NL63 HR2 peptide is a suitable drug candidate. The third target for virus inhibition is the viral genome itself. HCoV-NL63 is an RNA virus vulnerable to inhibition by siRNA. We explored the effectivity of the RNAi

mechanism with two synthetic siRNAs targeting the S gene. Transfection of these oligoribonucleotides in nanomolar concentration resulted in a profound decrease in virus yield (Chapter IX). The effectiveness of siRNA against respiratory track illnesses in a therapeutic setting was demonstrated recently in the mouse and monkey model with intranasal administration of naked siRNA or with transfection reagents targeting RSV, PIV and SARS-CoV[7,48,89]. Inhaled siRNA in low doses might offer a fast, potent and easily administrable antiviral tool against HCoV-NL63 infection in humans.

Different host receptors for cellular entry, poorly conserved structural proteins, and the high mutation and recombination rates of coronaviruses pose a significant problem in the development of wide-spectrum anti-CoV drugs and vaccines. M^{pro} is a key enzyme during post-translational processing and all coronaviral M^{pro} enzymes share a highly conserved substrate-recognition pocket. Mechanism-based inhibitors were designed based on this conserved enzyme pocket and tested in an *in vitro* assay and appeared to selectively inhibit several coronaviral M^{pro} enzymes including HCoV-NL63 M^{pro} [87].

Final Words

The VIDISCA method provides a powerful tool for identification of previously unknown viruses. After the discovery of a new virus the prevalence of infection should be determined. Ideally the Koch's postulates should be fulfilled but the lack of an animal model system often abolishes this option. In such a case, determining the association with disease is the best alternative. Still, identifying a virus is only the first step towards the final goal: treatment of patients by targeting the virus with an antiviral drug or with a vaccine to prevent future infections. The key element needed for evaluation of new antiviral compounds is an *in vitro* virus propagation system. Unfortunately, some viruses do not replicate in conventional cell culture (e.g. human bocavirus, HCoV-HKU1). In that case, employment of fully differentiated primary cell cultures (e.g. human airway epithelium cultures) may provide an alternative.

A relatively complete picture of HCoV-NL63 infection has emerged in a few years. After identification, the association with disease was determined, as well as the prevalence of infection. The most essential characteristics of the virus were determined (e.g. receptor usage) followed by evaluation of antiviral drugs in virus culture systems. At present there is an urgent need for an animal model system, but unfortunately it is not available yet.

In conclusion, the identification of novel viruses expands our knowledge on the *Viridae* kingdom and enables us to be prepared for the emergence of novel highly pathogenic viruses.

References

1. Allander, T., M. T. Tammi, M. Eriksson, A. Bjerkner, A. Tiveljung-Lindell, and B. Andersson. 2005. Cloning of a human parvovirus by molecular screening of respiratory tract samples. Proc. Natl. Acad. Sci. U. S. A 102:12891-12896.
2. Arden, K. E., M. D. Nissen, T. P. Sloots, and I. M. Mackay. 2005. New human coronavirus, HCoV-NL63, associated with severe lower respiratory tract disease in Australia. J. Med. Virol. 75:455-462.
3. Baranov, P. V., C. M. Henderson, C. B. Anderson, R. F. Gesteland, J. F. Atkins, and M. T. Howard. 2005. Programmed ribosomal frameshifting in decoding the SARS-CoV genome. Virology 332:498-510.
4. Bastien, N., K. Anderson, L. Hart, P. Van Caeseele, K. Brandt, D. Milley, T. Hatchette, E. C. Weiss, and Y. Li. 2005. Human coronavirus NL63 infection in Canada. J. Infect. Dis. 191:503-506.
5. Bastien, N., J. L. Robinson, A. Tse, B. E. Lee, L. Hart, and Y. Li. 2005. Human coronavirus NL-63 infections in children: a 1-year study. J. Clin. Microbiol. 43:4567-4573.
6. Benbacer, L., E. Kut, L. Besnardeau, H. Laude, and B. Delmas. 1997. Interspecies aminopeptidase-N chimeras reveal species-specific receptor recognition by canine coronavirus, feline infectious peritonitis virus, and transmissible gastroenteritis virus. J. Virol. 71:734-737.
7. Bitko, V., A. Musiyenko, O. Shulyayeva, and S. Barik. 2005. Inhibition of respiratory viruses by nasally administered siRNA. Nat. Med. 11:50-55.
8. Boivin, G., M. Baz, S. Cote, R. Gilca, C. Deffrasnes, E. Leblanc, M. G. Bergeron, P. Dery, and G. De Serres. 2005. Infections by human coronavirus-NL in hospitalized children. Pediatr. Infect. Dis. J. 24:1045-1048.
9. Bowman, E. J., A. Siebers, and K. Altendorf. 1988. Bafilomycins: a class of inhibitors of membrane ATPases from microorganisms, animal cells, and plant cells. Proc. Natl. Acad. Sci. U. S. A 85:7972-7976.
10. Brierley, I., M. E. Boursnell, M. M. Binns, B. Bilimoria, V. C. Blok, T. D. Brown, and S. C. Inglis. 1987. An efficient ribosomal frame-shifting signal in the polymerase-encoding region of the coronavirus IBV. EMBO J. 6:3779-3785.
11. Brierley, I., P. Digard, and S. C. Inglis. 1989. Characterization of an efficient coronavirus ribosomal frameshifting signal: requirement for an RNA pseudoknot. Cell 57:537-547.
12. Burns, J. C., D. R. Cayan, G. Tong, E. V. Bainto, C. L. Turner, H. Shike, T. Kawasaki, Y. Nakamura, M. Yashiro, and H. Yanagawa. 2005. Seasonality and temporal clustering of Kawasaki syndrome. Epidemiology 16:220-225.
13. Cavanagh, D. 1983. Coronavirus IBV: structural characterization of the spike protein. J. Gen. Virol. 64 (Pt 12):2577-2583.
14. Chang, L. Y., I. S. Chang, C. Y. Lu, B. L. Chiang, C. Y. Lee, P. J. Chen, J. T. Wang, H. N. Ho, D. S. Chen, and L. M. Huang. 2004. Epidemiologic features of Kawasaki disease in Taiwan, 1996-2002. Pediatrics 114:e678-e682.
15. Chang, L. Y., B. L. Chiang, C. L. Kao, M. H. Wu, P. J. Chen, B. Berkhout, H. C. Yang, and L. M. Huang. 2006. Lack of association between infection with a novel human coronavirus (HCoV), HCoV-NH, and Kawasaki disease in Taiwan. J. Infect. Dis. 193:283-286.
16. Chiu, S. S., K. H. Chan, K. W. Chu, S. W. Kwan, Y. Guan, L. L. Poon, and J. S. Peiris. 2005. Human coronavirus NL63 infection and other coronavirus infections in children hospitalized with acute respiratory disease in Hong Kong, China. Clin. Infect. Dis. 40:1721-1729.
17. Chou, C. T., J. S. Chang, S. E. Ooi, A. P. Huo, S. J. Chang, H. N. Chang, and C. Y. Tsai. 2005. Serum anti-Yersinia antibody in Chinese patients with Kawasaki disease. Arch. Med. Res. 36:14-18.
18. Crackower, M. A., R. Sarao, G. Y. Oudit, C. Yagil, I. Kozieradzki, S. E. Scanga, A. J. Oliveira-dos-Santos, J. da Costa, L. Zhang, Y. Pei, J. Scholey, C. M. Ferrario, A. S. Manoukian, M. C. Chappell, P. H. Backx, Y. Yagil, and J. M. Penninger. 2002. Angiotensin-converting enzyme 2 is an essential regulator of heart function. Nature 417:822-828.
19. Danilczyk, U., U. Eriksson, M. A. Crackower, and J. M. Penninger. 2003. A story of two ACEs. J. Mol. Med. 81:227-234.
20. de Haan, C. A., K. Stadler, G. J. Godeke, B. J. Bosch, and P. J. Rottier. 2004. Cleavage inhibition of the murine coronavirus spike protein by a furin-like enzyme affects cell-cell but not virus-cell fusion. J. Virol. 78:6048-6054.
21. Delmas, B., J. Gelfi, R. L'Haridon, L. K. Vogel, H. Sjostrom, O. Noren, and H. Laude. 1992. Aminopeptidase N is a major receptor for the entero-pathogenic coronavirus TGEV. Nature 357:417-420.

22. Denison, M. R. and S. Perlman. 1986. Translation and processing of mouse hepatitis virus virion RNA in a cell-free system. J. Virol. 60:12-18.
23. Doms, R. W. 2000. Beyond receptor expression: the influence of receptor conformation, density, and affinity in HIV-1 infection. Virology 276:229-237.
24. Drose, S. and K. Altendorf. 1997. Bafilomycins and concanamycins as inhibitors of V-ATPases and P-ATPases. J. Exp. Biol. 200:1-8.
25. Drose, S., K. U. Bindseil, E. J. Bowman, A. Siebers, A. Zeeck, and K. Altendorf. 1993. Inhibitory effect of modified bafilomycins and concanamycins on P- and V-type adenosinetriphosphatases. Biochemistry 32:3902-3906.
26. Drosten, C., S. Gunther, W. Preiser, S. van der Werf, H. R. Brodt, S. Becker, H. Rabenau, M. Panning, L. Kolesnikova, R. A. Fouchier, A. Berger, A. M. Burguiere, J. Cinatl, M. Eickmann, N. Escriou, K. Grywna, S. Kramme, J. C. Manuguerra, S. Muller, V. Rickerts, M. Sturmer, S. Vieth, H. D. Klenk, A. D. Osterhaus, H. Schmitz, and H. W. Doerr. 2003. Identification of a novel coronavirus in patients with severe acute respiratory syndrome. N. Engl. J. Med. 348:1967-1976.
27. Ebihara, T., R. Endo, X. Ma, N. Ishiguro, and H. Kikuta. 2005. Lack of association between New Haven coronavirus and Kawasaki disease. J. Infect. Dis. 192:351-352.
28. Esper, F., E. D. Shapiro, C. Weibel, D. Ferguson, M. L. Landry, and J. S. Kahn. 2005. Association between a novel human coronavirus and Kawasaki disease. J. Infect. Dis. 191:499-502.
29. Esper, F., C. Weibel, D. Ferguson, M. L. Landry, and J. S. Kahn. 2005. Evidence of a novel human coronavirus that is associated with respiratory tract disease in infants and young children. J. Infect. Dis. 191:492-498.
30. Fan, K., P. Wei, Q. Feng, S. Chen, C. Huang, L. Ma, B. Lai, J. Pei, Y. Liu, J. Chen, and L. Lai. 2004. Biosynthesis, purification, and substrate specificity of severe acute respiratory syndrome coronavirus 3C-like proteinase. J. Biol. Chem. 279:1637-1642.
31. Fouchier, R. A., N. G. Hartwig, T. M. Bestebroer, B. Niemeyer, J. C. de Jong, J. H. Simon, and A. D. Osterhaus. 2004. A previously undescribed coronavirus associated with respiratory disease in humans. Proc. Natl. Acad. Sci. U. S. A 101:6212-6216.
32. Gruber, W. C., S. Z. Wilson, B. J. Throop, and P. R. Wyde. 1987. Immunoglobulin administration and ribavirin therapy: efficacy in respiratory syncytial virus infection of the cotton rat. Pediatr. Res. 21:270-274.
33. Hegyi, A., A. Friebe, A. E. Gorbalenya, and J. Ziebuhr. 2002. Mutational analysis of the active centre of coronavirus 3C-like proteases. J. Gen. Virol. 83:581-593.
34. Hegyi, A. and J. Ziebuhr. 2002. Conservation of substrate specificities among coronavirus main proteases. J. Gen. Virol. 83:595-599.
35. Hemming, V. G., W. Rodriguez, H. W. Kim, C. D. Brandt, R. H. Parrott, B. Burch, G. A. Prince, P. A. Baron, R. J. Fink, and G. Reaman. 1987. Intravenous immunoglobulin treatment of respiratory syncytial virus infections in infants and young children. Antimicrob. Agents Chemother. 31:1882-1886.
36. Herold, J. and S. G. Siddell. 1993. An 'elaborated' pseudoknot is required for high frequency frameshifting during translation of HCV 229E polymerase mRNA. Nucleic Acids Res. 21:5838-5842.
37. Herrewegh, A. A., M. Mahler, H. J. Hedrich, B. L. Haagmans, H. F. Egberink, M. C. Horzinek, P. J. Rottier, and R. J. de Groot. 1997. Persistence and evolution of feline coronavirus in a closed cat-breeding colony. Virology 234:349-363.
38. Hofmann, H., G. Simmons, A. J. Rennekamp, C. Chaipan, T. Gramberg, E. Heck, M. Geier, A. Wegele, A. Marzi, P. Bates, and S. Pohlmann. 2006. Highly conserved regions within the spike proteins of human coronaviruses 229E and NL63 determine recognition of their respective cellular receptors. J. Virol. 80:8639-8652.
39. Huang, I. C., B. J. Bosch, F. Li, W. Li, K. H. Lee, S. Ghiran, N. Vasilieva, T. S. Dermody, S. C. Harrison, P. R. Dormitzer, M. Farzan, P. J. Rottier, and H. Choe. 2006. SARS coronavirus, but not human coronavirus NL63, utilizes cathepsin L to infect ACE2-expressing cells. J. Biol. Chem. 281:3198-3203.
40. Idell, S., F. Kueppers, M. Lippmann, H. Rosen, M. Niederman, and A. Fein. 1987. Angiotensin converting enzyme in bronchoalveolar lavage in ARDS. Chest 91:52-56.
41. Kaiser, L., N. Regamey, H. Roiha, C. Deffernez, and U. Frey. 2005. Human coronavirus NL63 associated with lower respiratory tract symptoms in early life. Pediatr. Infect. Dis. J. 24:1015-1017.

42. Kato, H., S. Koike, and T. Yokoyama. 1979. Kawasaki disease: effect of treatment on coronary artery involvement. Pediatrics 63:175-179.
43. Ksiazek, T. G., D. Erdman, C. S. Goldsmith, S. R. Zaki, T. Peret, S. Emery, S. Tong, C. Urbani, J. A. Comer, W. Lim, P. E. Rollin, S. F. Dowell, A. E. Ling, C. D. Humphrey, W. J. Shieh, J. Guarner, C. D. Paddock, P. Rota, B. Fields, J. DeRisi, J. Y. Yang, N. Cox, J. M. Hughes, J. W. LeDuc, W. J. Bellini, and L. J. Anderson. 2003. A novel coronavirus associated with severe acute respiratory syndrome. N. Engl. J. Med. 348:1953-1966.
44. Kuba, K., Y. Imai, S. Rao, H. Gao, F. Guo, B. Guan, Y. Huan, P. Yang, Y. Zhang, W. Deng, L. Bao, B. Zhang, G. Liu, Z. Wang, M. Chappell, Y. Liu, D. Zheng, A. Leibbrandt, T. Wada, A. S. Slutsky, D. Liu, C. Qin, C. Jiang, and J. M. Penninger. 2005. A crucial role of angiotensin converting enzyme 2 (ACE2) in SARS coronavirus-induced lung injury. Nat. Med. 11:875-879.
45. Larson, D. J., R. F. Solorzano, L. G. Morehouse, and L. D. Olson. 1980. Mild transmissible gastroenteritis in pigs suckling vaccinated sows. J. Am. Vet. Med. Assoc. 176:539-542.
46. Laude, H., M. Godet, S. Bernard, J. Gelfi, M. Duarte, and B. Delmas. 1995. Functional domains in the spike protein of transmissible gastroenteritis virus. Adv. Exp. Med. Biol. 380:299-304.
47. Leung, D. Y. 1989. The immunologic effects of IVIG in Kawasaki disease. Int. Rev. Immunol. 5:197-202.
48. Li, B. J., Q. Tang, D. Cheng, C. Qin, F. Y. Xie, Q. Wei, J. Xu, Y. Liu, B. J. Zheng, M. C. Woodle, N. Zhong, and P. Y. Lu. 2005. Using siRNA in prophylactic and therapeutic regimens against SARS coronavirus in Rhesus macaque. Nat. Med. 11:944-951.
49. Li, W., M. J. Moore, N. Vasilieva, J. Sui, S. K. Wong, M. A. Berne, M. Somasundaran, J. L. Sullivan, K. Luzuriaga, T. C. Greenough, H. Choe, and M. Farzan. 2003. Angiotensin-converting enzyme 2 is a functional receptor for the SARS coronavirus. Nature 426:450-454.
50. Liang, P. and A. B. Pardee. 1992. Differential display of eukaryotic messenger RNA by means of the polymerase chain reaction. Science 257:967-971.
51. Lim, K. P. and D. X. Liu. 1998. Characterization of the two overlapping papain-like proteinase domains encoded in gene 1 of the coronavirus infectious bronchitis virus and determination of the C-terminal cleavage site of an 87-kDa protein. Virology 245:303-312.
52. Liu, W., F. Tang, A. Fontanet, L. Zhan, Q. M. Zhao, P. H. Zhang, X. M. Wu, S. Q. Zuo, L. Baril, A. Vabret, Z. T. Xin, Y. M. Shao, H. Yang, and W. C. Cao. 2004. Long-term SARS coronavirus excretion from patient cohort, China. Emerg. Infect. Dis. 10:1841-1843.
53. Lu, Y., S. Y. Wang, and J. M. Lotz. 2004. The use of differential display to isolate viral genomic sequence for rapid development of PCR-based detection methods. A test case using Taura syndrome virus. J Virol Methods 121:107-114.
54. MacNaughton, M. R., M. H. Madge, and S. E. Reed. 1981. Two antigenic groups of human coronaviruses detected by using enzyme-linked immunosorbent assay. Infect. Immun. 33:734-737.
55. Mathews, D. H., J. Sabina, M. Zuker, and D. H. Turner. 1999. Expanded sequence dependence of thermodynamic parameters improves prediction of RNA secondary structure. J. Mol. Biol. 288:911-940.
56. McIntosh, K., J. H. Dees, W. B. Becker, A. Z. Kapikian, and R. M. Chanock. 1967. Recovery in tracheal organ cultures of novel viruses from patients with respiratory disease. Proc Natl Acad Sci U S A 57:933-940.
57. Moes, E., L. Vijgen, E. Keyaerts, K. Zlateva, S. Li, P. Maes, K. Pyrc, B. Berkhout, L. van der Hoek, and M. Van Ranst. 2005. A novel pancoronavirus RT-PCR assay: frequent detection of human coronavirus NL63 in children hospitalized with respiratory tract infections in Belgium. BMC. Infect. Dis. 5:6.
58. Nigro, G., M. Zerbini, A. Krzysztofiak, G. Gentilomi, M. A. Porcaro, T. Mango, and M. Musiani. 1994. Active or recent parvovirus B19 infection in children with Kawasaki disease. Lancet 343:1260-1261.
59. Oh, J. S., D. S. Song, and B. K. Park. 2003. Identification of a putative cellular receptor 150 kDa polypeptide for porcine epidemic diarrhea virus in porcine enterocytes. J. Vet. Sci. 4:269-275.
60. Oh, J. S., D. S. Song, J. S. Yang, J. Y. Song, H. S. Yoo, Y. S. Jang, and B. K. Park. 2004. Effect of soluble porcine aminopeptidase N on antibody production against porcine epidemic diarrhea virus. J. Vet. Sci. 5:353-357.
61. Peiris, J. S., S. T. Lai, L. L. Poon, Y. Guan, L. Y. Yam, W. Lim, J. Nicholls, W. K. Yee, W. W. Yan, M. T. Cheung, V. C. Cheng, K. H. Chan, D. N. Tsang, R. W. Yung, T. K. Ng, and K. Y. Yuen. 2003. Coronavirus as a possible cause of severe acute respiratory syndrome. Lancet 361:1319-1325.

62. Perez, L. and L. Carrasco. 1994. Involvement of the vacuolar H(+)-ATPase in animal virus entry. J. Gen. Virol. 75 (Pt 10):2595-2606.
63. Poon, L. L., D. K. Chu, K. H. Chan, O. K. Wong, T. M. Ellis, Y. H. Leung, S. K. Lau, P. C. Woo, K. Y. Suen, K. Y. Yuen, Y. Guan, and J. S. Peiris. 2005. Identification of a novel coronavirus in bats. J. Virol. 79:2001-2009.
64. Reed, S. E. 1984. The behaviour of recent isolates of human respiratory coronavirus *in vitro* and in volunteers: evidence of heterogeneity among 229E-related strains. J. Med. Virol. 13:179-192.
65. Sawicki, S. G. and D. L. Sawicki. 1990. Coronavirus transcription: subgenomic mouse hepatitis virus replicative intermediates function in RNA synthesis. J. Virol. 64:1050-1056.
66. Sawicki, S. G. and D. L. Sawicki. 1998. A new model for coronavirus transcription. Adv. Exp. Med. Biol. 440:215-219.
67. Schildgen, O., M. F. Jebbink, M. de Vries, K. Pyrc, R. Dijkman, A. Simon, A. Muller, B. Kupfer, and H. L. van der. 2006. Identification of cell lines permissive for human coronavirus NL63. J. Virol. Methods 138:207-210.
68. Shimizu, C., H. Shike, S. C. Baker, F. Garcia, H. L. van der, T. W. Kuijpers, S. L. Reed, A. H. Rowley, S. T. Shulman, H. K. Talbot, J. V. Williams, and J. C. Burns. 2005. Human coronavirus NL63 is not detected in the respiratory tracts of children with acute Kawasaki disease. J. Infect. Dis. 192:1767-1771.
69. Sieczkarski, S. B. and G. R. Whittaker. 2002. Dissecting virus entry via endocytosis. J. Gen. Virol. 83:1535-1545.
70. Simmons, G., D. N. Gosalia, A. J. Rennekamp, J. D. Reeves, S. L. Diamond, and P. Bates. 2005. Inhibitors of cathepsin L prevent severe acute respiratory syndrome coronavirus entry. Proc. Natl. Acad. Sci. U. S. A 102:11876-11881.
71. Stephensen, C. B., D. B. Casebolt, and N. N. Gangopadhyay. 1999. Phylogenetic analysis of a highly conserved region of the polymerase gene from 11 coronaviruses and development of a consensus polymerase chain reaction assay. Virus Res. 60:181-189.
72. Suzuki, A., M. Okamoto, A. Ohmi, O. Watanabe, S. Miyabayashi, and H. Nishimura. 2005. Detection of human coronavirus-NL63 in children in Japan. Pediatr. Infect. Dis. J. 24:645-646.
73. Takahashi, K., T. Oharaseki, M. Wakayama, Y. Yokouchi, S. Naoe, and H. Murata. 2004. Histopathological features of murine systemic vasculitis caused by Candida albicans extract--an animal model of Kawasaki disease. Inflamm. Res. 53:72-77.
74. Tipnis, S. R., N. M. Hooper, R. Hyde, E. Karran, G. Christie, and A. J. Turner. 2000. A human homolog of angiotensin-converting enzyme. Cloning and functional expression as a captopril-insensitive carboxypeptidase. J. Biol. Chem. 275:33238-33243.
75. Tresnan, D. B., R. Levis, and K. V. Holmes. 1996. Feline aminopeptidase N serves as a receptor for feline, canine, porcine, and human coronaviruses in serogroup I. J. Virol. 70:8669-8674.
76. Tyrrell, D. A. and M. L. Bynoe. 1965. Cultivation of a novel type of common-cold virus in organ cultures. Br. Med. J. 5448:1467-1470.
77. Vabret, A., T. Mourez, J. Dina, L. van der Hoek, S. Gouarin, J. Petitjean, J. Brouard, and F. Freymuth. 2005. Human coronavirus NL63, France. Emerg. Infect. Dis. 11:1225-1229.
78. van den Hoogen, B. G., J. C. de Jong, J. Groen, T. Kuiken, R. De Groot, R. A. Fouchier, and A. D. Osterhaus. 2001. A newly discovered human pneumovirus isolated from young children with respiratory tract disease. Nat. Med. 7:719-724.
79. van der Hoek, L., K. Pyrc, M. F. Jebbink, W. Vermeulen-Oost, R. J. Berkhout, K. C. Wolthers, P. M. Wertheim-van Dillen, J. Kaandorp, J. Spaargaren, and B. Berkhout. 2004. Identification of a new human coronavirus. Nat. Med. 10:368-373.
80. van der Hoek, L., K. Sure, G. Ihorst, A. Stang, K. Pyrc, M. F. Jebbink, G. Petersen, J. Forster, B. Berkhout, and K. Uberla. 2005. Croup is associated with the novel coronavirus NL63. PLoS. Med. 2:e240.
81. Vlasak, R., W. Luytjes, W. Spaan, and P. Palese. 1988. Human and bovine coronaviruses recognize sialic acid-containing receptors similar to those of influenza C viruses. Proc. Natl. Acad. Sci. U. S. A 85:4526-4529.
82. Wang, D., L. Coscoy, M. Zylberberg, P. C. Avila, H. A. Boushey, D. Ganem, and J. L. DeRisi. 2002. Microarray-based detection and genotyping of viral pathogens. Proc Natl Acad Sci U S A 99:15687-15692.
83. Wang, D., A. Urisman, Y. T. Liu, M. Springer, T. G. Ksiazek, D. D. Erdman, E. R. Mardis, M. Hickenbotham, V. Magrini, J. Eldred, J. P. Latreille, R. K. Wilson, D. Ganem, and J. L. DeRisi. 2003. Viral discovery and sequence recovery using DNA microarrays. PLoS. Biol. 1:E2.

84. Williams, R. K., G. S. Jiang, and K. V. Holmes. 1991. Receptor for mouse hepatitis virus is a member of the carcinoembryonic antigen family of glycoproteins. Proc. Natl. Acad. Sci. U. S. A 88:5533-5536.
85. Woo, P. C., Y. Huang, S. K. Lau, H. W. Tsoi, and K. Y. Yuen. 2005. In silico analysis of ORF1ab in coronavirus HKU1 genome reveals a unique putative cleavage site of coronavirus HKU1 3C-like protease. Microbiol. Immunol. 49:899-908.
86. Woo, P. C., S. K. Lau, C. M. Chu, K. H. Chan, H. W. Tsoi, Y. Huang, B. H. Wong, R. W. Poon, J. J. Cai, W. K. Luk, L. L. Poon, S. S. Wong, Y. Guan, J. S. Peiris, and K. Y. Yuen. 2005. Characterization and complete genome sequence of a novel coronavirus, coronavirus HKU1, from patients with pneumonia. J. Virol. 79:884-895.
87. Yang, H., W. Xie, X. Xue, K. Yang, J. Ma, W. Liang, Q. Zhao, Z. Zhou, D. Pei, J. Ziebuhr, R. Hilgenfeld, K. Y. Yuen, L. Wong, G. Gao, S. Chen, Z. Chen, D. Ma, M. Bartlam, and Z. Rao. 2005. Design of wide-spectrum inhibitors targeting coronavirus main proteases. PLoS. Biol. 3:e324.
88. Yeager, C. L., R. A. Ashmun, R. K. Williams, C. B. Cardellichio, L. H. Shapiro, A. T. Look, and K. V. Holmes. 1992. Human aminopeptidase N is a receptor for human coronavirus 229E. Nature 357:420-422.
89. Zhang, W., H. Yang, X. Kong, S. Mohapatra, H. Juan-Vergara, G. Hellermann, S. Behera, R. Singam, R. F. Lockey, and S. S. Mohapatra. 2005. Inhibition of respiratory syncytial virus infection with intranasal siRNA nanoparticles targeting the viral NS1 gene. Nat. Med. 11:56-62.
90. Ziebuhr, J. and S. G. Siddell. 1999. Processing of the human coronavirus 229E replicase polyproteins by the virus-encoded 3C-like proteinase: identification of proteolytic products and cleavage sites common to pp1a and pp1ab. J. Virol. 73:177-185.

Appendix A

VIDISCA: unraveling the unknown

In Press: Methods in Molecular Biology

Krzysztof Pyrc, Maarten F. Jebbink, Ben Berkhout and Lia van der Hoek

Laboratory of Experimental Virology, Department of Medical Microbiology, Center for Infection and Immunity Amsterdam (CINIMA), Academic Medical Center, University of Amsterdam, Meibergdreef 15, 1105 AZ, Amsterdam, The Netherlands.

Virus Discovery based on cDNA-AFLP (VIDISCA) is a novel approach that provides a fast and effective tool for amplification of unknown genomes, e.g. of human pathogenic viruses. The VIDISCA method is based on double restriction enzyme processing of a target sequence and ligation of oligonucleotide adaptors that subsequently serve as priming sites for amplification. As the method is based on the common presence of restriction sites, it results in the generation of reproducible, species-specific amplification patterns. The method allows amplification and identification of viral RNA/DNA, with a lower cutoff value of 10^5 copies/ml for DNA viruses and 10^6 copies/ml for the RNA viruses. Previously, we described the identification of a novel human coronavirus, HCoV-NL63, with the use of the VIDISCA method.

Introduction

To date, there are still a variety of human diseases with unknown etiology. That includes several chronic diseases like amyotrophic lateral sclerosis (ALS) and multiple sclerosis (MS), but also acute infections as Kawasaki disease or multiple respiratory diseases[3,6]. A viral origin has been suggested for many of these diseases, emphasizing the importance of a continuous search for new viruses. Identification of previously unrecognized viral agents in patient samples is of great medical interest, but remains a major technical challenge. Identification of novel viral pathogens is difficult with the virus discovery tools known to date. Several problems are encountered when searching for new viruses. First, most of the unidentified viruses do not replicate *in vitro*, at least not in the cells that are commonly used in viral diagnostics. Second, the molecular biology techniques previously used to identify unknown viruses have their specific drawbacks. Several techniques are in use for virus discovery, e.g. universal primer PCR, random priming based PCR, and representational difference analysis (RDA). Although each technique has proven to be useful for virus discovery in certain circumstances, they have serious limitations and restrictions.

Universal PCR-primers should amplify new members of an already known virus family. This method has two major drawbacks. First, a choice for a specific virus family has to be made. This limits the possibility of identifying a member of an unsuspected virus family or the founding member of a totally new virus family. Second, the universal primers may simply not match the genome sequence of novel members of a virus family. This is illustrated by the lack of success of universal coronavirus primers that were designed before the new members: SARS-CoV, HCoV-NL63 and HCoV-HKU1 were identified. None of the studies that used such primers was able to detect a novel human coronavirus[8,9]. Obviously, such primers gradually improve once more family members are known.

Another technique uses non-specific amplification of viral sequences in a random priming PCR at low annealing temperatures[5]. However, most ingredients of

this assay contain contaminating DNA. For instance, the enzymes used may contain trace amounts of DNA from the bacteria in which they are produced. This contaminating DNA is also amplified and it is therefore not possible to determine at an early stage whether amplification products represent a new virus or contaminating nucleic acids. This can be resolved only after excessive cloning and sequencing. Thus, high throughput screening of many clinical samples is therefore impractical.

Representational difference analysis (RDA) is a subtractive hybridization technique that enriches for nucleic acid sequences present in one tissue, but absent or present at lower concentration in an otherwise identical tissue sample. RDA utilizes PCR to generate sets of nucleic acids in a target and a (negative control) tester sample. After subtractive hybridization there is selective amplification of target enriched sequences. The method was developed for tissue material and not for non-tissue samples like serum / plasma or virus culture supernatants[4]. The fact that these liquid samples have low concentration of DNA and RNA in the tester sample may restrain the selective amplification of an unknown viral target. A disadvantage of this technique is that it requires a negative control tissue of the same person from which the disease tissue was obtained.

We recently developed a general, simple and easy to use new virus discovery method that allows large scale screening for any RNA or DNA virus in samples like serum/plasma or virus culture supernatant[10]. The method is based on the cDNA-AFLP technique[1] (Virus Discovery cDNA-AFLP: VIDISCA). The main feature of VIDISCA is that prior knowledge of the genome sequence is not required as the presence of restriction enzyme sites is sufficient to guarantee PCR amplification.

VIDISCA begins with a treatment to selectively enrich for viral nucleic acid, which includes a centrifugation step to remove residual cells and mitochondria. In addition, a DNase treatment is used to remove interfering chromosomal DNA and mitochondrial DNA from degraded cells, whereas RNases in the sample will degrade RNA. During this step the viral nucleic acid is specifically protected within the viral particle. Next, DNase/Rnases are inactivated and the viral nucleic acids are subsequently extracted from the particles, RNA is reverse transcribed into cDNA and second strand synthesis is performed to make dsDNA (from a viral RNA or DNA genome). The dsDNA is digested with frequently cutting restriction enzymes that are likely to be present in every viral target (HinP1-I and Mse-I), and HinP1-I- and Mse-I- anchors are ligated to the digested DNA. Essential to the method is that the restriction enzymes remain active during the ligase reaction, thus preventing concatamerization of digested fragments. The anchors themselves are not removed because they are designed such that the restriction site is lost. The target is subsequently PCR-amplified with primers that anneal to the anchor sequences, followed by a round of selective amplification with primers that are

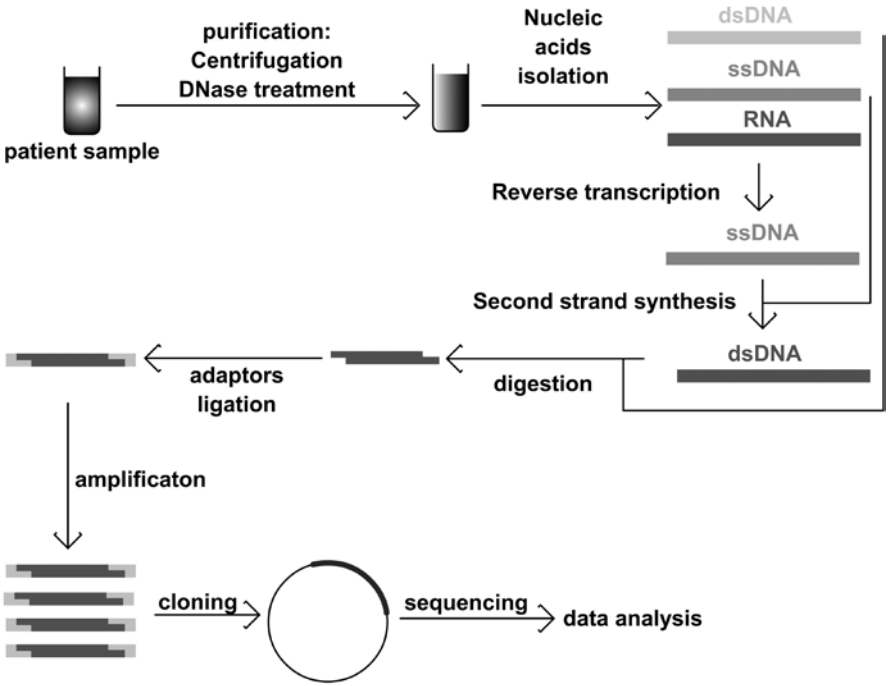


Figure 1. Overview of the VIDISCA method.

extended with one nucleotide (G, A, T or C). Thus, 16 primer combinations are used and each sample is compared to a representative negative control (negative serum or plasma or supernatant from an uninfected culture). The PCR fragments that are specific to the "infected" clinical sample can then be cloned and sequenced. Because amplification is based on the presence of restriction sites, the PCR is reproducible (in duplicate samples the same fragments are amplified) and these PCR products can be distinguished from background amplification. The assay is relatively high-throughput as multiple samples (about 10) can be tested per cycle of VIDISCA.

We were able to amplify viral nucleic acids from EDTA-plasma of a person with hepatitis B virus infection and a person with an acute parvovirus B19 infection. Using urine, we could detect adenoviral DNA and influenza B RNA in 2 patients. The technique can also detect HIV-1 and picornaviruses in cell culture. These results illustrate that the VIDISCA technique has the capacity to identify both RNA and DNA viruses directly from patient material or from cell cultures. In fact, it was the first experiment with a suspected virus culture that led to identification of a novel human coronavirus (HCoV-NL63[10]). Only three human coronaviruses were known at that time: HCoV-229E, HCoV-OC43 and SARS-CoV[5,7], and HCoV-NL63 represents the fourth member. The rapid identification of this novel coronavirus demonstrates the power of our virus discovery tool, which can now be used to test large sample sets suspected to contain viral pathogens.

Materials

Pretreatment of the sample

DNase I, RNase free at concentration 2U/μl (Ambion)

DNase buffer: 10 × concentrated (Ambion)

Sterile HPLC pure water (Baker)

Nucleic acid isolation

L2 buffer (0.1M Tris-HCl pH 6.4) Prepare by mixing: 12.1g Tris, 9.4ml of 32% HCl, and adjust with sterile water (Baker) to 1L[2].

L2 solution: prepare by mixing: 480g gunidinum thiocyanate (SIGMA) and 400ml of L2 buffer[2].

L6 solution: prepare by mixing: 480g gunidinum thiocyanate (SIGMA), 88ml of 0.2M EDTA, 10.4g Triton X-100 (Merck) and 400ml of L2 buffer[2].

Silica. Prepare 60g of silicon dioxide (Sigma) in a glass graduated cylinder of 500ml and adjust the volume to 500ml with sterile water (Baker). Resuspend the silica with vortexing and incubate at room temperature for 25 hours. Remove 430ml of top liquid. Adjust the volume with sterile water (Baker) to 500ml and resuspend. Incubate at room temperature for 5 hours and remove 440ml of water. Resusped the silica and stir adding 600μl of 32% HCl. Aliquot and autoclave. Store at room temperature[2].

70% ethanol (Merck)

100% acetone (Merck)

Sterile HPLC pure water (Baker)

Reverse transcription, digestion, ligation and PCR amplification

Sequenase 2.0, T7 DNA polymerase at concentration 13U/μl (Amersham Biosciences)

Random primers (hexamers; Amersham Biosciences). Working solution 1 μg/μl.

RnaseH, 5U/μl (Amersham Biosciences).

MMLV-RT (Moloney murine leukemia virus reverse transcriptase enzyme; 200U/μl; Invitrogen)

CMB buffer 10 × concentrated (100mM Tris-HCl pH 8.3, 500mM KCl, 1% Triton-

X100). Prepare by mixing: 1ml of 2M Tris pH 8.3, 5ml of 2M KCl, 2ml of 10% Triton X-100 and 12ml of sterile water (Baker). Store at –20°C in 250µl portions.

SEQII buffer 10 × concentrated (350mM Tris-HCl pH 7.5, 250mM NaCl, 175mM $MgCl_2$). Prepare by mixing: 2.25ml sterile water (Baker), 3.5ml of 1M Tris-HCl pH 7.5, 2.5ml of 1M NaCl, 1.75ml of 1M $MgCl_2$. Store at –20°C in 100µl portions.

Magnesium chloride (100mM).

dNTP's (25mM of each; Amersham Biosciences).

PCR buffer 10 × concentrated (100mM Tris-HCl pH 8.3, 500mM KCl, 100mg BSA). Prepare by mixing: 10ml of 2M Tris pH 8.3, 25ml of 2M KCl, 60ml of sterile water (Baker) and 5ml of BSA (Bovine serum albumin, 20mg/ml; Roche). Store at –20°C in 250µl portions.

First PCR primer set: HinP1-I standard primer 5′ - GACGATGAGTCCTGACCGC -3′ and MseI standard primer 5′- CTCGTAGACTGCGTACCTAA - 3′.

Nested PCR primer set: HinP1-I-X Selective primers. HinP1-I-A: 5′-GACGAT-GAGTCCTGACCGCA-3′; HinP1-I-T: 5′-GACGATGAGTCCTGACCGCT-3′; HinP1-I-C: 5′-GACGATGAGTCCTGACCGCC-3′; HinP1-I-G: 5′-GACGAT-GAGTCCTGACCGCG-3′.

Nested PCR primer set: MseI-X Selective primers. MseI-A: 5′ - CTCGTAGACTGCG-TACCTAAA - 3′; MseI-T: 5′ - CTCGTAGACTGCGTACCTAAT - 3′; MseI-C: 5′ - CTCG-TAGACTGCGTACCTAAC - 3′; MseI-G: 5′ - CTCGTAGACTGCGTACCTAAG - 3′.

HinP1-I anchors. Top strand: 5′ - GACGATGAGTCCTGAC - 3′; Bottom strand: 5′ - CGGTCAGGACTCAT - 3′ . Oligonucleotides should be diluted to the 10µM concentration.

MseI anchor: Top strand: 5′ - CTCGTAGACTGCGTACC - 3′; Bottom strand: 5′ - TAG-GTACGCAGTC - 3′. Oligonucleotides should be diluted to the 10µM concentration.

MseI restriction enzyme, 10U/µl (New England Biolabs). BSA and NEB buffer 2 are included.

HinP1-I restriction enzyme. 10U/µl (New England Biolabs).

Ligase, 5U/µl (Invitrogen).

Ligase buffer (Invitrogen).

UltraPure™ Phenol:Chloroform:Isoamyl Alcohol (25:24:1, v/v) (Invitrogen).

3M sodium acetate (pH 5.2).

100% ethanol.

70% ethanol.

AmpliTaq® DNA Polymerase polymerase (5U/µl; Applied Biosystems).

Sterile HPLC pure water (Baker).

Gel electrophoresis and gel extraction
MetaPhor agarose (Cambrex).

Agarose MP (Roche).

Ethidium bromide (BioRad).

Tris-Borate-EDTA buffer (Sigma).

25bp DNA ladder (Invitrogen).

smart ladder DNA size marker (Eurogentec).

sterile razor blades.

QIAquick Gel Extraction kit.

Sterile HPLC pure water (Baker).

Agarose gel loading buffer: 0.1% orange G, 30% glycerol in 0.5×TBE.

Cloning and sequencing
TOP10 E. Coli chemically competent bacteria (Invitrogen).

TOPO dual promoter or TOPO 2.1 kit (Invitrogen).

Luria-Broth (LB, Gibco) agar plates supplemented with ampiciline.

BigDye terminator kit (Applied Biosystems).

M13 reverse primer and T7 primer (10µM and 1µM) (Eurogentec).

Methods

Sample purification

Samples upon receipt are stored without thawing at -80°C to preserve the nucleic acids. On the day of the assay, sample is thawed, vortexed and 110µl is immediately centrifuged at room temperature with 13500rpm for 10 minutes, in order to remove the cells, cell debris and insoluble particles like mucus. Every analyzed sample is tested in duplicate and in every experiment an appropriate negative control is included. The negative control might be considered a sample of the same type derived from a healthy person or virus-negative cell culture of the same cell type if the pathogen was cultured.

Immediately after centrifugation, 100µl of sample is transferred into a fresh tube. Care should be taken that pelleted material is not transferred. If the sample is exceptionally full with cells / insoluble material, the primal volume may be increased as needed.

DNAse treatment. DNaseI solution is prepared in the nucleic acid free environment by mixing 15µl of DNaseI enzyme, 15µl of DNase1 buffer and 20µl of sterile water per 100µl of original sample. Subsequently, the DNase1 solution is added to the sample material and incubated at 37°C for 45 minutes.

Nucleic acid isolation using the Boom method (see note #1)

Immediately after the DNaseI treatment 900µl of L6 solution is added to the sample to lyse the material (see note #2,3,4,5). The lysis is done at room temperature for 10 minutes. Sample should by thoroughly mixed by inverting and vortexing.

Forty µl of silica is added and the sample is incubated at room temperature with mild shaking for 10 minutes. Sample is centrifuged (13200 rpm) for 10 seconds to pellet the silica particles, and the L6 supernatant is discarded.

The pelleted silica is washed two times with 900µl of L2. After addition of L2 solution, the sample is vortexed thoroughly until no pellet or large particles are visible and centrifuged for 10 seconds at 13200rpm. Washing with L2 is necessary to remove all traces of Triton-X100 and EDTA that may inhibit the following enzymatic reactions.

Sample is washed two times with room temperature 70% ethanol and one time with 100% acetone, in the same manner as described above for L2. Ethanol is added to wash out the guandine thiocyanate and residual traces of detergent and EDTA, while the acetone washing is mainly needed to speed up the drying process. After the removal of the acetone, silica is dried for 5 minutes at 56°C with the lid open.

To elute bound nucleic acids 50µl of sterile water is added, the sample is vortexed until all silica particles are in suspension and incubated at 56°C for 10 minutes with shaking (500rpm). After the elution, the sample is centrifuged for 2 minutes with 13200rpm. About 30µl of the liquid fraction is transferred into a fresh tube. Samples should be stored at -80°C until needed.

Reverse transcription and second strand synthesis
RT reaction

The reverse transcription (RT) reaction mixture is assembled under nucleic acid and nuclease free conditions and consists of a two-step reaction.

Two RT solutions (I and II) are prepared according to the formula:

RT solution I (10µl per sample)
2.5µl of random primers
3.0µl of 10 × concentrated CMB buffer
2.4µl of $MgCl_2$
2.1µl of sterile water

RT solution II (20µl per sample)
2.0µl of 10 × concentrated CMB buffer
1.0µl of MMLV-RT enzyme
0.8µl of dNTPs
16.2µl of sterile water

The nucleic acids isolated by the Boom method are centrifuged (1 minute, 13200rpm) in order to remove the residual silica particles.

After centrifugation, 20µl of the supernatant is mixed with 10µl of RT solution I and incubated at room temperature for 2 minutes in order to support primer-template annealing.

After 2 minutes of incubation, 20µl of RT solution II is added and samples are incubated for 90 minutes at 37°C to allow efficient reverse transcription. The RT reaction is followed by 5 minutes 95°C to deactivate the enzyme.

Second strand synthesis
After the RT reaction, the resulting single stranded cDNA cannot be used as a template for restriction enzyme cleavage or adaptor ligation. Therefore, second strand synthesis is performed using RNaseH to digest any residual RNA, and Sequenase enzyme, to synthesize the second strand DNA.

Second strand reaction mixture (100µl per sample)
10µl of 10 × concentrated SeqII buffer
2.0µl of Sequenase 2.0
1.5µl of RNAse H
1.0µl of dNTPs
85.5µl of water

The mixture is added to the 50.0µl RT reaction product.
Incubate for 90min at 37°C.

Phenol/chloroform extraction
After the second strand synthesis, the sample (150µl) is mixed with an equal volume of UltraPure™ Phenol:Chloroform:Isoamyl Alcohol and vortexed vigorously until the two phases are completely mixed.

The separation of phases is done by centrifugation (2 minutes, 13200rpm, room temperature) and the water phase containing ds-DNA is collected into a new tube. The usual volume recovery rate is about 93%.

Subsequently, the recovered ds-DNA is precipitated with ethanol. Water phase is mixed with 2.5 volumes of 100% ethanol and 0.1 volume of 3M sodium acetate and incubated for 14 hours at -20°C.

The ds-DNA is pelleted by 25 minutes centrifugation (15000 rpm) at 4°C, supernatant is discarded and the pellet is washed with 200 µl of freshly prepared 70% ethanol (Centrifugation for 25 minutes at 15000rpm at 4°C).

The ethanol is discarded, the pellet is air dried for 15 minutes at room temperature.

The pellet is dissolved in 30µl of sterile water by incubation at room temperature.

Construction of the adaptors
Adaptors are ds-DNA oligonucleotides designed to anneal to the cleavage site in the target DNA molecule. Introduction of the single mutation in the region recognized by the restriction enzyme prevents the cleavage of ligated adaptor-target DNA molecule (Figure 2). Adaptors are home-made, using single stranded oligonucleotides.

To prepare the functional adaptor, the bottom and top oligonucleotides are annealed by adding:
20.0µl of top adaptor (MseI or HinP1 I)
20.0µl of bottom adaptor (MseI or HinP1 I)
5.0µl of ligase buffer
45.0µl of sterile water

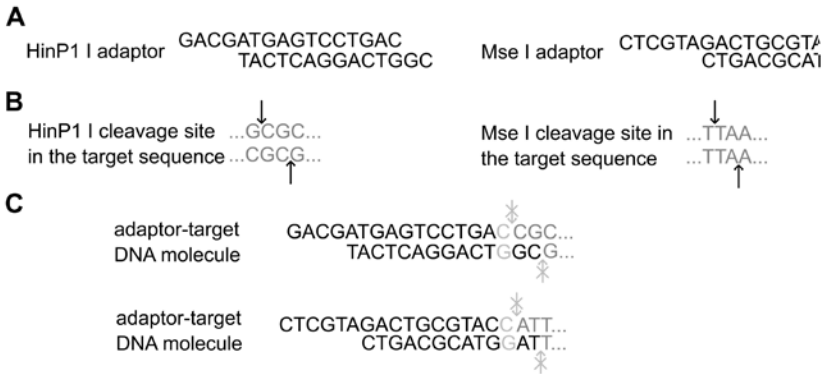


Figure 2. Ligation of adaptors to the target sequence. A) HinP1 I and Mse I adaptors. B) the restriction sites specific for HinP1 I and Mse I enzymatic cleavage C) The product of ligation of the adaptors to the target sequence. Incorporation of single nucleotide in the region of cleavage result in non-functional cleavage site.

Premixes for each adaptor should be prepared independently.

Solution should be heated up to 65°C for 5 minutes and cooled down slowly to the room temperature. Prepared adaptors are stored at -20°C.

Digestion of target sequence and ligation of adaptors

Digestion of the ds-cDNA is performed with restriction enzymes. In the protocol described here we included only digestion with HinP1 I and Mse1 enzymes, but this combination may be altered[1]. The use of two different restriction enzymes is essential as we observed that fragments that were cleaved on both sides by the same enzyme have lower chance to be amplified by PCR. If one is planning to change the enzyme combination, care should be taken that the combination of restriction enzymes should generate restriction fragments from virtually all templates.

For digestion of ds-cDNA material, the premix is prepared, containing per sample (10µl per sample):

4.0µl of NEB-2 buffer
4.0µl of 1:10 diluted BSA
1.0µl of Hinp1 I restriction enzyme
1.0µl of Mse1 restriction enzyme

Ten µl of the digestion premix is added to 30µl of purified ds-cDNA and incubated for 2 hours at 37 °C.

The ligation mix should be prepared before the digestion reaction is finished. The ligation premix contains per sample (15µl per sample):

1.0µl of HinP1 I adaptor
1.0µl of MseI adaptor
2.0µl of 5 × concentrated ligase buffer
1.0µl of ligase
10.0µl of sterile water

Fifteen µl of the ligation premix is added to the digested sample (40µl). There is no inactivation step between the digestion and ligation, as restriction activity prevents generation of the concatameric forms of the target templates. Fragments that are properly ligated with adaptors will not be cleaved, because of the point mutation introduced (Figure 2). The ligation should be performed for 2 hours at 37°C.

PCR reactions

The main part of the VIDISCA method is amplification of the genetic material without prior knowledge of the sequence. The pre-processed ds-cDNA with adaptors can be now amplified using the primers specific for the adaptors. During development of the method it was determined that a single PCR round does not provide sufficient specificity and sensitivity. Because of that, a second 'nested' PCR is included in the protocol. This PCR uses primers that are similar to the primers used in the first PCR, but with one nucleotide added to the 3' end of the primers.

First PCR reaction is done with the standard PCR thermocycling program (Table 1) and is optimized for 50µl reaction.

Ten µl of ligated sample is mixed with 40µl of PCR mix. The PCR mix is prepared as described below (the volumes are calculated per sample):

31.25µl of sterile water
0.75µl of $MgCl_2$
5.0µl of 10 × concentrated PCR buffer
0.5µl of dNTPs
1.0µl of Hinp1 I standard primer (10µM)
1.0µl of Mse I standard primer (10µM)
0.5µl of AmpliTaq® DNA Polymerase

The PCR reaction thermocycling is performed according to the scheme presented in Table 1 (see note #6). After the successful thermocycling the sample can be store at -20°C until needed.

Table 1. First PCR thermocycling profile.

Time	Temperature	Number of cycles
5min	94°C	1 cycle
1min 1min 2min	94°C 55°C 72°C	20 cycles
10min	72°C	1 cycle
∞	4°C	1 cycle

Second PCR - Selective amplifications.

The second, nested PCR reaction is necessary to provide the high specificity and sensitivity. This selective PCR is performed with primers with sequence identical as the standard primers, but with an additional nucleotide on its 3′ part. This additional nucleotide is outside the adaptor sequence and thus belongs already to the unknown material (Figure 2). Usage of additional nucleotide allows separation of the reactions in 16 different primer combinations and allows better analysis of the sample. To have a selectivity that is required when one wants to amplify only those fragments with a 100% match, the thermocycling profile is designed to increase the specificity of reaction by using the starting annealing temperature of 65°C that gradually decrease during first 10 cycles to 56°C. The PCR mix is prepared as described below (47.5µl per sample). The HinpI-X and MseI-X primers denote primers with an additional 3′ nucleotide.

40.3µl of sterile water
0.75µl of MgCl2
5.0µl of 10 × concentrated PCR buffer
0.2µl of dNTPs
0.5µl of HinpI-X primer (10µM)
0.5µl MseI-X primer (10µM)
0.25µl AmpliTaq® DNA Polymerase

Sixteen PCR premixes are prepared with different primer combinations (Hinp1 I - G,C,A,T; Mse I - G,C,A,T) and 47.5µl per sample of each premix is combined

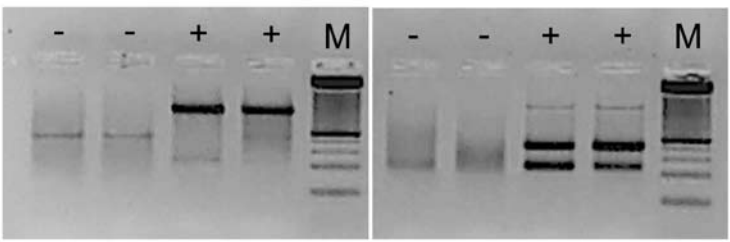


Figure 3. Representative VIDISCA fragments on MetaPhor agarose gel. Samples with '+' were supernatants of LLC-MK2 cells infected with HCoV-NL63 and samples '-' were supernatants of control LLC-MK2 cells.

with 2.5µl of the first PCR product. The second PCR thermocycling profile is presented in Table 2 (see note #6). The PCR product may be analyzed instantly or stored at -20°C until needed.

Table 2. Touch down PCR profile.

Time	Temperature	Number of cycles
5 min		1 cycle
60 sec 60 sec 90 sec	94°C 65 – 56°C[a] 72°C	10 cycles
30 sec 30 sec 60 sec	94°C 56°C 72°C	23 cycles
10 min	72°C	1 cycle
∞	4°C	1 cycle

[a] -1°C per cycle for each successive cycle

Gel analysis of the PCR product and purification of the amplified DNA

The second PCR product is analyzed on agarose gel. The majority of generated fragments is below 300 base pairs in size. Because of the need for high quality separation and small differences in fragment sizes, MetaPhor agarose is being used (it allows differentiate between fragments varying 1bp in size). Additionally, MetaPhor agarose provides an easy setup and high throughput processing for gel analysis and purification, compared to the polyacrylamide gels. The MetaPhor agarose gel is prepared as described below. One hundred and fifty ml of 0.5 × concentrated TBE buffer is poured into the erlenmeyer flask and stirred with the magnetic stirrer. Four gram of MetaPhor agarose is weighted and gently poured into the Erlenmeyer flask while mixing. Addition of all agarose powder at once will result in clumping of the agarose. The solution is stirred for another 10 minutes to soak the agarose grains and heated in the microwave for 60sec with low power. After the primal heating, the agarose is stirred and heated in 30sec cycles (low power) with extensive stirring in between. All agarose is solubilized during a final heating step for 60sec with medium power. The agarose is cooled down to ~65°C and 10µl of ethidium bromide (10mg/ml) is added. The agarose is poured in the electrophoresis tray and combs are inserted. It is crucial to remove all air bubbles from the gel (e.g. with pipette tip). Agarose is solidified at room temperature and further incubated at 4°C for at least 20 minutes (the incubation at 4°C improves the gel resolution). The gel is positioned in the electrophoresis box filled with 0.5 × TBE buffer.

Fifteen µl of the second PCR product is mixed with 5µl of the loading buffer and samples are layered on the prepared metaphor agarose gel. As a DNA size marker 5µl of the 25bp ladder is used. Electrophoretic separation is performed at 150V for about 1 hour.

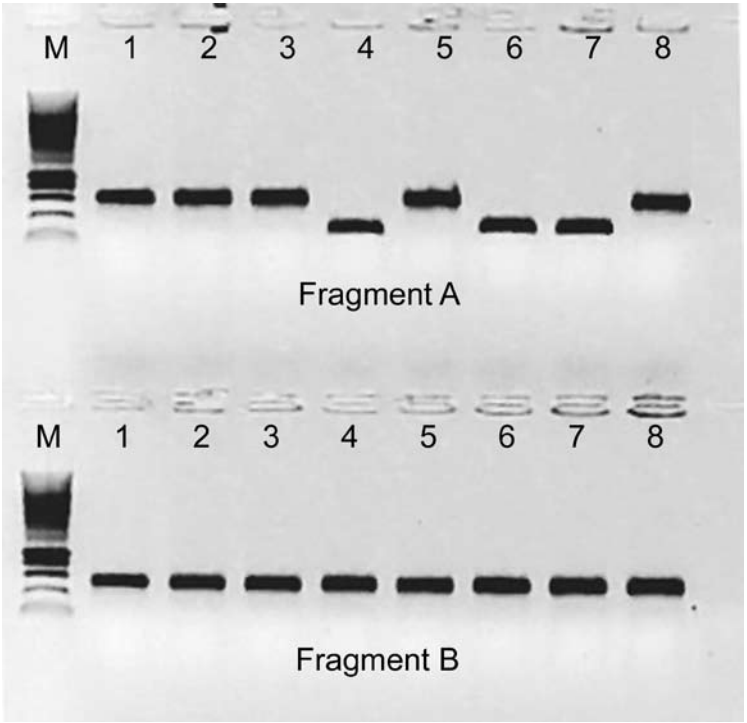


Figure 4. Gel analysis of colony PCR of VIDISCA fragments cloned into the TOPO 2.1 vector.

Immediately after the electrophoresis is finished, the gel is analyzed on the UV transiluminator. A picture is taken for analysis and the gel is stored at 4°C, wrapped in the plastic foil (Saran Wrap). The picture of the gel is used to search for fragments that are present in the sample of interest and not in the control sample All fragments that are exclusively present in the sample of interest are marked on the picture (Figure 3). If the bands appear very faint on the gel, the PCR products can be concentrated by vacuum centrifuge and re-analyzed on a MetaPhor gel. After fragment selection, the gel is again positioned on the UV transiluminator and the selected bands are excised with sterile razors (about 100mg per slice) and stored in coded, 1.5ml eppendorf tubes at 4°C (see note #7). After excision of all bands, a second picture of the gel should be taken, to document the proper excision.

The DNA fragments from the gel are extracted with the QIAquick gel extraction kit following the manufacturer protocol. The gel slices are solubilized in 600µl of QG buffer and 100 µl of isopropanol is added. After extraction, resulting DNA is dissolved in 30µl of EB buffer. Alternatively, any other gel extraction method may be used.

Cloning, selection of plasmids and sequencing

Purified DNA is subsequently cloned into a vector and transformed into bacteria. The usual procedure is to use the TOPO cloning kit from Invitrogen (TOPO TA Cloning® Kit

Dual Promoter). Cloning is done with 0.5µl of vector, 0.5µl of salt solution and 2µl of gel purified DNA. Chemically competent TOP10 E. Coli (Invitrogen) bacteria are transformed using the TOPO reaction (10µl of bacteria per reaction). The E.Coli are plated on LB agar plates supplemented with ampicilline. The growth on the LB plates is carried on for 16 hours at 37°C. Eight colonies per plate are collected with a pipette tip into 50µl of the BHI medium supplemented with ampiciline on a 96 well PCR plate. The suspended bacteria are subjected directly to a colony-PCR procedure, described below.

Colony PCR. The PCR mix is prepared by mixing (45µl per sample):

0.5µl of M13 reverse primer (10µM)
0.5µl of T7 primer (10µM)
5.0µl of 10 × concentrated PCR buffer
0.5µl of dNTPs
0.75µl of $MgCl_2$
0.2µl of AmpliTaq® DNA Polymerase
37.55µl of sterile water

Five µl of suspended E. Coli bacteria in BHI medium is added to the PCR mixture

Table 3. Colony PCR thermocycling scheme

Time	Temperature	Number of cycles
5 min	95 ºC	1 cycle
1 min 1 min 2 min	95 ºC 55 ºC 72 ºC	25 cycles
10min	72 ºC	1 cycle
∞	4 ºC	1 cycle

The thermocycling is performed as described in Table 3. After the PCR is finished, 10µl of the PCR product is mixed with gel loading dye and analyzed on 0.8% agarose MP gel with a Smart ladder DNA size marker. A representative picture of such a gel is presented in Figure 4.

The lanes that seem to contain the plasmid with proper insert are selected, and corresponding PCR products are subjected to sequencing reactions.

Sequencing reactions are performed on the colony-PCR product with the BigDye chemistry, using the M13 reverse and T7 primer, according to the manufacturers' instructions (Applied Biosystems).

Data analysis

The sequence data obtained in the survey is analyzed with the BLAST server (http://www.ncbi.nlm.nih.gov/BLAST/). The raw sequence is edited to remove the sequence derived from the vector and the adaptors. This procedure can be done manually or using a designated program e.g. CodonCode (http://www.codoncode.com/). After the cleanup, the sequences are analyzed for their quality and only those that show a clear, single signal are exported in fasta format for further analysis. Once imported to the BioEdit program (http://www.mbio.ncsu.edu/BioEdit/bioedit.html) the sequences are subjected to batch BLAST analysis with default settings. This batch analysis allows the pre-selection of the sequences of interest, as mRNA and rRNA fragments are frequently found as background. All results that indicate the presence of a virus, or an unknown sequence should be selected and re-analyzed with the BLAST server (nblast) with the expectation number of 1000 against all databases. If the results are still not clear the following steps might be taken:

- Analysis against translated database (tblastx)
- Search the conserved domain database (rpsblast)
- Analysis against virus database (nblast)

The sequences that in tblastx and rpsblast display similarity to viral sequences should be considered as possibly unknown pathogens. If the sequence is analyzed against viral database care should be taken with each hit, because virtually all fragments show some similarity to viral sequences. In that case, the pathogen might be considered identified only if the results from different fragments from one sample show similarity to the same virus family.

In all cases, it is essential to design a diagnostic primer set and re-test the original material for the presence of the pathogen. Only when the pathogen can be detected by the diagnostic (RT)-PCR in the original sample, efforts to sequence the entire genome can be undertaken.

Notes

1. For the nucleic acid isolation, any highly efficient method may be used. It is not advisable to use TRIzol isolation, as it is intended for isolation of nucleic acids from cells and tissues.

2. The L6 buffer lysis is sufficient to inactivate the virus. After 10 minutes incubation it is safe to process the sample in the normal biochemistry laboratory.

3. The L6 and L2 buffer contain concentrated guanidine thiocyanate (GTC), and thus should be considered as highly toxic. Remember to store the GTC waste separately with addition of one-tenth volume of 1N sodium hydroxide to prevent GTC degradation.

4. All RNA and cDNA handling before the first PCR should be performed in a contaminating nucleic acid free environment. The sequence independent amplification will result in overamplification of contaminating DNA.
5. The use of chlorine as a decontaminant should be limited as it may decrease the viability of reverse transcription enzyme.

6. If the thermocycling is performed in a PCR machine that does not include heating of the cover 2 drops of paraffin oil should be layered on top of the PCR solution to prevent evaporation during the PCR reaction.

7. It is advised to use a fresh razor for each band during excision. The exposition of the gel to ultraviolet light should be limited as it results in DNA degradation

References

1. Bachem, C. W., R. S. van der Hoeven, S. M. de Bruijn, D. Vreugdenhil, M. Zabeau, and R. G. Visser. 1996. Visualization of differential gene expression using a novel method of RNA fingerprinting based on AFLP: analysis of gene expression during potato tuber development. Plant J 9:745-753.
2. Boom, R., C. J. Sol, M. M. Salimans, C. L. Jansen, P. M. Wertheim-van Dillen, and J. van der Noordaa. 1990. Rapid and simple method for purification of nucleic acids. J. Clin. Microbiol. 28:495-503.
3. Burgner, D. and A. Harnden. 2005. Kawasaki disease: what is the epidemiology telling us about the etiology? Int. J. Infect. Dis. 9:185-194.
4. Chang, Y., E. Cesarman, M. S. Pessin, F. Lee, J. Culpepper, D. M. Knowles, and P. S. Moore. 1994. Identification of herpesvirus-like DNA sequences in AIDS-associated Kaposi's sarcoma. Science 266:1865-1869.
5. Drosten, C., S. Gunther, W. Preiser, S. van der Werf, H. R. Brodt, S. Becker, H. Rabenau, M. Panning, L. Kolesnikova, R. A. Fouchier, A. Berger, A. M. Burguiere, J. Cinatl, M. Eickmann, N. Escriou, K. Grywna, S. Kramme, J. C. Manuguerra, S. Muller, V. Rickerts, M. Sturmer, S. Vieth, H. D. Klenk, A. D. Osterhaus, H. Schmitz, and H. W. Doerr. 2003. Identification of a novel coronavirus in patients with severe acute respiratory syndrome. N. Engl. J. Med. 348:1967-1976.
6. Fujinami, R. S., M. G. von Herrath, U. Christen, and J. L. Whitton. 2006. Molecular mimicry, bystander activation, or viral persistence: infections and autoimmune disease. Clin. Microbiol. Rev. 19:80-94.
7. Holmes, K. V. and M. M. C. Lai. 1996. Coronaviridae: The viruses and their replication, p. 1075-1093. In B. N. Fields, D. M. Knipe, P. M. Howley, and et al (eds.), Fields Virology. Lippincott-Raven Publishers, Philadelphia.
8. Stephensen, C. B., D. B. Casebolt, and N. N. Gangopadhyay. 1999. Phylogenetic analysis of a highly conserved region of the polymerase gene from 11 coronaviruses and development of a consensus polymerase chain reaction assay. Virus Res. 60:181-189.
9. Stewart, J., P. Talbot, and S. Mounir. 1995. Detection of coronaviruses by the polymerase chain reaction, p. 316-327. In Y. Becker and G. Darai (eds.), Diagnosis of human viruses by polymerase chain reaction technology. Springer-Verlag, New York.
10. van der Hoek, L., K. Pyrc, M. F. Jebbink, W. Vermeulen-Oost, R. J. Berkhout, K. C. Wolthers, P. M. Wertheim-van Dillen, J. Kaandorp, J. Spaargaren, and B. Berkhout. 2004. Identification of a new human coronavirus. Nat. Med. 10:368-373.

Summary

To date, there are still a variety of human infections with unknown etiology. Identification of previously unrecognized viral agents in patient samples is of great medical interest, but remains a major technical challenge. Virus discovery based on cDNA-AFLP (VIDISCA) is a novel approach that provides a fast and effective tool for amplification of unknown nucleic acid species, e.g. of human viruses. The VIDISCA method is based on double restriction enzyme processing of a target sequence and ligation of oligonucleotide adaptors that subsequently serve as priming sites for amplification. As the method is based on the presence of restriction sites, it results in the generation of reproducible, specific amplification patterns. The method allows amplification and identification of viral RNA / DNA, with a lower cutoff value of 10^5 copies/ml for DNA viruses and 10^6 copies/ml for the RNA viruses (Chapter II, Appendix A). With this technique four human viruses were identified in this thesis: a human coronavirus (Chapter II) and three novel picornavirus types (Chapter XII).

Acute respiratory tract infections are responsible for considerable morbidity and mortality in humans and animals. A variety of viruses, bacteria, and fungi are associated with respiratory tract illness. Most of the respiratory viruses belong to the families of *Paramyxoviridae*, *Orthomyxoviridae*, *Picornaviridae*, *Adenoviridae*, and *Coronaviridae*. Nevertheless, pathogens cannot be detected in a relatively large proportion (~30%) of patients with respiratory disease. This is partially due to limitations of current diagnostic assays, but also because some infections are associated with yet unknown pathogens (Chapter XI). Chapter II describes the identification of a novel group I coronavirus, human coronavirus NL63 (HCoV-NL63) in a child with acute respiratory illness. This virus is observed mostly in young children, elderly persons and immunocompromised patients with upper and lower acute respiratory tract disease (1-10% of all respiratory infections). Additionally, virtually all sera from persons of 8 years and older are seropositive for HCoV-NL63, suggesting that infection of humans is very common and usually acquired during childhood (Chapter VI).

Investigation of the HCoV-NL63 genome variability led to the identification of two genetically distinct lineages that apparently have recombined, resulting in a mosaic genome structure in many HCoV-NL63 isolates (Chapter V). A study on coronaviral evolution revealed that HCoV-NL63 and HCoV-229E lineages may have diverged in the 11th century (Chapter V). Thus, HCoV-NL63 is not an emerging virus, but rather a previously unknown human pathogen.

The genome of HCoV-NL63 has the following gene order: 1ab-S-ORF3-E-M-N and during transcription all sub-genomic mRNAs are produced. Inspection of the genome sequence indicates that all open reading frames have functional TRS element, with the exception of the E gene. The TRS of the E gene possesses a defective core sequence that may result in decreased production of E mRNA

(Chapter III). Overall, the RNA genome composition is very low in the C nucleotide and high in U, which is also reflected in the codon usage. Inspection of the nucleotide composition along the genome indicates that this bias in nucleotide count is not constant along the genome: it is more moderate in the last one-third of the genome (Chapter III). A closer inspection of the HCoV-NL63 genome and encoded proteins is presented in chapter IV. In general, HCoV-NL63 has a typical coronaviral genome, with some characteristic features. One of these features is an altered substrate specificity of the main proteinase.

It was generally thought that all group I coronaviruses use CD13 (also known as aminopeptidase N) as receptor because all representatives (HCoV-229E, porcine, feline and canine coronaviruses) engage this molecule for cell entry. However, HCoV-NL63 can infect cells that are not susceptible for the closely related HCoV-229E, suggesting that HCoV-NL63 binds to a different surface molecule. An analysis of receptor engagement revealed that HCoV-NL63 uses angiotensin-converting enzyme 2 (ACE2) for cell entry, the receptor that is used by SARS-CoV (Chapter VI). ACE2 plays a protective role during lung damage and it has been suggested that the high pathogenicity of SARS-CoV is actually caused by downregulation of ACE2 during infection. However, HCoV-NL63 infection also results in a decrease of ACE2 protein (Chapter VII). This result illustrates that engagement of the ACE2 molecule as receptor, as well as its downregulation during infection, do not necessarily lead to the development of severe lung damage as observed during SARS-CoV infection.

It has been suggested that the overactivation of the innate immune system during SARS-CoV infection may explain its severe pathogenicity. We investigated the IL-6 and IL-8 levels during HCoV-NL63 infection and observed increased production of these two cytokines, similar as described previously for several respiratory viruses including SARS-CoV (Chapter VIII).

HCoV-NL63 infections are frequently involved in hospitalizations of patients with respiratory tract illness. Therefore, there is a need for an antiviral therapy to prevent disease induction or a vaccine to prevent new infections (Chapter X). We evaluated several existing antiviral drugs and small molecules as inhibitors of HCoV-NL63. These compounds target multiple stages of the replication cycle. Of the 31 compounds that were tested, several potently inhibit HCoV-NL63 at early steps of the replication cycle. Intravenous immunoglobulins, heptad repeat 2 peptide, small interfering RNAs, β-d-N4-hydroxycytidine, and 6-azauridine showed promising anti-NL63 activity and low cytotoxicity (Chapter IX).

Samenvatting

Er zijn ziektes waarbij men het vermoeden heeft dat er een virale infectie bij betrokken is terwijl geen van de bekende virussen aantoonbaar is. Het identificeren van de betrokken (onbekende) virussen is van groot belang omdat men door het bestuderen van het virus een diagnose en eventueel een behandeling kan ontwikkelen. Er zijn verschillende technieken om onbekende virussen te identificeren (Hoofdstuk XI). Een van de methodes is de VIDISCA methode (Hoofdstuk II, Appendix A). VIDISCA biedt de mogelijkheid om onbekende nucleïnezuursequenties te identificeren, zoals het genoom van nog onbekende virussen. Bij VIDISCA wordt gebruik gemaakt van restrictie-enzym herkenningsplaatsen die in het genoom van alle virussen aanwezig zijn en na digestie door de betreffende enzymen vindt ligatie aan oligonucleotide adaptors plaats. De sequenties van de adaptors worden vervolgens gebruikt voor amplificatie door middel van een PCR. Aangezien de methode gebaseerd is op restrictie-enzym digestie, waarbij de herkenningsplaatsen zich op een virus-specifieke positie bevinden zal elk virus een karakteristiek PCR patroon geven. De methode is geschikt voor het detecteren van RNA- of DNA-virussen, met een ondergrens van 105 kopieën voor DNA virussen en 106 kopieën voor RNA virussen per milliliter patiëntenmateriaal (Hoofdstuk II, Appendix A). In dit proefschrift staan vier nieuwe virussen beschreven die zijn geïdentificeerd met behulp van VIDISCA, een humaan coronavirus (Hoofdstuk II) en drie picornavirus serotypes (Hoofdstuk XII).

Acute respiratoire infecties zijn verantwoordelijk voor een aanzienlijke hoeveelheid ziekenhuisopnames. Een heel scala aan bekende virussen (Paramyxoviridae, Orthomyxoviridae, Picornaviridae, Adenoviridae, and Coronaviridae), bacteriën en schimmels kan hierbij betrokken zijn. Toch zijn er ook geregeld respiratoire infecties waarbij het verantwoordelijke pathogeen niet te identificeren is (ongeveer 30% van alle gevallen). Gedeeltelijk komt dit door beperkingen van de detectiemethodes, maar ook omdat niet alle pathogenen die een luchtweginfectie kunnen veroorzaken bekend zijn (Hoofdstuk XI). In hoofdstuk II wordt de identificatie van een groep I coronavirus beschreven, het humane coronavirus NL63 (HCoV-NL63). Dit is een respiratoir virus. Vergeleken met SARS-CoV - een zeer pathogeen respiratoir coronavirus - is de infectie met HCoV-NL63 relatief mild, alhoewel infectie van jonge kinderen, immuuun-gecompromiteerde volwassenen en ouderen kan leiden tot ziekenhuisopname. Het virus heeft zich wereldwijd verspreid en infecties treden relatief vaak op. Gedurende de eerste levensjaren maakt iedereen een infectie met HCoV-NL63 door, aangezien alle kinderen ouder dan 8 jaar antistoffen tegen het virus bij zich dragen (Hoofdstuk VI).

Onderzoek naar de variatie van het genetisch materiaal van HCoV-NL63 heeft uitgewezen dat er twee verschillende varianten te onderscheiden zijn. Toch is het typeren van de HCoV-NL63 varianten niet eenvoudig aangezien recombinatie

tussen de twee types regelmatig optreedt. Het gevolg is dat HCoV-NL63 een mozaïek genoomstructuur heeft met meerdere recombinatiesites (Hoofdstuk V). Het feit dat er twee types HCoV-NL63 circuleren doet vermoeden dat het virus niet recentelijk in de menselijke populatie is geïntroduceerd. Bestudering van de evolutiesnelheid en een vergelijking van HCoV-NL63 met het humane coronavirus 229E (het enige andere humane coronavirus van groep I) toont aan dat deze virussen ongeveer 900 jaar geleden een gemeenschappelijke voorouder hadden (Hoofdstuk V). Hieruit valt te concluderen dat HCoV-NL63 inderdaad niet recent in de humane populatie is geïntroduceerd.

Gedurende transcriptie van coronavirussen worden subgenome mRNAs geproduceerd indien er 5′ van het gen een Transcription Regulatory Sequence (TRS) aanwezig is. Het genoom van HCoV-NL63 bevat de volgende genen: 1ab, S, ORF3, E, M, N, en inspectie van het genoom en de geproduceerde subgenome mRNAs conformeren dat er bij alle genen een functioneel TRS element aanwezig is (Hoofdstuk III). Er is echter een opvallende bevinding: de TRS van het E gen heeft een alternatieve core sequentie. Toch is het E subgenome mRNA op Northern blot te identificeren, weliswaar in lage hoeveelheden (Hoofdstuk III). Een ander opvallend kenmerk in HCoV-NL63 is het nucleotidegebruik in het genoom. Het gehalte C-nucleotiden is laag terwijl het gehalte U-nucleotiden hoog is. Inspectie van de nucleotidecompositie laat zien dat deze bias niet constant is over het genoom: het is sterker aan de 5′ kant tot op tweederde van het genoom en minder geprononceerd aan de 3′ kant (Hoofdstuk III). In hoofdstuk IV wordt er in meer detail gekeken naar de eiwitten van HCoV-NL63, en het blijkt dat HCoV-NL63 een standaard coronavirussamenstelling heeft, met een aantal opvallende kenmerken. Een van de karakteristieke kenmerken is gelegen in de activiteit van het Main protease, waarschijnlijk heeft dit enzym een alternatieve substraatspecificiteit.

Voorheen werd aangenomen dat alle groep I coronavirussen dezelfde receptor gebruiken. Het eiwit CD13 wordt door meerdere groep I virussen op het celoppervlak herkend en gebruikt om de cel binnen te komen (HCoV-229E, en de groep I coronavirussen van varkens, katten en honden). Opvallend is daarom dat HCoV-NL63 de cellijnen die door HCoV229E geïnfecteerd kunnen worden juist niet kan infecteren. Dit doet vermoeden dat HCoV-NL63 een andere receptor gebruikt. Analyse van het receptorgebruik van HCoV-NL63 conformeert deze hypothese: HCoV-NL63 gebruikt angiotensin-converting enzyme 2 (ACE2) (Hoofdstuk III). Verassend is dit wel omdat het ACE2 molecuul ook wordt gebruikt door SARS-CoV (een groep II coronavirus). Onlangs is bekend geworden dat het ACE2 molecuul een schadebeschermende rol speelt in de longen, en men heeft gesuggereerd dat de ernstige pathogeniciteit van SARS-CoV wordt veroorzaakt door verlaagde expressie van ACE2 tijdens de infectie. Dit is echter in tegenspraak met de observaties tijdens HCoV-NL63

infectie. Tijdens HCoV-NL63 infectie is er ook verminderde expressie van ACE2 (Hoofdstuk VII), terwijl dit virus veel minder pathogeen is dan SARS-CoV.

Het aangeboren immuunsysteem is van groot belang bij de afweer van virale infecties. In hoofdstuk VIII wordt beschreven in hoeverre de eiwitten die betrokken zijn bij de aangeboren immuniteit tot expressie komen tijdens een HCoV-NL63 infectie. Het blijkt dat vooral interleukine (IL) 6 en IL8 sterk tot expressie komen. Deze verhoging is vergelijkbaar met de reactie tijdens een infectie met SARS-CoV. Dus het verschil in pathogeniciteit van SARS-CoV en HCoV-NL63 is niet terug te voeren tot een verschil in de expressie van IL6 of IL8.

Infecties met HCoV-NL63 kunnen leiden tot ziekenhuisopname vanwege een ernstige luchtweginfectie. Een effectieve behandelstrategie is daarom gewenst (Hoofdstuk X). In hoofdstuk IX worden een aantal antivirale middelen beschreven die een sterk remmend effect hebben op de replicatie van HCoV-NL63. Deze middelen remmen de infectie in een vroeg stadium van de replicatiecyclus, zoals tijdens receptorbinding (IVIG), membraanfusie (heptad repeat peptides) en transcriptie (siRNA, β-d-N4-hydroxycytidine en 6-azauridine).

Podsumowanie

Etiologia wielu chorób pozostaje nadal nieznana. Identyfikacja dotychczas nieznanych wirusów w próbkach klinicznych ma wielkie znaczenia dla współczesnej medycyny, pozostając jednocześnie jednym z największych wyzwań technicznych jakie przed nią stoją. Wykorzystywanie metody opartej na cDNA-AFLP (VIDISCA) do identyfikacji nowych wirusów jest nowatorskim podejściem dostarczającym szybkiego i efektywnego narzędzia amplifikacji kwasów nukleinowych o nieznanej sekwencji (np. ludzkich wirusów). Metoda VIDISCA wykorzystuje miejsca cięcia enzymami restrykcyjnymi do ligacji oligonukleotydów o znanej sekwencji, które następnie służą jako matryca dla primerów w czasie amplifikacji PCR. Wykorzystanie istnienia miejsc restrykcyjnych umożliwia uzyskanie podczas amplifikacji powtarzalnych wzorów fragmentów DNA, specyficznych dla danego gatunku. Metoda ta pozwala na amplifikację i identyfikację zarówno DNA, jak i RNA wirusów, z progiem detekcji na poziomie 10^5 kopii/ml dla wirusów DNA i 10^6 kopii/ml dla wirusów RNA (Rozdział II, Dodatek A). Dotychczas z pomocą tej techniki dokonano identyfikacji 4 ludzkich wirusów: ludzkiego koronawirusa (Rozdział II) i trzech nowych pikornawirusów (Rozdział XII).

Ostre infekcje układu oddechowego są związane z wieloma poważnymi, niejednokrotnie śmiertelnymi, chorobami ludzi i zwierząt. Wiele wirusów, bakterii i grzybów może być odpowiedzialnych za wywoływanie chorób górnych dróg oddechowych. Większość znanych wirusów wywołujących choroby układu oddechowego należy do rodzin *Paramyxoviridae*, *Orthomyxoviridae*, *Picornaviridae*, *Adenoviridae* i *Coronaviridae*. Mimo, że wiele wiadomo o etiologii infekcji układu oddechowego, nadal w wielu przypadkach (ok. 30%) nie udaje się zidentyfikować patogenu odpowiedzialnego za rozwój choroby. Wynika to w znacznej mierze z ograniczeń stosowanych obecnie metod, ale także z faktu, że część infekcji wywoływana jest przez nieznane patogeny (Rozdział IX). W rozdziale II opisano identyfikację nowego, ludzkiego koronawirusa z grupy I – koronawirusa NL63 (HCoV-NL63), odkrytego w próbce klinicznej pochodzącej od dziecka cierpiącego na ostrą infekcję dróg oddechowych. Późniejsze badania pokazały, że wirus ten jest związany z infekcjami górnych i dolnych dróg oddechowych (1-10% wszystkich infekcji układu oddechowego), głównie u małych dzieci, osób w podeszłym wieku oraz osób z obniżoną odpornością. Jest również główną przyczyną dławca u niemowląt. Wykazano również, że niemal wszystkie osoby powyżej 8 roku życia posiadają przeciwciała przeciwko białkom wirusa NL63, co sugeruje, że infekcje wywoływane przez ten wirus są szeroko rozpowszechnione i zazwyczaj pojawiają się po raz pierwszy już w dzieciństwie (Rozdział VI).

Badanie zmienności genetycznej HCoV-NL63 doprowadziło do identyfikacji dwóch, genetycznie odmiennych szczepów, które w przeszłości rekombinowały, czego skutkiem jest obecna mozaikowa struktura HCoV-NL63 (Rozdział V). Analiza ewolucyjna pozwoliła ustalić, że HCoV-NL63 jako odrębny gatunek

pojawił się już w XI wieku (Rozdział V). Odkrycie to pokazuje, że HCoV-NL63 nie jest nowo powstałym gatunkiem, lecz że nigdy wcześniej nie został zidentyfikowany i opisany.

Genom HCoV-NL63 zawiera następujące geny: 1ab-S-ORF3-E-M-N, które w czasie transkrypcji są przepisywane na sub-genomowe cząsteczki mRNA. Dokładna analiza wskazuje, że prawie wszystkie geny, z wyjątkiem jednego, kodującego białko E, posiadają poprawne sekwencje regulatorowe transkrypcji (TRS). Sekwencja TRS genu E posiada błędną sekwencje główną, co może skutkować obniżoną produkcją sub-genomowego E-mRNA (Rozdział III). Patrząc bardziej ogólnie na genom HCoV-NL63, można zauważyć znaczny deficyt cytydyny kosztem uracylu, co ma swoje odbicie również w wykorzystaniu kodonów. Dalsza analiza ujawnia, że to zachwianie równowagi w ilości cytydyny i uracylu nie ma jednakowego natężenia we wszystkich regionach i jest znacznie mniej nasilone w ostatnich dwóch-trzecich genomu (Rozdział III).

Szczegółowa analiza genomu HCoV-NL63 i kodowanych białek znajduje się w rozdziale IV. Generalnie, HCoV-NL63 ma wiele cech typowych dla ludzkich koronawirusów, ale posiada również wiele cech unikalnych (na przykład odmienną, w porównaniu z innymi koronawirusami, specyficzność substratową głównej proteazy).

Do niedawna uważano, że wszystkie koronawirusy grupy I wykorzystują białko CD13 (aminopeptydaza N) jako receptor, ponieważ wszystkie znane do tej pory gatunki (koronawirus 229E, świńskie, kocie i psie koronawirusy) wykorzystywały właśnie to białko do infekcji komórek gospodarza. Okazało się jednak, że HCoV-NL63 może zakażać komórki, które nie pozwalają na infekcje jego bliskiego kuzyna - koronawirusa 229E, co sugeruje że HCoV-NL63 oddziałuje z innymi białkami powierzchniowymi infekowanych komórek. Dokładniejsza analiza wykazała, że HCoV-NL63 wykorzystuje w trakcie infekcji białko ACE2 (angiotensin-converting enzyme 2), to samo które jest używane przez koronawirusa powodującego SARS (Rozdział VI). W dotychczasowych badaniach sugerowano, że wysoka patogenność koronawirusa SARS jest związana z obniżonym poziomem białka ACE2, które może działać ochronnie w przypadku uszkodzenia płuc. Infekcja mniej patogennym HCoV-NL63 również powoduje podobne obniżenie poziomu ACE2 (rozdział VII). Prowadzi to do konkluzji, że zarówno wykorzystanie białka ACE2 jako receptora komórkowego, jak i obniżenie poziomu tego białka w czasie infekcji, nie musi prowadzić do poważnych uszkodzeń płuc obserwowanych w czasie infekcji koronawirusem SARS.

Inną hipotezą tłumaczącą wysoką patogenność koronawirusa SARS jest nad-aktywacja systemu immunologicznego. Z badań prezentowanych w niniejszej pracy wynika, że poziom interleukiny 6 i 8 w czasie infekcji HCoV-NL63 jest

znacznie podwyższony, podobnie jak to opisano wcześniej dla innych wirusów układu oddechowego, włącznie z koronawirusem SARS (Rozdział VIII).

Infekcje powodowane przez HCoV-NL63 są częstą przyczyną hospitalizacji pacjentów cierpiących na choroby układu oddechowego, dlatego istnieje duże zapotrzebowanie na skuteczną terapie, która będzie w stanie zapobiegać rozwojowi choroby lub szczepionkę, która zapobiegnie nowym infekcjom (Rozdział X). W celu identyfikacji substancji, która mogłaby zostać wykorzystana w czasie terapii, przetestowano szereg istniejących leków i innych substancji. Przebadane substancje były wybrane tak, aby hamować replikację HCoV-NL63 na różnych etapach jego cyklu replikacyjnego. Immunoglobuliny, peptydy analogiczne do wirusowych białek (heptad repeat peptides), małe dwuniciowe cząsteczki RNA (siRNA), β-d-N4-hydroxycytydyna i 6-azaurydyna posiadają wysoką aktywność inhibicyjną w połączeniu z niską toksycznością (Rozdział IX).

Acknowledgments

And finally I want to say Thank You! to all these persons that made it possible for me to prepare this thesis.

First of all, I would like to say thank you to Lia for a marvelous guidance during last few years and for being a great friend. It was pleasure to work with you as a scientist and as a person, and I hope that we will keep in touch in future. Ben, you were a great promoter, thank you for all your comments and ideas – and of course thank you for giving me a chance 4 years ago! Thank you also to the members of my committee: Tom, René, Hans, Jaap, Ralph, Willy and Marc. For some of you also big thanks for traveling to Amsterdam, just for my dissertation.

I would also like to thank Maarten, for introducing me to the lab world and for supporting me through all the time. And of course for the nice work breaks!

Thanks Ronald for being a great guy and a great friend. It was great to have you with your sense of humor in our group! Thanks for all the work you did for me and with me and for all your ideas and input.

Thanks Anna for your work (especially all these ELISAs) and for being a great person.

I would like also to say thank you to Ralph, for having me in his laboratory for three months – it was a great time for me scientifically and socially. Thank you also for traveling all the way from North Carolina to the old continent! You have a marvelous group of people in your lab! I would like to say also thanks to all the people from the North Carolina that made my life easier and for sure much nicer: Amy, Damon, Anna, Boyd, Eric, Barry & Erica, Lisa, Leslie, Suzan, Matt, Tim, Will, Rhonda & all the others.

Thanks to all the people from the lab in Amsterdam that helped me through all these years, Elly, Joost, Rienk, Marcel, Marloes, Tony, Ellen, Jeroen, Karolina, Ying-Poi, Truus, Pavlina, Nienke, Rogier, Mireille, Xue, Chris, Olivier, Martine, Walter, Karin, Monique, Alex, Ilja, Edwin, Marc, Michel P. and Michel de V., Ruth, Volodya, Atze, Joost, Jens, Margreet and all the others – thanks! Also all other people from the AMC: Koen, Dave, Hans, Frits, Hettie, Gerrit, Mieke, Jan, Jacob and others.

Big thanks to all persons that collaborated with us: Volker, John, Lea, Heike, Stefan, Christian, Oliver, Howard, Rolf, Ralf, Elien, Leen, Els, Wilma, Ron, Pauline, Jos, Joke, David, Dave, Louis, Peter, Berend Jan and all others.

Thanks to you, Przemek and Ola, for being friends and housemates!

I would also like to say thank you to my girlfriend Kasia. You were great support for me, and I don't think I could do all these things if you were not there. Love you.

Thanks to my Mom and Dad for supporting me in all my crazy ideas and for raising me the way I am.

Thank you to all the people from the student houses on Weesperstraat (including the staff from 'the doose') and Plantage Muidergracht, especially Maria for making my life more entertaining!

And to all the people that I do not mention here but are very important to me

- thank you-

Curriculum Vitae



PERSONAL INFORMATION

NAME:	Krzysztof Antoni Pyrc
ADDRESS:	Academic Medical Center K3-106.F Meibergdreef 15 1105AZ Amsterdam The Netherlands
TELPHONE:	+48 692 696 863
E-MAIL ADDRESS:	k.a.pyrc@gmail.com
NATIONALITY:	Polish
DATE AND PLACE OF BIRTH:	29.10.1979 KRAKOW, POLAND
FAMILY STATUS:	Single, no children

EDUCATION AND TRAINING

29.06.2007	PhD thesis dissertation: "Virus discovery and human coronavirus NL63" at Department of Medical Microbiology, Center for Infection and Immunity Amsterdam (CINIMA), University of Amsterdam
20.04.2006 – 14.07.2006	3-month training at the Department of Epidemiology, University of North Carolina, Chapel Hill, United States of America.
01.09.2004 - 29.06.2007	PhD student position at Department of Medical Microbiology Center for Infection and Immunity Amsterdam (CINIMA), University of Amsterdam
June 2003	Master degree thesis: 'Oxidative damage of DNA, caused by the presence of etoposide and quercetin '. Jagiellonian University, Faculty of Biotechnology, Krakow, Poland
01.02.2003 – 31.05.2003	4- month training at Department of Medical Microbiology, Center for Infection and Immunity Amsterdam (CINIMA), University of Amsterdam in a framework of Socrates/Erasmus scholarship
1998 — 2003	Jagiellonian University, Department of General Biochemistry, Faculty of Biotechnology, Krakow, Poland
1994 — 1998	Stanislaw Wyspianski High School, Krakow, Poland

GRANTS AND AWARDS:

May 2006	American Society for Virology Student Travel Award for the 25th "Silver Anniversary"Annual Meeting 15-19 July 2006 ; University of Wisconsin-Madison.
January 2006	van Walree grant for working visit abroad from Royal Netherlands Academy of Arts and Sciences.
Autumn 2002	Socrates / Erasmus scholarship for working visit abroad from the Jagiellonian University in Cracow on behalf of the European Comission.

PROFESSIONAL MEMBERSHIPS:

American Society for Virology (ASV)

PUBLICATIONS:

1. Pyrc K., Berkhout B. and van der Hoek L., Identification of new human coronaviruses; (2007) Expert Review of Anti-infective Therapy, 5(2): 245-253.

2. Pyrc K., Berkhout B. and van der Hoek L., Antiviral Strategies Against Human Coronaviruses; (2007) Infect Disord Drug Targets. 7(1):59-66.

3. Pyrc K. and van der Hoek L., Human Coronavirus NL63, a long lost brother,; (2007) In: Coronaviruses: Molecular and Cellular Biology; Ch. 15: 295 - 315

4. Pyrc K., Jebbink MF., Berkhout B., van der Hoek L., VIDISCA: unraveling the unknown; (2007) In: SARS and other coronaviruses: strategies and protocols, *In Press*

5. Pyrc K, Berkhout B, van der Hoek L.; The novel human coronaviruses NL63 and HKU1.; (2007) Journal of Virology 81(7):3051-7.

6. Dijkman R, Jebbink MF, Wilbrink B, Pyrc K, Zaaijer HL, Minor PD, Franklin S, Berkhout B, Thiel V, van der Hoek L.; Human coronavirus 229E encodes a single ORF4 protein between the spike and the envelope genes.; (2006) Virology Journal 3(1):106

7. Pyrc K., Dijkman R., Lea Deng, Maarten F. Jebbink, Howard A. Ross, Ben Berkhout and Lia van der Hoek, Mosaic structure of human coronavirus NL63, one thousand years of evolution., Journal of Molecular Biology, (2006) Journal of molecular biology 364(5):964-973.

8. Schildgen O, Jebbink MF., de Vries M., Pyrc K., Dijkman R., Winke U., Simon A., Müller A., Kupfer B., van der Hoek L., Identification of cell lines permissive for human Coronavirus NL63, (2006) Journal of Virological Methods. 138(1-2):207-10.

9. Pyrc K., Bosch BJ., Berkhout B., Jebbink MF., Dijkman R., Rottier P., and van der Hoek L.; Inhibition of Human Coronavirus NL63 Infection at Early Stages of the Replication Cycle; (2006) Antimicrobial Agents and Chemotherapy, 50(6): 2000–2008

10. van der Hoek, L., Pyrc, K., Berkhout, B.; Human coronavirus NL63, a new respiratory virus.; (2006) FEMS Microbiology Reviews, September 30(5): 760-773

11. Pohlmann S, Gramberg T, Wegele A, Pyrc K, van der Hoek L, Berkhout B, Hofmann H.; Interaction between the spike protein of human coronavirus NL63 and its cellular receptor ACE2; (2006) In: The Nidoviruses: The control of SARS and Other Nidovirus Diseases.; Advances in experimental medicine and biology 581:281-4.

12. Piotrowski, Y., van der Hoek, L., Pyrc, K., Berkhout, B., Moll, R. and R. Hilgenfeld. Non-structural proteins of human coronavirus NL63; (2006) In: The Nidoviruses: The control of SARS and Other Nidovirus Diseases.; Advances in experimental medicine and biology 581:97-100.

13. Hofmann H., Marzi A., Gramberg T., Geier M., Pyrc K., van der Hoek L., Berkhout B., Pöhlmann S. Attachment factor and receptor engagement of SARS coronavirus and human coronavirus NL63; (2006) In: The Nidoviruses: The control of SARS and Other Nidovirus Diseases.; Advances in experimental medicine and biology 581:219-27.

14. van der Hoek L., Sure K., Ihorst G., Stang A., Pyrc K., Maarten F. Jebbink, Petersen G., Forster J., Berkhout B., Überla K., Human coronavirus NL63 infection is associated with croup; (2006) In: The Nidoviruses: The control of SARS and Other Nidovirus Diseases.; Advances in experimental medicine and biology 581:485-491

15. van der Hoek, L., Pyrc, K., Berkhout, B.; Coronavirus NL63, the new Dutch.; (2006) Tijdschrift voor Infectieziekten, 1(3): 108-114

16. van der Hoek L, Sure K, Ihorst G, Stang A, Pyrc K, Jebbink MF, Petersen G, Forster J, Berkhout B, Uberla K., Croup Is Associated with the Novel Coronavirus NL63. (2005), PLoS Medicine 23;2(8):e240

17. Hofmann H, Pyrc K, van der Hoek L, Geier M, Berkhout B, Pöhlmann S, Human coronavirus NL63 employs the severe acute respiratory syndrome coronavirus receptor for cellular entry; (2005) Proceedings of National

Academy of Sciences. USA, 31;102(22):7988-93

18. Moes E., Vijgen L., Keyaerts E., Zlateva K., Li S., Maes P., Pyrc K., Berkhout B., van der Hoek L., Van Ranst M. A novel pancoronavirus RT-PCR assay: frequent detection of human coronavirus NL63 in children hospitalized with respiratory tract infections in Belgium. (2005) BMC Infectious Diseases 5:6

19. Pyrc K., Berkhout B, van der Hoek L, Molecular characterization of human coronavirus NL63 (2005): in Recent Research in Infection and Immunity, 3: 325-48

20. Pyrc K, Jebbink MF, Berkhout B, van der Hoek L. Genome structure and transcriptional regulation of human coronavirus NL63. (2004) Virology Journal. 1(1):7

21. van der Hoek L, Pyrc K, Jebbink MF, Vermeulen-Oost W, Berkhout RJ, Wolthers KC, Wertheim-Van Dillen PM, Kaandorp J, Spaargaren J, Berkhout B. Identification of a new human coronavirus. (2004) Nature Medicine, 10(4):368-73

22. Kapiszewska M., Pyrc K. Anticancer and antiartheriosclerosis action of flavonoids. Vegetables and fruits in the nutrition. (2003) Medycyna i Społeczenstwo, Acta Academiae Modrevianae, 101-108